

University of Alberta

**Role of Triacylglycerol Hydrolase in Hepatic Lipid Droplet
Metabolism**

by

Huajin Wang

A thesis submitted to the Faculty of Graduate Studies and Research
in partial fulfillment of the requirements for the degree of

Doctor of Philosophy

Department of Cell Biology

©Huajin Wang
Fall, 2009
Edmonton, Alberta

Permission is hereby granted to the University of Alberta Libraries to reproduce single copies of this thesis and to lend or sell such copies for private, scholarly or scientific research purposes only. Where the thesis is converted to, or otherwise made available in digital form, the University of Alberta will advise potential users of the thesis of these terms.

The author reserves all other publication and other rights in association with the copyright in the thesis and, except as herein before provided, neither the thesis nor any substantial portion thereof may be printed or otherwise reproduced in any material form whatsoever without the author's prior written permission.

Examining Committee

Dr. Richard Lehner, Department of Pediatrics and Cell Biology

Dr. Dennis Vance, Department of Biochemistry

Dr. Tom Hobman, Department of Cell Biology

Dr. Thomas Simmen, Department of Cell Biology

Dr. Dawn Brasaemle, Department of Nutritional Sciences, Rutgers University

Dedication

To grandma, an amazing woman, fighter, and human being.

Abstract

The majority of triacylglycerol (TG) utilized for very-low density lipoproteins (VLDL) assembly is derived from lipolysis-reesterification of TG stored in lipid droplets (LDs). At least two types of LDs exist in hepatocytes – cytosolic LDs (CLDs) and the microsomal-associated luminal LDs (LLDs). An endoplasmic reticulum luminal lipase, triacylglycerol hydrolase (TGH), was shown to participate in mobilizing intracellular TG stored in LDs. However, it is not clear which pool of TG is hydrolyzed by TGH. LLDs are present in the same subcellular compartment as TGH and thus may serve as the substrate pool for this enzyme.

Results presented in this thesis describe the isolation and characterization of LLDs from mouse liver microsomes, providing the first biochemical evidence for the presence of these LDs. LLDs differ from CLDs or VLDL particles in both protein and lipid compositions. TGH was found to associate with LLDs, suggesting it may hydrolyze this pool of TG. Other VLDL secretion related proteins were also found on LLDs, including apolipoprotein E and microsomal triglyceride transfer protein. It was determined that LLDs constitute a minor pool of intracellular TG. Thus, quantitatively TG stored in CLDs may provide the major TG source for VLDL assembly. Overexpression of TGH resulted in increased mobilization of not only LLDs but also CLDs.

The mechanism by which TGH may regulate the metabolism of CLDs was investigated in wild type and TGH-deficient mouse hepatocytes. It was found that TGH deficiency led to morphological changes in CLDs and diminished the rate at

which preformed CLDs obtain newly formed TG (CLD growth). An alternative mechanism for CLD growth was also explored by tracing the incorporation of fluorescent fatty acids analogues into CLDs by live-cell imaging. The results suggested that newly synthesized TG are assembled into LDs through TGH-dependent and TGH-independent mechanisms.

The role of apoE as cofactor for TGH mediated lipolysis was investigated. Obtained results suggested that the absence of apoE in hepatocytes compromised the lipolysis/reesterification process mediated by TGH. Future studies in this direction should further explore the interaction of apoE with TGH and whether the interaction affects the stability of TGH at the lipid-water interface.

Acknowledgements

First and foremost, I am deeply grateful to my supervisor, Dr. Richard Lehner. Thank you for taking me on in your laboratory and introducing me to the stimulating world of lipids. The experience working with you towards my PhD degree has been challenging and rewarding. Not only did you teach me knowledge, experimental and writing skills, and scientific thinking, but also a diligent and perseverant attitude towards anything worthwhile in life.

I would like to thank members of my supervisory committee: Dr. Richard Lehner, Dr. Dennis Vance and Dr. Tom Hobman for your valuable discussions and comments throughout my PhD program. The critical thinking I learned from you will benefit me my entire scientific career.

Thanks to all who have given me a helping hand in my research. I would especially like to thank Dr. Nicolas Touret for your tremendous help with time-lapse microscopy. I am deeply grateful for the immeasurable assistance you warmly offered on data analysis and interpretation, as well as tricks with immunofluorescence and even image editing software, which would otherwise take me forever to learn. Dr. Xuejun Sun, thank you so much for the time you spent teaching me image analysis. It would have been impossible on my own. I would also like to extend my thanks to our extremely helpful lab technicians Johanne Lamoureux and Lena Li, and the present and past technical experts who contributed greatly to my research: Honey Chan (confocal microscopy), Russ Watts (ER and Golgi preparation), Priscilla Gao (GC and hepatocyte preparation), Randy Nelson (molecular biology), Audric Moses (GC and FPLC), and Laura Hargreaves (animal work).

All the present and past members of Lehner lab and the MCBL group – thank you all so much for the memorable experience we had together during the past 5 years. It has been a great pleasure to work with a group of talented people with curious minds. I enjoyed your companionship at or after work, and you have gradually become my family here in Edmonton.

As well, my graduate peers and office staff at the department of Cell Biology have been extremely helpful throughout the years. My special thanks to Sue-Ann Mok for sharing your valuable experience in writing and formatting of this thesis.

I cannot thank enough all the friends that I have been so lucky to make since I came to Edmonton. You have made my life colorful and made Edmonton a significant and memorable place for me in the years to come.

A special thanks to Pat, for being there for me when I needed mental support. Talking to you always calms me down, even over the phone. Thank you for teaching me to appreciate non-science books and for all our philosophical discussions that help me keep an open mind.

Last but not least, I extend my utmost gratitude to my amazing parents, who have always believed in me, and taught me to be sincere and to be strong. Mom and Dad, I always look up to you. Thanks for the unconditional love that you are always prepared to offer!

Table of Contents

| | |
|--|-----------|
| CHAPTER I: INTRODUCTION..... | 1 |
| 1.1 Preface | 2 |
| 1.2 Overview of TG metabolism..... | 2 |
| 1.2.1 Digestion and transport of dietary fat | 5 |
| 1.2.2 <i>De novo</i> FA synthesis | 7 |
| 1.2.3 TG biosynthesis..... | 10 |
| 1.2.3.1 The generation of DG | 10 |
| 1.2.3.1.1 Glycerol-3-phosphate pathway | 10 |
| 1.2.3.1.2 The MG pathway | 13 |
| 1.2.3.2 Conversion of DG to TG | 14 |
| 1.2.4 TG storage and utilization..... | 16 |
| 1.2.4.1 Hormone Sensitive Lipase (HSL)..... | 17 |
| 1.2.4.2 ATGL / desnutrin | 18 |
| 1.2.4.3 Regulation of basal and stimulated lipolysis by perilipin A..... | 21 |
| 1.3 Biology and metabolism of TG-containing lipid droplets | 23 |
| 1.3.1 LD associated proteins..... | 25 |
| 1.3.1.1 PAT family proteins | 25 |
| 1.3.1.1.1 Perilipin and adipophilin/ADRP – the constitutively TG-associated PAT proteins..... | 26 |
| 1.3.1.1.2 TIP47 and the exchangeable TG-associated PAT proteins..... | 27 |
| 1.3.1.2 Other LD associated proteins and the implications | 29 |
| 1.3.2 Formation and growth of LDs | 31 |
| 1.3.3 Organelle connection and motility of LDs | 33 |
| 1.4 Hepatic LDs and VLDL assembly | 37 |

| | | |
|---|--|-----------|
| 1.4.1 | LDs in the liver..... | 37 |
| 1.4.1.1 | Cytosolic LDs | 37 |
| 1.4.1.2 | Luminal apoB-free LDs | 38 |
| 1.4.2 | Mechanisms for VLDL assembly..... | 39 |
| 1.4.2.1 | Composition of VLDL particles..... | 39 |
| 1.4.2.2 | Two-step model of VLDL assembly | 40 |
| 1.4.2.3 | Location of the second-step lipidation | 42 |
| 1.4.3 | Regulation of VLDL assembly – availability of lipids | 44 |
| 1.4.3.1 | TG and PL synthesis for VLDL secretion..... | 44 |
| 1.4.3.2 | Provision of lipids by MTP..... | 46 |
| 1.4.3.3 | ApoB100 secretion is regulated by degradation..... | 47 |
| 1.4.3.4 | Mobilization of TG stores for VLDL assembly – lipolysis and reesterification | 48 |
| 1.5 | Triacylglycerol hydrolase | 51 |
| 1.5.1 | TGH belongs to the carboxylesterase gene family | 52 |
| 1.5.2 | Conserved motifs and structure of TGH | 53 |
| 1.5.3 | Role of TGH in different tissues..... | 59 |
| 1.5.3.1 | Role of TGH in the liver – VLDL secretion..... | 59 |
| 1.5.3.2 | Role of TGH in adipose tissue | 61 |
| 1.5.3.3 | Role of TGH in macrophages..... | 61 |
| 1.6 | Focus of this thesis | 63 |
| CHAPTER II: MATERIALS AND METHODS..... | | 64 |
| 2.1 | Materials..... | 65 |
| 2.1.1 | Chemicals and Reagents | 65 |
| 2.1.2 | Plasmids..... | 69 |
| 2.1.3 | Antibodies | 69 |
| 2.1.4 | Buffers and solutions | 71 |

| | | |
|------------|--|-----------|
| 2.2 | Animals | 72 |
| 2.3 | Cell culture and manipulation | 73 |
| 2.3.1 | Culture of mammalian cell lines..... | 73 |
| 2.3.2 | Preparation and culture of primary mouse hepatocytes | 73 |
| 2.3.3 | Augmentation of intracellular TG stores..... | 75 |
| 2.3.4 | Stable transfection of McA cells | 75 |
| 2.3.5 | Transfection of primary mouse hepatocytes..... | 76 |
| 2.4 | Protein manipulation and analysis | 77 |
| 2.4.1 | Determination of protein concentration | 77 |
| 2.4.2 | SDS-PAGE | 77 |
| 2.4.3 | Native PAGE..... | 78 |
| 2.4.4 | Immunoblotting..... | 78 |
| 2.4.5 | Protein identification by mass spectrometry | 79 |
| 2.4.6 | Immunoprecipitation | 80 |
| 2.5 | Subcellular fractionation | 80 |
| 2.5.1 | Isolation of microsomal luminal contents | 80 |
| 2.5.2 | Isolation of microsomal LLDs by density gradient ultracentrifugation | 81 |
| 2.5.3 | Preparation of ER and Golgi fractions..... | 82 |
| 2.5.4 | Isolation of cytosolic lipid droplets (CLDs)..... | 83 |
| 2.6 | Lipid manipulation and analysis | 84 |
| 2.6.1 | Lipid extraction for thin-layer chromatography (TLC)..... | 84 |
| 2.6.2 | TLC | 84 |
| 2.6.3 | Gas chromatography (GC) analysis of lipids | 85 |
| 2.6.4 | Gel filtration chromatography..... | 86 |
| 2.6.5 | Metabolic labeling of lipids | 87 |
| 2.7 | Microscopy | 87 |

| | | |
|------------|--|-----------|
| 2.7.1 | Fluorescence labeling of hepatocytes | 87 |
| 2.7.2 | Immunofluorescent staining..... | 88 |
| 2.7.3 | Confocal fluorescence scanning microscopy | 89 |
| 2.7.4 | Time-lapse microscopy..... | 90 |
| 2.7.5 | Image processing and analysis with Velocity Software..... | 90 |
| 2.8 | Other methods | 91 |
| 2.8.1 | Generation and purification of rabbit anti-mouse TGH antibodies..... | 91 |
| 2.8.2 | <i>In vitro</i> lipase assay | 92 |
| 2.8.3 | RNA isolation and real-time PCR for TGH expression | 92 |
| 2.8.4 | Statistical Analysis | 93 |

**CHAPTER III: ISOLATION AND CHARACTERIZATION OF
APOLIPOPROTEIN B-FREE LUMINAL LIPID DROPLETS 94**

| | | |
|------------|---|------------|
| 3.1 | Overview..... | 95 |
| 3.2 | Results..... | 95 |
| 3.2.1 | Isolation of LLDs | 96 |
| 3.2.2 | Lipid composition of LLDs..... | 100 |
| 3.2.3 | Protein composition of LLDs | 103 |
| 3.2.4 | LLDs are heterogeneous in size..... | 106 |
| 3.2.5 | TGH is mainly present in the ER but not Golgi | 110 |
| 3.2.6 | TGH decreases neutral lipid stores | 111 |
| 3.3 | Discussion | 114 |

**CHAPTER IV: ROLE OF TRIACYLGLYCEROL HYDROLASE IN
CYTOSOLIC LIPID DROPLET BIOGENESIS 120**

| | |
|---|------------|
| 4.1 Overview | 121 |
| 4.2 Results..... | 121 |
| 4.2.1 TGH is localized in the ER surrounding cytosolic LDs | 121 |
| 4.2.2 Ablation of TGH leads to cytosolic TG accumulation in hepatocytes | 122 |
| 4.2.3 Ablation of TGH alters the morphology of LDs..... | 125 |
| 4.2.4 TGH deficiency does not alter the formation of nascent LDs | 125 |
| 4.2.5 TGH deficiency delays LD maturation | 131 |
| 4.2.6 Nascent LDs interact with preformed LDs dynamically | 134 |
| 4.3 Discussion | 137 |

**CHAPTER V: IDENTIFICATION OF POTENTIAL COFACTORS FOR
TGH 146**

| | |
|--|------------|
| 5.1 Overview..... | 147 |
| 5.2 Results..... | 147 |
| 5.2.1 ApoE partially colocalizes with TGH and co-immunoprecipitates with TGH..... | 147 |
| 5.2.2 ApoE deficiency does not alter TGH expression but alters TGH activity against 4- MUH..... | 150 |
| 5.2.3 Decreased TG secretion from apoE deficient hepatocytes due to compromised lipolysis. | 153 |
| 5.2.4 ApoE is not required for TGH association with lipid droplets | 158 |
| 5.3 Discussion | 165 |

CHAPTER VI: PERSPECTIVES AND FUTURE DIRECTIONS 168

| | |
|---------------------------|------------|
| 6.1 Synopsis | 169 |
|---------------------------|------------|

| | |
|---|------------|
| 6.2 Perspectives..... | 169 |
| 6.2.1 Differential pools of intracellular LDs..... | 169 |
| 6.2.2 Lipases and the destiny of FAs – is it the location that matters? | 173 |
| 6.2.3 Proposed role of TGH in regulating different pools of LDs..... | 177 |
| 6.2.4 Some remaining questions pertinent to TGH function..... | 180 |
| 6.2.4.1 Which pool of luminal TG does TGH really hydrolyze? | 180 |
| 6.2.4.2 Cofactor for TGH..... | 183 |
| 6.2.4.3 Apolipoprotein binding domain | 185 |
| 6.3 Concluding remarks | 186 |

CHAPTER VII: REFERENCES 193

APPENDICES 223

| | |
|--|------------|
| Digital data available on CD..... | 223 |
| Video S1. Lipid transfer from nascent LDs to preformed LDs | 223 |
| Video S2. Dynamic interactions between nascent and preformed LDs | 223 |

List of Tables

| | |
|--|-----|
| Table 2-1. Plasmids | 69 |
| Table 2-2. Primary antibodies | 69 |
| Table 2-3. Secondary antibodies..... | 70 |
| Table 2-4. Common buffers and solutions | 71 |
| Table 2-5. List of mouse strains used..... | 72 |
| Table 3-1. Identification of LLD associated proteins by Mass Spectrometry..... | 105 |

List of Figures and Illustrations

| | |
|---|-----|
| Figure 1-1. Structure of a triacylglycerol molecule | 4 |
| Figure 1-2. Overview of TG transport in circulation | 6 |
| Figure 1-3. TG biosynthesis pathways | 12 |
| Figure 1-4. Regulation of basal and stimulated lipolysis by perilipin A | 22 |
| Figure 1-5. Structure of LDs | 24 |
| Figure 1-6. Proposed mechanisms for CLD formation and growth | 34 |
| Figure 1-7. Two-step model for VLDL assembly..... | 41 |
| Figure 1-8. Lipolysis and reesterification..... | 50 |
| Figure 1-9. Subcellular localization of TGH | 54 |
| Figure 1-10. Conservative domains in TGH amino acid sequence | 56 |
| Figure 1-11. Three-dimensional structure of human TGH..... | 58 |
| Figure 3-1. Isolation of LLDs..... | 97 |
| Figure 3-2. Release of PDI from the microsomal lumen..... | 98 |
| Figure 3-3. Release of TGH and apoB from the microsomal lumen..... | 99 |
| Figure 3-4. Lipid composition of LLDs | 101 |
| Figure 3-5. Protein profile of LLDs | 104 |
| Figure 3-6. Protein profile of LLDs | 107 |

| | |
|---|-----|
| Figure 3-7. TGH associates with small LLDs that may contain apoE or MTP, but not apoB | 108 |
| Figure 3-8. TGH associates with small LLD that may contain apoE or MTP but not apoB..... | 109 |
| Figure 3-9. Analysis of subcellular fractions from mouse liver..... | 112 |
| Figure 3-10. Ectopic expression of TGH decreases neutral lipid stores in McA cells | 113 |
| Figure 3-11. Model for the role of LLDs in VLDL assembly | 119 |
| Figure 4-1. TGH is localized in the ER surrounding cytosolic LDs. | 123 |
| Figure 4-2. Ablation of TGH leads to TG accumulation in OA treated hepatocytes | 124 |
| Figure 4-3. TGH affects LD morphology..... | 126 |
| Figure 4-4. Structures of Bodipy FA analogues | 128 |
| Figure 4-5. Characterization of Bodipy FA analogues..... | 129 |
| Figure 4-6. TGH does not affect nascent LD formation..... | 132 |
| Figure 4-7. Nascent LDs extensively associate with TIP47 but not ADRP..... | 133 |
| Figure 4-8. TGH deficiency delays the merge of nascent and preformed LDs..... | 135 |
| Figure 4-9. Live-imaging of LD formation | 136 |
| Figure 4-10. Interaction of nascent LDs and preformed LDs | 138 |
| Figure 4-10. Interaction of nascent LDs and preformed LDs..... | 139 |
| Figure 4-11. Lipid transfer into the core of preformed LDs | 140 |
| Figure 4-12. Model for the role of TGH in LD maturation | 143 |
| Figure 5-1. Colocalization of TGH with apoE and MTP | 149 |

| | |
|---|-----|
| Figure 5-2. Characterization of anti-mouse TGH antibodies..... | 151 |
| Figure 5-3. ApoE co-immunoprecipitates with TGH..... | 152 |
| Figure 5-4. Expression of TGH mRNA in apoE deficient livers | 154 |
| Figure 5-5. TGH protein level in apoE deficient livers..... | 155 |
| Figure 5-6. ApoE deficiency leads to compromised TGH activity | 156 |
| Figure 5-7. TG turnover and secretion in WT and apoE KO hepatocytes..... | 159 |
| Figure 5-8. Absence of apoE does not affect TGH targeting to CLDs..... | 162 |
| Figure 5-9. ApoE is associated with LDs..... | 163 |
| Figure 5-10. Absence of apoE does not affect TGH targeting to LLDs | 164 |
| Figure 6-1. Hepatic LDs are at close proximity with peroxisomes..... | 174 |
| Figure 6-2. Proposed role of TGH in LD metabolism..... | 178 |
| Figure 6-3. Immunoprecipitation of TGH and apoB..... | 182 |
| Figure 6-4. Model for apoE stabilizing TGH on lipid-water interface..... | 184 |
| Figure 6-5. Putative lipoprotein binding domain of TGH | 187 |
| Figure 6-6. McA cells stably expressing wild type or mutant human TGH | 189 |
| Figure 6-7. In vitro lipase activity of wild type or mutant human TGH..... | 190 |

List of Abbreviations

| | |
|--------|---|
| 4-MUH | 4-methylumbelliferyl heptanoate |
| AADA | arylamide deacetylase |
| ACAT | acyl-CoA: cholesterol acyltransferase |
| ADRP | adipose differentiation-related protein |
| apoB | apolipoprotein B |
| apoE | apolipoprotein E |
| ATGL | triglyceride lipase |
| BSA | bovine serum albumin |
| CE | cholesteryl ester |
| Ces1 | carboxylesterase 1 |
| CGI-58 | comparative gene identification-58 |
| CLD | cytosolic lipid droplet |
| CM | chylomicrons |
| CPAT | constitutively TG-associated PAT protein |
| CT | CTP: phosphocholine cytidylyltransferase |
| DG | diacylglycerol |
| DGAT | acyl-CoA: diacylglycerol acyltransferases |
| DMEM | Dulbecco's modified Eagle's medium |
| E600 | diethyl- <i>p</i> -nitrophenyl phosphate |
| EPAT | exchangeable TG-associated PAT proteins |
| ER | endoplasmic reticulum |

| | |
|------|--|
| FA | fatty acid |
| FPLC | fast protein liquid chromatography |
| GC | gas chromatography |
| GPAT | acyl-CoA: glycerol-3-phosphate acyltransferase |
| GSKi | GR148672X, TGH-specific inhibitor |
| HDL | high density lipoprotein |
| HSL | hormone sensitive lipase |
| IP | immunoprecipitation |
| KLH | keyhole limpet hemocyanin |
| LD | lipid droplet |
| LDL | low density lipoprotein |
| LLD | luminal lipid droplets |
| McA | McArdle RH7777 |
| MG | monoacylglycerol |
| MGAT | acyl-coenzyme A:monoacylglycerol acyltransferase |
| MTP | microsomal triglyceride transfer protein |
| NCEH | neutral cholesteryl ester hydrolase |
| NLBD | neutral lipid binding domain |
| OA | oleic acid |
| PA | phosphatidic acid |
| PAGE | polyacrylamide gel electrophoresis |
| PAT | perilipin, adipophilin, TIP47 |
| PBS | phosphate buffered saline |

| | |
|-------|--|
| PC | phosphatidylcholine |
| PDI | protein disulphide isomerase |
| PE | phosphatidylethanolamine |
| PEMT | phosphatidylethanolamine N-methyltransferase |
| PKA | protein kinase A |
| PL | phospholipid |
| PLD | phospholipase D |
| PMSF | phenylmethylsulphonyl fluoride |
| SCD1 | stearoyl-coenzyme A desaturase 1 |
| TBS | Tris-buffered saline |
| TG | triacylglycerol |
| TGH | triacylglycerol hydrolase |
| TIP47 | tail-interacting protein of 47 kDa |
| TLC | thin-layer chromatography |
| VLDL | very-low density lipoprotein |
| WAT | white adipose tissue |

Chapter I: Introduction

1.1 Preface

Through the long history of evolution, humans and our ancestors have evolved a set of sophisticated mechanisms to maintain body fat and carefully regulate energy preservation during times of chronic energy insufficiency / starvation. Today, however, human beings live in a modern, industrialized society where mass-produced, energy-dense and nutrient-poor foods with high levels of sugar and saturated fats have never been so abundant in history. The “thrifty” genes (Neel, 1962) that have evolved to conserve energy and protect us from starvation can no longer precisely maintain the energy balance under such energy-excess conditions. On the other hand, industrialization also liberated humans from heavy labor which used to be a necessity for survival. Reduced activity and sedentary life-style has led to reduced energy output, worsening the problems caused by excessive energy input. As a consequence, a series of diseases and clinical conditions has arisen rapidly during the past a few decades. Obesity, type 2 diabetes and cardiovascular disease are recognized as part of a rising global pandemic related to energy imbalance, especially in industrialized countries.

The major cause for obesity and one of the key contributing factors for type 2 diabetes and cardiovascular disease is the extra storage of triacylglycerols (TG), a water-insoluble substance commonly known as triglycerides or “fat”. In this introduction, the key biochemical, cellular and physiological events involved in TG metabolism will be discussed.

1.2 Overview of TG metabolism

A TG molecule is composed of three fatty acids attached to a glycerol backbone through ester bonds (Figure 1-1). Despite the aforementioned clinical conditions associated with excessive TG storage, TG serves many important functions in the body under physiological conditions. It is the most condensed form of energy source (9 kcal/g) in the body and stores 6 times the metabolic energy of an equal weight of hydrated glycogen (Voet et al., 2002). The primary function of TG is to serve as the major storage for molecules of fatty acid (FA) required for energy utilization. Partial hydrolysis of TG can generate diacylglycerol (DG), which not only provides a precursor for phospholipid (PL) synthesis (Coleman and Lee, 2004), but also serves as an important signaling molecule. On the other hand, conversion of DG and FA to TG serves to attenuate DG signals and to avoid toxicity of excessive FA accumulation. TG stored in adipose tissue provides insulation for animals to protect important organs from severe conditions. In liver and intestine, TG synthesized from endogenous or dietary FA is assembled into lipid emulsion particles called lipoproteins that are then transported to peripheral tissues for utilization or storage. However, overproduction of these particles is known to contribute to clinical conditions including obesity, atherosclerosis and type 2 diabetes.

Liver and adipose tissue play central roles in the regulation of lipid metabolism and homeostasis by forming an interactive metabolic cycle. During fasting, TG stores in the adipose are hydrolyzed by lipases such as adipose triglyceride lipase (ATGL) and hormone-sensitive lipase (HSL), and the FAs are bound to albumin and delivered to other tissues through circulation for energy

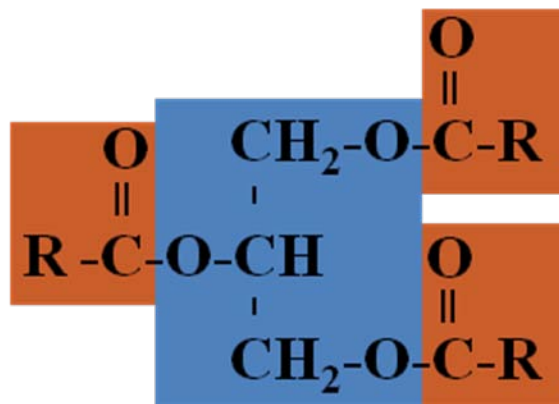


Figure 1-1. Structure of a triacylglycerol molecule. A TG molecule is composed of a glycerol backbone (blue) attached to three FA side chains (brown) by ester bonds.

utilization. Adipose tissue-derived FA is the major substrate for the production of TG incorporated into hepatic very-low density lipoprotein (VLDL). VLDL-TG secreted by the liver is hydrolyzed by lipoprotein lipase in the circulation and the released FAs are used for energy production in the target tissues. Some of the VLDL-TG derived FA is delivered to adipose tissue for reesterification and storage (Figure 1-2). This review will mainly focus on TG synthesis, storage and mobilization in the liver and the white adipose tissue (WAT).

1.2.1 Digestion and transport of dietary fat

The primary sources of FA for TG synthesis come from either hydrolysis of dietary fat or *de novo* FA synthesis. The digestion of dietary fat takes place in both the stomach and the intestine. The ingested dietary fat is first partially hydrolyzed into DG and FA by gastric lipase in the stomach (Lowe, 2002). The major digestion comes from hydrolysis by pancreatic lipases in the duodenum (the first section of the small intestine) where the TG emulsion is mixed with bile and pancreatic juice that contain pancreatic lipase and other lipases released from the pancreatic tissue. Pancreatic lipase specifically hydrolyses FA located at *sn*-1/3 positions, leading to the generation of *sn*-2-monoacylglycerol (MG) and FA (Mu and Hoy, 2004). Efficient dietary fat digestion requires fat emulsification by bile salts and the association of pancreatic lipase with a small protein cofactor called colipase. Colipase is required for the efficient dietary lipid hydrolysis by stabilizing the active conformation of pancreatic lipase on the lipid-water interface [see (Lowe, 2002; van Tilbeurgh et al., 1999) for reviews].

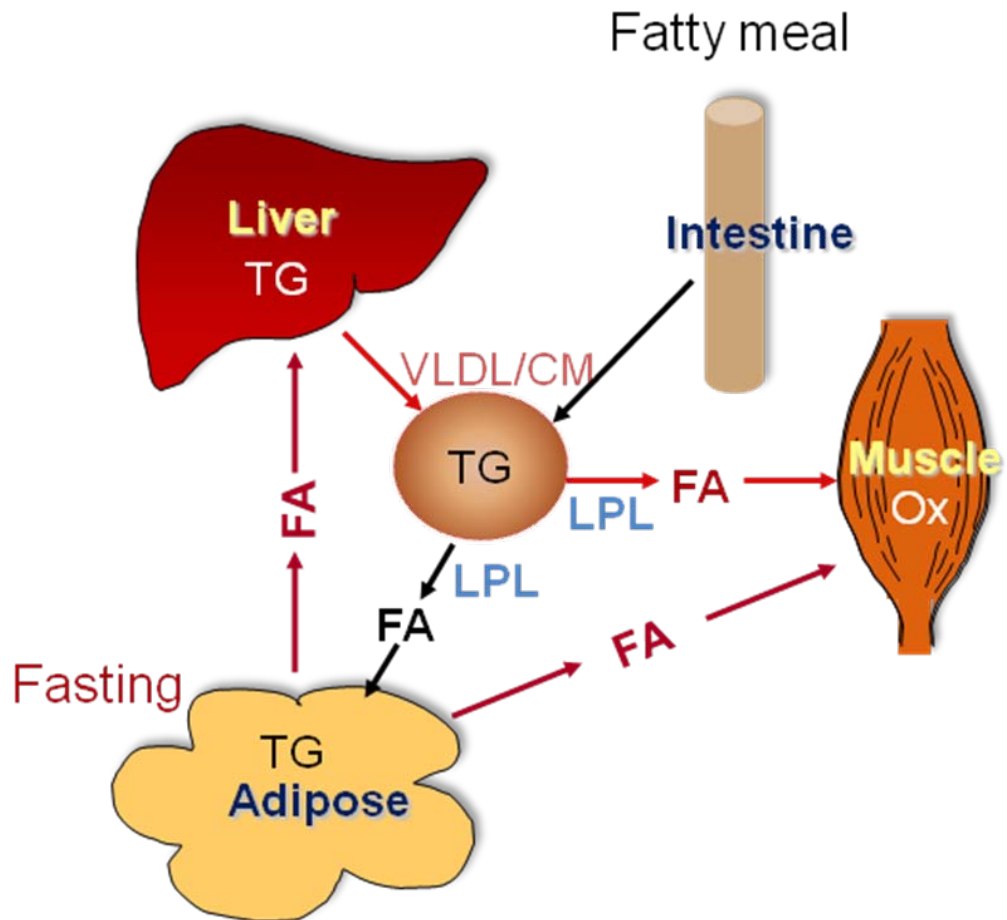


Figure 1-2. Overview of TG transport in circulation. FAs are esterified into TG and incorporated into TG-rich lipoprotein particles (VLDL and chylomicrons, CM). TG content in VLDL and CM particles can be hydrolyzed by lipoprotein lipase to provide FA to peripheral tissues for oxidation, or to adipose tissue for storage. During fasted condition, FAs are released from adipose tissue and transported in circulation in an albumin-bound form. Illustration provided by Dr. R. Lehner, University of Alberta.

The digestion products, FA and *sn*-2-MG, are absorbed across the apical membrane of the enterocytes and resynthesized into TG and packaged into chylomicrons (CM) in these cells. The assembly of CM resembles that of VLDL in the liver and requires apolipoprotein B48 (apoB48) (see **Section 1.4**). CM particles are secreted into circulation via lymph and experience rapid remodeling by exchanging apolipoproteins and PL with other lipoprotein particles such as high-density lipoproteins (HDL) (Redgrave and Small, 1979; Wu and Windmueller, 1978). Apolipoproteins play important roles in CM metabolism. CM particles will obtain apolipoprotein E (apoE) and apoC-II and lose apoA-I. TG content in the CM particles is rapidly hydrolyzed by lipoprotein lipase at or close to the capillary endothelial wall and the released FA is taken up by surrounding tissues, such as skeletal muscles or cardiac muscles for oxidation, or adipose tissue for storage. Large amounts of FA are bound to albumin and are eventually delivered to the liver. It is estimated that about 70-90% TG is removed from CM during this process (Redgrave and Carlson, 1979). As a consequence, CM are converted to much smaller, cholesteryl ester (CE)-rich CM remnants, which are removed from plasma by the liver via a receptor-mediated uptake (Redgrave and Carlson, 1979). The transport of TG in circulation is illustrated in Figure 1-2.

1.2.2 *De novo* FA synthesis

Another primary source of FA for TG synthesis is *de novo* synthesis which takes place rapidly under fed conditions, especially when the diet has little or no fat

(Lehner and Kuksis, 1996). Only a small amount of caloric intake in the form of carbohydrate is stored as glycogen, while most is converted to fat via lipogenesis (*de novo* FA synthesis). Liver is the primary location for *de novo* FA synthesis and adipose tissue is also engaged in FA synthesis at least in rodents. All carbon atoms of *de novo* synthesized FA are derived from the two-carbon precursor, acetyl-CoA, generated by catabolism of carbohydrates. In eukaryotes, FA synthesis is carried out by covalently linked multienzyme complexes referred to as type I fatty acid synthase system, as opposed to the individual enzymes present in prokaryotes known as the type II fatty acid synthase system (Wakil et al., 1983). Two multifunctional polypeptides are required for the entire FA synthesis pathway in animals, the acetyl-CoA carboxylase and fatty acid synthase. Acetyl-CoA carboxylase catalyzes the first committed step and one of the rate-limiting steps of FA biosynthesis, generating the only free intermediate in the entire pathway, malonyl-CoA. Subsequently, malonyl-CoA undergoes cycles of two-carbon chain elongation catalyzed by the second multifunctional polypeptides, fatty acid synthase, leading to the final formation and release of FA. It is worth noting that, except for some specialized tissues, the final product in mammalian systems is predominantly palmitic acid (16:0) with minor amounts of stearic acid (18:0) and myristic acid (14:0).

The endogenously synthesized or dietary fatty acids are subject to 2-carbon chain elongation and desaturation to generate long-chain fatty acids or unsaturated fatty acids. Many eukaryotic cells have capacity for these processes. In liver, brain and other tissues, there are at least two locations for fatty acid chain

elongation, the endoplasmic reticulum (ER) and the mitochondria (Cook and McMaster, 2002). The chain elongation system in the ER is highly active and predominates quantitatively. It appears to be the most important source for acyl chains greater than 16 carbons for membrane phospholipids during growth and maturation.

Unsaturated fatty acids are generated by introducing double bonds into saturated acyl chains. The mammalian system is able to introduce double bonds at the $\Delta 9$, $\Delta 6$, $\Delta 5$ positions, however, the first double bond is always introduced at $\Delta 9$ position. The animal system cannot introduce double bonds beyond the $\Delta 9$ position (Lessire et al., 1993) and therefore depends on the diet (plants or insects) to obtain essential fatty acids such as linoleic acid (18:2, $\Delta 9,12$). Stearoyl-coenzyme A desaturase 1 (SCD1) is responsible for introducing double bonds at the $\Delta 9$ position in the liver and adipose tissue (Enoch and Strittmatter, 1978). The preferred substrates for SCD1 are palmitoyl (16:0)- and stearoyl (18:0)-CoAs, which are converted into palmitoleoyl (16:1)- and oleoyl (18:1)-CoAs, respectively (Enoch and Strittmatter, 1978). Oleic acid (18:1) is the most abundant FA found in TG and PL, therefore, SCD1 has been proposed to play a critical role in lipid metabolism. Mice absent in SCD1 expression are lean and protected from diet-induced obesity, and exhibit marked increases in energy expenditure (Cohen et al., 2002; Ntambi et al., 2002). Liver-specific knockout of SCD1 protected mice from carbohydrate-induced adiposity (Miyazaki et al., 2007), while skin-specific deletion of this gene caused a severe skin defect

including sebaceous gland hypoplasia and depletion of sebaceous lipids (Sampath et al., 2009).

1.2.3 TG biosynthesis

In mammals, liver, intestine and adipose tissue are the most active locations for TG synthesis. It is generally accepted that TG synthesis is largely controlled by the amount of FA available, i.e., TG is synthesized only when FA is in excess. Several excellent reviews have discussed TG synthesis pathways and key enzymes involved in this process (Coleman and Lee, 2004; Lehner and Kuksis, 1996; Takeuchi and Reue, 2009; Wendel et al., 2009; Yen et al., 2008). There are two major TG synthesis pathways, the glycerol-3-phosphate or Kennedy pathway, and the monoacylglycerol (MG) pathway (Figure 1-3). While the glycerol-3-phosphate pathway is present in most cell types, the MG pathway functions predominantly in enterocytes, hepatocytes, and adipocytes where TG undergoes hydrolysis and resynthesis (Xia et al., 1993). Both pathways require fatty acyl-CoAs, the “activated form” of FA, as acyl donors (Coleman et al., 2002), which are synthesized by acyl-CoA synthetases. The two pathways use different sets of enzymes to synthesize DG, where the two routes subsequently merge and share the same enzymes to complete the final conversion to TG.

1.2.3.1 The generation of DG

1.2.3.1.1 Glycerol-3-phosphate pathway

The glycerol-3-phosphate pathway is the main route of TG biosynthesis in most cells except for enterocytes. It is proposed to produce 93% of TG in the liver under normal physiological conditions (Declercq et al., 1984).

The first and committed step in the glycerol-3-phosphate pathway is the acylation of glycerol-3-phosphate at the *sn*-1 position by acyl-CoA: glycerol-3-phosphate acyltransferase (GPAT) (EC 2.3.1.15), resulting in the production of 1-acylglycerol-3-phosphate (lysophosphatidic acid, lyso-PA) (Coleman and Lee, 2004; Kornberg and Pricer, 1953). Four mammalian GPATs have been found to date. GPAT1 and GPAT2 are associated with mitochondria and the other two, GPAT3 and GPAT4 are localized to the ER. In the liver, mitochondrial GPAT accounts for at least 50% of the total GPAT activity (Coleman and Lee, 2004). The mitochondrial GPAT1, the first cloned and most characterized mammalian GPAT isoform, was found to play an important role in hepatic lipid metabolism, channeling fatty acyl-CoA away from FA oxidation and towards TG biosynthesis (Hammond et al., 2002). In addition to controlling TG synthesis, GPAT1 is also critical for PL synthesis due to its preference to esterify palmitate (16:0) at the *sn*-1 position of glycerol-3-phosphate (Hammond et al., 2002). Following the formation of lyso-PA, it is further acylated at *sn*-2 position by acyl-CoA:1-acylglycerol-*sn*-3-phosphate acyltransferase (also called lysophosphatidate acyltransferase or LPAAT) (EC 2.3.1.51) to form phosphatidic acid (PA). PA stands at a central branch point in glycerolipid biosynthetic pathways. It is a mutual intermediate for the synthesis of DG and phosphatidylinositol, both of which are lipid second messengers that are involved in cell signaling. DG is also

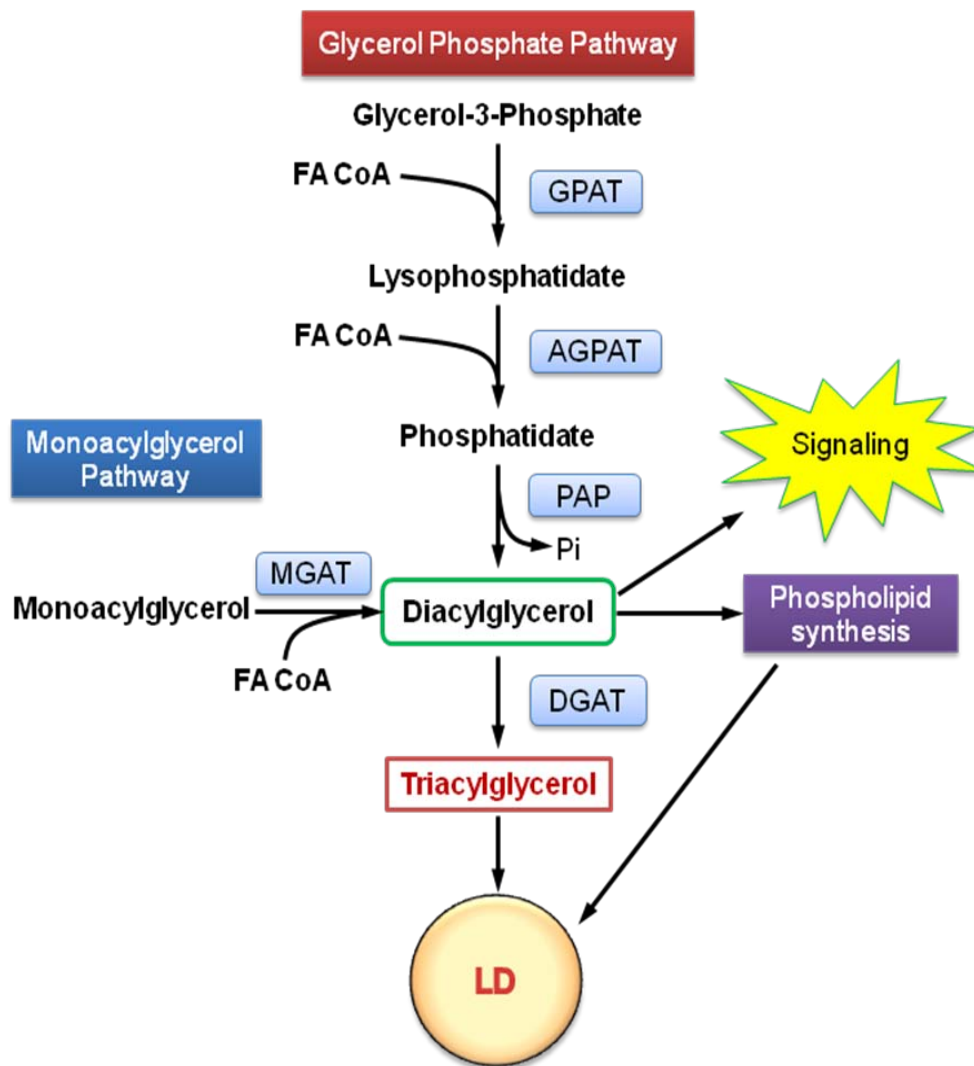


Figure 1-3. TG biosynthesis pathways. Two major pathways control TG synthesis, the glycerol phosphate pathway and the monoacylglycerol pathway. The reaction sequence and key enzymes regulating each pathway are shown. The two pathways merge at diacylglycerol, which is a branching point for TG synthesis, PL synthesis, as well as cell signaling. Synthesized TG and PL can be incorporated into TG storage droplets (LDs).

an important precursor at the convergence of TG and phospholipids [phosphatidylserine, phosphatidylcholine (PC) and phosphatidylethanolamine (PE)] synthetic pathways. The synthesis of DG from PA is catalyzed by phosphatidic acid phosphatases, including the lipin family proteins [see (Carman and Han, 2006; Coleman et al., 2000; Takeuchi and Reue, 2009) for reviews].

1.2.3.1.2 The MG pathway

MG pathway is prominent in enterocytes of the small intestine and is estimated to account for ~75% of TG synthesis in the intestine (Kayden et al., 1967; Mattson and Volpenhein, 1964). MG is mainly derived from hydrolysis of dietary TG by pancreatic lipases. The main products, *sn*-2-MG and FA are taken up by enterocytes where the MG undergoes stepwise acylation by acyl-CoA: monoacylglycerol acyltransferase (MGAT) (EC 2.3.1.22) and acyl-CoA: diacylglycerol acyltransferase (DGAT) (EC 2.3.1.20) to resynthesize TG for CM production.

At least 3 isoforms of MGAT have been described: MGAT1, MGAT2, and MGAT3. They were first identified as members of the DGAT2 family (Cases et al., 2001). MGAT1 mRNA is extensively expressed in mice, including stomach, kidney and adipose tissue, but is absent in the intestine (Yen et al., 2002). MGAT2 and MGAT3 are primarily expressed in small intestine, suggesting that they are the main isoforms mediating fat absorption (Shi and Cheng, 2009). It was recently reported that mice lacking MGAT2 expression are resistant to diet-induced obesity and metabolic disorders and show delayed fat absorption, but not

malabsorption of dietary fat (Yen et al., 2009). All three MGAT isoforms are believed to reside in the ER (Coleman and Lee, 2004). It has been shown that MGAT3 has a subcellular localization similar to that of DGAT2 but distinct from that of DGAT1 (see below) when exogenously expressed in COS-7 cells (Cao et al., 2007), suggesting a metabolic link between these two enzymes.

1.2.3.2 Conversion of DG to TG

The final step of TG synthesis is the acylation of DG to form TG, catalyzed by DGAT. Two mammalian forms of DGAT have been identified, DGAT1 and DGAT2.

DGAT activity was first reported 40 years ago, however, the purification of the corresponding enzyme proved to be difficult. In 1998, the gene encoding DGAT1 was identified by its similarity to acyl-CoA: cholesterol acyltransferase (ACAT) (Cases et al., 1998). It was further shown that DGAT1 is ubiquitously expressed in mice and humans, with the highest levels of expression in small intestine (Cases et al., 1998). However, the subsequent generation of DGAT1 knockout mice revealed that, although these mice are lean and resistant to diet-induced obesity, they maintain the ability to synthesize TG and have normal fasting plasma TG (Smith et al., 2000). These findings led to the prediction of a second DGAT. As a consequence, DGAT2 was found and cloned (Cases et al., 2001; Lardizabal et al., 2001). Strikingly, DGAT1 and DGAT2 do not share sequence homology at either the DNA or the protein level. DGAT2 is also ubiquitously expressed in humans and mice, with the highest expression in

adipose tissue and the liver. Unlike the mild phenotypes found in DGAT1 deficient mice, DGAT2 knockout mice are neonatal lethal and have a severe defect in skin barrier function (Stone et al., 2004). DGAT2 knockout mice also presented with decreased hepatic TG and decreased plasma TG, suggesting that this enzyme is involved in providing TG for VLDL secretion. The different phenotypes observed in DGAT deficient mice raised the question whether DGAT1 and DGAT2 are functionally different. It was proposed that this may be due to differences in topology and subcellular localization. Although DGAT activity has been predominantly localized to ER membranes, different DGAT activities have been found on the cytosolic and luminal faces of rat liver microsomes, referred to as “overt” and “latent” activities, respectively (Abo-Hashema et al., 1999; Owen et al., 1997). It was suggested that DGAT1 contributes to both overt and latent activities, while DGAT2 only contributes to the overt activity (Yen et al., 2008). It has been hypothesized that the overt DGAT activity may be associated with TG synthesis for storage, while the latent activity may contribute to synthesizing TG for lipoprotein secretion. However, mixed data exist concerning whether overexpression of DGAT1 increases TG secretion from the liver. Overexpression of human DGAT1 in McArdle RH7777 (McA) cells led to intracellular TG accumulation and VLDL secretion (Liang et al., 2004). Long-term adenoviral overexpression also demonstrated that both DGAT1 and DGAT2 increased hepatic TG accumulation, but only DGAT1 overexpression was associated with increased VLDL secretion (Yamazaki et al., 2005). However, this observation was challenged by another group who showed that short-term

overexpression of DGAT1 did not change VLDL or apoB production (Millar et al., 2006). Recent results obtained from liver-specific DGAT1 and DGAT2 transgenic mice also suggested that hepatic overexpression of neither enzyme led to increased plasma TG (Monetti et al., 2007).

1.2.4 TG storage and utilization

TG is stored in the body when there is a positive energy balance. Adipose tissue is the predominant location for TG storage. Mammalian livers also have the capacity to store a considerable amount of TG. Newly synthesized TG is packaged into TG-containing lipid droplets (LDs) for storage. However, little is known about the mechanisms by which TG is incorporated into LDs and how it is mobilized when needed for energy production. In the past decade, the biology and metabolism of LDs have been under intensive study. Recent advances in this area will be reviewed in depth in **section 1.3**.

There are three main control points in TG utilization (Fukao et al., 2004). The first is the mobilization of TG through lipolysis, a process by which TG molecules are hydrolyzed by lipases to release FA and glycerol. The other two are FA entry into mitochondria for β -oxidation and FA entry into the ketogenic pathway, controlled by carnitine palmitoyl transferase and hepatic mitochondrial 3-hydroxy-3-methylglutaryl (HMG)-CoA synthase, respectively. The latter two pathways are beyond the scope of this thesis; only TG mobilization will be included in this section with a focus on white adipose tissue (WAT). TG mobilization in the liver will be discussed in detail in **section 1.4**.

The majority of TG mass in the body is stored in the LDs present in WAT during the fed state. During prolonged fasting or metabolic stress, TG is hydrolyzed from LDs in adipocytes in response to hormonal signals, such as catecholamines and glucagon, to provide FA for energy production. Complete hydrolysis of TG includes a series of enzymatic reactions catalyzed by lipases to break the three ester bonds to liberate three FA and one molecule of glycerol. Major enzymes catalyzing these sequential reactions include ATGL, HSL and monoglyceride lipase.

1.2.4.1 Hormone Sensitive Lipase (HSL)

The first and rate limiting step of TG hydrolysis is the conversion of TG to DG and FA. Historically, HSL has long been recognized as the single rate-limiting lipase catalyzing hormonally regulated lipolysis for both TG and DG. However, studies from HSL-deficient mice generated in four independent laboratories (Haemmerle et al., 2002; Mulder et al., 2003; Osuga et al., 2000; Wang et al., 2001) revealed that these animals were not obese and did not accumulate large amounts of TG. There was still 45-50% residual TG lipase activity in adipocytes lacking HSL expression, and these adipocytes were able to maintain some degree of catecholamine-stimulated lipolysis, suggesting the presence of alternative lipase(s). Instead of accumulating TG, HSL-deficient mice accumulated DG in adipose tissue and muscle, indicating a role of HSL as a DG lipase instead of TG lipase. It is worth noting that earlier studies have shown that HSL has a broad spectrum of substrate specificity and is capable of hydrolyzing TG, DG, MG, CE,

and retinyl esters. (Zimmermann et al., 2009). However, the *in vitro* activity of HSL against DG is much greater (10-20-fold) than that against TG and MG (Fredrikson and Belfrage, 1983).

HSL is activated in response to β -adrenergic stimulation, leading to the phosphorylation of this enzyme at multiple serine sites by protein kinase A (PKA; cAMP-dependent protein kinase) (Garton and Yeaman, 1990; Small et al., 1991; Stralfors and Belfrage, 1985; Stralfors et al., 1984). PKA mediated phosphorylation of HSL increases its *in vitro* activity by only 2-3-fold; however, it also promotes the translocation of HSL to LDs (Egan et al., 1992), accounting for the 30-100-fold increase in lipolytic activity observed in intact cells upon β -adrenergic stimulation or PKA activation. A LD-coat protein, perilipin, plays a critical role in the translocation of HSL (Brasaemle et al., 2000a; Sztalryd et al., 2003). It is viewed that perilipin forms a regulated barrier on the surface of LD to restrain access by HSL (Brasaemle et al., 2000b). Under stimulated conditions, PKA phosphorylates perilipin on six serine residues, leading to translocation of HSL to LDs and initiation of lipolysis (Miyoshi et al., 2006; Sztalryd et al., 2003; Tansey et al., 2003). Perilipin phosphorylation is therefore essential for full enzymatic activation of HSL (Sztalryd et al., 2003).

1.2.4.2 ATGL / *desnutrin*

In 2004, three groups independently identified the lipase alternative to HSL (see above) responsible for TG hydrolysis, named ATGL (adipose triglyceride lipase), also known as desnutrin and phospholipase A₂ - ζ (Jenkins et al., 2004; Villena et

al., 2004; Zimmermann et al., 2004). Surprisingly, ATGL shares no clear sequence similarity with classical lipases (Schneider et al., 2006). An active Ser47 was identified within a GX SXG consensus sequence for serine lipases in the N-terminal patatin domain. Instead of having a catalytic triad as HSL or other traditional lipases, ATGL contain a Ser-Asp catalytic dyad in the active site, indicating that it could be regulated differently from traditional lipases (Watt and Steinberg, 2008).

ATGL is predominantly expressed in WAT and BAT, but is also present at much lower levels in other tissues (Watt and Steinberg, 2008). In contrast to HSL, ATGL activity is highly specific to TG, with 10-fold higher activity against TG than DG and no activity against MG, CE or retinyl ester. It selectively catalyzes the first step of TG hydrolysis, converting TG into DG and FA (Zimmermann et al., 2004). Studies in murine adipocytes have demonstrated that ATGL is involved in both basal and catecholamine-stimulated lipolysis (Kershaw et al., 2006; Zimmermann et al., 2004), in contrast to HSL, which almost exclusively contributes to stimulated lipolysis. However, ATGL deficient mice seem to demonstrate a marked decrease in stimulated lipolysis but not basal lipolysis (Haemmerle et al., 2006). In the same paper, it was reported that ATGL deficiency caused lipid accumulation in multiple tissues especially in cardiac myocytes, leading to premature death. However, the increased TG accumulation in WAT and the liver are mild. There was a drastic decrease in FA release from WAT and these animals were extremely cold-sensitive, indicating that ATGL is essential for mobilizing sufficient amounts of FA to maintain energy homeostasis.

Posttranslational regulation of ATGL activity is largely unknown. ATGL is phosphorylated at two serine residues, but phosphorylation is not mediated by PKA (Zimmermann et al., 2004). Phosphorylation also does not seem to affect translocation of ATGL to LDs since similar amounts of ATGL were found on LD in the basal state and stimulated state (Granneman et al., 2007; Zimmermann et al., 2004). Interestingly, it was recently reported that delivery of ATGL to LDs may be regulated through the COPI pathway (Soni et al., 2009), a vesicular transport pathway that retrieves proteins from the Golgi complex and delivers them to the ER.

In 2006, it was found that ATGL activity is strongly stimulated by the interaction with CGI-58 (Comparative Gene Identification-58, also known as ABHD5) (Lass et al., 2006), a protein accounting for a rare neutral lipid storage disease, Chanarin-Dorfman syndrome (MIM 275630) (Lefevre et al., 2001), which is characterized by ichthyosis (a group of skin disorders characterized by dry, thickened, scaly or flaky skin) and excessive TG deposition in most tissues except for adipose tissue. CGI-58 is a member of the esterase/thioesterase/lipase subfamily, but lacks the nucleophilic serine residue within the GX SXG motif (Lefevre et al., 2001). The purified form of CGI-58 does not possess lipase activity *in vitro*, but its presence stimulates ATGL activity up to 20-fold (Lass et al., 2006), indicating a role of CGI-58 as cofactor for ATGL to facilitate its full activation. CGI-58 was shown to bind to LDs via interaction with perilipin A under basal conditions, but rapidly dissociate from LDs and disperse into the cytosol upon β -adrenergic stimulation (Subramanian et al., 2004). This process

may require phosphorylation of, and dissociation from, perilipin A. Interestingly, CGI-58 was recently identified to have lysophosphatidic acid acyltransferase activity (Ghosh et al., 2008). Overexpression of CGI-58 in yeast showed increased formation of phosphatidic acid and an overall increase in PL. This was accompanied with decreased intracellular TG and increased FA, suggesting CGI-58 may be involved in an alternative PA biosynthetic pathway synergizing TG lipolysis and PL synthesis.

1.2.4.3 Regulation of basal and stimulated lipolysis by perilipin A

As described above, perilipin A plays a critical role in regulating basal and stimulated lipolysis. Under basal conditions, perilipin A associates with CGI-58 on LDs and serves as a barrier that prevents lipases from accessing the neutral lipid core (Subramanian et al., 2004). Under this condition, HSL is mainly in the cytosol and ATGL is partially associated with LDs. Following hormonal stimulation, activation of PKA leads to phosphorylation of HSL and perilipin A (Greenberg et al., 1991; Stralfors and Belfrage, 1985; Stralfors et al., 1984). The phosphorylation of perilipin A leads to the release of CGI-58, which further interacts and activates ATGL, initiating the first step of TG hydrolysis (TG to DG) (Granneman et al., 2007). The phosphorylation of HSL leads to its translocation to LDs and the subsequent second step of TG hydrolysis (DG to MG) (Brasaemle et al., 2000a). MG is then hydrolyzed by monoglyceride lipase to release FA and glycerol. This process is illustrated in Figure 1-4. This role of perilipin has been supported by functional studies both in cell culture and in animal models. It has

been reported that ectopic expression of perilipin A in fibroblasts leads to elevated intracellular TG accumulation, caused by a decreased rate of TG turnover (Brasaemle et al., 2000b). On the other hand, perilipin knockout mice exhibited reduced body fat and were resistant to diet-induced obesity. Adipocytes isolated from these mice also showed elevated basal lipolysis and diminished stimulated lipolysis (Martinez-Botas et al., 2000; Tansey et al., 2001).

1.3 Biology and metabolism of TG-containing lipid droplets

In conditions when intracellular FAs are in excess, cells rapidly form TG that is deposited in LDs. LDs (also known as lipid bodies) are depots of neutral lipids in essentially all organisms. LDs in mammalian cells are comprised of a neutral lipid core, mainly TG and CE, which is surrounded by a monolayer of amphipathic lipids [PL and free (unesterified) cholesterol] and LD-associated proteins (Fujimoto et al., 2008; Martin and Parton, 2005) (Figure 1-5). Historically, LDs have been viewed as inert storage particles to accommodate fat. Although their importance in providing energy and maintaining intracellular lipid homeostasis has been slowly revealed, it was not until recently that LDs have been recognized as highly dynamic, *bona fide* organelles that play central roles in energy metabolism (Brasaemle, 2007; Martin and Parton, 2006; Murphy, 2001). Great interest has been raised and intensive studies have been engaged in during the last decade (Beckman, 2006) to elucidate the mechanisms involved in LD biogenesis. Complex roles of LDs in multiple cellular functions have also been revealed, which include lipid metabolism and transport, cell signaling and trafficking,

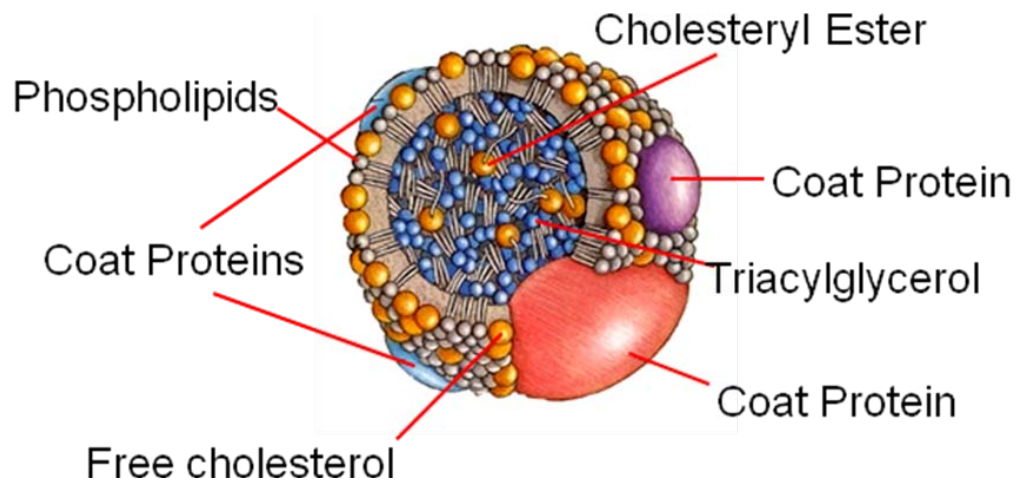


Figure 1-5. Structure of LDs. LDs contain a neutral lipid core comprised of TG and a small amount of CE. The hydrophobic core is surrounded by a monolayer of amphipathic lipid, mainly PL, and a small amount of free cholesterol. LD-associated proteins on the surface of the LDs play critical roles in LD metabolism. Figure adapted from (Grundy, 1990).

cytoskeleton organization, protein degradation, etc. Numerous reviews have been published recently on this topic (Brasaemle, 2007; Fujimoto et al., 2008; Goodman, 2008; Martin and Parton, 2006; Murphy et al., 2009; Ohsaki et al., 2009; Olofsson et al., 2009; Walther and Farese, 2009).

1.3.1 LD associated proteins

Like traditional organelles, LDs also contain specific associated proteins. However, the LD has a unique structure; in contrast to the bilayer membrane found in most organelles, the LD surface is comprised of a single layer of PL with the hydrophobic acyl-chains of FA dissolved in the TG-rich core and the hydrophilic head groups facing the aqueous environment in the cytosol. As a consequence, proteins associated with LDs are either embedded into the phospholipid monolayer with hydrophobic anchors (such as perilipin and ADRP), or associate electrostatically with the head groups or with hydrophobically anchored proteins (Wolins et al., 2006a).

1.3.1.1 PAT family proteins

The first discovery of LD-associated proteins traces back to 1991 to the laboratory of C. Londos, where they found perilipin on LDs in adipocytes (Greenberg et al., 1991). Subsequently, four other proteins with sequence similarities were discovered and classified as the PAT (Perilipin, Adipophilin, TIP47) family of LD proteins (Lu et al., 2001). Five members of PAT proteins have been identified in vertebrates to date which include perilipin, adipophilin (also known as Adipose

Differentiation-Related Protein, ADRP), TIP47 (for Tail-Interacting Protein of 47 kDa), S3-12 and OXPAT, with an additional two proteins in insects, LSD1 and LSD2 (for Lipid Storage Droplet proteins 1 and 2) (Brasaemle, 2007). Except for S3-12, PAT family members share a ~100 amino acid homologous motif at the N-termini, referred to as the PAT domain (Lu et al., 2001).

1.3.1.1.1 Perilipin and adipophilin/ADRP – the constitutively TG-associated PAT proteins

At least three isoforms of perilipin proteins exist in mice and humans (perilipin A, B and C) generated from alternative splicing from a single gene. The most abundant isoform, perilipin A, is predominantly present in adipocytes (Bickel et al., 2009; Brasaemle, 2007). Under physiological conditions, it is constitutively associated with LDs through a central hydrophobic region, which may anchor this protein to the hydrophobic core of LDs (Bickel et al., 2009). Excessive perilipin that does not bind to LDs is rapidly degraded (Brasaemle et al., 1997). ADRP is another constitutively TG-associated PAT protein (CPAT) (Wolins et al., 2006a) extensively expressed in many tissues other than adipocytes (Heid et al., 1998). Non-LD-associated ADRP has been shown to be degraded via the ubiquitin / proteasome pathway (Xu et al., 2005).

Numerous functional studies have depicted that PAT proteins regulate dynamics of neutral lipid storage and breakdown. In adipocytes, perilipin A plays a central regulating role in basal and stimulated lipolysis by interacting with lipases and CGI-58 under different phosphorylation states (see **section 1.2.4** for

details). The perilipins are the only known PAT proteins subjected to acute regulation by phosphorylation (Bickel et al., 2009). In many tissues other than adipose, ADRP seems to play a similar role as perilipin in protecting LDs from lipolysis. Overexpression of ADRP leads to increased intracellular TG stores in cultured cells, similar to overexpression of perilipin (Fukushima et al., 2005; Gao and Serrero, 1999; Imamura et al., 2002). ADRP knockout mice also showed reduced hepatic TG accumulation and attenuated hepatic steatosis in response to a high-fat diet (Chang et al., 2006). These phenomena may be due at least partially to reduced TG lipolysis since exogenous expression of ADRP in HEK293 cells led to reduced localization of the major TG lipase, ATGL, to LDs (Listenberger et al., 2007). However, evidence has also shown that ADRP is not functionally identical to perilipin in regard to the regulation of lipolysis. In perilipin-null mice, basal lipolysis is increased in spite of the presence of ADRP on LDs (Martinez-Botas et al., 2000; Tansey et al., 2001), suggesting that ADRP is less effective in protecting LDs from lipase attack. Ectopic expression of perilipin A in fibroblasts (in which the major CPAT is ADRP) have shown that perilipin A out-competed ADRP for LD binding (Souza et al., 2002; Tansey et al., 2003), suggesting that perilipin is a more robust LD shield with a stronger binding affinity.

1.3.1.1.2 TIP47 and the exchangeable TG-associated PAT proteins

The other three PAT proteins, TIP47, S3-12 and OXPAT, are referred to as exchangeable TG-associated PAT proteins (EPAT) (Wolins et al., 2006a). They are dispersed in the cytosol under lipid-poor conditions, and translocate to LDs

during rapid TG synthesis (see below). TIP47 was the first reported EPAT and was identified by sequence similarity to perilipin and ADRP (Wolins et al., 2001). It was demonstrated that in HeLa cells (Wolins et al., 2001) and 3T3-L1 adipocytes (Wolins et al., 2005), as well as in the liver (Wolins et al., 2006b), TIP47 was stable in the cytosol under lipid-poor conditions, and translocated onto LDs in response to lipid-loading. More recent research has shown that knockdown of TIP47 resulted in smaller but more numerous LDs in AML12 cells, contrary to the knockdown of ADRP which yielded no change in LD number or size (Bell et al., 2008). Interestingly, the combined knockdown of TIP47 and ADRP led to larger and fewer LDs, accompanied with elevated lipolysis, increased ATGL and CGI-58 at LD surface, and compromised insulin signaling (Bell et al., 2008). Functional roles of other EPATs, S3-12 and OXPAT, are less well known. However, studies on different EPATs, especially the ones addressing S3-12, have led to the understanding of fat packaging as a dynamic process (Wolins et al., 2005; Wolins et al., 2003). Under basal conditions, LDs in 3T3-L1 adipocytes were predominantly large, centrally localized and coated with perilipin. When cells were incubated with long-chain FA, small, peripherally localized LDs emerged rapidly, with TIP47, S3-12 or ADRP coating the surfaces, distinct from the pre-existing, perilipin-coated LDs (Wolins et al., 2005). These newly formed small LDs eventually differentiated into different subpopulations bearing different coat proteins, with TIP47 and S3-12 concentrated on the smallest LDs, ADRP concentrated on intermediate-sized LDs, and perilipin concentrated on the largest LDs. Based on these observations, it was proposed (Wolins et al., 2006a; Wolins

et al., 2005) that EPATs represent a pre-existing reservoir of LD-coat proteins that package newly synthesized TG into nascent LDs for delivery into the storage LDs. CPATs, on the other hand, are believed to coat the storage LDs and are responsible for regulating lipase access. It is worth mentioning, however, that these observations have been made mainly in adipocytes. Evidence for these processes in other tissues such as the liver (which is the focus of this thesis) is scarce.

1.3.1.2 Other LD associated proteins and the implications

Since the discovery of PAT family proteins, a long list of LD-associated proteins were subsequently identified individually or by proteomics approaches (Bartz et al., 2007; Brasaemle et al., 2004; Fujimoto et al., 2004; Liu et al., 2004; Ozeki et al., 2005; Sato et al., 2006; Turro et al., 2006). In addition to PAT proteins, a few categories of proteins have been found repeatedly in proteomics studies of purified LDs by different groups.

ER resident proteins (such as calnexin, protein disulphide isomerase) have been reported in essentially all these proteomics efforts. Since the prevailing hypothesis for LD formation proposes that LDs originate from the ER and possibly remain associated with the ER during maturation (see **section 1.3.2**), it is not surprising to find ER resident proteins on LDs. It has been observed by electron microscopy in a variety of cell types that LDs are often tightly associated or embraced by sheets of the ER membrane (Blanchette-Mackie et al., 1995; Cushman, 1970). Some key enzymes in lipid synthesis machinery have been

located at the ER membrane, such as phospholipase D1 (Andersson et al., 2006; Marchesan et al., 2003) and DGATs (see **section 1.2.3**), consistent with the hypothesis that LDs are generated at the ER where lipid biosynthesis takes place.

Enzymes involved in lipid metabolism, such as ATGL, HSL, acyl-CoA synthetases, were also frequently found on LDs, suggesting that TG and potentially some other lipids are synthesized locally on LDs. This point has been recently well addressed in COS-7 cells, where DGAT2 was localized to areas where ER and LDs were tightly associated under conditions when rapid TG synthesis takes place (Kuerschner et al., 2008).

Initially surprising, proteins involved in vesicular transport or membrane trafficking (such as Arf1, multiple Rab GTPases, and COPI components), as well as cytoskeleton components that are closely related to organelle motility (such as tubulin and dynein), were also frequently identified on purified LDs. The findings led to the fresh perspective that LDs are motile organelles and may extensively interact with other organelles (see **section 1.3.3** for details).

Another class of proteins repeatedly found on LDs is the caveolin family. Caveolins are integral membrane proteins that are major components of caveolae, the cholesterol-rich invaginations at the plasma membrane (Parton and Simons, 2007). The adipose tissue is especially enriched in caveolae, indicating caveolae and caveolins may contribute to specialized roles of adipose tissue in lipid metabolism. Caveolin-1 and caveolin-2 have demonstrated regulated association with LDs in cell culture and during liver regeneration (Fernandez et al., 2006; Fujimoto et al., 2001; Pol et al., 2004) and can be internalized in response to

excessive FA or cholesterol (Le Lay et al., 2006; Pol et al., 2005). Caveolin-1 knockout mice exhibited lean phenotype, with decreased LD accumulation in hepatocytes and mouse embryonic fibroblasts over-expressing perilipin (Cohen et al., 2004; Fernandez et al., 2006). These phenomena depicted a role for caveolins in regulating lipid transport and facilitating LD formation. On the other hand, caveolin-1 was also found to associate with PKA and is required to maintain the interaction of PKA and perilipin (Cohen et al., 2004; Razani and Lisanti, 2001; Razani et al., 1999), indicating that caveolin-1 may also play a role in stimulated lipolysis by facilitating phosphorylation of perilipin A.

1.3.2 Formation and growth of LDs

It is generally believed that LD biogenesis in eukaryotes initiates from the ER where TG biosynthesis takes place. It has been proposed that newly synthesized TG accumulates between the two leaflets of the ER bilayer, forming a lens-like structure, which will further separate from the ER and form an independent nascent LD through budding or “hatching” (Fujimoto et al., 2008; Murphy and Vance, 1999). However, little is known about the mechanism by which nascent LDs accrue additional TG and grow in size after nascent formation. Some studies suggest that LDs remain in contact with the ER, while other reports argue that LDs likely pinch off from the ER and become independent structures (Brasaemle, 2007; Walther and Farese, 2009). It was recently reported that in COS7 cells and adipocytes DGAT2 was present in close proximity with LDs suggesting that TG

may be transferred into the LD via a tight ER-LD association (Kuerschner et al., 2008).

Walther and Farese in their recent review (Walther and Farese, 2009) proposed a few possibilities for LD maturation based on recent advances in the field. The first and simplest is that LDs remain attached to the ER after nascent formation so that lipids could enter LDs from the ER bilayer simply by lateral diffusion. The second possibility is that LDs accrue additional lipids after they detach from the ER. Many studies have found resident ER proteins (in certain instances even transmembrane proteins) in LD preparations, which would support the first hypothesis. Confocal microscopy studies in yeast have claimed that 92-97% of LDs could not be resolved from the ER (Szymanski et al., 2007). However, evidence has also shown that LDs travel long distances along microtubules (Bostrom et al., 2005; Welte et al., 1998) and undergo dynamic remodeling (Brasaemle et al., 2004; Marcinkiewicz et al., 2006; Yamaguchi et al., 2007), supporting the possibility that LDs may detach from the ER under certain conditions. If this were the case, lipids would either be synthesized locally on the surface of LDs, or a transfer protein would be required, otherwise LDs would have to grow in size by fusion. However, no such cytosolic lipid transfer protein has been identified so far.

Homotypic fusion events between LDs have been observed by time-lapse microscopy in oleic acid (OA) treated NIH 3T3 cells (Bostrom et al., 2005). However, the observation could not exclude the possibility that the LDs that underwent fusion separate again (fission) immediately after the observed fusion.

The most convincing evidence to support fusion has been recently reported by Bostrom et al. (Bostrom et al., 2007). By knocking down the SNAREs (SNAP23, syntaxin-5, VAMP4), proteins that mediate membrane fusion (Jahn and Scheller, 2006), it was shown that SNAREs are essential for LD fusion and growth in NIH 3T3 cells. The fusion did not seem to be regulated by TG synthesis. The current proposed mechanisms for LD formation and growth are summarized in **Figure 1-6**.

1.3.3 Organelle connection and motility of LDs

TG metabolism involves multiple organelles (Murphy et al., 2009). For example, FA mobilized from TG needs to undergo β -oxidation in mitochondria or peroxisomes to provide energy. TG is primarily synthesized in the ER and stored in the LDs. A few recent studies also reported that LDs are associated with autophagic components during nutrient deprivation (Ohsaki et al., 2006; Singh et al., 2009). The functional links point to an enticing hypothesis that LD, as a central organelle regulating neutral lipid metabolism, may interact with other organelles in order to efficiently share the metabolites (Murphy et al., 2009).

Many organelles that contribute to TG metabolism are found in close apposition to LDs by microscopic studies, including the ER (Ozeki et al., 2005; Turro et al., 2006), mitochondria (Sturmeijer et al., 2006), endosomes (Liu et al., 2007), and peroxisomes (Binns et al., 2006; Schrader, 2001). It is proposed that interaction of LDs with the ER is through a structure called membrane contact site (Levine, 2004; Levine and Loewen, 2006), referring to specific regions of an

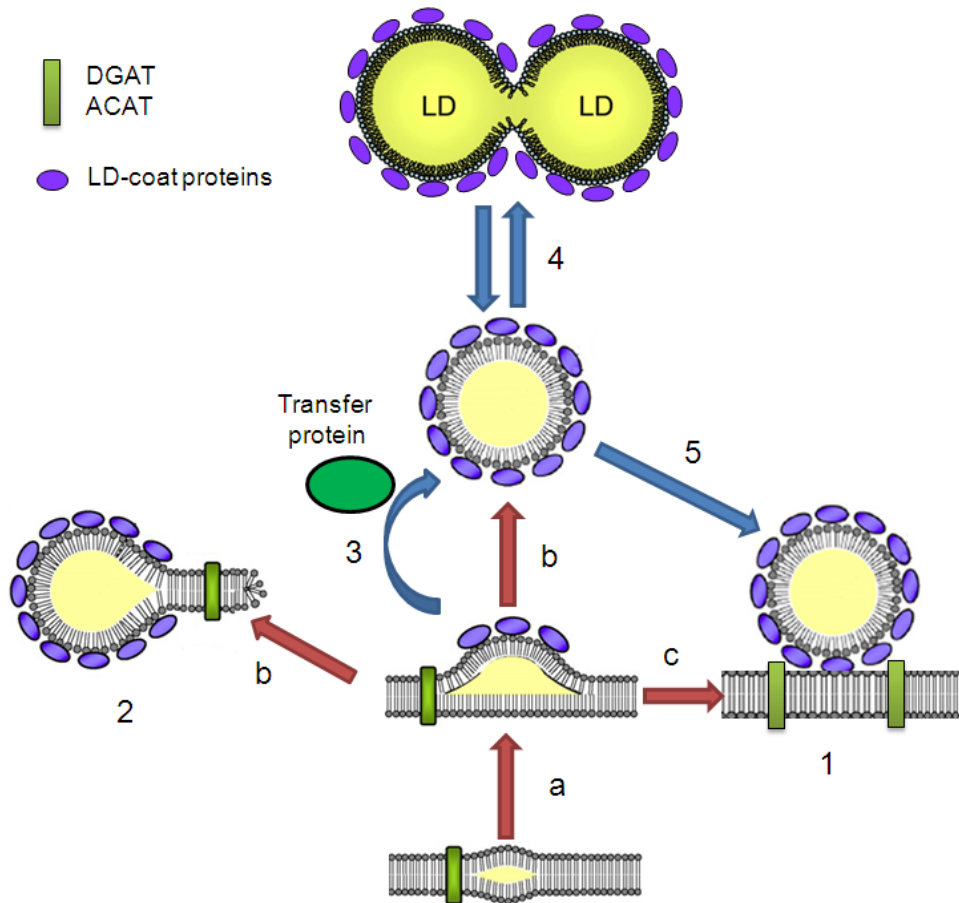


Figure 1-6. Proposed mechanisms for CLD formation and growth. Neutral lipid synthesis occurs on the ER by acyltransferases (DGAT, ACAT). Newly synthesized lipids accumulate between ER bilayer, forming a lens-like structure. This structure can recruit LD-coat proteins and grow in size by obtaining more lipids (a). The newly formed CLDs either separate from the ER through “budding” or “hatching” (b), or remain attached to the ER (c). A few mechanisms have been proposed for CLD growth. CLDs could obtain additional lipids from the ER directly if they remain attached (1). Alternatively, lipids can be synthesized locally by enzymes attached to the CLDs (2). A lipid transfer protein could also be involved to transfer lipid between the ER and independent CLDs (3). CLDs were also proposed to grow in size by homotypic fusion (4). CLDs that are already detached from the ER could also dock back to access the lipid synthesis mechanism (5).

organelle involved in budding or fusion in vesicular trafficking. Membrane contact site may allow transfer of lipid and proteins between organelles. Such a structure is commonly described for many organelles. However, LDs are organelles of unique structure in that the contents of LDs are surrounded by monolayer of PL, unlike all other organelles or vesicles that contain two leaflets of PL. It is not clear how such distinctive structures would interact with bilayer-containing organelles. Murphy et al. proposed that LDs can associate with other bilayer organelles through a mechanism called “hemifusion”, involving formation of a “stalk” between the LD monolayer and the outer leaflet of the target organelle (Murphy et al., 2009). The hemifusion mechanism has been employed to describe the intimate connection between LDs and peroxisomes observed in yeast (Binns et al., 2006). Proteins involved in hemifusion are largely unknown. It would be interesting to investigate the role of SNAREs, proteins proposed to mediate homotypic fusion between LDs (Bostrom et al., 2007), in this process.

LDs are motile organelles. It has been observed that insulin stimulation promotes LD formation via the activation of phospholipase D 1 and ERK2 (Extracellular signal-Related Kinase 2) (Andersson et al., 2006), which in turn phosphorylates the motor protein dynein. The activated dynein then targets to LDs and facilitates the transport of LDs along microtubules. It was proposed that LD fusion and growth is dependent on the integrity of the microtubule-mediated transport (Andersson et al., 2006; Bostrom et al., 2005).

Rab GTPases, proteins mediating vesicle motility, docking and fusion to target membranes were identified as LD-associated proteins (see **section 1.3.1.2**). Some of the Rab family members, especially Rab18 (Martin et al., 2005; Ozeki et al., 2005), were recently speculated to facilitate links between LDs and other organelles (Bostrom et al., 2007; Murphy et al., 2009; Walther and Farese, 2009). In response to lipolytic stimulation, Rab18 in adipocytes was found to be recruited to a subpopulation of LDs that are closely associated with the ER (Martin et al., 2005), suggesting that Rab18 may function as a “molecular switch” to induce LD-ER association and facilitate transfer of FA or neutral lipids between LDs and the ER (Martin and Parton, 2006).

Another type of GTPase, Arf1, has also been identified on LDs during proteomics studies (Bartz et al., 2007). Knockdown of Arf1-COPI machinery in *Drosophila* cells led to larger and more dispersed LDs and a defect in lipolysis (Guo et al., 2008), as well as increased lipid storage (Beller et al., 2008). Arf1-COPI has been known to mediate vesicular transport from Golgi to the ER. It was proposed that this machinery may also function on the surface of LDs, returning LD membrane and coat proteins to the ER (Beller et al., 2008). An alternative hypothesis proposed that Arf1-COPI may mediate the budding of smaller LDs and increase surface area for lipolysis (Walther and Farese, 2009). Nonetheless, accumulating evidence started to support the attractive possibility that traditional vesicular trafficking and LD biogenesis may share some common machineries (Wolins et al., 2006a).

1.4 Hepatic LDs and VLDL assembly

Liver is a specialized organ for mobilizing and secreting TG into the blood as VLDL particles, in addition to its critical roles in TG synthesis and ketogenesis. VLDL is the precursor of low-density lipoprotein (LDL). Elevated plasma VLDL and LDL are risk factors for cardiovascular disease and atherosclerosis. Surprisingly, however, relatively little is known about TG storage and mobilization in this organ, compared to our knowledge of adipose tissue. Three sources of FA contribute to the hepatic TG storage pool: *de novo* synthesis, plasma FA mobilized from the adipose tissue, and the uptake of lipoprotein remnants (Gibbons et al., 2000). In humans, the majority (~77%) of VLDL-TG is derived from FA released from the adipose tissue under fasted conditions (Barrows and Parks, 2006). Even under fed conditions, *de novo* hepatic lipogenesis contributes to only a small amount (~8%) of VLDL-TG (Barrows and Parks, 2006; Gibbons et al., 2000). Several lines of evidence have indicated that FAs incorporated into VLDL-TG first enter LDs before being utilized through a lipolysis/reesterification process (Gibbons et al., 1992; Gibbons et al., 2000).

1.4.1 LDs in the liver

1.4.1.1 Cytosolic LDs

Liver has a great capacity to store TG, mainly in the cytosolic LDs (CLDs) of hepatocytes. Very little is understood about the biology of hepatic LDs compared to LDs in the adipocytes. Very few studies investigating protein components on hepatic LDs have been performed, two of which are proteomics studies in

hepatocytes (Turro et al., 2006) and in the HuH7 hepatoma cell line (Fujimoto et al., 2004). Available information revealed that, although having simpler compositions than the adipose LDs, hepatic LDs seem to contain numerous common components found in adipocytes and other cell types, such as ER resident proteins, Rab GTPases and cytoskeleton components, indicating LDs in both cell types, and likely other cell types as well, share some similar regulation. However, and importantly, LDs in liver cells also contain proteins different from those found in adipocytes. The most distinct difference is that instead of perilipin, ADRP is the only CPAT in hepatocytes (see **section 1.3.1**). Interestingly, major lipases regulated by perilipin in adipocytes, ATGL and HSL, are poorly represented in the liver.

Hepatic CLDs have been strongly implicated in VLDL formation (Gibbons et al., 2000; Olofsson et al., 2009; Wiggins and Gibbons, 1992). It was recently reported that increased ADRP expression led to elevated neutral lipid storage and reduced entry of lipids into secretory pathways (Magnusson et al., 2006). In contrast, treatments promoting LD fusion caused decreased VLDL secretion and increased CLD number (Li et al., 2006).

1.4.1.2 Luminal apoB-free LDs

In addition to CLDs, hepatocytes (as well as enterocytes which also produce apoB-containing lipoproteins) contain at least two more types of LDs in the lumen of secretory pathway where VLDL is assembled: the luminal apoB-free lipid droplets (LLDs) and the apoB-containing particles (VLDL and its precursors).

The existence of LLDs was first observed by immuno-gold electron microscopy, where they were identified as VLDL-sized particles in the smooth ER lacking immuno-detectable apoB (Alexander et al., 1976). Subsequently, CM-sized particles were detected in the ER of enterocytes lacking apoB expression, further supporting this observation (Hamilton et al., 1998). LLDs have been proposed to provide TG source for the bulk lipidation of VLDL assembly (see below), however, this notion remains speculative. Few advances have been made to increase our knowledge of this matter since 1998, despite intensive research and advances made on VLDL assembly during the past decade. Characterization of LLDs is necessary and will be one of the main subjects of this thesis.

1.4.2 Mechanisms for VLDL assembly

1.4.2.1 Composition of VLDL particles

VLDL is a class of lipoproteins present in the circulation. Like other types of LDs, a VLDL particle is composed of a neutral lipid core surrounded by a monolayer of amphipathic PL and free cholesterol. Compared to other lipoproteins (except for CM), VLDL is larger in size and has a higher lipid-to-protein ratio, with diameters ranging from 30 to 80 nm (Shelness and Sellers, 2001), and contains over 90% lipids. The core of VLDL is rich in TG, which comprises over 50% of VLDL lipids. PL comprises 19-21% of VLDL lipids, over 60% of which is phosphatidylcholine (PC) (Jonas, 2002).

Proteins associated with lipoproteins are referred to as apolipoproteins generally divided into two types, the non-exchangeable and the exchangeable. In

VLDL, the constitutive, non-exchangeable apolipoprotein is apoB. Each VLDL particle has one, and only one, copy of apoB (Elovson et al., 1988). VLDL also contains some exchangeable apolipoproteins such as apoE and apoA-I, which can transfer between lipoprotein particles in circulation.

ApoB is essential for VLDL assembly in the liver (as well as CM in the intestine). It is a large amphipathic protein that comprises the major structural protein of VLDL. Two forms of apoB exist in the circulation, derived from differential RNA editing of the same gene (Chen et al., 1987; Powell et al., 1987). The larger form, apoB100, corresponds to the full-length protein, while the smaller form, apoB48, corresponds to the N-terminal 48% of the gene product. In humans, apoB100 (4536 amino acid residues) is the only form expressed in the liver while apoB48 (2152 residues) is expressed in the intestine. In some rodents (mice and rats), however, both forms exist in the liver and both can be assembled into VLDL particles and secreted.

1.4.2.2 Two-step model of VLDL assembly

Most of the current models of hepatic VLDL assembly describe a “two-step” process (Alexander et al., 1976; Fisher and Ginsberg, 2002; Gordon and Jamil, 2000; Olofsson et al., 2000; Rustaeus et al., 1995; Shelness and Sellers, 2001) (**Figure 1-7**). The first step involves the formation of a small, partially lipidated apoB-containing VLDL precursor particle in the lumen of the ER. While apoB is being synthesized by the ribosomes attached to the surface of the rough ER, the nascent polypeptide translocates to the lumen of the ER through a channel in the

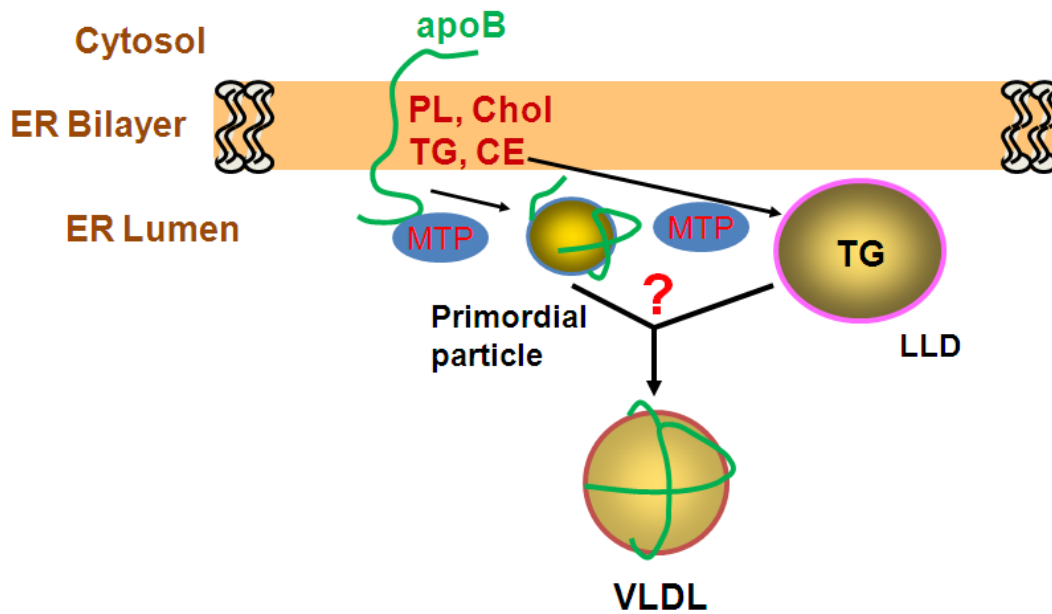


Figure 1-7. Two-step model for VLDL assembly. VLDL assembly initiates from the cotranslational translocation of apoB. During the first step, small amounts of lipids are added to nascent apoB to form the HDL-sized primordial particle. In the second step, the bulk of lipids are added to the primordial particle to form large, mature VLDL. An apoB-free LLD is proposed to combine with the primordial particle and provides the bulk TG. It is not clear whether a fusion event takes place. Microsomal triglyceride transfer protein (MTP) is proposed to mediate lipid transfer to the primordial particle and the formation of the LLD.

ER membrane. Chaperones such as heat shock protein 70 (hsp70) are required to facilitate proper folding of apoB (Fisher and Ginsberg, 2002). During the translocation, small amounts of lipids (TG, PL and cholesterol) are added to the growing apoB polypeptide, forming a small, dense primordial particle referred to as pre-VLDL (Olofsson and Boren, 2005). The existence of pre-VLDL has been immunodetected by electron microscopy. It was found that apoB positive particles smaller than VLDL were present in the rough ER, while apoB-containing, VLDL-sized particles were located in smooth termini of the rough ER and the Golgi (Alexander et al., 1976), providing the foundation for the two-step model of VLDL assembly.

During the second step of VLDL assembly, the bulk of TG is transferred to the precursor particles to form larger, fully lipidated VLDL particles. The source of TG for the second-step lipidation of apoB is believed to be preformed intracellular LDs. Since VLDL is assembled in the lumen of the secretory pathway, the pool of stored TG for the provision of VLDL-TG substrates most likely resides in the lumen of these organelles, where the LLDs were found (Hamilton et al., 1998; Kulinski et al., 2002).

1.4.2.3 Location of the second-step lipidation

While the initial formation of the VLDL precursor particles in the ER is well accepted, the identity of the compartment involved in the second step bulk lipidation has remained controversial. It was first proposed by electron microscopy studies that mature VLDL-sized apoB-containing particles are present

in the ER and that the primordial particle must diffuse laterally from the rough ER to smooth ER to acquire the bulk TG (Alexander et al., 1976; Hamilton et al., 1998). This theory has later been supported by pulse-chase studies in McA cells by interrupting vesicular transport. It was found that when OA-induced apoB-containing particles were trapped in the ER, cells retain the ability to produce mature VLDL, while when these particles were trapped in the Golgi, mature VLDL was no longer formed in response to OA-treatment (Yamaguchi et al., 2003). VLDL sized particles were also directly recovered from purified ER fractions (Rusinol et al., 1993). Recently, Cideb, a protein associated with hepatic LDs and the smooth ER, was found to mediate VLDL lipidation and maturation by interacting with apoB (Ye et al., 2009). These studies provide compelling evidence for the “ER lipidation” theory. However, the model has been challenged by several studies which suggest post ER / Golgi lipidation (Bamberger and Lane, 1990; Gusarova et al., 2003; Valyi-Nagy et al., 2002), mostly through kinetic studies and by comparing lipid compositions of particles isolated from different subcellular compartments. It was suggested that there is a 15 minute delay in apoB100 secretion compared to TG secretion (Adiels et al., 2005). Studies from Olofsson’s group demonstrated that the maturation of VLDL was dependent on the Golgi-localized Arf1 GTPase activity and involves the activation of phospholipase D (Asp et al., 2000; Rustaeus et al., 1995), suggesting VLDL maturation may happen in the post-ER compartment. However, the presence of apoB-free LLDs in the Golgi has never been demonstrated by electron microscopy.

1.4.3 Regulation of VLDL assembly – availability of lipids

ApoB is normally continuously synthesized in hepatocytes and is considered in excess. The major factor limiting the rate of VLDL assembly is the availability of lipids (Dixon and Ginsberg, 1993), mainly TG and PL. Insufficient lipid supply will lead to the degradation of excess apoB (see **section 1.4.3.2**) and compromised VLDL secretion (Davidson and Shelness, 2000).

1.4.3.1 TG and PL synthesis for VLDL secretion

It is commonly accepted that supplementing cells with FA such as OA stimulates TG and PL synthesis and boosts VLDL and apoB secretion (Vance, 2002). In contrast, inhibition of TG synthesis blocks OA-induced secretion (Vance, 2002). Enzymes catalyzing lipid synthesis have been implicated in modulating apoB assembly and secretion. The rate limiting enzymes for the synthesis of TG, which comprises over 50% of VLDL lipids, are DGAT1 and DGAT2, discussed in **section 1.2.3.2**. It is not yet certain, which form of DGAT contributes to VLDL secretion. Although a few studies involved in DGAT1 overexpression suggested a role of DGAT1 in VLDL secretion (**section 1.2.3.2**), data obtained from knockout mice seem to suggest DGAT2 plays a more prominent role in this process (Smith et al., 2000; Stone et al., 2004). This observation was supported by Rader's group who recently reported that knockdown of DGAT2 expression in both wild type and DGAT1 deficient mice resulted in decreased apoB and TG secretion, suggesting that DGAT2 is the isoform responsible for synthesizing TG targeted for secretion (Liu et al., 2008).

The availability of PL was also found to be critical for VLDL secretion, especially PC (Vance, 2008), which comprises the majority of PL on the surface monolayer of VLDL particles (Agren et al., 2005). In the liver, PC is synthesized via two major pathways. About 70% of hepatic PC synthesis comes from the glycerol-3-phosphate pathway where PC synthesis occurs through the transfer of CDP-choline and the rest (30%) is synthesized by the phosphatidylethanolamine N-methyltransferase (PEMT) pathway that involves tri-methylation of phosphatidylethanolamine (PE) (Vance, 2008). The rate-limiting enzymes for these two pathways are CTP: phosphocholine cytidyltransferase (CT) and PEMT, respectively. Studies using PEMT knockout mice and liver-specific CT α (the major form of CT in the liver) knockout mice have demonstrated that both enzymes are required for normal VLDL secretion (Jacobs et al., 2004; Jacobs et al., 2008; Noga et al., 2003; Noga et al., 2002). However, PEMT deficiency led to compromised VLDL secretion despite the normal hepatic PC level (Noga et al., 2002; Walkey et al., 1997) while liver-specific CT α deficiency affected both hepatic- and VLDL- PC levels (Jacobs et al., 2004).

It is controversial as to whether CE synthesis plays a regulatory role in VLDL assembly and secretion. CE is a relatively minor component of VLDL core lipid (5-15%). Two major enzymes control the final step of CE synthesis in mice, ACAT1 and ACAT2. ACAT2 is the predominant form in mouse liver and intestine (Buhman et al., 2000), and has been implicated in production of CE for VLDL and CM secretion. Although ACAT2-null mice retained the ability to secrete apoB, the secreted VLDL particles were of a much smaller particle size

(Buhman et al., 2000), indicating a role of ACAT2 in assembling large, mature VLDL. However, ACAT1 rather than ACAT2 seems to be the predominant ACAT isoform in human liver (Chang et al., 2000); the physiological relevance of ACAT in lipoprotein assembly in humans has yet to be elucidated.

1.4.3.2 Provision of lipids by MTP

Microsomal triglyceride transfer protein (MTP) is a 97 kDa protein implicated to play a major role in provision of lipids for VLDL and apoB secretion. It is confined to the lumen of the ER and possibly the Golgi (Levy et al., 2002; Swift et al., 2003; Wetterau and Zilversmit, 1984; Wetterau and Zilversmit, 1986). MTP forms an obligatory heterodimer with the ER chaperone protein disulfide isomerase (PDI) (Wetterau et al., 1991b). MTP has been shown to physically bind to apoB and was proposed to transfer lipids from the ER membrane or other donor sites to nascent apoB polypeptides (Patel and Grundy, 1996; Wu et al., 1996).

The critical role of MTP during apoB secretion has been well supported by abundant experimental evidence. In liver-specific MTP knockout mice, plasma apoB100 levels were reduced over 90% while the levels of apoB48 were largely unaffected (Raabe et al., 1999). The difference between apoB100 and apoB48 secretion was because apoB100 requires full lipidation to be secreted while apoB48 can be secreted in small, partially lipidated particles. Hepatocytes isolated from these mice contained very few VLDL-sized particles in the secretory compartments, accompanied with cytosolic LD accumulation, indicating that transfer of lipids into the lumen requires MTP (Raabe et al., 1999). On the other

hand, adenoviral introduction of MTP into mouse livers led to increased apoB and TG secretion (Tietge et al., 1999). It has been clearly demonstrated that MTP mediates lipid transfer to the nascent apoB and regulates the first-step lipidation of apoB. Inhibition of MTP activity mimics the effect of insufficient lipid, targeting apoB for proteasomal degradation (Gordon and Jamil, 2000). It is controversial, however, whether or not MTP contributes to the second-step bulk lipidation (Gordon and Jamil, 2000). MTP is required for the formation of LLDs. Generation of LLDs was greatly diminished in liver-specific MTP knockout mice (Raabe et al., 1999) and in hepatocytes treated with MTP inhibitors (Kulinski et al., 2002; Wang et al., 1999).

1.4.3.3 ApoB100 secretion is regulated by degradation

The fate of apoB, especially apoB100, is tightly regulated by the availability of lipids. Earlier studies in HepG2 cells and rat hepatocytes have indicated that a considerable amount of nascent apoB is degraded intracellularly (Borchardt and Davis, 1987; Bostrom et al., 1986). Multiple mechanisms have been found to contribute to apoB degradation co-translationally or post-translationally (Ginsberg and Fisher, 2009). Under the conditions when lipids are limited or when MTP activity is low, apoB undergoes a retrograde translocation from the ER lumen to the cytosol, exposing the loop-like sequences, which are subsequently ubiquitinated and targeted for proteasomal degradation (Ginsberg and Fisher, 2009; Olofsson and Boren, 2005; Shelness and Sellers, 2001). This process is

referred to as ER-associated degradation and requires interaction with cytosolic chaperone proteins, such as Hsp70 and Hsp 90 (Ginsberg and Fisher, 2009).

ApoB can also undergo ER-associated degradation after the completion of translation and translocation of the full protein. It has been estimated that over 50% of apoB is degraded post-translationally via a mechanism independent of proteasomes (Ginsberg and Fisher, 2009). It is believed that an ER protease, ER-60, may be involved in this process (Avramoglu and Adeli, 2004). Some studies also suggest that proteasomal degradation may also contribute to the degradation of full-length apoB protein, presumably when the protein is misfolded in a under-lipidated, aberrant particle (Davidson and Shelness, 2000).

It is worth mentioning that post-ER machinery was also proposed to contribute to apoB degradation. This pathway does not seem to be regulated by availability of lipids (Ginsberg and Fisher, 2009).

1.4.3.4 Mobilization of TG stores for VLDL assembly – lipolysis and reesterification

Although LLDs have been implicated in the bulk lipidation of apoB-containing primordial particles during the second step of VLDL assembly, the mechanisms by which the lipids from LLDs are transferred remain speculative. Some models of VLDL assembly suggest “fusion” between the LLDs and the primordial pre-VLDL particles (Alexander et al., 1976; Shelness and Sellers, 2001). However, the occurrence of any fusion between the partially lipidated apoB particles and LLDs has never been experimentally demonstrated. Another possible mechanism

may involve an indirect transfer of lipids from LLDs to the primordial pre-VLDL particle through a series of enzymatic events. Metabolic labeling of preformed lipids have demonstrated that up to 70% of TG in VLDL is derived from hydrolysis and reesterification of preformed TG stores (Lankester et al., 1998; Wiggins and Gibbons, 1992; Yang et al., 1996). It appears that the FAs used for VLDL secretion mainly come from lipolysis of intracellular storage TG, while that used for oxidation and ketogenesis are derived from extracellular FA (Gibbons et al., 2000). The process of lipolysis-reesterification is illustrated in **Figure 1-8**.

A question raised by the lipolysis-reesterification model is the identity of the lipase responsible for the mobilization of storage TG. Compared to our knowledge on lipases in adipose tissue, little is known about lipases in the liver. The major lipases responsible for TG mobilization from adipocytes, ATGL and HSL, are essentially absent in the liver. It is also unlikely that a cytosol-localized lipase would be involved in the provision of substrates for VLDL assembly based on studies by Pease et al. (Pease et al., 1999) who reported that FA released from CLDs by overexpression of HSL were directed for mitochondrial oxidation but not for VLDL assembly. A recent study also demonstrated that adenovirus-mediated overexpression of ATGL and HSL in the liver led to increased FA oxidation but not apoB and TG secretion (Reid et al., 2008). On the other hand, overexpression of CGI-58 (a co-activator of ATGL) in McA cells led to increased VLDL-TG secretion (Brown et al., 2007; Caviglia et al., 2009). Acidic lipase is also unlikely to contribute to VLDL-TG, since lysosomal acid lipase has been

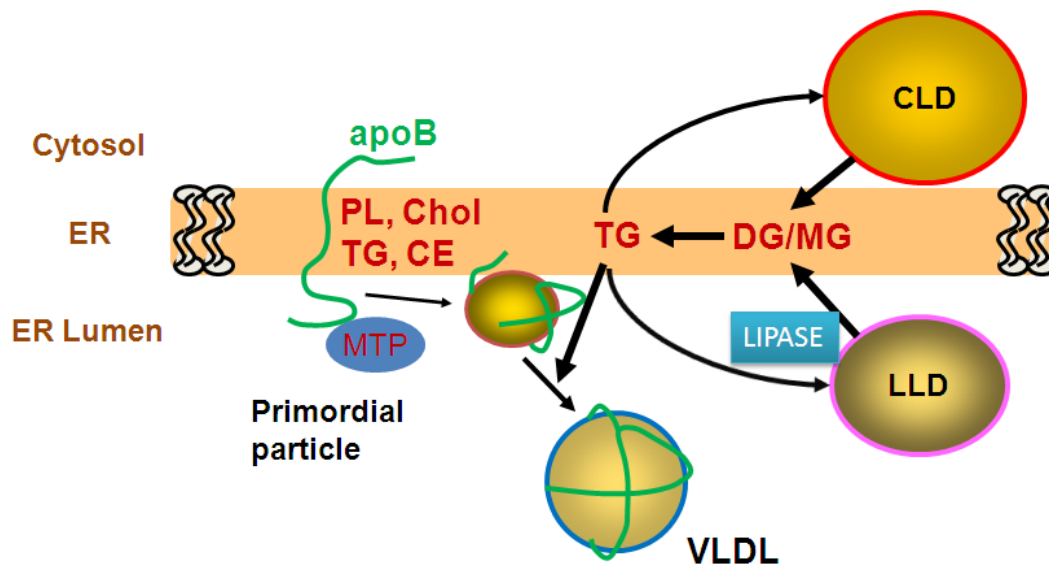


Figure 1-8. Lipolysis and reesterification. During the second step of VLDL assembly, a lipolysis-reesterification process is proposed to mediate the provision of bulk TG. TG stores in either CLD or LLD are mobilized by lumenally localized lipases, the lipolytic products (DG/MG) are then resynthesized into TG and incorporated into the primordial particle to form mature VLDL. Excessive TG can be recycled to the TG storage pool (CLD or LLD) via a futile cycle.

shown to only contribute to the breakdown of endocytosed lipoprotein (LDL) TG, but not the endogenously formed TG (Hilaire et al., 1993; Hilaire et al., 1994). It was proposed that the responsible lipase for VLDL secretion should meet at least the following two conditions: Firstly, it should be a non-lysosomal lipase capable of hydrolyzing TG. Secondly, results from several groups have shown independently that the responsible lipase should be ER-associated in order to properly channel the released FA to the ER for reesterification (Gibbons et al., 2000; Lehner et al., 1999; Pease et al., 1999). Based on these hypotheses, two candidate ER-localized neutral lipases have been identified including triacylglycerol hydrolase (TGH) and arylacetamide deacetylase (AADA) (Gibbons et al., 2000). The role of TGH is the focus of this thesis and will be reviewed below in much detail.

1.5 Triacylglycerol hydrolase

As discussed above, the identity of the lipase responsible for mobilizing storage TG for VLDL secretion has been an enigma. It was a major advance when Lehner and colleagues (Lehner and Verger, 1997) successfully isolated a 60 kDa TG lipase with a neutral pH optimum from porcine liver microsomes in 1997, and named it triacylglycerol hydrolase (TGH). It was demonstrated TGH has lipase activity towards medium- and long- chain TG, but does not hydrolyze PL. Its hydrolytic activity can be inhibited by serine reagents such as diethyl-*p*-nitrophenyl phosphate (E600), suggesting that it is a serine esterase. Shortly after the purification of TGH, cDNAs encoding rat (Lehner and Vance, 1999a), murine

(Dolinsky et al., 2001) and human (Alam et al., 2002a) TGH were successively cloned by our laboratory; biochemistry, cell biology, and physiological roles of this enzyme have been extensively characterized during the past decade [see below and (Dolinsky et al., 2004; Dolinsky et al., 2001; Gilham and Lehner, 2004) for reviews].

1.5.1 TGH belongs to the carboxylesterase gene family

Sequence analysis has shown that TGH belongs to the mammalian carboxylesterase family (E.C. 3.1.1.1) (Dolinsky et al., 2001). The TGH gene in human is also termed carboxylesterase 1 (CES1) and in mouse, carboxylesterase 3 (Ces3). Murine and human TGH proteins share 92% identity at amino acid level and those of rat and human share 93% identity. Mouse TGH has been mapped to chromosome 8 at 8C5 in a cluster of 6 carboxylesterase genes encoding proteins of the carboxylesterase family. Of these, Es22 (also termed egasyn) and Ces1 (also termed Esterase-x or Es-x) are the most closely related to TGH and share 76% identity at the amino acid level. Es-x is expressed in the liver and the intestine and is absent in adipose tissue, while TGH is expressed in all three tissues. Not much is known about the role of Es-x in lipid metabolism except that ectopic expression of Es-x cDNA in McA cells leads to decreased cellular TG accumulation (Ko et al., 2009). However, the role of Es-x in VLDL secretion is not yet clear. To date no other member of these TGH homologues has been shown to hydrolyze lipid substrates or mobilize TG stores from the liver.

1.5.2 Conserved motifs and structure of TGH

Several conserved motifs are present in the primary amino acid sequence of TGH, including N-glycosylation sites (2 in mouse and rat, 1 in human), a putative tyrosine phosphorylation site and seven consensus serine phosphorylation sites for casein kinase II (CK II). However, data from our laboratory have shown that neither insulin nor glucagon induces phosphorylation of TGH or affects TGH activity *in vitro* (Gilham et al., 2005b). The glycosylation state of TGH was also found not to be important for TGH activity *in vitro* (Gilham et al., 2005a).

TGH resides in the lumen of the ER (Gilham et al., 2005a; Lehner et al., 1999; Lehner and Verger, 1997) (**Figure 1-9**). A cleavable N-terminal 18-amino acid signal peptide directs the protein into the ER lumen (Lehner and Verger, 1997). An ER retrieval sequence, HIEL, was identified in the C-terminal of human TGH. Equivalent sequences in mice and rats are HVEL and HAEL, respectively. Interestingly, this sequence is different from the classic ER retrieval sequence, KDEL, and was found to be necessary to properly localize TGH to peripheral ER elements (Gilham et al., 2005a). Deletion of the HIEL motif from exogenously expressed TGH in McA cells led to secretion of TGH into the culture media. More importantly, substitution of HIEL with KDEL directed TGH to a region in the ER that was different from where HIEL-bearing TGH resided (**Figure 1-9**), and this alternate localization was accompanied with impaired TGH-mediated mobilization of intracellular TG. The result suggests that the localization of TGH is important for its intracellular function, likely due to TGH accessibility to LDs.

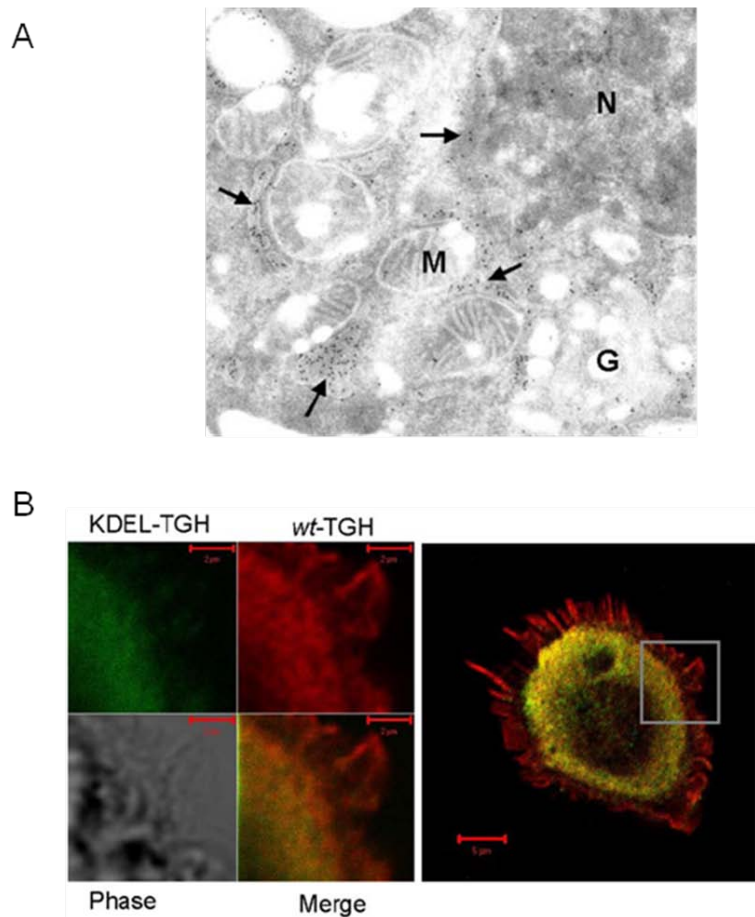


Figure 1-9. Subcellular localization of TGH. (A) Immunogold labeling and electron microscopy of ectopically expressed TGH in McA cells. Arrow, ER structures containing TGH labeling; N, nucleus; M, mitochondria; G, Golgi. TGH is enriched in the ER around mitochondria and nucleus and is absent in the Golgi. (B) McA cells expressing flag-tagged wt-TGH and a myc-tagged TGH mutant with the ER retention signal replaced by KDEL (KDEL-TGH). The subcellular localization of wt and mutant TGH were immunodetected by anti-flag or anti-myc antibodies and visualized by confocal microscopy. Figures adapted from (Gilham et al., *Mol Biol Cell*. 2005).

Several distinct lipase / esterase domains are predicted in TGH structure based on its primary sequence (**Figure 1-10**). The conserved Ser221, Glu353 (354) and His466 (468) in murine (human) TGH are predicted to form the catalytic triad found in all carboxylesterases (Dolinsky et al., 2001; Lehner and Vance, 1999a; Satoh and Hosokawa, 1998). The Ser221 residue is located within the GESAG pentapeptide that matches the GX SXG consensus found in serine esterases and is predicted to be the active site serine. Substitution of any of the catalytic triad residues to Ala abolished the esterase activity of TGH (Alam et al., 2002b). Another conserved region found in the deduced TGH sequence contains a stretch of eight amino acids (414-429) comprising the putative neutral lipid binding domain (NLBD) which has been proposed to facilitate binding of neutral lipids based on similar motifs found in other neutral lipid utilizing enzymes (Alam et al., 2002b). However, site-directed mutagenesis of the conserved residues did not affect TGH activity (Alam et al., 2006), suggesting that an alternative domain might be responsible to mediate neutral lipid binding.

A 3-dimensional model of TGH was predicted based on crystal structure coordinates of acetylcholine esterase and overlapping active sites with pancreatic lipase (Alam et al., 2002b; Dolinsky et al., 2004) (**Figure 1-11**). The protein contains a central catalytic domain located at the bottom of a deep active site cleft, providing a hydrophobic environment for substrates. Near the entrance of the active site cleft, there are several α -helices controlling the access of substrates to the active site. The highly conserved α -helix 1 works as a lid domain and might

Figure 1-10. Conservative domains in TGH amino acid sequence. Alignment of TGH amino acid sequences of mouse, rat, monkey and human is shown. *, identical amino acid residues; \Rightarrow , β sheets; \blacksquare , α helices; \square , highly conserved residues; NLBD, putative neutral lipid binding domain; 1, GXSXG catalytic serine motif; 2, catalytic glutamic acid; 3, catalytic histidine. Figure reproduced from (Dolinsky et al. *Cell Mol Life Sci.* 2004.)

| | | | | | | | | |
|--------|------------|-------------|-------------|------------|-------------|-------------|------------|-----|
| | | | | 1 | 2 | 3 | | |
| mouse | MRLYLPLIWL | LAACAW-GY | PSSPPVNTV | KGKVLGKYVN | LEGFTQPVAV | | 49 | |
| rat | *****V**F | *****-* | ***** | ***** | *****A**** | | 49 | |
| rabbit | *W*CA*ALA* | *****-H | **A****D** | H*****F*S | *****A**** | | 49 | |
| monkey | *W*RA*VLAT | **F***-H | *****D** | H*****F*S | *****A**** | | 49 | |
| human | *W*RAF*LAT | *S*SA**A*H | *****D** | H*****F*S | ***** | | 50 | |
| | | | | 4 | 5 | 1 | | |
| mouse | FLGVFFAKPP | LGSLRFAPPQ | PAEPWSFVKN | TTSYPPMCSQ | DAVGGQVLSE | | 99 | |
| rat | ***I***** | ***** | ***N**** | ***** | ***** | | 99 | |
| rabbit | ***** | ***** | **S**H*** | ***** | ***S*HM*** | | 99 | |
| monkey | ***I***** | **P**T*** | ***** | ***** | ***A**** | | 99 | |
| human | ***I*G**** | **P**T*** | ***** | A*****T* | *PKA**L*** | | 100 | |
| | 1 | Lid | 6 | 7 | 8 | | | |
| mouse | LFTNRKENIP | LQFSEDQLYL | NIYTPADLTK | NSRLPVMVNI | HGGGLVVGGA | | 149 | |
| rat | ***** | ***** | *V***** | ***** | ***** | | 149 | |
| rabbit | ***** | *K***** | ***** | RG***** | *****M**** | | 149 | |
| monkey | ***** | *KL***** | ***** | KN***** | *****A**** | | 149 | |
| human | *****T* | *KL***** | ***** | KN***** | *****M**A* | | 150 | |
| | 2 | | 3 | 10 | 4 | | | |
| mouse | STYDGLALSA | HENVVVVTIQ | YRLGIWFFS | TGDEHSRGNW | GHLDQVAALR | | 199 | |
| rat | *****QV** | ***** | ***** | ***** | *****H | | 199 | |
| rabbit | ***** | ***** | ***** | ***** | ***** | | 199 | |
| monkey | *****A* | ***** | ***** | ***** | *****L**** | | 199 | |
| human | *****A* | ***** | ***** | ***** | ***** | | 200 | |
| | 4 | 12 | 1 | 5 | 13 | | | |
| mouse | WVQDNIANFG | GNPGSVTIF | GESAG | GFSVSV | LVLSPLAKNL | FHRAISESGV | 249 | |
| rat | ***** | ***** | ***** | *****A | ***** | ***** | 249 | |
| rabbit | ***** | *D***** | ***** | *Q**I | *L***T*** | ***** | 249 | |
| monkey | *****S* | ***** | ***** | *E**** | ***** | ***** | 249 | |
| human | *****S* | ***** | ***** | *E**** | ***** | ***** | 250 | |
| | 14 | 6 | 7 | 8 | | | | |
| mouse | SLTAALITT- | DVKPIAGLVAT | LSGCKTTTSA | VMVHCLRQKT | EDELLETSLK | | 299 | |
| rat | V**S***** | *S****K*I** | ***** | ***** | ***** | | 299 | |
| rabbit | A*LSS*FRK- | NT*SL*EK*I | EA***** | ***** | *E**M*VT** | | 299 | |
| monkey | A**V*VKKG | ***L*EQI*I | AA**Q**** | ***** | *E****TT** | | 300 | |
| human | A**SV*VKKG | ***L*EQI*I | TA***** | ***** | *E****TT** | | 301 | |
| | | 15 | 9 | 16 | | | | |
| mouse | LNLFKLDDLG | NPKESYFPLP | TVIDGVVLPK | APEEILAERK | FSTVPYIVGI | | 349 | |
| rat | ***** | ***** | ***** | T***** | *N***** | | 349 | |
| rabbit | MKFLS***H* | D**NTA**T | *****L** | **A*****K | YNML**M** | | 349 | |
| monkey | MKFLS***V* | D**R**H**G | *****LL** | T**LQ**RN | *N*****M**F | | 350 | |
| human | MKFLS***Q* | D**R**Q*L*G | *****ML*L* | T**LQ**RN | *H*****M**I | | 351 | |
| | 2 | 10 | 11 | 12 | | | | |
| mouse | NEQ | FCWIIP | TLM-GVPLAEG | KLDQRTANSL | LWKSYPPLKI | SENMI PVVAE | 399 | |
| rat | *** | ***** | *M*-****S** | *****K** | ***** | ***** | 399 | |
| rabbit | *Q* | ***** | MQML****S** | *****TE* | *****VNV | *KELT**AT* | 400 | |
| monkey | *** | ***** | M*-****S** | *****M** | *****LVY* | AKEL**EAT* | 400 | |
| human | *** | ***** | MLMS****S** | Q*****M** | *****LVC* | AKEL**EAT* | 402 | |
| | | | NLBD | | | | | |
| | | | 13 | 14 | 17 | | | |
| mouse | KYLGTTDDL | KKKD | LFQDLM | ADVFGVPSV | IVSRSHRDAG | ASTYMYEFY | 449 | |
| rat | **F*****PA | *R** | *****V | ***** | M***** | *P*F***** | 449 | |
| rabbit | *****PV | *** | *L*ML | *L***** | N*A*H***** | *P*****YR* | 450 | |
| monkey | *****E*PV | *** | R*L*L | *M*S**** | *A*H***** | VP*****Q* | 450 | |
| human | *****TV | *** | *L*I | *M*I*** | *A*N***** | *P*****Q* | 452 | |
| | | 3 | 15 | 16 | | | | |
| mouse | RPSFVSAMRP | KAVIGD | H | GDE | IFSVFGSPFL | KDGASEEETN | LSKMVMKFWA | 499 |
| rat | ***** | *T**** | * | *** | L***** | ***** | *****Y** | 499 |
| rabbit | ****S*D*** | *T**** | * | *** | L**A*** | *E*****IK | *****Y** | 500 |
| monkey | ****S*D*** | *T**** | * | *** | L**A*** | *E*****IR | ***** | 500 |
| human | ****S*D*K* | *T**** | * | *** | L**A*** | *E*****IR | ***** | 502 |
| | | 16 | | 17 | | | | |
| mouse | NFARNGNFNG | GGLPHWPEYD | QKEGYLKIGA | STQAAQLRKD | KEVSFWAELR | | 549 | |
| rat | *****S** | ***** | ***** | ***** | ***A**S** | | 549 | |
| rabbit | ***** | E**Q**A*N | Y*****Q** | T****K*** | ***A**T**W | | 550 | |
| monkey | ***** | E**R****N | *E*****Q** | NA***K*** | ***A**T**F | | 550 | |
| human | ***** | E***** | *****Q** | N**G*K*** | ***A**T**F | | 552 | |
| mouse | AKESAQRPSH | REHVEL | | | | | 565 | |
| rat | ***A*EE** | ***A** | | | | | 565 | |
| rabbit | ***A*-**RE | T**I** | | | | | 568 | |
| monkey | **KAVEK*PQ | T**I** | | | | | 566 | |
| human | **KAVEK*PQ | T**I** | | | | | 568 | |

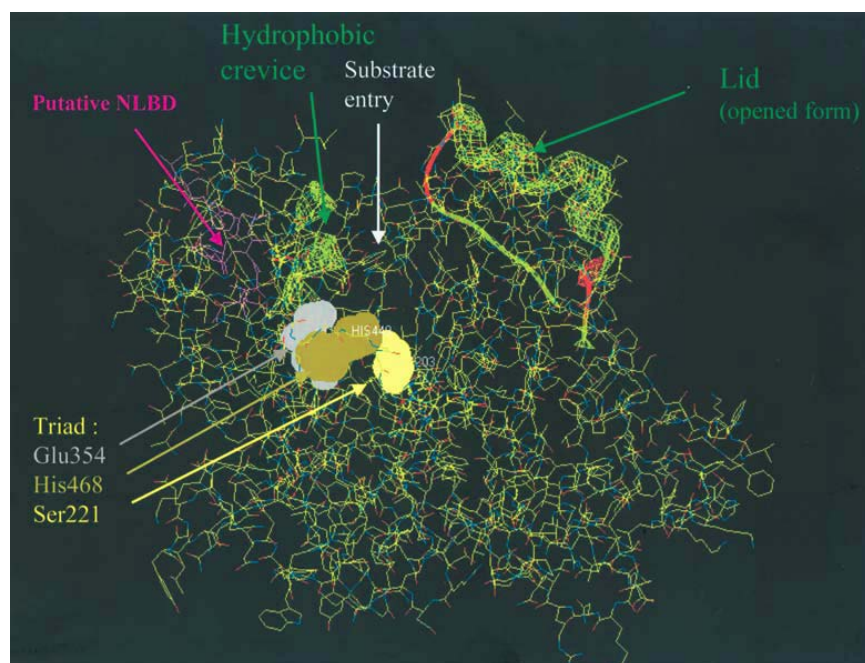


Figure 1-11. Three-dimensional structure of human TGH. TGH contains a catalytic triad (Glu-His-Ser) at the bottom of a hydrophobic cavity. A lid-domain controls the entry of substrate. A putative NLBD potentially mediates interaction with lipids. Figure reproduced from (Dolinsky et al. *Cell Mol Life Sci.* 2004.)

control the activity of TGH at the lipid-water interface via interfacial activation. In the absence of a lipid-water interface, the lid covers the entrance and prevents the substrate from accessing the active site, while in the presence of lipid, the lid domain undergoes a conformational change to an open conformation, which allows the entry of substrates (Dolinsky et al., 2004). Disulfide bonds formed by Cys87 and Cys116 may help to stabilize the lid structure (Dolinsky et al., 2004). This model was subsequently confirmed by X-ray crystallography (Bencharit et al., 2003).

1.5.3 Role of TGH in different tissues

TGH is highly expressed in the liver, adipose tissue and, to a lesser extent, small intestine and kidney (Dolinsky et al., 2001). TGH was also found in human macrophages where the protein was defined as neutral cholesteryl ester hydrolase (NCEH or CEH) (Ghosh, 2000). Several cell and animal models have been generated to study the function of TGH in different tissues. Major advances have been made with the help of these models, especially with the generation of genetically modified mice, including liver-specific TGH transgenic mice and TGH knockout mice.

1.5.3.1 Role of TGH in the liver – VLDL secretion

TGH is highly expressed in the liver; however, its expression is undetectable in HepG2 and McA cells (Lehner et al., 1999), hepatoma derived cell lines known to have impaired VLDL secretion, suggesting that the absence of TGH may

contribute to the defective VLDL secretion in these cells. It has been shown that compared to control cells, ectopic expression of rat TGH in McA cells has led to a decrease in the pre-labeled storage TG pool, accompanied with a 20% elevation in TG secretion (Lehner and Vance, 1999a), suggesting that TGH plays a role in mobilizing preformed TG for VLDL secretion. This role of TGH was further elucidated by using lipase inhibitors in primary rat hepatocytes. Inhibition of TGH activity with a TGH-specific inhibitor, GR148672X (will be referred to as GSKi hereafter), developed in collaboration with GlaxoSmithKline, resulted in significantly decreased TG and apoB secretion (Gilham et al., 2003), further implicating the contribution of TGH-specific activity to VLDL assembly.

Wei et al. generated an inducible transgenic mouse model expressing human TGH specifically in the liver to address the *in vivo* function of hepatic TGH. It was shown that induction of hepatic expression of human TGH led to increased apoB secretion into the plasma, however, the elevated level of VLDL-TG was only observed in male, but not female, animals (Wei et al., 2007a).

It was not until recently that the physiological role of TGH was systematically elucidated, owing to the generation of TGH knockout mice by our group (unpublished data). Global deletion of TGH leads to a drastic decrease in plasma TG and apoB100 levels, confirming the central role of TGH in providing lipids for VLDL assembly. Interestingly, no concomitant hepatic TG accumulation was observed. Further investigation demonstrated that this phenomenon could be explained by the elevated hepatic FA β -oxidation and

reduced FA mobilization from adipose tissue found in TGH deficient mice (see below section 1.5.3.2.).

1.5.3.2 Role of TGH in adipose tissue

Although HSL and ATGL are claimed to account for essentially all lipolytic activity in adipose tissue, a role of TGH in adipose tissue and cultured adipose-like cells has also been demonstrated. Inhibition of TGH expression in 3T3-L1 adipocytes by RNA interference led to decreased basal, but not isoproterenol-stimulated, FA efflux from these cells, accompanied by augmented intracellular TG and CE levels (Wei et al., 2007b). TGH deficient mice also exhibited decreased FA and glycerol release into plasma in both fasted and fed conditions (unpublished data). In accordance with observations from our laboratory, another group has also identified TGH as a major non-HSL adipose lipase using proteomic approaches (Soni et al., 2004).

1.5.3.3 Role of TGH in macrophages

Macrophages accumulate CE-containing LDs when loaded with cholesterol. CE accumulation in macrophages has been implicated in the development of atherosclerotic lesions. It was proposed that neutral CE hydrolases (NCEH) are required to remove CE from these macrophages, but no consensus has been reached regarding the identity of macrophage NCEH. HSL has demonstrated NCEH activity when ectopically expressed in macrophage foam cells (Escary et al., 1998; Okazaki et al., 2002). However, hydrolysis of CE in macrophages was

unchanged in HSL-null mice (Osuga et al., 2000). NCEH activity of CES1/TGH was reported by Ghosh's group and hypothesized to be the potential NCEH in human macrophages. Expression of NCEH (CES1/TGH) in CHO-K1 cells overexpressing ACAT led to a 2-fold increase in cholesterol efflux (Ghosh et al., 2003). Macrophage expression of NCEH (CES1/TGH) in LDL receptor deficient mice was reported to reduce atherosclerosis and lesion (Zhao et al., 2007). Although intriguing, a few potential problems exist with these studies. First, macrophages were incubated with [³H]-cholesterol instead of the commonly used acetylated LDL, the former may not be sufficient to augment intracellular CE stores. Second, this group reported the localization of NCEH in the cytosol, conflicting with the well-demonstrated ER localization of CES1/TGH (see **section 1.5.2**). Third, the observed increase in NCEH (CES1/TGH) expression in cholesterol-loaded macrophages conflicts with decreased NCEH activity under the same conditions (Dolinsky et al., 2004; Gilham and Lehner, 2004). Fourth, although CES1/TGH/NCEH is expressed in human macrophages (low levels) it is absent in mouse macrophages, which strongly suggests the presence of another NCEH in these cells (unpublished data). However, results recently obtained from our group using TGH inhibitors also suggest a role of TGH in CE mobilization and cholesterol efflux, but the effect seems to be minor (unpublished data). Whether or not TGH plays a major role in metabolizing CE in human macrophages has yet to be evaluated.

1.6 Focus of this thesis

This thesis intends to address hepatic LD metabolism as it is related to TG secretion, as well as the potential contribution of TGH to these events. A broad spectrum of biochemistry and cell biology approaches have been employed to investigate the following probing questions: 1) What are the characteristics of LLDs, the proposed luminal TG storage particles responsible for VLDL maturation; 2) What are the contributions of each TG storage pool (cytosolic or luminal) to VLDL secretion; 3) How is TGH involved in the regulation of these TG storage pools; 4) What are the identities of cofactors required for TGH to play such a role?

Chapter II: Materials and Methods

2.1 Materials

2.1.1 Chemicals and Reagents

| <u>NAME OF CHEMICAL</u> | <u>SOURCE</u> |
|--|----------------------|
| [9,10(n)- ³ H]Oleic acid (10 Ci/mmol) | GE Healthcare |
| [U- ¹⁴ C] Glycerol (140-186 mCi/mmol) | GE Healthcare |
| 4-Methylumbelliferyl heptanoate | Sigma-Aldrich |
| Acetone | BDH |
| Albumin, Bovine (FA free) | Sigma-Aldrich |
| Ammonium persulfate | |
| β-Mercaptoethanol | Sigma-Aldrich |
| Bodipy 493/503 dye | Molecular Probes |
| Bodipy 558/568 C ₁₂ | Molecular Probes |
| Bodipy FL C ₁₂ | Molecular Probes |
| Bovine serum albumin (BSA) | Roche Diagnostics |
| Bradford protein assay reagent | Bio-Rad Laboratories |
| Chloroform | Fisher Scientific |
| Cholesteryl oleate | Sigma-Aldrich |
| Collagen Solution from calf skin (type I) | Sigma-Aldrich |
| Collagenase, Type IV | Sigma-Aldrich |
| Complete TM protease inhibitor cocktail tablets | Roche Diagnostics |
| deoxynucleotides triphosphates (dNTPs) | Invitrogen |
| Diethyl p-Nitrophenyl Phosphate (E600) | Sigma-Aldrich |

| | |
|---|------------------------|
| Dimethyl 3,3'-dithiobispropionimidate (DTBP) | Pierce Biotechnologies |
| Dimethyl Sulfoxide (DMSO) | Sigma-Aldrich |
| Di-Sodium hydrogen orthophosphate anhydrous | BDH |
| DNase I | Invitrogen |
| Dulbecco's modified Eagle's medium (DMEM) | Invitrogen |
| ECL immunoblotting reagents | GE Healthcare |
| Enhance Spray | PerkinElmer |
| Ethanol, 95% | Biochemistry Store |
| Ethidium Bromide | Sigma-Aldrich |
| Ethyl Ether, anhydrous | Caledon |
| Ethylene-diaminetetra-acetic acid disodium salt (EDTA) | BDH |
| Fetal bovine serum (FBS) | Invitrogen |
| Formaldehyde, 16% EM grade | Canemco-Marivac |
| Freund's Adjuvant complete | Sigma-Aldrich |
| Freund's Adjuvant incomplete | Sigma-Aldrich |
| Freund's complete and incomplete adjuvants | Roche Diagnostics |
| Full-range rainbow protein molecular weight markers | GE Healthcare |
| G418 (Geneticin) | Gibco |
| Glutaraldehyde, 10% EM grade | Canemco-Marivac |
| glycerol | Anachemia |
| glycine | Fisher Scientific |

| | |
|--|-------------------|
| HEPES | Sigma-Aldrich |
| Hexane | EMD Chemicals |
| HMW native protein standards | GE Healthcare |
| Horse serum | Invitrogen |
| Infinity Triglyceride Reagent | Sigma-Aldrich |
| Insulin (bovine pancreas) | Sigma-Aldrich |
| Iodine | Fisher Scientific |
| Iso-Propyl alcohol | BDH |
| L-a-Phosphatidylcholine | Sigma-Aldrich |
| Lipofectamine 2000 | Invitrogen |
| Methanol | Biochem Store |
| Metophen (Methoxyflurane) | Janssen |
| Nile Red | Molecular Probes |
| Nonidet P-40 | Sigma-Aldrich |
| Normal goat serum | Invitrogen |
| Oleic acid | Sigma-Aldrich |
| oligo dT primers | Invitrogen |
| Opti-MEM | Invitrogen |
| Penicillin-streptomycin liquid | Gibco |
| Phenylmethanesulfonyl fluoride (PMSF) | Sigma |
| Phospholipase C (Clostridium welchii) | Sigma-Aldrich |
| Platinum® SYBR®Green qPCR SuperMix-UDG | Invitrogen |

| | |
|--|--|
| Platinum® Taq DNA Polymerase | Invitrogen |
| ProLong Anti-fade Kit | Molecular Probes |
| Protease Inhibitors, Complete | Roche |
| Protein A-Sepharose, 4B fast flow | Sigma-Aldrich |
| QTB fatty acid uptake assay kit | Molecular Devices |
| Saponin | Dr. N. Touret (University of Alberta) |
| SDS | BioRad |
| Sodium Bicarbonate | Caledon |
| Sodium Carbonate anhydrous | BDH |
| Sodium Chloride | BDH |
| Sodium dihydrogen orthophosphate anhydrous | BDH |
| Sodium hydrogen carbonate | BDH |
| Sodium Hydroxide | BDH |
| Sucrose | BDH |
| Superscript™ II reverse transcriptase | Invitrogen |
| Sylon BFT (BSTFA + TMCS, 99:1) | Supelco (Sigma) |
| Targefect-Hepatocyte / Virofect | Targeting Systems |
| Taurodeoxycholate | Sigma-Aldrich |
| TGH inhibitor (GSKi) | GlaxoSmithKline |
| Triolein | Sigma-Aldrich |
| Tris (Ultra Pure Tris) | Invitrogen |
| Triton X-100 | BDH |

TRIZOL Reagent

Invitrogen

2.1.2 Plasmids

Plasmids used in this thesis are listed in Table 2-1.

Table 2-1. Plasmids

| Name | Vector | Insert | Comments |
|------------|----------|------------------|---|
| EGFP | pEGFP-N1 | None | From Clontech |
| TGH-EGFP | pEGFP | human TGH | EGFP cDNA was placed at C-terminus of human TGH sequence with a linker and immediately before the C-terminal "HIEL" encoding sequence of human TGH. |
| AA/KK-EGFP | pEGFP | mutant human TGH | Two "A"s in human TGH apolipoprotein binding domain were mutated to two "K"s. |
| KDEL-EGFP | pEGFP | KDEL | (Touret et al., 2005) |

2.1.3 Antibodies

Antibodies used in this thesis are listed in Tables 2-2 and 2-3.

Table 2-2. Primary antibodies

| Name | Species | Dilution (IB) | Dilution (IF) | Source |
|---------|---------|---------------|---------------|--|
| ADRP | Rabbit | 1:5000 | 1:200 | Dr. C. Londos (NIH, Bethesda) |
| albumin | rabbit | 1:5,000 | N/A | Dr. D. E. Vance (University of Alberta) |
| apoB | goat | 1:5,000 | N/A | Chemicon |
| apoE | goat | 1:2,000 | 1:100 | BioDesign |

| | | | | |
|----------------|-----------------|----------|-------|---|
| Calnexin | rabbit | 1:8,000 | 1:200 | Stressgen |
| GFP | Goat/ rabbit | 1:10,000 | N/A | Dr. L. Berthiaume (University of Alberta) |
| human TGH | rabbit | 1:1,000 | N/A | (Alam et al., 2002a) |
| mouse TGH | rabbit | 1:50,000 | 1:500 | (Wang et al., 2007) |
| MTP | mouse | 1:5,000 | 1:100 | BD Biosciences |
| PDI | rabbit | 1:5,000 | 1:200 | Stressgen Biotechnologies |
| porcine TGH | rabbit | 1:1,000 | N/A | (Lehner and Verger, 1997) |
| SKL | rabbit | N/A | 1:200 | Dr. R. Rachubinski (University of Alberta) |
| TIP-47 | rabbit | N/A | 1:200 | Dr. C. Sztalryd (Univ. of Maryland) |

Table 2-3. Secondary antibodies*

| NAME | SOURCE |
|---|---------------------------|
| Horseradish peroxidase-conjugated goat-anti-rabbit IgG | Pierce Biotechnologies |
| Horseradish peroxidase-conjugated goat-anti-mouse IgG | Pierce Biotechnologies |
| Horseradish peroxidase-conjugated donkey-anti-goat IgG | Pierce Biotechnologies |
| Alexa 488-conjugated donkey-anti-goat IgG | Molecular Probes |
| Alexa 488-conjugated goat-anti- rabbit IgG | Molecular Probes |
| TexasRed-conjugated goat-anti-rabbit IgG | Molecular Probes |

* All secondary antibodies were used at 1:10,000 dilutions for IB and 1:100 for IF.

2.1.4 Buffers and solutions

Compositions of commonly used buffers and solutions are listed in Table 2-4.

Table 2-4. Common buffers and solutions

| Name | Composition |
|--------------------------------|---|
| Perfusing Solution | Hanks Balance Salt Solution (Gibco 14185), 20mM glucose, 4.0 mM NaHCO ₃ , 2.5 mM HEPES, 0.5 mM EGTA, pH 7.4 |
| Collagenase Solution | Hanks Balance Salt Solution (Gibco 14065), 20mM glucose, 4.0 mM NaHCO ₃ , 2.5 mM HEPES, 100 U/ml collagenase, pH 7.4 |
| 1x PBS | 137mM NaCl, 2.7mM KCl, 10mM Na ₂ HPO ₄ , 2mM KH ₂ PO ₄ , pH 7.4 |
| 1xTBS | 20 mM Tris-HCl, pH 7.4, 150 mM NaCl |
| 1xT-TBS | 50 mM Tris-HCl, pH 7.4, 150 mM NaCl, 0.1% Tween 20 |
| 1x transfer buffer | 192 mM Glycine, 24 mM Tris, 20% Methanol |
| 4x SDS-PAGE loading buffer | 200 mM Tris-HCl, pH 6.8, 8% SDS, 40% glycerol (v/v), 40% β-mercaptoethanol (v/v), 0.4% Bromophenol Blue |
| 2x native PAGE loading buffer | 100 mM Tris-HCl, pH 6.8, 40% glycerol (v/v), 0.4% Bromophenol Blue |
| 10x SDS-PAGE running buffer | 10g of SDS, 30.3g of Tris base, 144.1g glycine, dissolved in 1 L ddH ₂ O, pH 8.3 |
| 10x native PAGE running buffer | 30.3g of Tris base, 144.1g glycine, dissolved in 1 L ddH ₂ O, pH 8.3 |
| Coomassie Blue stain | 45% Methanol (v/v), 10% acetic acid (v/v), 0.25% Coomassie Brilliant Blue R-250 |
| Destain solution | 40% Methanol (v/v), 10% acetic acid (v/v) |

| | |
|------------------------------|---|
| Ponceau stain | 0.2% Ponceau S, 3% trichloroacetic acid, 3% sulfosalicylic acid |
| Homogenization buffer | 250 mM sucrose, 20 mM Tris-HCl, pH 7.4, 1 mM EDTA |
| Lipase Activity Assay Buffer | 20 mM Tris pH 8.0, 1 mM EDTA, 300 μ M taurodeoxycholate |

2.2 Animals

All animal procedures were approved by the University of Alberta's Animal Care and Use Committee and were in accordance with guidelines of the Canadian Council on Animal Care. All mice used in this thesis were females of 3-4 months old and age-matched, where applicable. They were exposed to 12 h light / dark cycle and maintained on a chow diet (from LabDiet, PICO laboratory Rodent Diet 20) with free access to distilled water. Unless otherwise stated, all mice were fasted for 4 h before experiments. Mouse strains used are listed below in Table 2-5.

Table 2-5. List of mouse strains used.

| Name | Description |
|------------------------|--|
| C57BL/6J; 129P2-Tgh WT | TGH wild type bred from the litter mates of TGH knockout; mixed background |
| C57BL/6J; 129P2-Tgh KO | TGH knockout; mixed background |
| C57BL/6J | wild type; pure background (Jackson's Laboratory) |
| C57BL/6J-Apoe KO | ApoE knockout; pure background (from Dr. D.E. Vance laboratory) |

2.3 Cell culture and manipulation

2.3.1 Culture of mammalian cell lines

McArdle RH7777 (McA) cells were obtained from American Type Culture Collection (Manassas, VA). McA cells stably transfected with pCI-neo vector containing human TGH cDNA and with empty pCI-neo vector have been produced and maintained in our laboratory (Gilham et al., 2005a). Cells are cultured in DMEM containing 10% FBS (v/v) and 10% horse serum (v/v) and in the presence of 100 U/ml penicillin and 100 µg/ml streptomycin. G418 (400 µM) was also added to pCI-neo and TGH stable cell lines. All cell culture and incubations were performed at 37°C in humidified air enriched with 5% CO₂.

2.3.2 Preparation and culture of primary mouse hepatocytes

Primary mouse hepatocytes were isolated by collagenase perfusion of the livers from mice based on previously published method (Yao and Vance, 1988). Mice were anesthetized by inhalation of Metophen and the abdominal cavity was opened by making a midline incision through the skin and abdominal muscle. Then the hepatic portal vein was exposed by carefully moving the intestines away from the abdominal cavity with a cotton swab. Ligatures were then loosely set around the portal vein and the lower vena cava, to be closed later. The key step of this surgery is to make a minor cut on the portal vein and to insert a feeding needle through the cut in the portal vein. Once inserted, the ligature set around the portal vein was closed to keep the needle in place. The perfusion was then

performed at 4 ml/min through a peristaltic pump with the perfusing solution (Table 2-4). The left side of the rib cage and the diaphragm were then cut to expose the heart. Once exposed, the atrium was cut to release the perfusate. Another ligature was then loosely set around the upper vena cava. Once no visible blood ran out of the heart and the liver appeared pale in color, the solution running through the pump was switched to collagenase solution (Table 2-5) and the ligatures around the upper vena cava and lower vena cava were tied off, and the liver was allowed to swell and digest. The digestion process takes approximately 5-10 min and was monitored by pressing with forceps (Livers are well digested if pressure with forceps leaves a distinct mark on the tissue.)

The digested liver was removed from the animal, transferred to a 60 mm culture dish and disrupted with scissors. The disrupted tissues were transferred to a 50 ml sterile centrifuge tube containing ~2ml collagenase solution, further disrupted by pipetting, and suspended in 25 ml DMEM containing 10% FBS. Cells were then filtered through a sterilized coarse filter, centrifuged for 2 min at 200 x g, resuspended in 25 ml DMEM+10% FBS, and filtered through another sterilized fine filter. Cells were then centrifuged again and resuspended in 20 ml DMEM+10% FBS. Cell numbers were counted with a hemocytometer. For metabolic studies, 1.5×10^6 cells were plated in 60 mm collagen-coated culture plates. For microscopy, 0.2×10^6 cells were plated in 6-well plates containing coverslips coated with collagen. Hepatocytes were maintained in DMEM supplemented with 10% FBS at 37°C in humidified air containing 5% CO₂ for a maximum of 48 h before experiments.

2.3.3 Augmentation of intracellular TG stores

To augment intracellular TG storage, cells (cell lines or primary hepatocytes) were incubated with DMEM containing 0.4 mM oleic acid complexed to 0.5% (w/v) BSA (essentially fatty acid free). The 20x OA/BSA stock solution was made by dissolving 5 g BSA in 50 ml DMEM, which was warmed to 56°C in a water bath. This DMEM/BSA was then added to a beaker containing 0.106 g oleate pre-warmed to 56°C. The mixture was stirred vigorously until clarified and then sterilized through a 0.22 µm filter and stored at 4°C.

2.3.4 Stable transfection of McA cells

Plasmids encoding TGH-EGFP and AA/KK-EGFP were constructed by our laboratory by inserting the EGFP coding sequence into the human TGH cDNA immediately before the region encoding the C-terminal “HIEL” ER retrieval sequence.

Before transfection, McA cells were grown in 6-well plates to 70% confluency. Plasmid DNAs were introduced into cells using Lipofectamine 2000 according to the manufacturer’s instructions. Briefly, for each well of cells, 5 µg of plasmid DNA in TE buffer (Tris-EDTA, pH 8.0) was diluted in 250 µl Opti-MEM. At the same time, 7.5 µl of Lipofectamine 2000 reagent was diluted in 250 µl Opti-MEM and incubated for 5 min at room temperature. The Lipofectamine 2000 mixture was then mixed with the DNA mixture and incubated at room temperature for 20 min to allow DNA-Lipofectamine complex formation.

Following incubation, the complex was added to each well of cells containing 1 ml serum free-DMEM. After overnight incubation, the transfection media were replaced by regular culture media. Expression of proteins of interest was monitored by fluorescence microscopy after 16 h of transfection.

To select stable cell lines, the regular media were replaced with media containing 800 μ M G418 the day following transfection. Cells were cultured in this condition for 2 weeks until massive cell death occurred. Single colonies were then transferred into 24-well plates and monitored for fluorescence. The fluorescing colonies with at least 95% of cells showing similar degree of fluorescence were kept and maintained in media containing 400 μ M G418. The expression of the protein of interest in these colonies was further confirmed by Western blotting using anti-GFP antibodies.

2.3.5 Transfection of primary mouse hepatocytes

Transfection of KDEL-EGFP and TGH-EGFP plasmids into hepatocytes was performed using the Targefect-Hepatocytes reagent following the user manual. Hepatocytes were maintained in DMEM containing 10% FBS that was heat-inactivated at 56°C for 30 min. The media were replaced with serum-free DMEM for at least 2 h before transfection. To transfect a well in a 24-well plate, 0.8 μ g plasmid DNA was mixed with 250 μ l DMEM. At the same time, 1.5 μ l Targefect reagent and 3 μ l enhancer (Virofect) were mixed with 250 μ l DMEM. The DNA and Targefect mixtures were then mixed and incubated for 20 min at 37°C to yield the transfection complex. Cells were incubated with the transfection complex for

4 h in serum-free DMEM, then replaced with DMEM containing 10% FBS and maintained for at least 14 h before visualization by fluorescence microscopy.

2.4 Protein manipulation and analysis

2.4.1 Determination of protein concentration

Protein concentrations were determined using the BioRad Protein Assay kit (Bradford method). The reagent was diluted 5-fold before use. Each protein sample (usually 4-18 μg) was mixed with 1 ml diluted reagent in a cuvette and incubated at RT for 5 min before measuring absorbance at 595 nm. Protein concentrations were determined according to the standard curve plotted by measuring the absorbance of known concentrations (0.2-0.9 mg/ml) of BSA standard.

2.4.2 SDS-PAGE

Samples were mixed with 4x SDS-PAGE loading buffer to the final concentration of 1x and boiled for 5 min to denature. Unless otherwise stated, an equal amount of protein was loaded in each well. Proteins were resolved by 10% denaturing discontinuous polyacrylamide gels containing 0.1% SDS and 0.05% ammonium persulfate at 80-120 V using a BioRad Mini-PROTEAN 3 system.

For analyses of LLD fractions after density gradient fractionation, the top three fractions were concentrated 15-fold using Millipore Amicon® Ultra-4 Centrifugal Filter Units (Mississauga, Ontario, Canada). An equal volume of each

concentrated fraction was analyzed by 4-15% pre-cast gradient polyacrylamide gels (BioRad) at 80-120 V using a BioRad Mini-PROTEAN 3 system.

2.4.3 Native PAGE

For the analysis of particle size by gradient native PAGE, 25 μ l aliquots of each sample were mixed with an equal volume of 2x native PAGE loading buffer and applied to a 2-10% gradient non-denaturing polyacrylamide gel. The gradient gel was cast using a gradient maker (Hoefer, Inc.). Proteins were resolved in native PAGE running buffer without SDS (Table 2-4) at 80-120 V using a BioRad Mini-PROTEAN 3 system.

2.4.4 Immunoblotting

Proteins resolved by PAGE were transferred to nitrocellulose membranes in transfer buffer for a total of 800-1200 mAmp-Hours. For native PAGE, positions of HMW native protein standards were determined by Ponceau staining. Membranes were blocked with 5% skim milk in T-TBS for 1 h, washed 3 times for 5 min with T-TBS, and probed with primary antibodies diluted (see Table 2-2 for ratio of dilution) in either 2.5% skim milk or 3% BSA in T-TBS for 1 h at room temperature or overnight at 4°C. The membranes were then washed again with T-TBS and probed with secondary antibodies diluted at 1:10,000 in 2.5% skimmed milk in T-TBS. Following incubation, membranes were washed again before chemiluminescent detection using ECL reagents.

2.4.5 Protein identification by mass spectrometry

Proteins resolved by SDS-PAGE were stained with coomassie blue stain for at least 1 h and destained to visualize distinct bands. Visible bands were excised on a clean stage in a clean room. Precaution was taken throughout the procedure not to touch the gel with bare skin.

Later procedures were performed by the Institute for Biomolecular Design (University of Alberta, Edmonton). Briefly, automated in-gel tryptic digestion was performed on a MassPrep Station (Waters Corporation, Milford, MA). Proteins in the gel were de-stained, reduced (DTT), alkylated (iodoacetamide), and digested with trypsin (Promega Sequencing Grade Modified); the resulting peptides were extracted from the gel and analyzed via LC/MS/MS. LC/MS/MS was performed on a CapLC HPLC (Waters Corporation, Milford, MA) coupled with a Q-ToF-2 mass spectrometer (Waters Corporation). Tryptic peptides were separated using a linear water/acetonitrile gradient (0.2% formic acid) on a Picofrit reversed-phase capillary column, (5 micron BioBasic C18, 300 Angstrom pore size, 75 micron ID x 10 cm, 15 micron tip from New Objective Inc., Woburn, MA) with an in-line PepMap column (C18, 300 micron ID x 5 mm from LC Packings, Sunnyvale, CA) used as a loading/desalting column.

Protein identification from the resulting MS/MS data was done by searching the NCBI non-redundant database using Mascot Daemon (Matrix Science, UK). Search parameters included carbamidomethylation of cysteine, possible oxidation of methionine and one missed cleavage per peptide.

2.4.6 Immunoprecipitation

For immunoprecipitation using anti-mouse TGH antibodies (R13 sera), 1 ml of microsomal luminal content (containing approximately 0.5 mg protein) was adjusted to 20 mM Tris-HCl (pH 7.4) and 150 mM NaCl. Protease inhibitor cocktail was added according to the manufacturer's instructions. The sample was incubated with 3 µg anti-mouse affinity purified anti-mTGH antibodies while rotating the tube end-over-end at 4 °C overnight. Then 20 µl of washed protein A-Sepharose beads were added and incubated with the sample rotating end-over-end for 2 h at 4 °C. The protein-beads complex was pelleted by centrifugation for 30 s at 6,000 xg. Immunoprecipitates were washed and denatured by boiling in SDS-PAGE loading buffer for 5 min. Proteins were separated by 10% SDS-PAGE and subjected to immunoblotting.

2.5 Subcellular fractionation

2.5.1 Isolation of microsomal luminal contents

Microsomes from female C57BL/6J mouse liver homogenates were prepared essentially as previously described (Lehner and Kuksis, 1993). Usually 4 livers would provide enough material for an experiment. In brief, mice were exsanguinated via cardiac puncture, and livers were removed and washed with ice-cold TBS. Livers were then homogenized with a motor-driven Potter-Elvehjem homogenizer (Wheaton Science Products, Millville, NJ) at medium speed (level 3-4) for 10 strokes in homogenization buffer (see Table 2-4) to yield a 20% (w/v) homogenate. Cellular debris were removed by centrifugation at 500

x g for 10 min. Crude mitochondrial pellets were obtained by centrifugation of the 500 x g supernatant at 15,000 x g for 10 min, and microsomes (pellet) and cytosol (supernatant) were separated by centrifugation of the 15,000 x g supernatant at 106,000 x g for 1 h. Microsomes were then resuspended in 20 mM Tris-HCl, 0.5 M NaCl (pH 7.4) to remove peripherally associated membrane proteins and lipid droplets. Washed microsomes were recovered by centrifugation at 106,000 x g for 1 h. To release microsomal luminal contents, microsomes were suspended with 1/3 the original volume of 1 mM Tris-HCl (pH 8.8) or 0.2 M Na₂CO₃ (pH 12) for 30 min on ice, followed by centrifugation at 106,000 x g for 1 h to obtain luminal contents (supernatant) and microsomal membranes (pellet) (Lehner and Kuksis, 1993; Wetterau et al., 1991a). Protease inhibitor cocktail was included to all of the solutions used in this isolation procedure.

2.5.2 Isolation of microsomal LLDs by density gradient ultracentrifugation

Microsomal luminal contents were adjusted to 50 mM Tris-HCl, 150 mM NaCl (pH 7.4), and immunoprecipitation with anti-apoB polyclonal antibodies was performed in the absence of detergents. The immunoprecipitation was performed using the same conditions as in section 2.4.6. For luminal content prepared from 4 livers, 20 µl of anti-apoB antibodies and 160 µl protein A sepharose beads were used. Following immunoprecipitation, the protein-beads complex and the supernatant (post-IP) were collected. Two ml of post-IP supernatant were combined with an equal volume of glycerol and transferred to a Beckman Ultra-ClearTM centrifuge tube (Palo Alto, CA). Samples were overlaid with 4 ml of

homogenization buffer (Table 2-4) and an additional layer of 4 ml TBS. The solution was centrifuged at 35,000 rpm (160,000 x g) in a Beckman SW40 rotor for 2 h at 8°C. Fractions of 2 ml were collected from bottom to top of the centrifuge tube (6 fractions in total) for analysis.

2.5.3 Preparation of ER and Golgi fractions

Separation of ER and Golgi was performed following a protocol obtained from Dr. J. E. Vance's group. A C57BL/6J female mouse was fasted overnight and exsanguinated via cardiac puncture. The liver was removed rapidly and immediately rinsed in ice-cold H-buffer (37.5 mM Tris-HCl, pH 6.5; 0.5 M sucrose; 1% dextran; 5 mM MgCl₂; 0.1 mM PMSF). The entire procedure was performed on ice or at 4°C. To make liver homogenate, the liver was weighed, chopped up, and H-buffer with a volume of 4x the liver weight was added. The sample was homogenized with a polytron homogenizer at medium setting (speed 5) for 30 sec and centrifuged in JS 13.1 rotor at 5700 rpm (3300 x g) for 15 min. The fat cake was discarded and the supernatant was collected and set aside for further ER preparation. The top 2/3 of the pellet was scraped and transferred into a 15 ml Corex tube for Golgi preparation. The collected pellet was resuspended in ~2 ml H-buffer and layered on top of the 2.4 ml of 1.2 M sucrose (all sucrose solutions used for gradient formation were made in 37.5 mM Tris-HCl, pH 6.4; 1% dextran; 5 mM MgCl₂; 0.1 mM PMSF) in a 4.4 ml ultraclear Beckman tube, followed by ultracentrifugation in SW60 rotor at 31,000 rpm (99,000 x g) for 30 min (brake to 800). The Golgi band was enriched between the two layers of

sucrose and the pellet contained ER. The Golgi band was collected carefully and transferred to a 15 ml Corex tube. Liquid above the ER pellet was discarded and the pellet was set aside for further use. The collected Golgi band was further diluted in H-buffer and centrifuged in JA-20 rotor at 5700 rpm (2500 x g) for 20 min. The pellet from this step (purified Golgi) was resuspended in 300 μ l Buffer R (10 mM Tris-HCl, pH7.4; 0.25 M sucrose; 0.1 mM PMSF) and stored. The ER pellet that was set aside was resuspended with ER supernatant obtained from the first centrifugation step. This mixture was diluted 1:3 in ER buffer (55 mM Tris-HCl, pH 7.0; 5 mM MgCl₂; 0.1 mM PMSF) and centrifuged in 30 ml Corex tubes in JS13.1 rotor at 7300 rpm (5400 x g) for 5 min. The supernatant was collected and layered on top of a sucrose gradient set in 38.5 ml ultraclear Beckman tubes composed of 6 ml of 2.0 M, 8 ml of 1.5 M and 8ml of 1.3 M sucrose solutions. Following a centrifugation in a SW32 rotor at 27,000 rpm (90,000 x g) for 75 min (brake to 800), the two bands (ER1 and ER2) between the lower three layers of sucrose were collected, diluted with ER buffer and centrifuged in SW32 rotor at 27,000 rpm (90,000 x g) for 20 min. The pellets containing purified ER1 and ER2 were collected and resuspended in Buffer R (200 μ l and 40 μ l, respectively).

2.5.4 Isolation of cytosolic lipid droplets (CLDs)

Microsomes and cytosol were isolated from livers or hepatocytes of WT or TGH KO mice, as described in section 2.5.1. CLDs were floated on top of the cytosol and formed a layer of fat cake after 106,000 x g 1h centrifugation of post-mitochondrial supernatants. The crude fat cake layer was collected carefully,

washed with TBS and subjected to ultracentrifugation at 106,000g for 1 h to re-float CLDs. CLDs were collected and suspended in TBS. The protein concentration of each fraction was determined by the Bradford method.

2.6 Lipid manipulation and analysis

2.6.1 Lipid extraction for thin-layer chromatography (TLC)

Samples were transferred into glass tubes and total lipids were extracted with chloroform/methanol (2:1, v/v) (Folch et al., 1957). Four ml of chloroform/methanol were added to each 1 ml sample and mixed thoroughly by vortex for 20 s. The mixture was then centrifuged at 350 x g for 10 min to separate lipid and aqueous phases. The lower phase (lipid phase) was collected with a Pasteur pipette and evaporated under N₂. The residues were dissolved in 100 µl chloroform and were analyzed by TLC. If radioactive samples were to be analyzed, 100 µg each of non-radioactive lipid carrier (phosphatidylcholine, oleic acid, trioleoylglycerol and cholesteryl oleate) was added in chloroform/ methanol for visualization of these lipids after separation by TLC. To extract lipids from fluorescently labeled samples, 4 ml chloroform (without methanol) was used to avoid quenching of fluorophores by methanol.

2.6.2 TLC

Lipids extracted from samples (2.6.1.) were spotted onto silica gel H TLC plates (Whatmann Inc., Florham Park, NJ), developed to 1/3 the height of the plate with phospholipid solvent (chloroform/ methanol/ acetic acid/ water, 25:15:4:2, v/v) to

allow separation of glycerol phospholipids, followed by separation of neutral lipids with neutral lipid solvent (heptane/ isopropyl ether/ acetic acid, 60:40:4, v/v) (Lehner and Vance, 1999a). The lipid classes were visualized by exposure of TLC plates to iodine vapor and identified by comparing to the migration of lipid standards. For non-radioactive samples, images were taken with a digital camera. For radioactive samples, bands were scraped off of the plates and dissolved in 5 ml of CytoScint scintillation fluid (ICN Biomedicals, Irvine, CA). Radioactivity incorporated into different lipid classes was analyzed with a scintillation counter (Beckman LS 6000TA). For fluorescently labeled lipid samples, the TLC plate was developed in neutral lipid solvent only. The fluorescent fatty acid incorporation into lipid classes was visualized under UV light (365 nm) and images were captured with a digital camera.

2.6.3 Gas chromatography (GC) analysis of lipids

The mass of cholesterol, phospholipids, cholesteryl ester and TG were quantified by gas chromatography. Lipids were extracted from samples in the presence of tridecanoyl glycerol (internal standard) as previously described (Myher et al., 1989; Sahoo et al., 2004). Typically, 200 μ l of sample was mixed with 2 ml PL-C solution (17.5 mM Tris, pH 7.3; 10 mM CaCl_2 and 2 units of PL-C from *Clostridium welchii*) and 2 ml diethyl ether, and shaken vigorously for 2 h at 30°C. One ml of internal standard of known concentration in chloroform and 6 ml of chloroform/methanol 2:1 were added to the samples and mixed, and lipid and aqueous phases were separated by centrifugation. The lower phase was then

collected, passed through a Pasteur pipette containing anhydrous Na₂SO₄, and evaporated under N₂. The residue was then dissolved in 100 µl of Sylon BFT (Supelco) and incubated at room temperature for 1 h. The reactant was evaporated again under N₂ and re-dissolved in 50-100 µl of hexane. 1 to 5 µl was injected and analyzed by GC (Agilent Technologies, 6890 Series equipped with a flame ionization detector; Palo Alto, CA).

2.6.4 Gel filtration chromatography

Luminal apoB-free contents were applied to a Superose 6 size exclusion fast protein liquid chromatography (FPLC) column (Pharmacia, Uppsala, Sweden). For TG analysis, eluted fractions were mixed in-line with the InfinityTM Triglyceride Reagent (Thermo Fisher Scientific, Inc., Waltham, MA) using a post-column T-connector/Solvent Delivery Module (model 110B, Beckman Coulter, Mississauga, Ontario, Canada) and passed through a CH-30 Column Heater (Eppendorf, Mississauga, Ontario, Canada) set at 37 °C. Reaction products were monitored at 500 nm in real-time using a Programmable Detector Module (model 166, Beckman Coulter). For protein analysis, fractions (2 ml) were collected every four minutes from the 22nd to 58th minute. Fraction #1 (eluted from the 22nd to 25th minute) contains VLDL sized particles and fractions #5 to #8 (eluted from the 38th to 53th minute) contain HDL sized particles based on the elution of plasma lipoproteins used as standards. Proteins in collected fractions were precipitated with 2 volumes of ice-cold acetone for 30 min at -20°C,

resuspended in 50 μ l SDS-PAGE sample buffer, and analyzed by SDS-PAGE and immunoblotting.

2.6.5 Metabolic labeling of lipids

To label intracellular lipids with radioactive isotopes, hepatocytes were freshly prepared and McA cells were grown to 70% confluency. Cells were serum starved overnight and then incubated with serum-free DMEM containing 0.4 mM [3 H]-oleic acid (125 μ Ci / μ mol) complexed to 0.5% BSA for 4 h (pulse). In the case where labeling of glycerol backbone is needed, 25 μ Ci / μ mol [14 C]-glycerol were also included in labeling media. At the end of the incubation, media were aspirated and cells were washed with DMEM/0.5% BSA for 30 min. If no chase period was needed, cells were washed with ice-cold PBS and harvested. Otherwise, cells were incubated with DMEM containing 100 μ M E600, 10 μ M GSKi, or DMSO for 12 h (chase). Media were collected after incubation and cells were washed with ice-cold PBS before being harvested. Where applicable, cytosolic and luminal contents were isolated as described in **2.5.1**. Lipids were extracted and analyzed by TLC as described in **2.6.1** and **2.6.2**.

2.7 Microscopy

2.7.1 Fluorescence labeling of hepatocytes

To stain LDs with Bodipy 493/503, freshly isolated hepatocytes were grown on collagen-coated coverslips for 4 h to allow attachment, and washed 3 times with PBS, followed by incubation with 2 μ g / ml of Bodipy 493/503 in PBS. To label

cells with fluorescent fatty acid analogues, cells grown on collagen-coated coverslips were washed with PBS and incubated overnight in DMEM containing 0.4 mM oleic acid complexed to 0.5% BSA. 6 μ M of Bodipy FL C₁₂ or Bodipy 558/568 C₁₂ were added to the oleic acid-containing media described above to make labeling media. For confocal imaging of fixed cells, cells were incubated with labeling media containing Bodipy FL C₁₂ overnight, then washed with PBS and incubated with labeling media containing Bodipy 558/568 C₁₂ for 15 min, 30min, 1 h or 4 h. The labeling reaction was stopped by washing off labeling media with PBS followed by immediate fixation with 4% paraformaldehyde in PBS. For live-imaging, cells were first incubated with labeling media containing Bodipy 558/568 C₁₂ overnight to label preformed LDs. Nascent LDs were labeled with QTB fatty acid uptake reagent (containing Bodipy FL C₁₂) reconstituted in 10 ml DMEM containing 0.5% BSA and 0.4 mM oleic acid added to cells immediately before image capture.

2.7.2 Immunofluorescent staining

Hepatocytes grown on collagen-coated coverslips were incubated with DMEM containing OA/BSA for 4 h or overnight to build up neutral lipid stores before immunostaining. For colocalization with nascent LDs, cells were incubated with DMEM containing OA/BSA and 6 μ M Bodipy 558/568 C₁₂ for 15 min before staining. Cells were then rinsed 3x with PBS and immediately fixed with 4% paraformaldehyde and 0.025% glutaraldehyde in PBS at 4 °C for 10 min, quenched with 50 mM NH₄Cl in PBS for 10 min, and then permeabilized with

0.05% Saponin in PBS for 15 min at room temperature and blocked with 3% normal goat serum in PBS at room temperature for 1 h or 4 °C overnight. Following each of the above steps, cells were rinsed 3x with PBS. Then cells were incubated with primary antibodies diluted at desired concentrations (Table 2-2) in PBS containing 3% BSA for 1 h at 37 °C, and washed thoroughly with PBS, followed by incubation with secondary antibodies (Table 2-3) for 1 h at 37 °C. Thorough washes were applied following every antibody incubation step, normally 3 washes of 5 min. Where applicable, LDs were stained with Nile Red or Bodipy 493/503 for 10 min after the incubation with antibodies was completed. Cells were then rinsed and mounted on microscope slides with Prolong antifade reagent.

2.7.3 Confocal fluorescence scanning microscopy

Images of fixed cells were collected with a Zeiss (Carl Zeiss, Jena, Germany) Confocal Laser Scanning Microscope (LSM510, software version 3.2) mounted on a Zeiss Axiovert 100M inverted microscope with a Plan-Apochromat differential interference contrast (DIC) 63x (1.40 NA) objective. To image Bodipy 493/503 staining, the 488 nm laser line was used and signals were collected with a long pass filter of 505 nm. For dual-color images, the 488 nm laser line was used to image Bodipy FL C₁₂ and the 543 nm laser line was used to image Bodipy 558/568 C₁₂. Signals were collected with a band pass 500 to 530 nm filter - IR blocking, and a long pass 560 nm filter, respectively. Quantification

of LD number and sizes was done with MetaMorph software (ver. 7.5, Molecular Devices, Sunnyvale, CA).

2.7.4 Time-lapse microscopy

Cells grown on coverslips were mounted onto an adaptor (Chamlide, Seoul, Korea) and placed in an environment chamber thermostated at 37°C with 5% CO₂. Confocal microscopy was performed on a spinning-disk microscope (WaveFx from Quorum Technologies, Guelph, Canada) set up on an Olympus IX-81 inverted stand (Olympus, Markham, Canada). Images were acquired through a 60X objective (N.A. 1.42) with an EMCCD camera (Hamamatsu, Japan). The fluorescent fatty acid analogues Bodipy FL C₁₂ and Bodipy 558/568 C₁₂ were successively excited by a 491 nm (GFP channel) and a 543 nm (Cy3 channel) laser line (Spectral Applied Research, Richmond Hill, Canada), respectively. Z-slices of 0.5 µm steps were acquired using Volocity software (Improvision) through the cells using a piezo z-stage (Applied Scientific Instrumentation, Eugene, USA) with image capture every 1 minute over a period of 30 minutes. Quantification of fluorescent intensity was done using Volocity software (Ver. 5.0.0) (see below).

2.7.5 Image processing and analysis with Volocity Software

Images captured with time-lapse microscopy were processed with Volocity software. Brightness, contrast, density and blackness were adjusted to obtain sharp images. To calculate transfer of newly synthesized lipids (green) to

performed LDs (red), areas with red staining were selected by choosing objects within a defined density range in the Cy3 channel and touching objects were separated. This selection was defined as areas of interest (performed LDs) and the same algorithm was applied to all time points for both WT and KO cells. Fluorescence intensity within areas of interest at each point was quantified for both GFP and Cy3 channels and presented as the percentage of initial fluorescent intensity (at time “0”).

2.8 Other methods

2.8.1 Generation and purification of rabbit anti-mouse TGH antibodies

Rabbits were immunized with a synthetic peptide corresponding to the C-terminus of mouse TGH conjugated to Keyhole Limpet Hemocyanin (KLH) (KLH-C-ESAQRPSHREHVEL). 0.5 mg of this antigen (0.5 ml) was combined with 0.5 ml of Freund's complete adjuvant, and the emulsion was injected subcutaneously into two rabbits. Two booster intramuscular injections were given at 4 week intervals with 0.5 mg of antigen in Freund's incomplete adjuvant. Rabbits were bled prior to (preimmune) and 8 weeks after the initial immunization; sera were prepared and titer was determined. The sera were then affinity purified with the same TGH peptide conjugated to BSA bound to a nitrocellulose membrane. The bound antibodies were eluted with 100 mM Glycine, pH 3.0, neutralized with 1 M Tris-HCl, pH 8.0, and dialyzed. The IgG concentration was determined by measuring OD₂₈₀.

2.8.2 *In vitro* lipase assay

An *in vitro* lipase activity was performed using the fluorogenic substrate 4-methylumbelliferyl heptanoate (4-MUH), which releases the fluorescent group 4-methylumbelliferone (4-MU) when hydrolyzed. A fluorometer, Fluoroskan Ascent FL Type 374 (Thermo LabSystems), was used to dispense substrates and measure the fluorescence intensity of 4-MU. Briefly, samples to be tested were loaded into a 96-well black masked microplate and brought to a total volume of 180 μ l in assay buffer (1 mM 4-MUH in 20 mM Tris-HCl, pH 8.0, 1 mM EDTA, 300 μ M taurodeoxycholate). Typically, 5 μ g cell lysate or 2 μ g microsomes were used for each well. Immediately before reactions, 1 mM 4-MUH substrate solution was prepared by diluting the 100 mM stock in the assay buffer listed above. The initiation of each enzymatic reaction was performed by automatically dispensing 20 μ l of substrate solution into each well (total volume 200 μ l; final substrate concentration 100 μ M). The plate was then agitated and read (excitation / emission: 355 / 460 nm) in a kinetic fashion every 20 sec for up to 5 min. Triplicate samples were measured. The amount of substrate hydrolyzed was quantified by comparing to a standard curve generated with standard solutions containing 4-MU (sodium salt). Data were analyzed using Ascent software version 2.4.2.

2.8.3 RNA isolation and real-time PCR for TGH expression

Total RNA from livers of WT or apoE KO mice was isolated using Trizol® reagent according to the manufacturer's instructions. First strand cDNA synthesis

from 2 µg of total RNA was performed using Superscript™ II reverse transcriptase primed by oligo (dT)₁₂₋₁₈ primers. Primers for the amplification of mouse TGH were: ' 5'-GGAGGGCAGGTGCTCTCA-3' and 5'-GCCTTCAGCGAGTGGATAGC-3'. The housekeeping gene cyclophilin was also amplified as an internal control. Primers for cyclophilin amplification were: 5'-TCC AAA GAC AGC AGA AAC TTT CG-3' and 5'-TCT TCT TGC TGG TCT TGC CAT TCC-3'. All primers were synthesized at the DNA Core Facility of the University of Alberta. PCR amplification of TGH cDNA was performed using the following conditions: 95 °C for 4 min, 94 °C for 30 seconds, 59 °C for 30 seconds, and 72 °C for 30 seconds, with repetitions of the second to fourth steps for 30 cycles, followed by a final elongation step at 72 °C for 5 min. Quantification of cDNAs was performed using Platinum® SYBR®Green qPCR SuperMix-UDG. Transcripts were detected by Rotor-Gene 3000 (Montreal Biotech, Montreal, Quebec, Canada) and analyzed with Rotor-Gene 6.0 software. A standard curve was used to calculate mRNA levels of TGH relative to that of cyclophilin.

2.8.4 Statistical Analysis

Data are presented as means ±S.D. unless otherwise stated. Statistical significance was evaluated by two-tailed Student's *t*-test.

Chapter III: Isolation and characterization of apolipoprotein B-free luminal lipid droplets

Portions of this work have been published in:

Wang, H., D. Gilham, and R. Lehner. 2007. Proteomic and lipid characterization of apolipoprotein B-free luminal lipid droplets from mouse liver microsomes: implications for very low density lipoprotein assembly. *J Biol Chem.* 282:33218-26.

3.1 Overview

It has been demonstrated that a large portion of TG incorporated into VLDL particles is derived from storage TG by the hydrolysis and reesterification cycle (Gibbons et al., 1992; Lankester et al., 1998; Yang et al., 1996). TGH was shown to be involved in mobilizing TG for VLDL assembly (Gilham et al., 2005a; Gilham et al., 2003; Lehner et al., 1999); however, it is not clear which TG pool TGH accesses. In vitro studies have indicated that apoB containing particles are not substrates for TGH (Gilham et al., 2005a). LLDs, the putative TG storage particles localized in the same compartment where VLDL assembly takes place, have been proposed to be involved in the second-step lipidation during VLDL assembly (Alexander et al., 1976; Hamilton et al., 1998; Raabe et al., 1999). However, LLDs have never been isolated and biochemically analyzed. Understanding the physical properties and lipid/protein composition of LLDs should provide insight into their physiological role and metabolic fate. In this study, I have isolated LLDs from mouse liver microsomes and analyzed their lipid and protein compositions. LLDs are variably sized particles relatively poor in TG content when compared to the lipid composition of CLDs. They are devoid of apoB, adipophilin and albumin but contain numerous proteins different from those found on CLDs, including TGH, Ces1/Es-x, MTP, and apoE. Ectopic expression of TGH in McA hepatoma cells resulted in decreased CLD-TG levels, demonstrating a role for TGH in the mobilization of hepatic neutral lipid stores.

3.2 Results

3.2.1 Isolation of LLDs

To isolate mouse liver LLDs, female C57BL/6J mice were fasted overnight in order to accumulate liver TG stores. The procedure used to isolate LLDs is illustrated in Figure 3-1. Livers from these mice were harvested and microsomes were prepared by subcellular fractionation. To release microsomal luminal contents, a hypotonic solution of 1 mM Tris-HCl (pH 8.8) was used instead of the commonly used alkaline Na_2CO_3 . This method preserves the integrity of LLDs without stripping loosely associated peripheral membrane proteins. Compared to 0.2 mM Na_2CO_3 (pH 12), 1 mM Tris-HCl released only about 1/4 of the total protein released by Na_2CO_3 , estimated by a protein concentration assay. The majority of the ER resident protein PDI was released by 0.2 mM Na_2CO_3 treatment and only a minor portion remained associated with microsomal membranes. In contrast, less than a half of the total PDI was released by 1 mM Tris-HCl treatment (Figure 3-2). However, the majority of lumenally localized apoB and TGH were released efficiently by the hypotonic buffer treatment (Figure 3-3).

Luminal contents include apoB-containing particles (VLDL and its precursors) in addition to LLDs. ApoB-containing particles were removed by immunoprecipitation with anti-apoB antibodies (Figure 3-3). The post-apoB immunoprecipitation (post-IP) supernatant contains non-apoB-associated luminal proteins including those associated with LLDs. The majority of TGH is recovered in this supernatant and is not present in the apoB immunoprecipitation pellet.

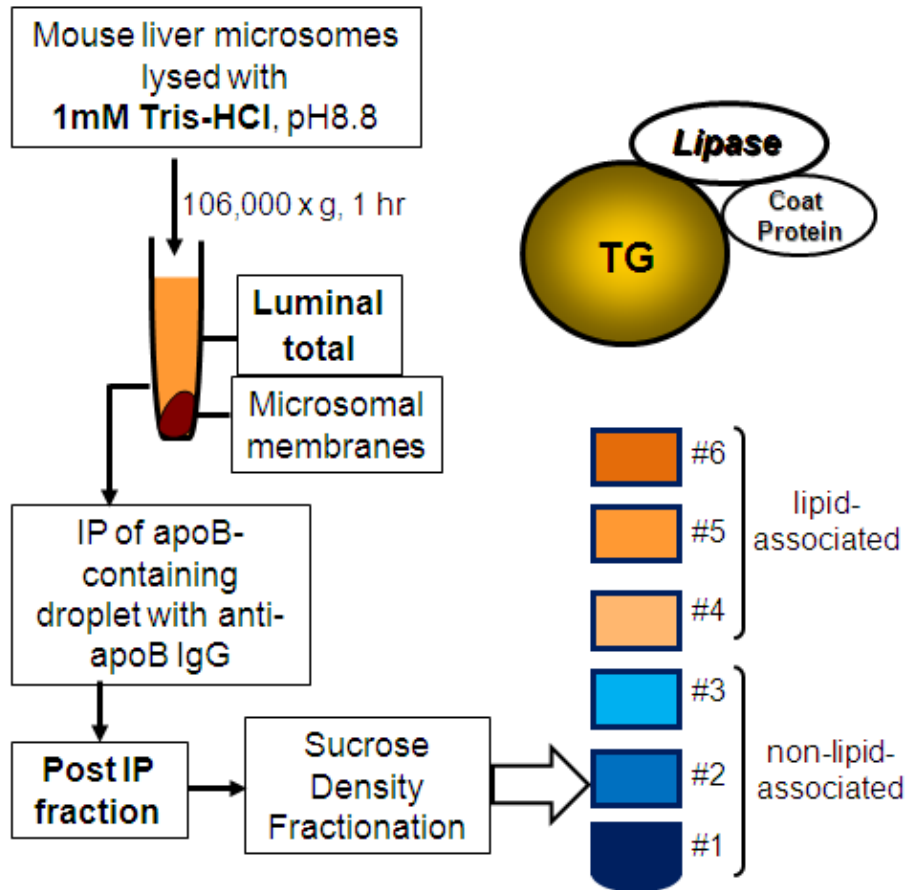


Figure 3-1. Isolation of LLDs. Microsomal luminal contents were released from mouse liver microsomes by incubating with 1 mM Tris-HCl (pH 8.8). The apoB containing components were removed by immunoprecipitation with α -apoB IgG, and the LLDs were subsequently isolated by sucrose density fractionation of the post-IP supernatant. See Chapter 2 for details.

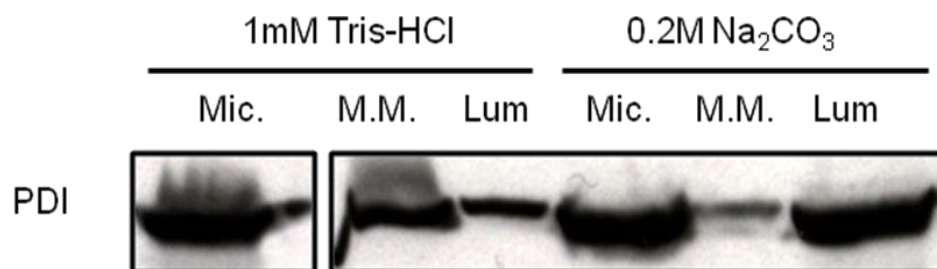


Figure 3-2. Release of PDI from the microsomal lumen. Salt-washed microsomes (Mic.) were suspended in either 1 mM Tris-HCl (pH 8.8) or 0.2 M Na₂CO₃ (pH 12), and centrifuged to prepare microsomal soluble luminal contents (Lum) and microsomal membranes (M.M.). Equal volumes of each sample were loaded and the release of PDI into the luminal fraction was determined. Na₂CO₃ released the majority of PDI while 1 mM Tris-HCl released less than a half of this ER resident protein.

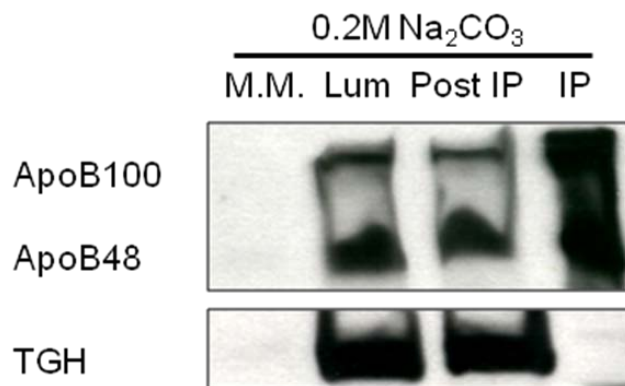
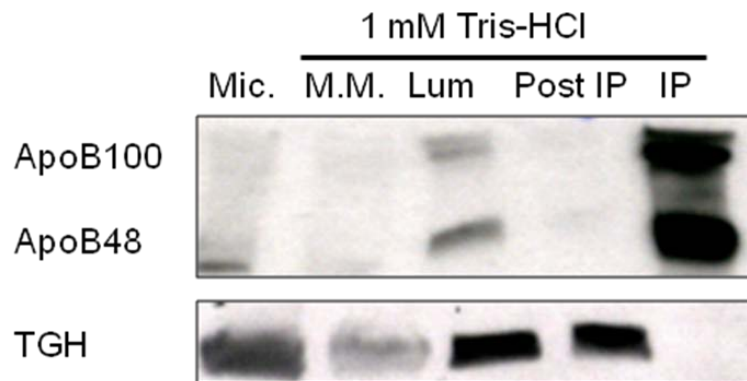


Figure 3-3. Release of TGH and apoB from the microsomal lumen. Salt-washed microsomes were centrifuged and resuspended in 1 mM Tris-HCl (pH 8.8) or 0.2 M Na₂CO₃ (pH 12), with a volume equals to 1/3 the volume of the original microsomes. Samples were then centrifuged to prepare microsomal soluble luminal contents (Lum) and microsomal membranes (M.M.). An equal volume of each sample was analyzed. The majority of TGH and apoB were released by 1 mM Tris-HCl and all were released by Na₂CO₃. ApoB was immunoprecipitated from luminal contents with anti-apoB antibodies using non-denaturing conditions to yield an immunoprecipitate (IP) and a post-IP supernatant (Post IP). Essentially all apoB was removed by IP from luminal contents released by 1 mM Tris-HCl.

LLDs were further isolated from the apoB-free post-IP fraction by glycerol-sucrose density centrifugation. Densities for the collected fractions are (from bottom to top): 1.1312, 1.1070, 1.0382, 1.0270, 1.0105 and 1.0036 g/ml, respectively. LLDs and the associated proteins were enriched in the top three fractions of the gradient. Lipid and protein composition of the LLD-associated fractions were analyzed and are discussed below.

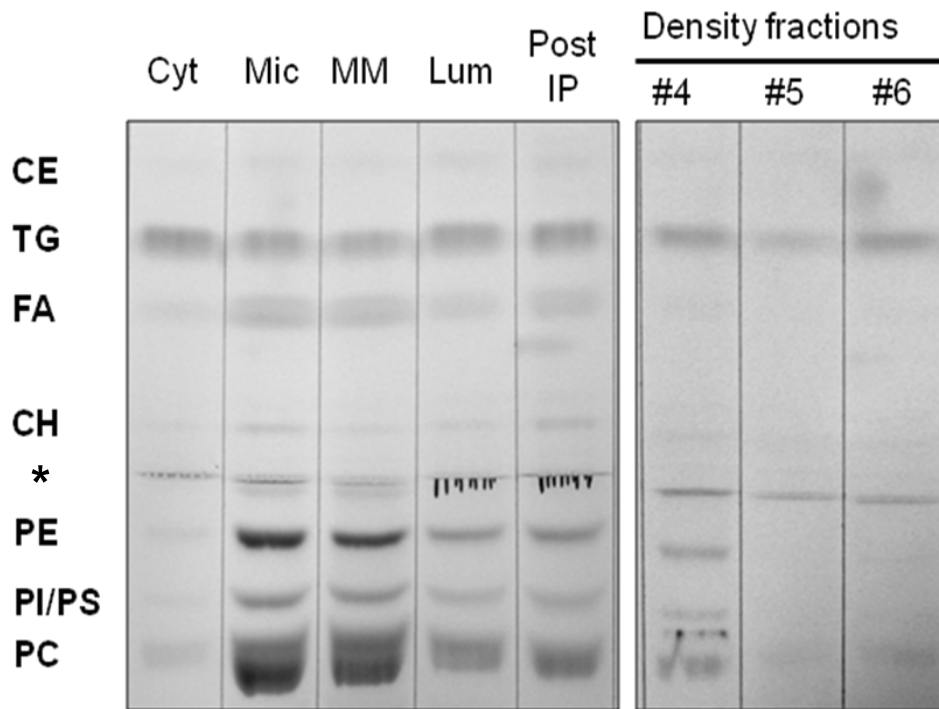
3.2.2 Lipid composition of LLDs

Lipid analysis of subcellular fractions isolated from fasted animals revealed that about 93% of cellular TG resided in the cytosol (CLDs) and 7% in microsomes. Thirty % of luminal TG associated with apoB and 70% was found in the post IP supernatant. The observed partition of TG to various subcellular locations suggested that LLDs comprise a very small pool (less than 3%, assuming that a half or less of the lipids residing in the lumen were released) of intracellular neutral lipid stores under fasted conditions.

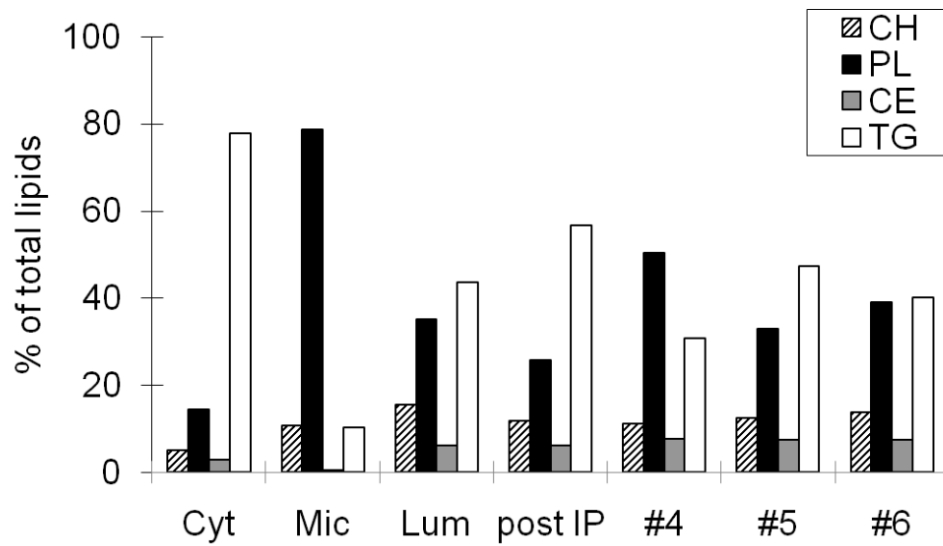
About half of the lipids present in the post-IP supernatant were recovered in LLDs. The lipid content of LLDs (fractions #4-6) was analyzed by thin-layer chromatography (Figure 3-4A) and gas chromatography (Figure 3-4B). Significant differences were found in the lipid composition of LLDs and CLDs. While CLDs contained about 80% TG and less than 20% glycerophospholipids, LLDs were less enriched in TG (ranging from 40% to 60%) and contained a near equal percentage of phospholipids (Figure 3-4A and 3-4B). Less TG and more PL in the lipid composition indicates that LLDs may be relatively small in size.

Figure 3-4. Lipid composition of LLDs. Cytosol (Cyt), microsomes (Mic), microsomal membranes (MM) and microsomal luminal contents (Lum) were isolated from mouse livers. Luminal contents were depleted of apoB by immunoprecipitation under non-denaturing conditions and the post-IP supernatants (Post IP) were subjected to density fractionation via centrifugation. Fractions were collected from the bottom of the gradient. Fractions #4-6 represent LLDs. Lipids were extracted and analyzed by TLC (**A**) and GC (**B**). For TLC analysis, livers from 3 mice (about 2.4 g) were homogenized in 12 ml homogenization buffer. Four ml of 1 mM Tris-HCl (pH 8.8) were used to resuspend/lyse microsomes and microsomal membranes. 0.5% of the total cytosolic fraction and 2.5% of the microsome-derived fractions were used for analyses. Figure is representative of three independent preparations. CE, cholesteryl ester; TG, triacylglycerol; Ch, unesterified (free) cholesterol; PL, phospholipids; PE, phosphatidylethanolamine; PC, phosphatidylcholine; PI, phosphatidylinositol; PS, phosphatidylserine; *, solvent interface.

A



B



3.2.3 Protein composition of LLDs

All biological lipid droplets contain a specific set of associated proteins. To determine the protein composition of LLDs, a proteomic approach was employed. Proteins present in combined fractions #4-6 were resolved by SDS-PAGE and individual protein bands were subjected to analysis by mass spectrometry (Figure 3-5 and Table 1). The LLD-associated proteins include TGH and a homologous protein of unknown function, carboxylesterase1/esterase-x (Ces1/Es-x), VLDL secretion related proteins (MTP and apoE), and ER resident proteins (such as PDI). The identification of MTP and apoE is of particular interest as these proteins are implicated participants in VLDL assembly. MTP has been suggested to play an important role in lipid transfer from the cytosol/ER membranes to the lumen of the ER (Jamil et al., 1995; Raabe et al., 1999; Wiggins and Gibbons, 1992). It forms an obligatory heterodimer with PDI (Wetterau et al., 1990), which was also found in the analysis (Table 1). Some mitochondrial and cytosolic proteins were also found in the analysis. They represent possible contaminants that were non-specifically adsorbed to the droplets during preparation. Importantly, transmembrane proteins from either the ER or the Golgi were not found in LLD preparations. The CLD coat protein, ADRP, was also absent from the LLDs both by proteomic and immunoblotting analyses, indicating the lack of contamination of LLDs with CLDs.

The presence of apoE and TGH in the LLD fractions was confirmed by immunoblotting (Figure 3-6). The LLDs were devoid of albumin (secretory protein), which partitioned to the bottom fractions of the gradient (fractions #1-3).

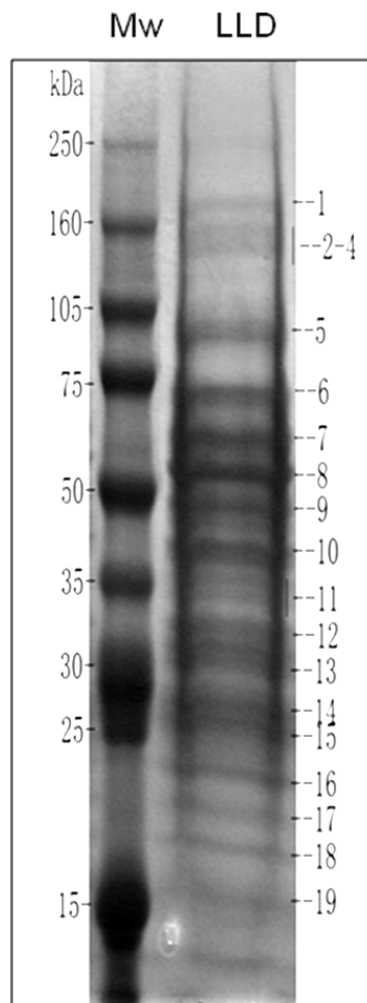


Figure 3-5. Protein profile of LLDs. Combined LLD fractions (fractions #4-6) were concentrated and subjected to SDS-PAGE followed by staining with Coomassie Blue. The identities of proteins indicated by numbers on the right are listed in Table 1. The protein profile is representative of three independent analyses.

Table 3-1. Identification of LLD associated proteins by Mass Spectrometry. LLD associated proteins separated by SDS-PAGE were identified by LC/MS/MS. Raw data obtained from the database were evaluated according to the significance of ion scores and species where matching peptides were found. Reproducible results from two independent experiments are presented.

| Category | Name | GI # | Band |
|------------------------|--|-------------|-------------|
| Carboxylesterases | triacylglycerol hydrolase (TGH) | 16716505 | 7,8 |
| | carboxylesterase 1(Ces1/Es-x) | 20070717 | 8 |
| VLDL secretion related | apolipoprotein E | 6753102 | 12 |
| | MTP | 15215161 | 5 |
| ER resident proteins | BiP | 2598562 | 6 |
| | tumor rejection antigen gp96 | 6755863 | 5 |
| | calreticulin | 13097432 | 9 |
| | protein disulfide isomerase | 860986 | 9 |
| | protein disulfide isomerase associated 3 | 6679687 | 9 |
| | protein disulfide isomerase associated 4 | 86198316 | 6 |
| | microsomal protease ER-60 | 1583929 | 9 |
| | sorbitol dehydrogenase 1 | 22128627 | 11 |
| | carbonic anhydrase III | 10717134 | 14 |
| Possible contaminants | heat shock protein 70 | 1661134 | 6 |
| | albumin | 26986064 | 7,8 |
| | clathrin heavy chain 1 | 51259242 | 1,2 |
| | complement component 3 | 23956044 | 2 |
| | transferrin | 17046471 | 6 |
| | catalase | 1066114 | 8 |
| | alcohol dehydrogenase 1 (class I) | 32449839 | 11 |
| | regucalcin | 6677739 | 13 |
| | ribosomal proteins | multiple | 15-19 |

Interestingly, although both TGH and apoE partitioned into LLDs, the levels of the two proteins varied in the individual fractions, suggesting a degree of heterogeneity in the LLD protein composition.

3.2.4 LLDs are heterogeneous in size

The unique lipid composition of LLDs (Figure 3-4) suggested that these particles might be relatively dense, resembling high-density lipoproteins in size. Gel filtration chromatography of apoB-free luminal contents was performed to determine the size of LLDs (Figure 3-7A). Surprisingly, TG was eluted in three distinct peaks with sizes corresponding to VLDL, HDL, and smaller-than-HDL. The peak at >54 min corresponds to the elution of free glycerol. The source of luminal glycerol is unclear; however, it might be derived from lipolysis of membrane or luminal lipids.

Eluted fractions from the sizing column were collected and analyzed for the presence of TGH, apoE and MTP (Figure 3-7B). TGH was present in most fractions (26-58 min), with the highest enrichment in particles corresponding to small HDL (42-50 min). Interestingly, apoE co-eluted with TGH in the larger molecular mass fractions (presumably less dense LLDs), while MTP co-eluted with TGH on smaller particles. No significant levels of MTP co-eluted with apoE. It is unlikely that apoE or TGH are present as free proteins in the lipoprotein-sized fractions. The M_r of apoE and TGH are about 35 and 60 kDa, respectively, and the M_r of the obligate MTP/PDI heterodimer is approximately 150 kDa. Neither TGH nor apoE were detected to any significant amount in fractions 22-25

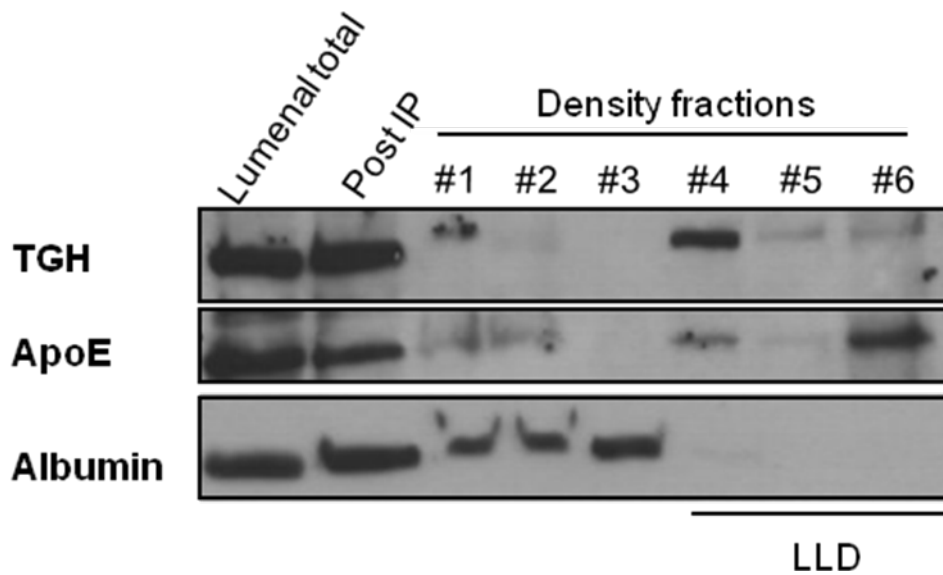


Figure 3-6. Protein profile of LLDs. Microsomal luminal contents and fractions from density centrifugation were analyzed for the presence of TGH, apoE and albumin by immunoblotting. LLD fractions were concentrated 15-fold before analysis. The result is representative of several preparations.

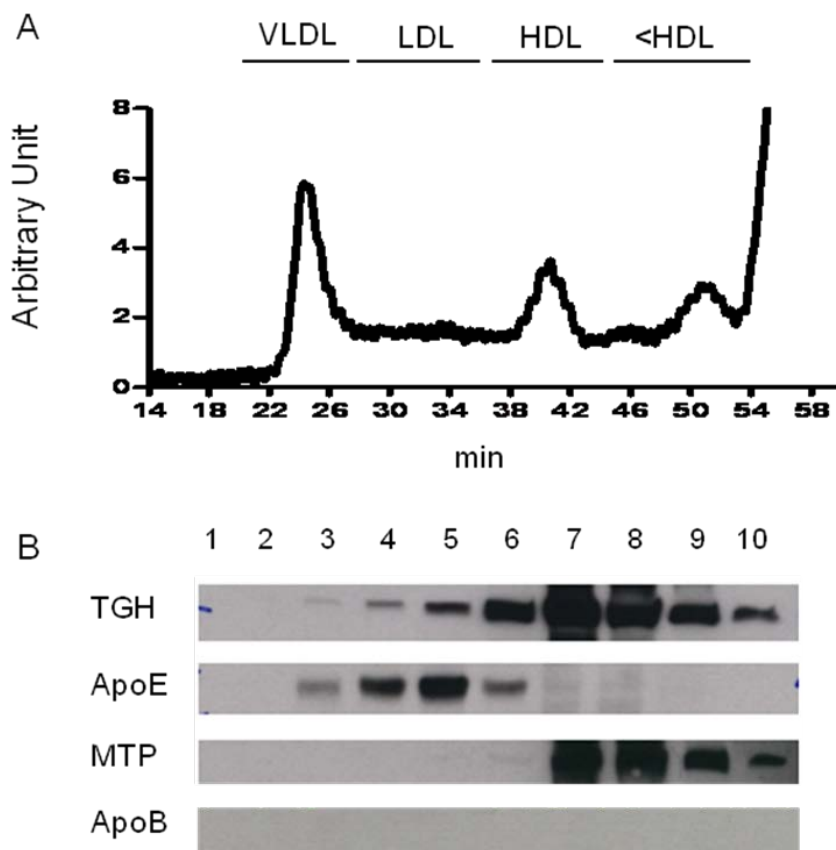


Figure 3-7. TGH associates with small LLDs that may contain apoE or MTP, but not apoB. (A) FPLC gel filtration profile of microsomal luminal apoB-free contents. Post-apoB immunoprecipitation supernatant was applied to a FPLC gel filtration column and fractions were assayed for the presence of TG, as described in **Chapter 2**. The elution profile of plasma lipoprotein standards (VLDL, LDL, HDL) is indicated. (B) Fractions were collected every four minutes (2 ml fractions), and proteins were precipitated with ice-cold acetone. The presence of TGH, apoE and MTP were assessed by immunoblotting. Each lane corresponds to fractions eluted from: 1, 18-21 min; 2, 22-25 min; 3, 26-29 min; 4, 30-33 min; 5, 34-37 min; 6, 38-41min; 7, 42-45 min; 8, 46-49 min; 9, 50-53 min; 10, 54-57 min.

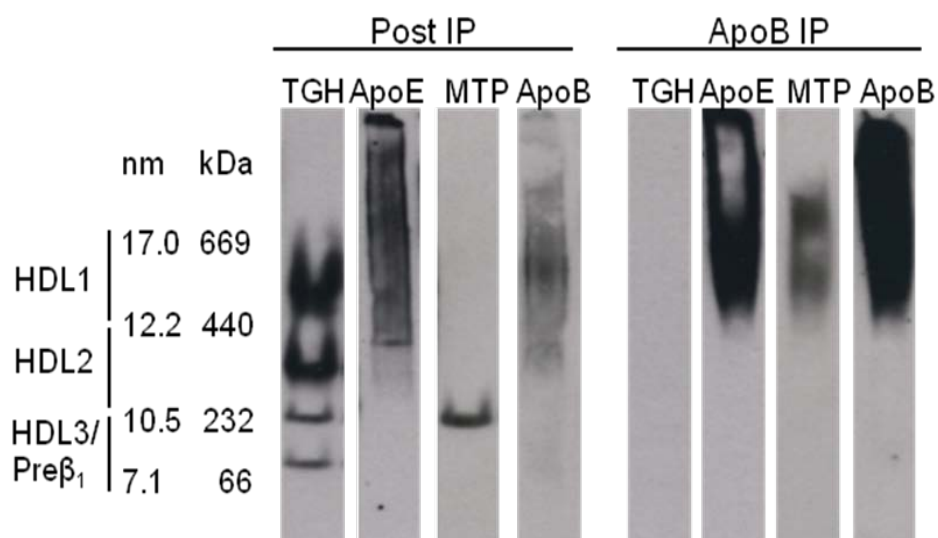


Figure 3-8. TGH associates with small LLD that may contain apoE or MTP but not apoB. ApoB was immunoprecipitated from luminal contents and beads (apoB IP) and supernatants (Post IP) were resolved by 2-10% native PAGE. The presence of TGH, apoE, MTP and apoB were determined by immunoblotting. Mobility of known lipoprotein standards and the sizes of molecular mass markers are indicated on the left.

corresponding to VLDL-sized particles and none of the fractions contained immunodetectable apoB100 or apoB48 even after overexposure of the film.

Similar results were obtained when post-IP contents were analyzed using a native gradient PAGE approach (Figure 3-8, left panel). TGH migrated as four distinct bands corresponding to relatively small particles ranging in size from HDL1 (17.0 nm) to HDL3 (10.5 nm). ApoE migrated as a smear corresponding to sizes larger than HDL2 (12.2 nm) that partially overlapped with TGH containing particles. MTP migrated as a distinct band with the size of HDL3 (10.5 nm), overlapping with one of the TGH bands, but not with apoE. A small amount of residual apoB was found in the post-IP fraction in this preparation. Immunoprecipitated luminal apoB-containing lipoproteins exhibited slower mobility as expected for larger-size particles (Figure 3-8, right panel). Both apoE and MTP were present in the apoB immunoprecipitation pellet, which is in agreement with published data (Bradbury et al., 1999; Hussain et al., 1997; Wu et al., 1996), while TGH was absent, supporting previous results (Gilham et al., 2005a).

3.2.5 TGH is mainly present in the ER but not Golgi

The microsomal fraction contains both ER and Golgi membranes. To evaluate whether the isolated LLDs were from the ER and Golgi, subcellular fractionation was performed as described in 2.5.3. Western blotting confirmed that the isolated Golgi fraction was enriched in the Golgi marker, mannosidase II, while the ER fraction was enriched in the ER membrane protein, calnexin (Figure 3-9A). TGH

was found mainly in the ER, while a small amount was also found in the Golgi, likely due to contamination from the ER. The secretory protein apoE was found enriched in both ER and Golgi fractions (Figure 3-9A). TG content in both ER and Golgi-derived fractions were analyzed by GC to assess the proportion of luminal lipids in these compartments (Figure 3-9B). Because ER and Golgi have different levels of recovery during preparation, membrane, luminal, apoB-associated or apoB-free TG in each compartment was calculated as the percentage of total TG in the corresponding compartments. Golgi seems to contain ~8 times more TG than the ER (1874.2 $\mu\text{g}/\text{mg}$ protein in Golgi and 224.1 $\mu\text{g}/\text{mg}$ protein in ER). The majority of TG in the Golgi was associated with membrane while about equal amounts of membrane and luminal TG were found in the ER. It is difficult to evaluate the exact proportion of apoB-associated versus apoB-free TG because very low values were obtained from GC analysis in the luminal fractions.

3.2.6 TGH decreases neutral lipid stores

TGH has been shown to play a role in the mobilization of intracellular neutral lipid stores for VLDL assembly (Gilham et al., 2005a; Gilham et al., 2003; Lehner et al., 1999; Wei et al., 2007a). However, it is not entirely clear which lipid pool TGH accesses. The association of TGH with LLDs suggested that LLDs are the likely TG storage pool utilized by TGH for VLDL assembly. To explore this hypothesis, McA cells stably transfected with human TGH cDNA, as well as wild type McA cells (lacking TGH expression), were incubated with [^3H]OA and examined for intracellular and secreted lipid content. Surprisingly, no

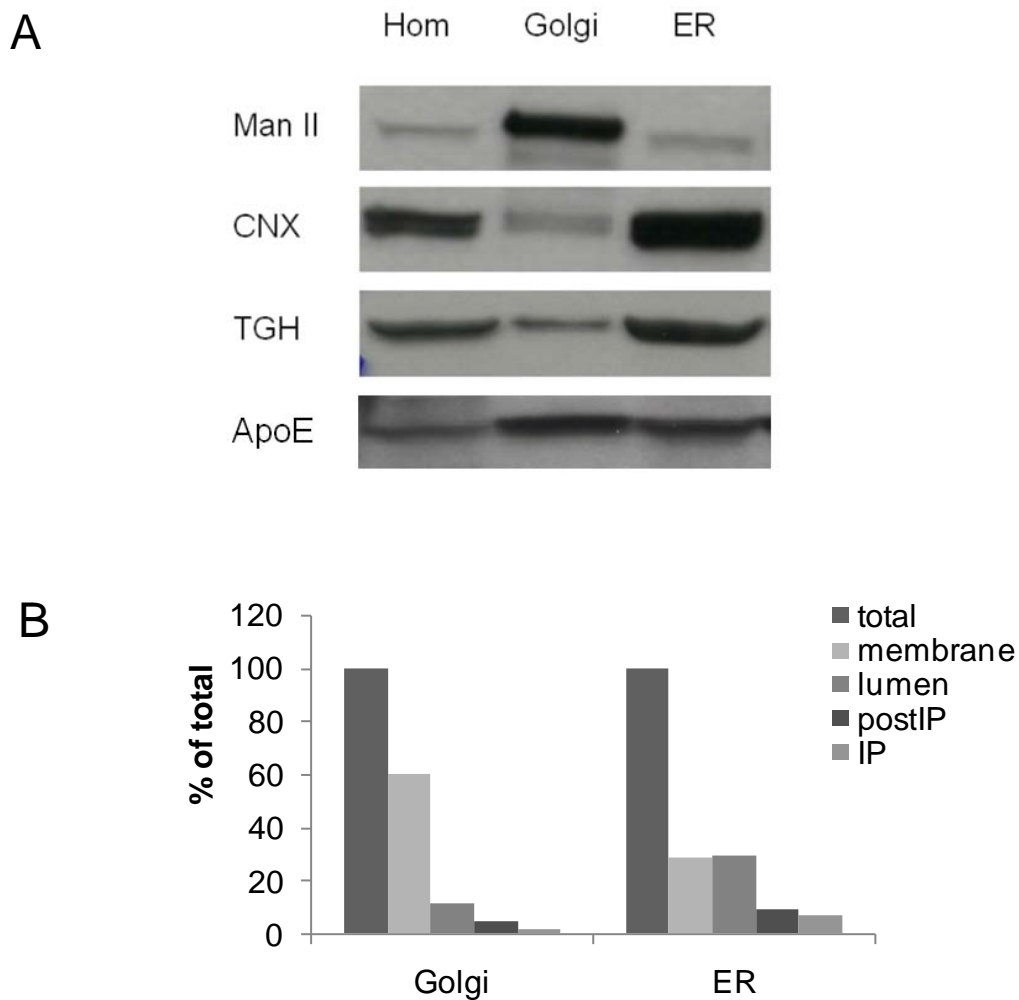


Figure 3-9. Analysis of subcellular fractions from mouse liver. (A) protein composition. Enrichment of TGH was obtained in the ER fraction (ERI and ERII combined) but not the Golgi fraction. ApoE was enriched in both ER and Golgi fractions. Hom: total liver homogenate. Man II, mannosidase II; CNX, calnexin (CNX). (B) TG content in ER and Golgi. Membrane, luminal, apoB-associated (IP) or non-apoB-associated (postIP) TG in Golgi or ER were analyzed by GC and calculated as the percentage of the total Golgi or ER TG.

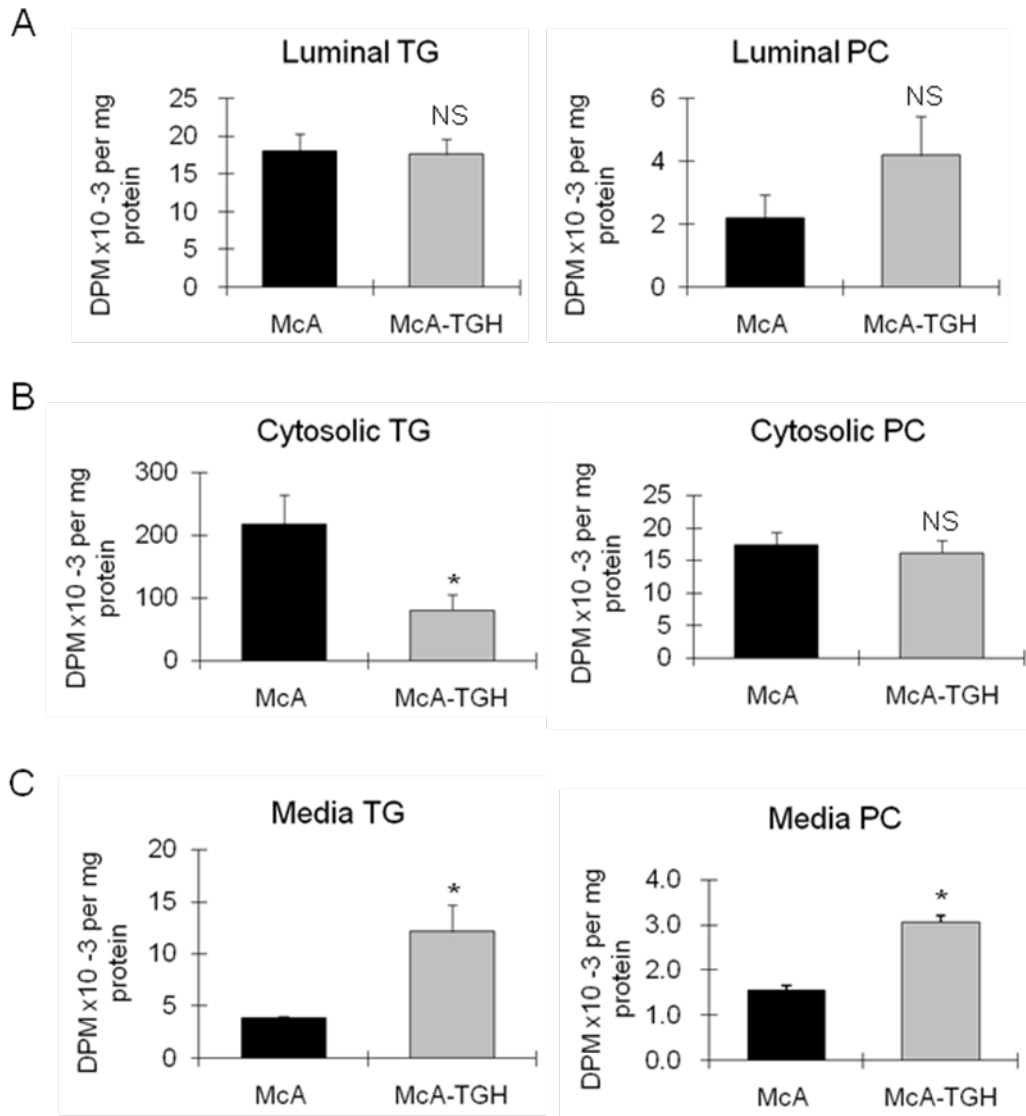


Figure 3-10. Ectopic expression of TGH decreases neutral lipid stores in McA cells. Wild type McA cells or McA cells stably expressing human TGH (McA-TGH) were incubated with [³H]OA for 4hr. Cells were homogenized, LLDs (A) and CLDs (B) were isolated, and media (C) were collected. Lipids were extracted and separated by thin-layer chromatography. Radioactivity associated with TG and PC was determined by scintillation counting. *, $p < 0.01$; NS, not significant.

decrease in luminal TG in TGH-expressing cells was observed (Figure 3-10A). However, when levels of cytosolic lipids were examined in parallel, a marked decrease in TG labeling was observed in TGH expressing cells (Figure 3-10B), while no significant changes in PC labeling were seen in either luminal or cytosolic content. Correspondingly, a 3-fold increase in media TG labeling was obtained from TGH-transfected cells (Figure 3-10C), suggesting that TGH mediates alterations in intracellular neutral lipid stores and the redirection of the lipolytic products to VLDL secretion.

3.3 Discussion

To our knowledge, this is the first study reporting isolation and characterization of hepatic LLDs that may serve as a reservoir of lipids for VLDL assembly. The isolation was performed using conditions that did not affect LLD integrity and did not strip peripherally associated proteins. CLDs contain a phospholipid monolayer and specific coat proteins that play a role in droplet metabolism (**Section 1.3.1**). This study suggests that like the CLDs, LLDs also contain a variety of proteins on their surfaces. The LLD proteome differs significantly from that of CLDs, which is expected, given their physical separation in distinct subcellular compartments. Some proteins were common for both LLDs and CLDs, such as the chaperone protein BiP, which predominantly localize in the ER, suggesting continuity of LDs with the ER bilayer, or derivation of both LDs from the ER. Neither transmembrane proteins nor known CLD coat proteins (ADRP, TIP-47) were found on LLDs. Instead, LLDs contained apoE, which may perform a lipid

droplet coat function, and MTP, which plays a crucial role in apoB-containing lipoprotein assembly (Davis, 1999; Gordon and Jamil, 2000). Genetic ablation of apoE in mice results in the impairment of VLDL-TG secretion (Kuipers et al., 1997; Kuipers et al., 1996; Mensenkamp et al., 2001) and leads to intracellular accumulation of lipids (Mensenkamp et al., 2004). Conversely, overexpression of apoE in mice promotes VLDL-TG production (Maugeais et al., 2000). Interestingly, recent *in vitro* experiments demonstrated that large VLDL can be secreted from apoE-deficient hepatocytes when these cells are supplemented with exogenous FA (Gusarova et al., 2007), suggesting that apoE is not absolutely required in this process. Although a definitive role for apoE in VLDL assembly and secretion has not been demonstrated, an enticing hypothesis is that apoE may be involved in the mobilization of LLDs for lipidation of apoB. Because apoE and TGH are both present on LLDs, it is possible that apoE plays a role in modulating TGH function. This aspect of apoE will be explored in **Chapter 5**. MTP has also been implicated in the biogenesis of LLDs, in addition to its crucial role in the co-translational/co-translocational lipidation of apoB. Genetic ablation of MTP expression (Raabe et al., 1999) or chemical inhibition of MTP activity (Kulinski et al., 2002; Wang et al., 1999) was shown to decrease LLD levels. The observed co-migration of MTP with LLDs supports its proposed role in LLD generation. MTP may also be involved in transporting lipids (phospholipids, TG and CE) from LLDs to nascent apoB-containing particles (Gordon et al., 1996; Mitchell et al., 1998; Rustaeus et al., 1998). Another protein of interest found associated with LLDs is Ces1/Es-x. Ces1/Es-x shares a high degree of homology with TGH and

therefore may play a role in hepatic lipid metabolism (Dolinsky et al., 2004; Ellinghaus et al., 1998).

Compared to CLDs that contain 80% TG (Fig 3-4B), LLDs have higher phospholipid/TG ratios. Because phospholipids form a lipid monolayer surrounding the neutral lipid core of LDs, the higher phospholipid/TG ratio found in LLDs suggests smaller particles. Gel filtration chromatography revealed that the apoB-free lipid particles are heterogeneous, ranging from the size of VLDL to smaller than HDL. LLDs of various sizes might represent particles with different roles or particles at different stages of biogenesis/hydrolysis. TGH associates primarily with the smaller HDL-size lipid droplets and is absent from the larger VLDL-size particles.

Several groups have reported that the maturation of VLDL (the addition of bulk lipid to primordial apoB lipoproteins) may occur in the Golgi (Bamberger and Lane, 1990; Gusarova et al., 2003; Valyi-Nagy et al., 2002; Yamaguchi et al., 2003). One of the key questions that needs to be resolved in the Golgi-localized apoB-lipidation model is the source of non-lipoprotein associated TG in the Golgi. Because TG is synthesized by the ER-localized acyltransferases DGAT1 and DGAT2 (Man et al., 2006; Stone et al., 2006), LLDs generated in this organelle would be required to be sorted into transport vesicles and exported to the Golgi. However, some LLDs, at least the subpopulation that bears TGH, could not undergo this transport process because TGH is exclusively localized to the ER and has not been detected in the Golgi (Gilham et al., 2005a). Therefore, non-TGH-containing LLDs would have to be sorted from TGH-containing LLDs into

transport vesicles in the ER before being exported to the Golgi. It is likely that LLDs in the Golgi would be depleted of other ER proteins identified in our screen but would not be expected to acquire any new proteins since the Golgi does not contain any luminal resident proteins. ApoE and apoB were reported to be present in different subpopulations of ER-derived transport vesicles (Gusarova et al., 2007), and thus it is possible that apoE-containing LLDs that do not contain TGH are transferred to the Golgi. In support of this hypothesis, enrichment of apoE was found in the Golgi compartment by subcellular fractionation (Figure 3-9). A small amount of TGH was found in the Golgi by this approach likely due to contamination from the ER since a small amount of the ER resident protein calnexin was cofractionated with TGH in the Golgi.

Previous metabolic labeling studies in our laboratory showed that expression of TGH in McA cells significantly increased the turnover of preformed TG (Lehner and Vance, 1999a) and that inhibition of TGH in hepatocytes had the opposite effect (Gilham et al., 2003). In this study, cytosolic neutral lipid levels were depleted markedly in TGH-expressing McA cells, but no significant decrease of luminal neutral lipid levels was observed (Figure 3-10). Because luminal TG comprises a relatively minor fraction of total TG storage in hepatocytes, these studies suggested TGH-mediated depletion of cytosolic TG pools in addition to mobilization of luminal TG for VLDL assembly. It is not clear how TGH, a luminal lipase, would access cytosolic TG. One possibility is that TG could egress from CLDs that are in continuum with the ER membrane and TGH would mobilize such membrane-associated TG. Up to 3 mol% of TG

can be solubilized within phospholipid membranes without disturbing bilayer structures (Hamilton, 1989; Hamilton and Small, 1981; Spooner and Small, 1987). Because proteomic analyses of CLDs identified the presence of ER resident proteins, such as BiP and calnexin (Brasaemle et al., 2004; Liu et al., 2004), it is also plausible that CLD-ER association represents a hemifusion of the cytosol-facing phospholipid monolayer of the ER with a phospholipid monolayer surrounding CLDs, providing access of luminal ER proteins (TGH, MTP) to CLDs. LLDs may represent intermediate reservoirs that regulate the transfer of neutral lipids from CLDs to VLDL. The proposed model is shown in Figure 3-11. In this model, TG for the lipidation of primordial apoB containing particles is provided through lipolysis/reesterification of pre-existing ER-associated TG pools. TG that is in excess can be returned to either LLDs or to CLDs (futile cycle). An unresolved issue regards the possible access of TGH and MTP to cytosol-derived TG. If hemifusion of the ER leaflet with CLDs takes place, TG would be expected to become available for either hydrolysis by luminal lipases or for binding to MTP.

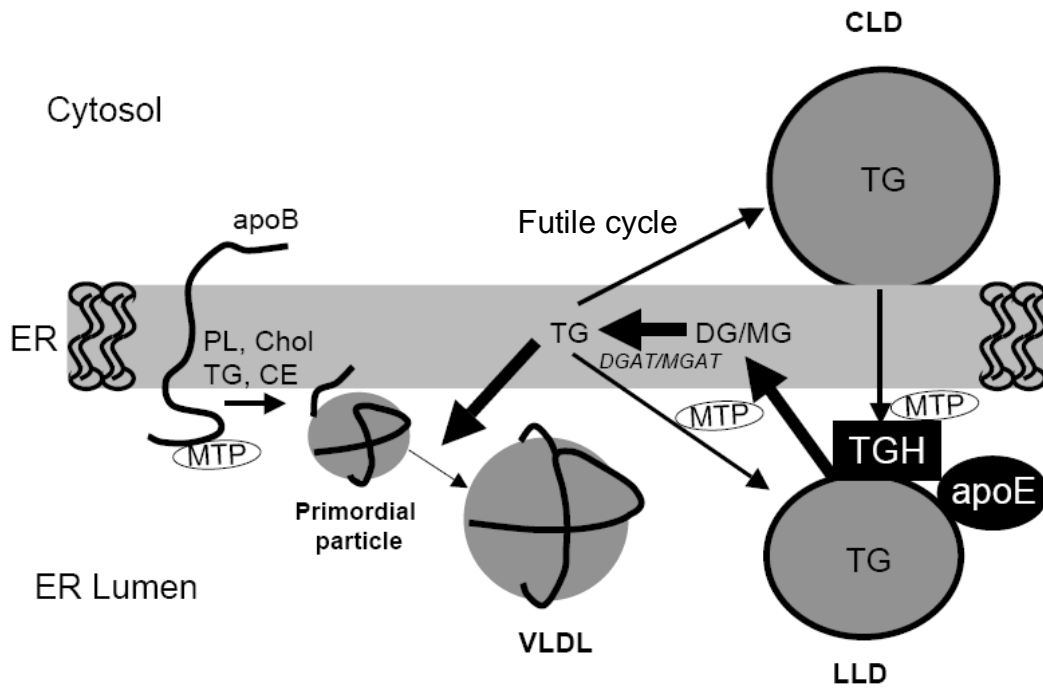


Figure 3-11. Model for the role of LLDs in VLDL assembly. TGH localizes to the lumen of the ER, associates with LLDs and mobilizes this pool of TG for VLDL assembly. The hydrolysis of TG by TGH may be modulated through interactions with apoE. LLDs serve as a direct source for VLDL-TG. TG from the CLDs replenishes LLDs. The transfer of TG from CLDs to LLDs may involve MTP and TGH. Excessive TG can be returned to either LLDs or to CLDs (futile cycle).

Chapter IV: Role of triacylglycerol hydrolase in cytosolic lipid droplet biogenesis

This work has been submitted and is currently under revision:

Wang, H, Wei E, Quiroga A, Sun X, Touret N, and Lehner R. 2009. Altered lipid droplet dynamics in hepatocytes lacking triacylglycerol hydrolase expression. *Mol Biol Cell*.

4.1 Overview

Luminal TG makes up only a small portion of total hepatic TG (Wang et al., 2007). Metabolic labeling studies described in the previous chapter have revealed that ectopic expression of TGH in McA cells resulted in decreased TG levels not only in LLDs but also in CLDs. Therefore, it is hypothesized that TGH may gain access to cytosolic TG and regulate CLD metabolism. In this study, we investigated TGH-mediated changes in LD dynamics. We have found that TGH deficiency resulted in decreased size and increased number of LDs in hepatocytes. Using fluorescent fatty acid analogues to trace LD formation, we observed that TGH deficiency did not affect the formation of nascent LDs on the ER. However, the lipid transfer rate from nascent LDs to preformed LDs was significantly slower in the absence of TGH. Therefore, altered maturation (growth) rather than nascent formation (de novo synthesis) may be responsible for the observed morphological changes of LDs in TGH deficient hepatocytes. It is suggested that a TGH-dependent mechanism and an alternative mechanism could coexist and regulate LD maturation in hepatocytes.

4.2 Results

4.2.1 TGH is localized in the ER surrounding cytosolic LDs

To address the potential interaction of TGH with cytosolic LDs, hepatocytes transfected with a cDNA encoding TGH-EGFP fusion protein were incubated with OA, and subcellular localization of TGH-EGFP and LDs was observed using confocal microscopy. TGH-EGFP is excluded from the nucleus and assumes the

expected ER localization manifested by a reticular pattern throughout the cells (Figure 4-1A). TGH-EGFP also localized extensively to areas surrounding the cytosolic LDs (Figure 4-1A, right panel). However, the resolution of confocal microscopy precludes the possibility of determining unequivocally whether TGH resides in the ER surrounding the LDs, or whether it physically associates with LDs. Subcellular fractionation was performed to address this question. The results revealed that TGH predominantly co-fractionated with the microsomal fraction together with the ER resident protein PDI and the ER polytopic membrane protein PEMT (Figure 4-1B). The LD fraction was enriched in the known LD coat protein ADRP (Figure 4-1B).

4.2.2 Ablation of TGH leads to cytosolic TG accumulation in hepatocytes

We have shown (Wang et al., 2007) that ectopic expression of TGH in McA cells led to decreased cytosolic TG accumulation, suggesting that TGH activity can either prevent cytosolic LD formation or increase LD turnover. To address the role of TGH in cytosolic LD homeostasis we utilized primary hepatocytes isolated from mice in which *Tgh* expression has been genetically ablated. Our working hypothesis was that lack of TGH expression would increase OA-mediated TG accumulation in the cytosol. As expected, there is a 2.8-fold increase in the cytosolic TG level in TGH deficient (KO) hepatocytes incubated with OA compared to WT cells (Figure 4-2A). Correspondingly, a 1.7-fold increase in ADRP was also observed (Figure 4-2B).

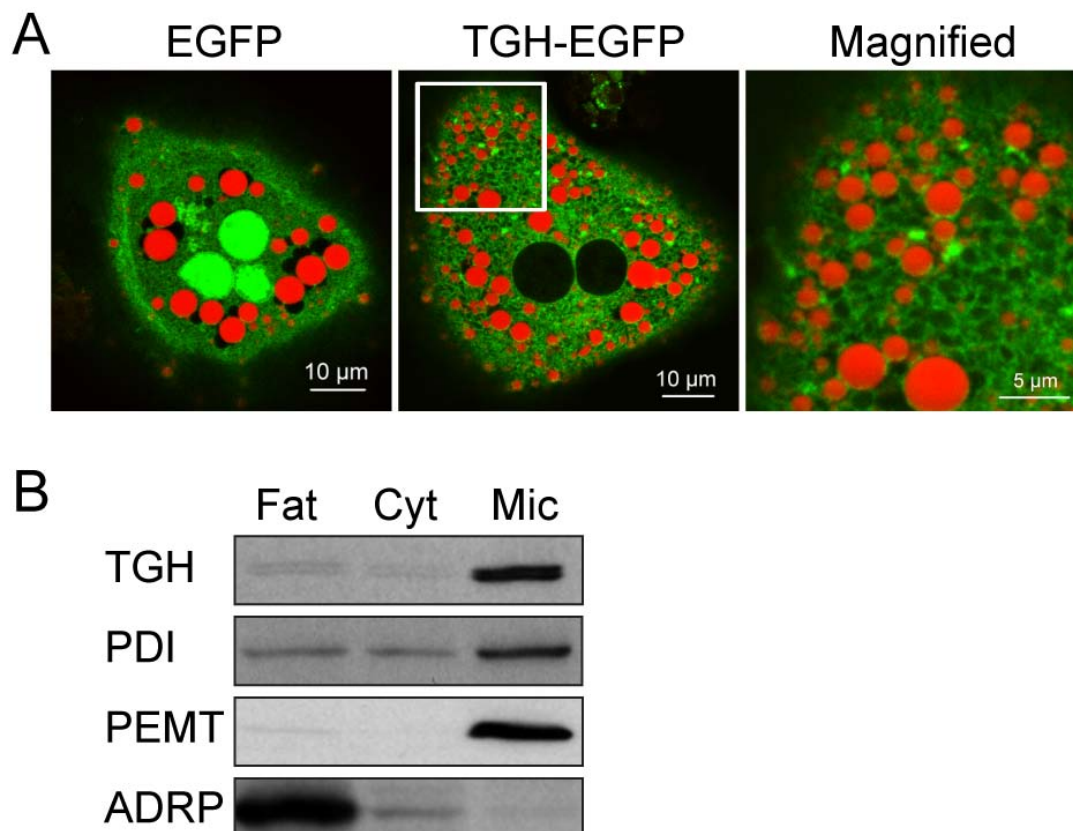


Figure 4-1. TGH is localized in the ER surrounding cytosolic LDs. (A) Confocal images of hepatocytes transfected with plasmids encoding EGFP or TGH-EGFP. Green, EGFP; red, Nile Red (LDs). A close up of the area within the white box is shown as “Magnified”. TGH is found in close proximity to LDs. Bar: 10 μ m (EGFP and TGH-EGFP) and 5 μ m (Magnified). (B) Endogenous TGH cofractionates with LDs (fat cake) and microsomes. Subcellular fractions from mouse liver homogenates were obtained as described under the “Materials and Methods”. An equal volume from each fraction was analyzed. Fat, fat cake; Cyt, cytosol; Mic, microsomes.

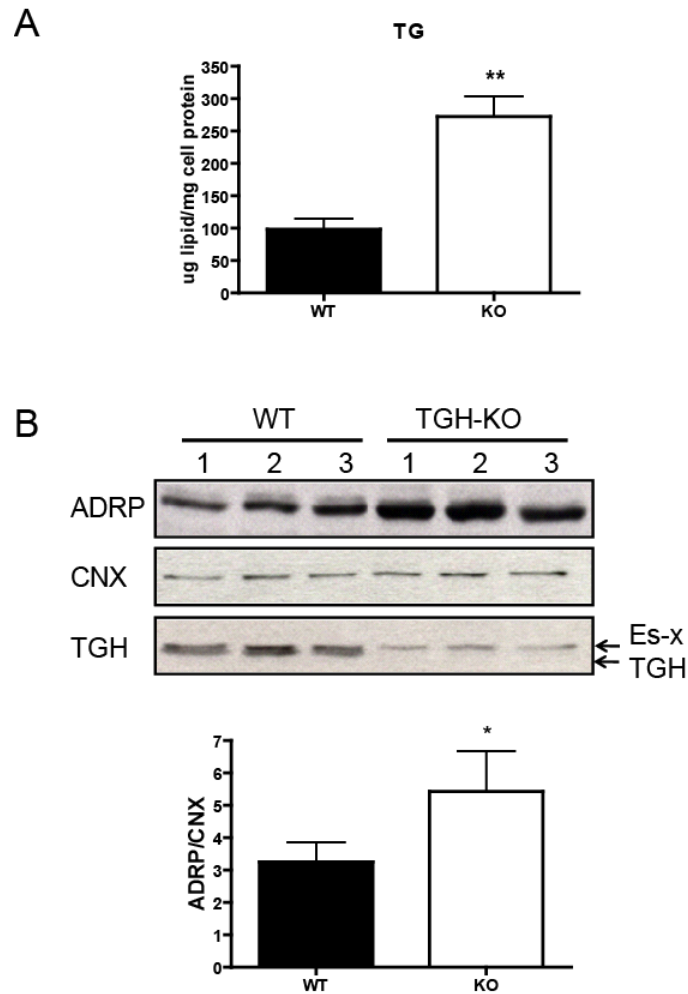


Figure 4-2. Ablation of TGH leads to TG accumulation in OA treated hepatocytes. WT and TGH KO hepatocytes were incubated overnight with DMEM containing 0.4 mM oleic acid complexed to 0.5% BSA. Three dishes of each cell type were analyzed. **(A)** Cytosol fractions were isolated from cell homogenates and TG mass was determined by GC. **(B)** Cell homogenates were analyzed for ADRP, calnexin (CNX) and TGH levels by western blotting. Twenty μ g of cell protein from cell homogenates were analyzed. ADRP levels were determined by densitometry and normalized to calnexin. Note that anti-TGH sera recognize both TGH (lower band) and a protein highly homologous to TGH, Es-x (upper band). *, $p < 0.05$; **, $p = 0.001$.

4.2.3 Ablation of TGH alters the morphology of LDs

Freshly isolated TGH-deficient hepatocytes from fasted mice contained LDs that were significantly smaller in size but more numerous compared to those in control (WT) cells (Figure 4-3A, B). The size of LDs varies from below $0.01 \mu\text{m}^2$ to up to $50 \mu\text{m}^2$. Although the majority of LDs was below $10 \mu\text{m}^2$ in both genotypes, WT cells contained more LDs larger than $10 \mu\text{m}^2$ (Figure 4-3C, D). TGH-deficient cells exhibited a 34% decrease in the average area of an individual LD, but 45% increase in LD number. As a result, total LD area (fluorescent area) was comparable to that in control cells (Figure 4-3E), indicating similar TG content. It is important to note that these results were obtained from freshly isolated hepatocytes from fasted mice without incubation with OA and thus reflect *in vivo* conditions, distinct from conditions used in Figure 4-2. The lack of hepatic TG accumulation in TGH deficiency agrees with the proposed role of TGH in fatty acid mobilization from adipose tissue (Soni et al., 2004; Wei et al., 2007b). Our recent studies also indicate that fasting hepatic TG levels in TGH deficient mice were not significantly different from that in WT mice due to decreased FA influx from the adipose tissue (unpublished data).

4.2.4 TGH deficiency does not alter the formation of nascent LDs

LDs are dynamic intracellular bodies that are initially formed as nascent particles probably at the site of TG synthesis on the ER. This is followed by expansion through additional transfer of lipids into the preformed LDs and finally lipolysis

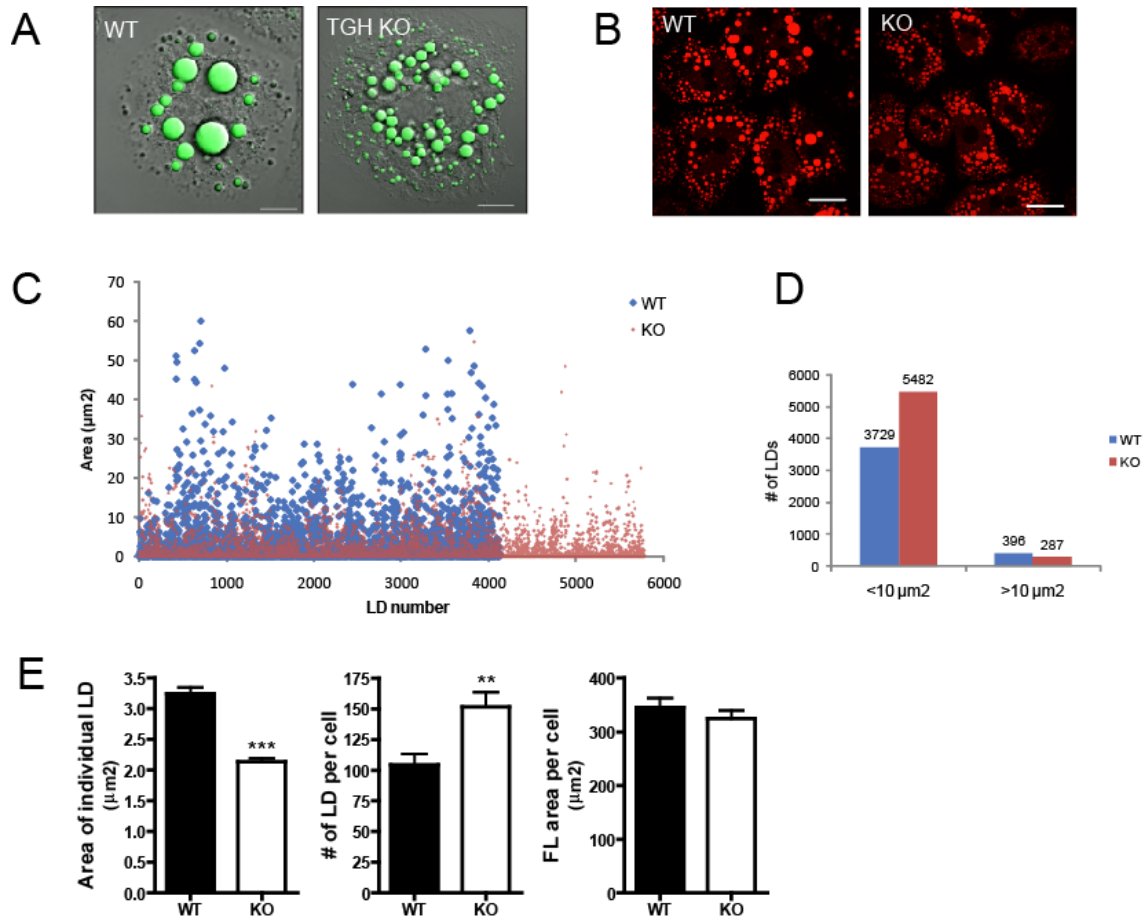
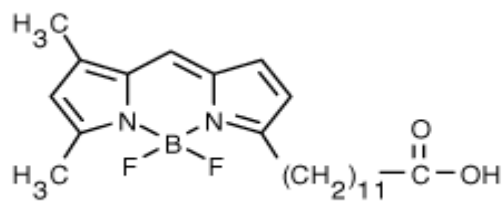


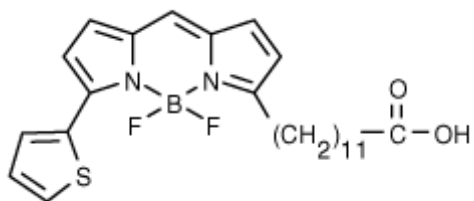
Figure 4-3. TGH affects LD morphology. Freshly isolated WT or TGH KO hepatocytes were incubated with DMEM+10%FBS for 4 h without OA supplementation. LDs in WT or TGH KO hepatocytes were stained with Bodipy 493/503 and visualized by confocal microscopy. **(A)** Morphology of LDs in representative cells. Bar, 10 μm. **(B)** A representative field containing multiple cells stained with Nile Red. Bar, 20 μm. **(C)** Images of 38 random cells from each genotype were captured at the centre slice and analyzed by MetaMorph for their LD numbers and areas. Results from all 38 cells were pooled and graphed in a scatter plot. Each data point represents an individual LD. **(D)** Numbers of LDs with areas <10 μm² or >10 μm² were counted and presented in a bar graph. **(E)** Average area of an individual LD, number of LDs per cell, and total area of LDs per cell were quantified. **, p=0.001; ***, p<0.0001. Data are presented as means ± SEM.

of LD-associated TG for energy production and other cellular events. Because we have previously demonstrated that TGH is involved in hepatic TG metabolism (Gilham et al., 2003; Lehner and Vance, 1999b; Wang et al., 2007; Wei et al., 2007a) and that TGH is localized to the ER where TG synthesis and therefore biogenesis of LDs occurs, we rationalized that TGH activity might regulate LD dynamics. We wished to first address whether TGH plays a role in nascent LD formation. To this end, we introduced fluorescent FA analogues (Figure 4-4) as tracers for TG synthesis and the integration of TG into LDs. The two FA analogues used were Bodipy 558/568 C₁₂ (will be referred to as Red C₁₂ hereafter) and Bodipy FL C₁₂ (will be referred to as Green C₁₂). Both Red C₁₂ and Green C₁₂ can be integrated into LDs with a similar distribution (Figure 4-5A).

To further examine whether the FA analogues were incorporated into LDs in an esterified form, neutral lipids from McA cells labeled with these fluorescent FA analogues were isolated and the lipid species were resolved by thin layer TLC. The method used for lipid extraction differs from the standard lipid extraction protocol which uses a mixture of chloroform and methanol. Because methanol was shown to quench the fluorescent signal, we utilized either chloroform only or neutral lipid solvent (see Section 2.6.2) to extract neutral lipids. Both methods were able to extract free FA analogues and their esterified forms, as demonstrated by the migration of the extracted lipids in neutral lipid solvent in TLC (Figure 4-5B, left panel). Both Green and Red C₁₂ were esterified into a lipid species that migrated faster than the unesterified form (Figure 4-5B, left panel).



Bodipy FL C12 (green)



Bodipy 558/568 (red)

Figure 4-4. Structures of Bodipy FA analogues. Bodipy fluorescent groups are attached to the 12-carbon acyl chain.

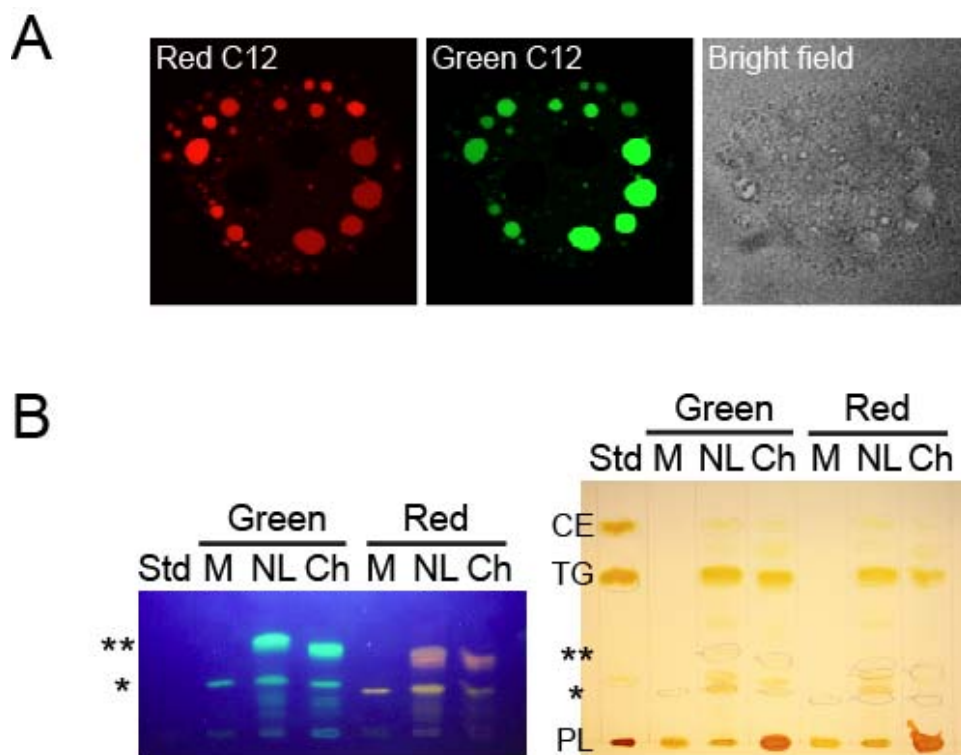


Figure 4-5. Characterization of Bodipy FA analogues. (A) WT hepatocytes were labeled with Green- and Red- C₁₂ for 4 h, and incorporation into LDs was visualized by confocal microscopy. (B) McA cells were labeled with Green or Red C₁₂ for 4 h. Lipids were then extracted with chloroform (Ch) or neutral lipid solvent (NL) and different lipid classes were resolved on TLC plates in neutral lipid solvent. The mobility of FL analogues was visualized by excitation with UV-light (left). The same plate was also stained with iodine to visualize natural FA (right). *, unesterified Bodipy FA analogues; **, esterified Bodipy FA analogues; ◀, PL.

It is difficult to identify the lipid species present in the observed bands because the Bodipy FA analogues are composed of bulky hydrophobic fluorescent groups attached to the acyl chain (Figure 4-4) and thus migrate differently from natural FA (Figure 4-5B, right panel). Nonetheless, these analyses suggested that both Bodipy FA analogues were esterified to chloroform-extractable neutral lipids. Later experiments demonstrated that they entered the hydrophobic cores of LDs (Figure 4-11), a process that would require an esterified, non-polar molecule.

To study LD dynamics, cells were first incubated with Green C₁₂ supplemented with OA/BSA overnight to label LDs to represent preformed LDs in experiments (green globules, Figure 4-6A). Cells were then incubated for 15 min with Red C₁₂/OA/BSA to label newly formed LDs. At the end of 15 min, Red C₁₂ distributed mainly within the ER, manifested as red reticular structures (Figure 4-6A). This reticular structure coincided with the areas of ER where TGH was localized (Figure 4-6B). Distribution of newly synthesized lipids in the ER may be due to initial incorporation of FA into membrane phospholipids, since the incorporation of Green or Red C₁₂ into PL seemed to take place earlier than into neutral lipids (Figure 4-5C). Alternatively, it could be due to lipid accumulation within the ER bilayer or ER lumen. Most preformed LDs were apposed to these red-fluorescing ER structures (Figure 4-6A). Small, nascent LDs were seen to emerge from discrete areas of the ER. We compared nascent LD formation between WT and KO cells. Similar amounts of nascent LDs with diameters ranging from 0.2-0.6 μm were observed in both genotypes (Figure 4-6C), indicating that the absence of TGH did not affect nascent LD formation. A few of

these nascent LDs colocalized with small, preformed LDs (Figure 4-6A), suggesting ongoing merging events between these two types of LDs. However, the majority of LDs remained unmixed after the 15 min incubation.

We intended to elucidate whether these nascent LDs were associated with known LD-coat proteins at this stage. Wild type hepatocytes were briefly labeled with Red C₁₂ for 15 min, followed by immunofluorescent staining for ADRP and TIP47. We had technical difficulty in completely preventing labeled lipids from entering preformed LDs during immunostaining because lipids cannot be fixed and may diffuse between LDs where contact takes place. Nevertheless, the majority of nascent LDs were distinguishable from preformed LDs that were lightly stained. The results demonstrated that numerous Red C₁₂-stained nascent LDs were at close proximity with TIP47, but not with ADRP, which was localized mainly on the surface of preformed LDs (Figure 4-7). The partial colocalization of nascent LDs with TIP47 suggests an early stage of LD formation and commencement of LD coat protein recruitment.

4.2.5 TGH deficiency delays LD maturation

Differences between LD dynamics were revealed upon longer incubation periods with Red C₁₂. In WT cells, some preformed LDs were seen to colocalize with nascent LDs at 30 min, suggesting TG transfer from nascent to preformed LDs at this stage (Figure 4-8). No apparent lipid transfer was observed in KO hepatocytes until 1 h of incubation (Figure 4-8). These results suggest delayed transfer of lipids from nascent to preformed LDs in the absence of TGH. However,

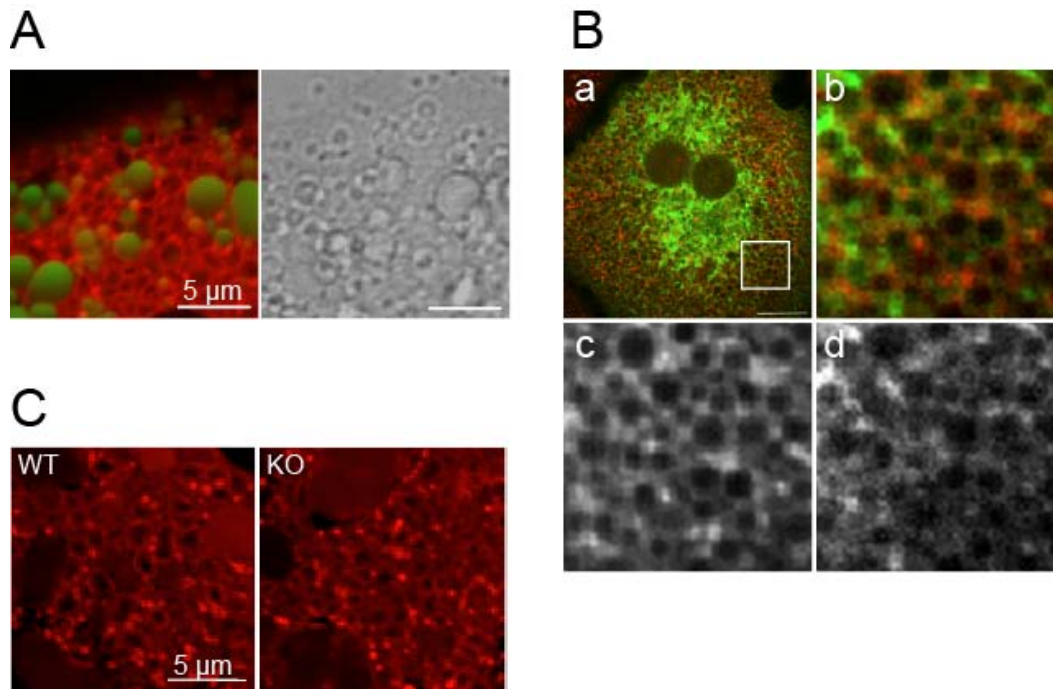


Figure 4-6. TGH does not affect nascent LD formation. (A) Cells were labeled with Bodipy FL C₁₂ overnight (performed LDs, green), followed by Bodipy 558/568 C₁₂ for 15 min (nascent LDs, red). Nascent LDs (arrow) emerge at discrete ER locations surrounding the performed LDs. (B) TGH deficient hepatocytes were transfected with TGH-EGFP and fluorescently labeled with Red C₁₂ for 15 min. The colocalization of TGH-EGFP and integration of Red C₁₂ was determined by confocal microscopy. A representative cell is presented (a). The area in white box is magnified (b). (c), Red C₁₂; (d), TGH-EGFP. Bar, 10 μm. (C) Formation of nascent LDs in WT and TGH KO cells at 15 min is similar.

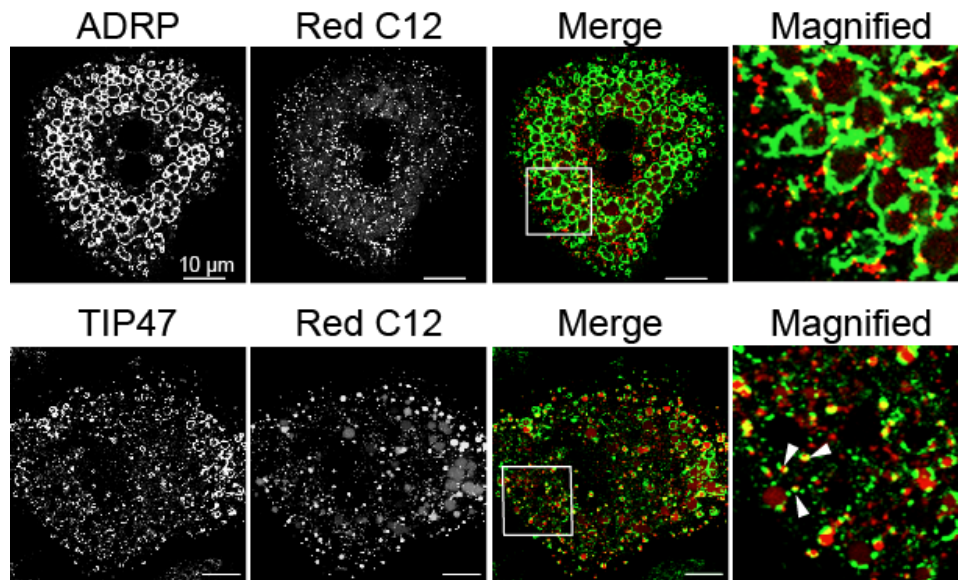


Figure 4-7. Nascent LDs extensively associate with TIP47 but not ADRP. WT hepatocytes were incubated with OA/BSA overnight. Nascent LDs were then labeled with Red C₁₂ for 15 min and immunostained for ADRP and TIP47 as described in Section 2.7.2. Arrowhead: association of TIP47 with surface of nascent LDs.

the process is only delayed rather than completely abolished, since after 4 h incubation, essentially all preformed LDs have incorporated newly synthesized lipids from the nascent LDs in the presence or absence of TGH. Therefore, TGH appears to affect the rate of lipid transfer from nascent to preformed LDs. This phenomenon can be seen more clearly in live-cell imaging (Figure 4-9 and Video S1). In the video, Red C₁₂ globules represent preformed LDs and Green C₁₂ labels nascent LDs. The preformed LDs were relatively static while the nascent LDs were highly dynamic. In WT cells, nascent lipids were integrated into the preformed LDs rapidly and extensively, while in TGH deficient cells, the incorporation was only seen in a few LDs. The amount of newly synthesized lipids that became incorporated into preformed LDs over time was quantified (Figure 4-9B). The signal intensity of preformed lipids (Red C₁₂) remained relatively stable in both WT and KO cells during the 30 minute incubation. However, the curve for incorporation of newly synthesized lipids into preexisting LDs was much steeper in WT cells than that in KO cells, with 3-fold increase in WT cells at the end of 30 min incubation compared with only 50% increase in KO cells (Figure 4-9B), indicating that in the presence of TGH, preformed LDs obtain lipids from newly synthesized LDs much faster than when this lipase is absent. These results strongly suggest a positive role of TGH in LD maturation.

4.2.6 Nascent LDs interact with preformed LDs dynamically

Fusion between LDs is generally believed to be an important mechanism for LD growth (Fujimoto et al., 2008; Goodman, 2008; Olofsson et al., 2008). We

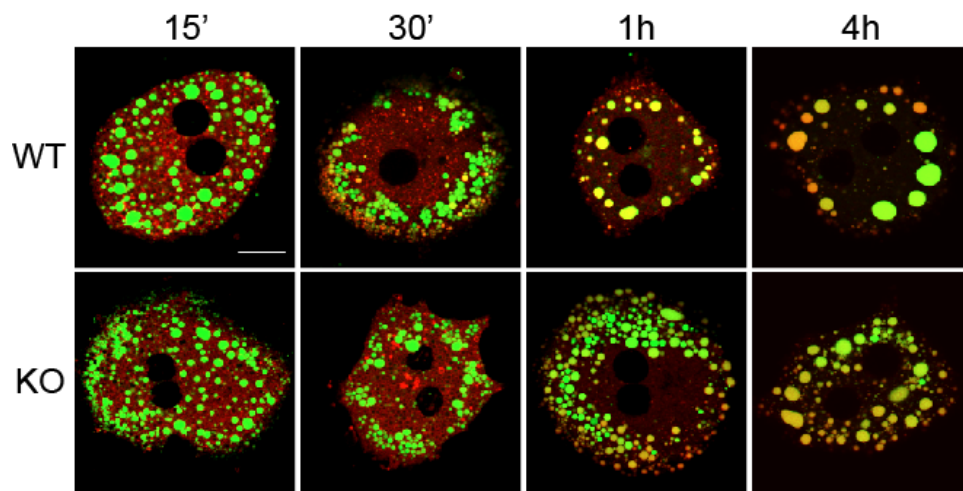


Figure 4-8. TGH deficiency delays the merge of nascent and preformed LDs. WT and TGH KO hepatocytes were labeled with labeling media containing Green C₁₂ overnight, followed by incubation with Red C₁₂ containing labeling media for indicated period of time. Cells were then fixed and mounted onto coverslips. Confocal images were captured and representative cells are presented. Bar, 10 μ m.

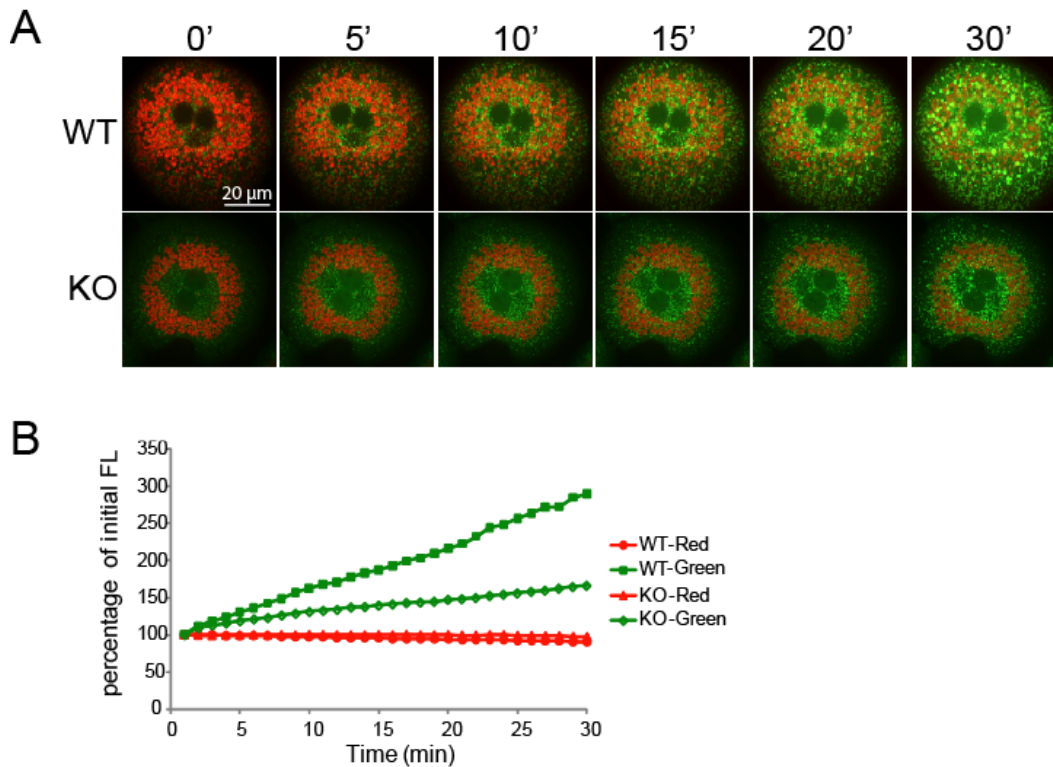


Figure 4-9. Live-imaging of LD formation. (A) WT and TGH KO hepatocytes were labeled with Red C₁₂ containing media overnight and fatty acid uptake reagent (containing Green C₁₂) was added immediately before the start of image acquisition (0 min) with time-lapse confocal microscopy. Image stacks were taken every 1 min for 30 min. Images at indicated time points were presented at extended focus mode. The corresponding videos were shown in Supplementary data (Video S1A and S1B). Data presented in this figure are representative of 5-8 cells obtained during each experiment for 2 repeated experiments. (B) Acquired images at all time points were analyzed for fluorescent intensity according to criteria described in Section 2.7.5. Fluorescent intensity at each time point is presented as percentage of initial fluorescence (0 min).

attempted to address whether fusion was the mechanism responsible for the transfer of lipids from nascent to preformed LDs in primary hepatocytes. Live cell-images of WT and TGH deficient hepatocytes were taken at the same resolution and magnified after image capture to analyze LD interactions (Figure 4-10 and Video S2). In WT cells, nascent LDs rapidly formed around and dynamically interacted with preformed LDs. Although the net result of these brief interactions seemed to be the transfer of newly synthesized lipids into the core of preformed LDs (Figure 4-11), no apparent full-fusion was observed, at least within the 30 min duration that the movie represents. Transfer of lipids seemed to follow a gradual process rather than “bulk” lipidation. These results indicate that if fusion is employed in the growth of hepatic LDs, it appears to be a series of dynamic, transient fusions instead of full-collapse fusions. In TGH deficient cells, the dynamic movement of nascent LDs and their contact with preformed LDs remained intact despite the decreased amount of nascent LDs (Figure 4-10B and Video S2B), indicating that this process may be independent of TGH activity. However, we cannot exclude the possibility that TGH may play a role in facilitating the transfer of lipids once the contact has been made.

4.3 Discussion

We report that TGH, in addition to being a key enzyme in hepatic VLDL secretion, also regulates LD maturation in hepatocytes. This is the first time an ER luminal lipase has been reported to regulate the metabolism of cytosolic LDs. Our results indicate that TGH localizes in areas of ER at close proximity with

A

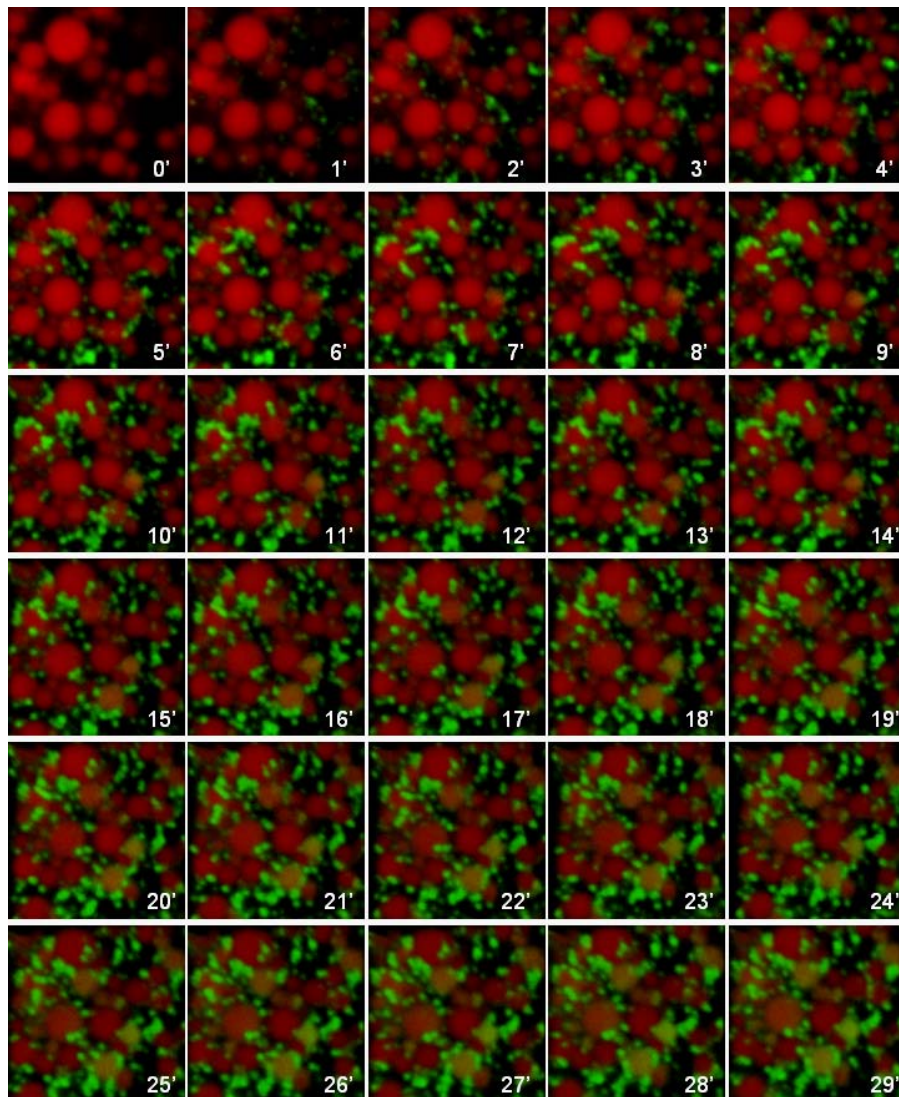


Figure 4-10. Interaction of nascent LDs and preformed LDs. Image stacks were taken in the same conditions as in Figure 4-9. Obtained images were magnified and presented at 3-D opacity mode. **(A) WT. (B) TGH-KO** (see next page). The corresponding videos are shown in Supplementary data (Video S2A and S2B). Red, preformed LDs; green, nascent LDs.

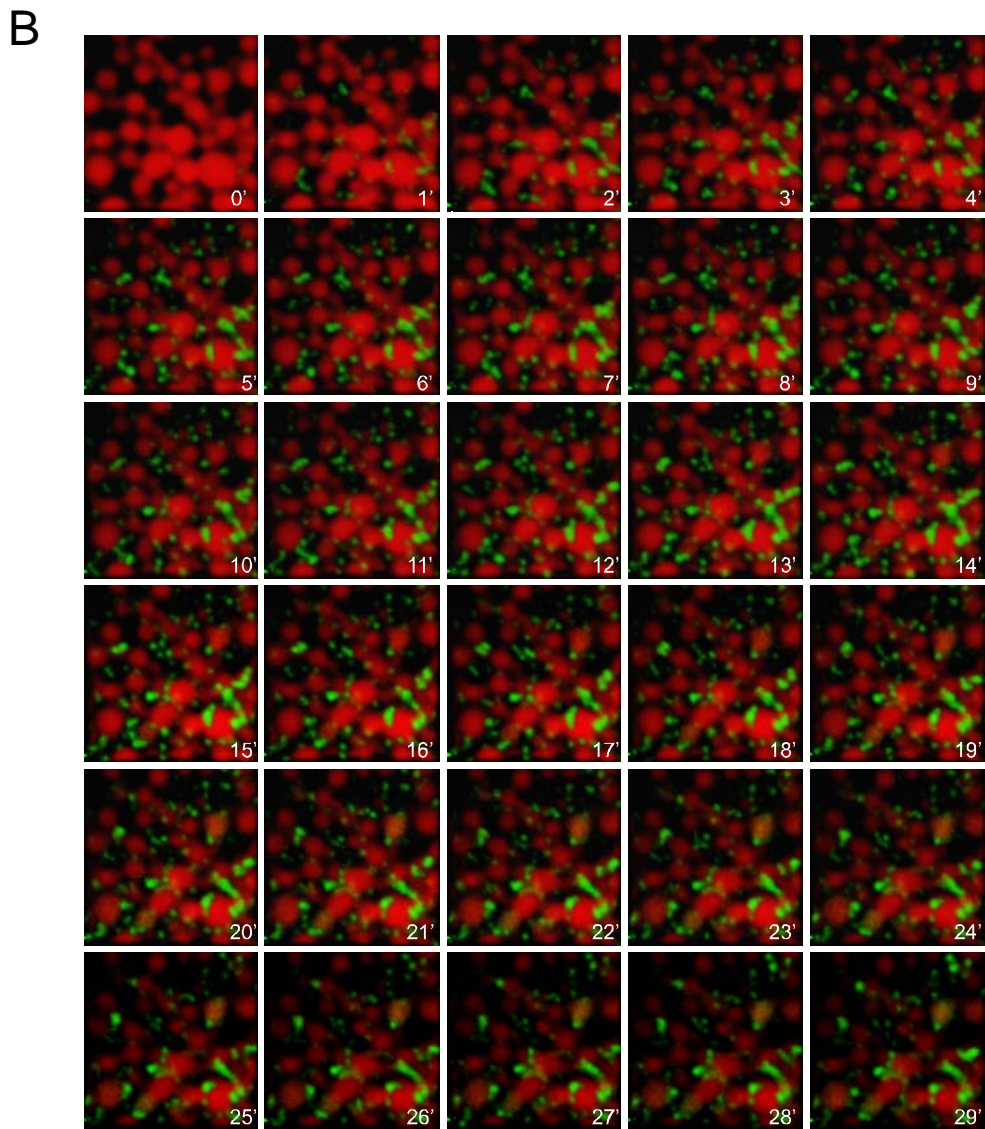


Figure 4-10. Interaction of nascent LDs and preformed LDs. Image stacks were taken in the same conditions as in Figure 4-9. Obtained images were magnified and presented at 3-D opacity mode. **(B) TGH-KO.** The corresponding videos are shown in Supplementary data (Video S2A and S2B). Red, preformed LDs; green, nascent LDs.

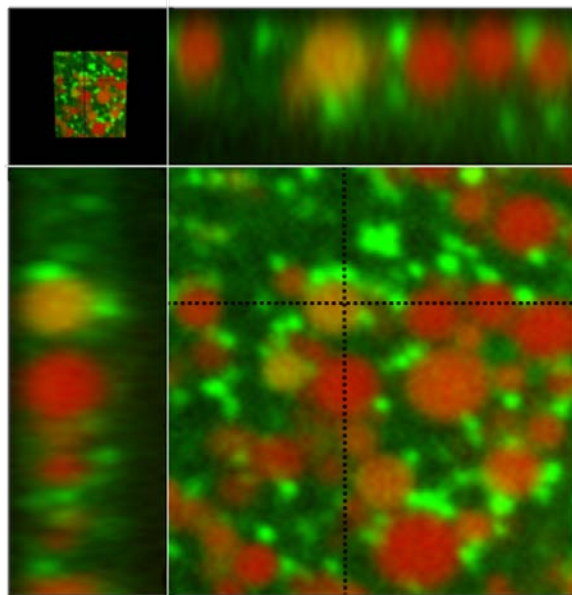


Figure 4-11. Lipid transfer into the core of preformed LDs. Image stacks were obtained in the same conditions as in Figure 4-9 and the image at 26 min is presented at XYZ-plane mode. Top and left panels are projected images from the Z-axis sliced at positions indicated with dotted lines.

cytosolic LDs. In a recent functional genomics screening for genes that affect LD formation and utilization in drosophila, inhibition of a gene (CG34127) encoding a protein with carboxylesterase activity was found to affect the total signal of Bodipy 493/503 staining from OA treated drosophila S2 cells (Guo et al., 2008), supporting our finding that TGH (which also exhibits a carboxylesterase activity) could play a role in regulating LD metabolism.

We intended to investigate the formation and turnover of TG containing LDs in hepatocytes under conditions when FA supply is sufficient. This condition mimics the fasted state in vivo when large amounts of FA are mobilized from the adipose tissue and delivered to the liver. We observed that nascent LDs with a diameter ranging from 0.2-0.6 μm rapidly formed from discrete areas of the ER (Figure 4-6A, B), consistent with the general consensus that ER is the location for LD formation (Section 1.3.2). Fusion has been proposed to be an important mechanism for LD growth after nascent formation. In the present research, we did not observe apparent fusion events in primary mouse hepatocytes. Instead, the nascent LDs appeared to prefer transferring their lipid content into preformed LDs gradually, through dynamic contact between LDs, leading to lipid transfer from the nascent to preformed LDs. TGH deficiency delayed the transfer process. These phenomena were observed when cells were under continuous supply of excess FA, thus providing an alternative mechanism for LD growth. When FAs are in excess, TG is synthesized rapidly to prevent cytotoxicity of FA. Because the ER bilayer where TG synthesis takes place can accommodate only limited amounts of this neutral lipid, excess TG must be incorporated into new LDs or

into preexisting LDs. Preformed LDs may represent a relatively inert pool, the content of which is not readily available for metabolism, as evidenced by the relatively constant Red C₁₂ intensity in both cell types (Figure 4-9B). In contrast, nascent LDs represent a metabolically active pool that undergoes dynamic formation and breakdown. The proposed mechanism by which preformed LDs obtain TG after nascent formation is illustrated in Figure 4-12. We propose that TGH hydrolyzes TG content in LDs, most likely when nascent LDs are attached to the ER. The hydrolytic products can then be re-synthesized into TG by the ER-localized acyltransferases (DGAT) and enter preformed LDs via this futile cycle, possibly through membrane contact sites when the LDs “dock back” to the ER (Murphy et al., 2008). The role of DGAT2 in this process is supported by the association of DGAT2 and its substrate diacylglycerol with LDs (Kuerschner et al., 2008). In TGH deficient cells, the excess TG failed to be transferred back to the inert preformed pool efficiently and this instead resulted in the accumulation of smaller LDs. Lipids from this relatively active pool, however, cannot be channeled for VLDL secretion due to the absence of TGH-mediated lipolysis. We speculate that they are channeled for energy production. In accordance with this hypothesis, TGH deficient mice present with elevated hepatic FA β -oxidation (unpublished data). Although it may not be immediately apparent how inactivation of an enzyme localized in the lumen of the ER leads to increased FA oxidation in mitochondria or peroxisomes; the simplest interpretation would be that generation of a larger number of smaller LDs would provide increased surface area for cytosolic lipolysis. Increased lipolysis by cytosolic lipases has

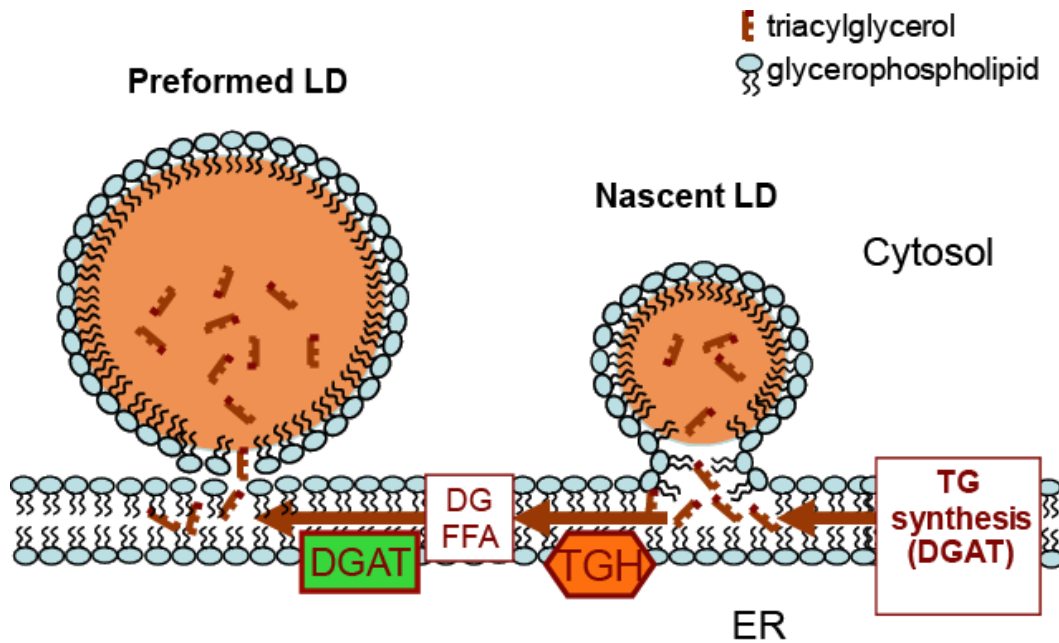


Figure 4-12. Model for the role of TGH in LD maturation. DGAT synthesizes TG in the ER and provides content for nascent LDs. TGH accesses the nascent LDs when they are still in contact with the ER and hydrolyzes this pool of TG. The hydrolytic products are reesterified by DGAT and the resulting TG is transferred into preformed LDs. Potential alternative mechanisms independent of TGH activity are not shown in this illustration for simplicity.

been demonstrated to augment FA oxidation (Reid et al., 2008).

TGH deficiency did not abolish lipid transfer between LDs but only delayed the process, suggesting that other mechanisms exist for LD maturation, such as the fusion mechanism proposed by Bostrom et al (Bostrom et al., 2007). We failed to observe fusion in the present study, possibly because fusion was a transient event that may occur much faster than the time interval between image acquisitions during time-lapse microscopy. Instead, data from the time-lapse microscopy (Figure 4-10 and Video S2) suggest a dynamic interaction and gradual lipid transfer between nascent and preformed LDs. It is possible that a transient fusion and fission occurred during the contact between the two participating LDs, leading to the transfer of content from nascent to preformed LDs. It is unknown why lipids only transferred from nascent to preformed LDs but not the other direction, if this mechanism plays a role. It may represent a tightly regulated mechanism. On the other hand, the dynamic contact of LDs may also represent a state when both nascent and preformed LDs are close to the same TG synthesis mechanism. In this case, the mechanism would resemble the situation depicted in Figure 4-12. Since at least 1/3 of lipid transfer seems to be independent of TGH (Figure 4-9B), either the lipids incorporated into preformed LDs are synthesized locally and independent of the nascent LDs, or a lipase other than TGH is involved.

In conclusion, our research identified a new role for TGH in regulating the biogenesis of cytosolic LDs. It is also proposed that more than one mechanism is

responsible for the regulation of LD maturation. The two mechanisms could coexist during physiological conditions of continual fatty acid supply to the liver.

Chapter V: Identification of potential cofactors for TGH

Portions of this work have been published in:

Wang, H., D. Gilham, and R. Lehner. 2007. Proteomic and lipid characterization of apolipoprotein B-free luminal lipid droplets from mouse liver microsomes: implications for very low density lipoprotein assembly. *J Biol Chem.* 282:33218-26.

5.1 Overview

Most lipases need cofactors to facilitate optimal lipolysis. Examples include apolipoprotein CII for lipoprotein lipase (Havel et al., 1970; LaRosa et al., 1970), perilipin for hormone sensitive lipase (Holm, 2003; Miyoshi et al., 2006; Tansey et al., 2004), and CGI-58 for adipose triglyceride lipase (Lass et al., 2006). Likewise, it is possible that TGH also has a cofactor(s) to facilitate its optimal lipolytic activity. TGH activity and protein eluted in two different fractions from gel filtration and correspond to protein / protein complexes of different sizes (D. Gilham, thesis 2005), indicating the potential association of TGH with cofactor(s). ApoE and MTP were both found to cofractionate with TGH, suggesting a potential role as binding partners for TGH. Proteomic studies of LLDs (Chapter 3) have found that apoE and MTP both co-exist with TGH on LLDs. In native PAGE performed to resolve LLDs of different sizes, apoE partially co-migrated with TGH, while MTP consistently appeared as a single band that co-migrates with the third band of TGH, corresponding to a molecular mass of around 232 kDa (Chapter 3). Research described in this Chapter investigated the potential role of apoE as a cofactor for TGH. It was hypothesized that the lack of apoE expression will lead to compromised TGH activity and therefore decreased channeling of TG for VLDL assembly.

5.2 Results

5.2.1 ApoE partially colocalizes with TGH and co-immunoprecipitates with TGH

A cofactor is expected to physically associate with its lipase. To address whether apoE associates with TGH, we first assessed intracellular localization of these proteins by immunofluorescence. Wild type mouse hepatocytes were immunostained for TGH and apoE and images were taken by confocal microscopy. Both TGH and apoE distributed throughout the cells in a reticular pattern, representing typical ER staining. TGH and apoE extensively colocalized with each other, however, the magnified image revealed that the two proteins only partially colocalize at certain granulated areas (Figure 5-1A). It is worth mentioning that MTP staining demonstrated similar patterns as that of TGH and apoE; it also colocalized with TGH at granulated areas, suggesting the three proteins may be spatially adjacent to each other and therefore function in concert with each other.

Both TGH and apoE were found on LLDs (Figure 3-5 and Table 3-1). We wished to further assess whether apoE and TGH were present on separate or the same LLDs. If both of these proteins could be found on the same LLDs, we then ask whether these two proteins directly interact with each other. It was previously shown in intact cells expressing exogenous flag-tagged TGH that TGH and apoE can be crosslinked and co-immunoprecipitated with anti-flag antibodies under denaturing conditions (Wang et al., 2007), suggesting spatial proximity of the two proteins. However, the association of endogenous TGH and apoE has never been demonstrated due to the lack of anti-mouse TGH antibodies that could immunoprecipitate the endogenous protein. I raised anti-mouse TGH antisera (R13) in rabbits using the synthetic 14 amino acid polypeptide corresponding to

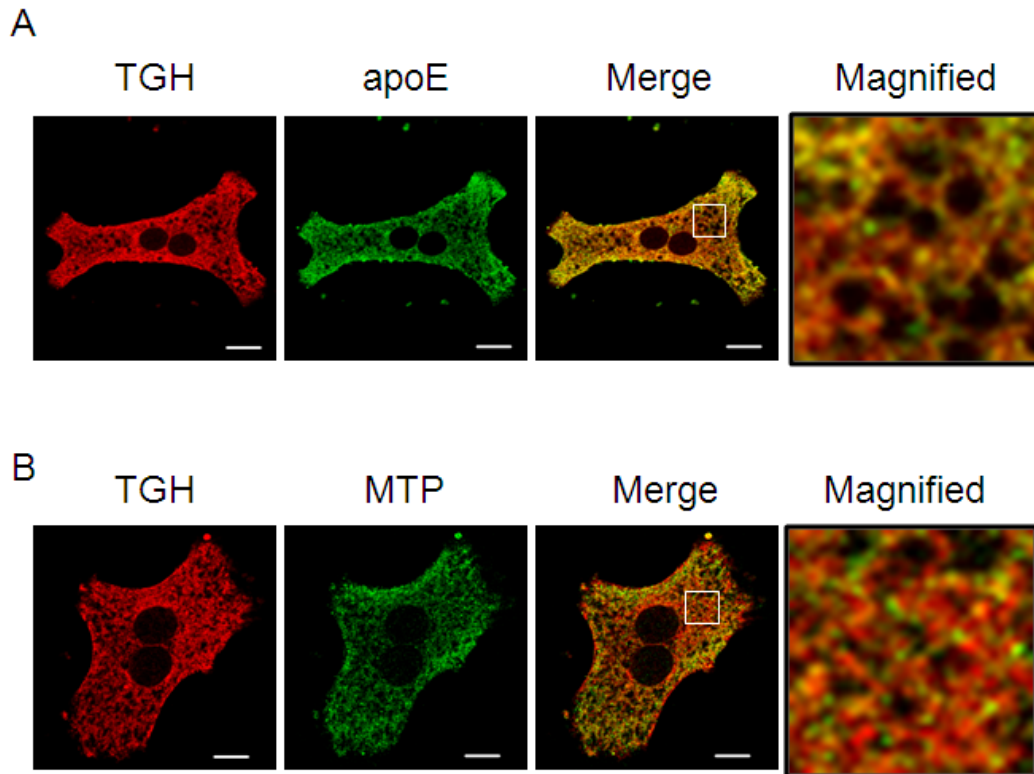


Figure 5-1. Colocalization of TGH with apoE and MTP. Wild type hepatocytes were incubated with OA/BSA for 4 h and immunostained with rabbit α -mTGH (red) and goat- α -apoE (**A**, green) or goat- α -MTP (**B**, green). Images were captured with confocal microscopy. Magnified images represent areas in the white box in the corresponding panels. Bar: 10 μ m.

the C-terminus of mouse TGH conjugated to KLH (KLH-CESAQRPSHREHVEL) for immunization. R13 antisera specifically recognized mouse, but not human, derived TGH (Figure 5-2A). Anti-mouse TGH antibodies (α -mTGH) were then affinity purified from R13 sera and tested for effectiveness for IP procedures (Figure 5-2B).

The purified R13 antibodies were further used to detect co-immunoprecipitation of TGH and apoE under non-denaturing conditions (in the absence of detergent). I found that the IP resulted in a significant recovery of apoE in the pellet (Figure 5-3). Co-immunoprecipitation of TGH and apoE further demonstrated that TGH and apoE co-exist on the same LLDs and may interact with each other. However, we failed to demonstrate the same result when 1% NP-40 was introduced. This could either suggest that TGH does not interact with apoE directly, or that the TGH-apoE interaction was disrupted by the conditions used for IP.

5.2.2 ApoE deficiency does not alter TGH expression but alters TGH activity against 4-MUH

An activating lipase cofactor usually functions by keeping the corresponding lipase at the lipid/water interface. It can either facilitate the lipolytic activity of the lipase by stabilizing the lipase in open-lid conformation, as is the case for co-lipase activation of pancreatic lipase (van Tilbeurgh et al., 1999), or facilitate the targeting of a lipase to its substrates (i.e. LDs). I therefore hypothesized that if apoE were a cofactor for TGH, absence of apoE would lead to either attenuated

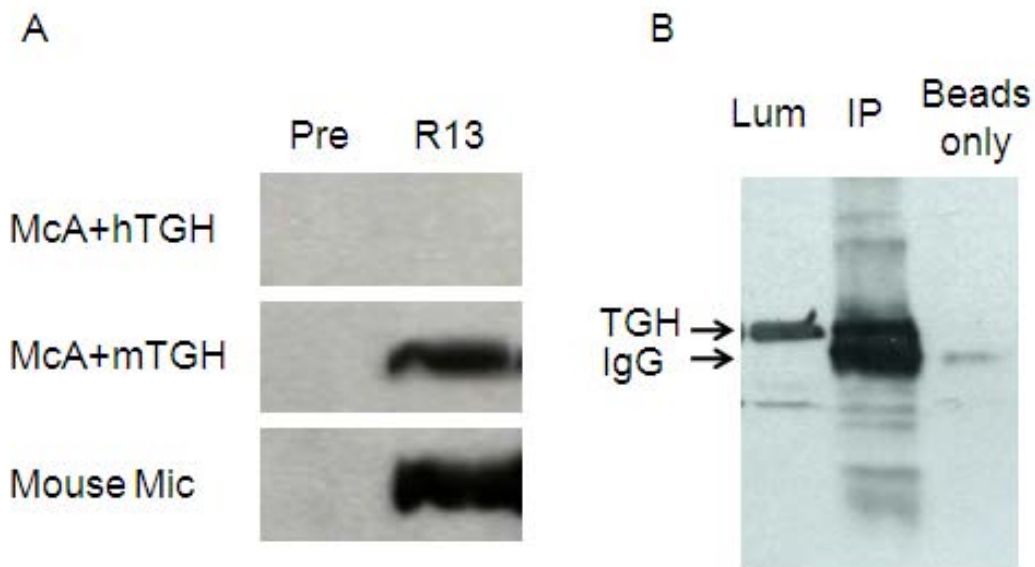


Figure 5-2. Characterization of anti-mouse TGH antibodies. (A) R13 sera specifically recognize mouse TGH but not human TGH. Equal amounts of protein from McA cell lysates expressing human TGH (McA+hTGH) or mouse TGH (McA+mTGH), or mouse microsomes (mouse Mic) were analyzed by western blotting using R13 sera or pre-immune sera (Pre). (B) Purified α -mTGH antibodies are effective in immunoprecipitation of mouse TGH. Three μ g of purified α -mTGH antibodies were used to immunoprecipitate endogenous TGH in the mouse microsomal luminal contents. Two bands were detected: one corresponds to endogenous TGH (higher band), the other corresponds to the IgG heavy chain (lower band).

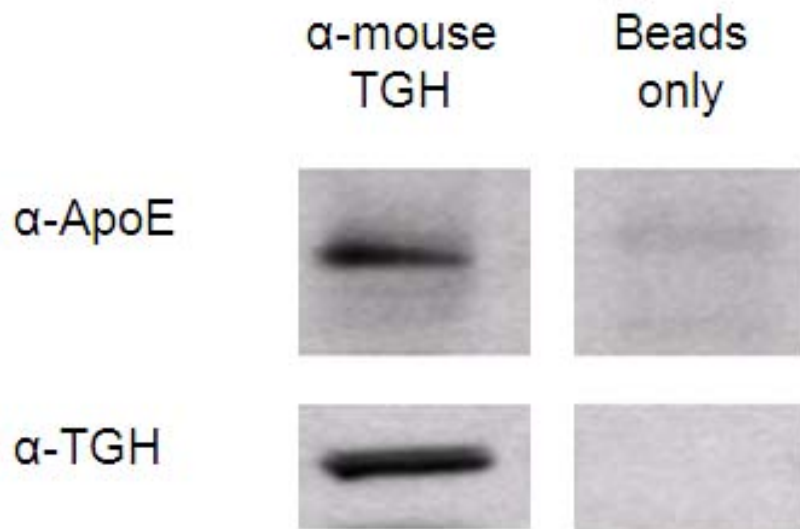


Figure 5-3. ApoE co-immunoprecipitates with TGH. Immunoprecipitations with α -mTGH antibodies were performed in the absence of detergents. Immunoprecipitates were analyzed for the presence of TGH and apoE by immunoblotting. The specificity of immunoprecipitations was assessed by parallel experiments using protein A-Sepharose beads without inclusion of the α -mTGH antibodies (beads only).

TGH activity and/or potentially altered TGH levels on LLDs. To this end, livers collected from apoE knockout (KO) mice were employed. First, I evaluated TGH expression and protein levels in the absence of apoE. Results from quantitative PCR (qPCR) showed unaltered TGH mRNA levels in both female and male mice (Figure 5-4). TGH protein levels were further analyzed in WT or apoE KO livers collected from at least three animals. No difference in TGH protein content was observed in the presence or absence of apoE expression in either males or females (Figure 5-5).

In vitro lipase activity of TGH against 4-MUH was determined to evaluate the influence of apoE on TGH activity. Although the expression of TGH remained unchanged (Figures 5-4 and 5-5), the *in vitro* lipase activity was significantly compromised when apoE expression was ablated in female mice (Figure 5-6A). The difference was mainly due to the decrease in TGH-specific activity but not that of other lipases, as determined by the addition of GSKi, an inhibitor that specifically inhibits TGH activity (Figure 5-6B). However, the difference has only been observed in female mice but not in males.

5.2.3 Decreased TG secretion from apoE deficient hepatocytes due to compromised lipolysis

An *in vitro* lipase assay is a direct method to evaluate lipase activity; however, it does not necessarily reflect the metabolism *in vivo*. To further investigate the intracellular effect of apoE deficiency on TGH activity, metabolic labeling was employed to assess TG turnover and secretion in WT and apoE KO hepatocytes

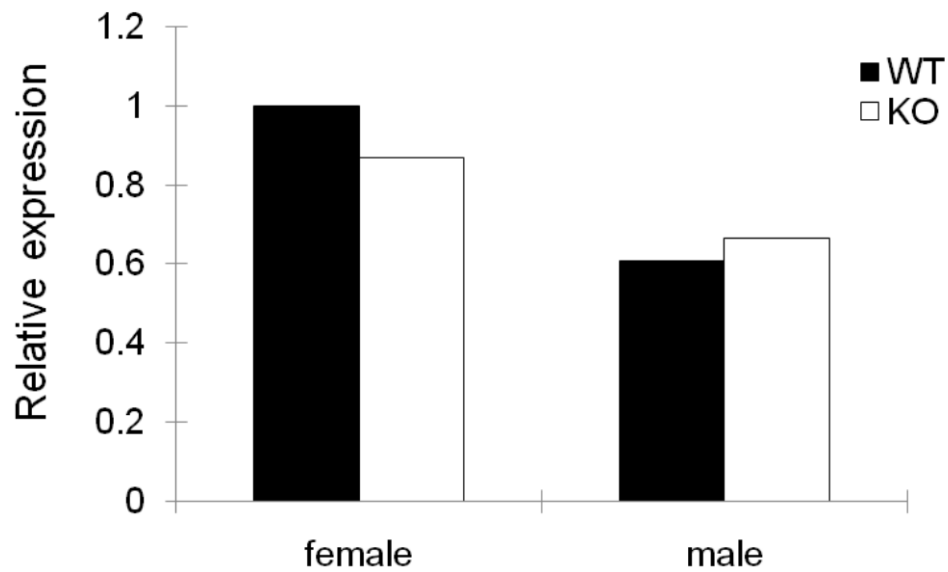


Figure 5-4. Expression of TGH mRNA in apoE deficient livers. ApoE deficiency does not alter TGH mRNA levels. TGH mRNA expression in WT and apoE KO livers was quantified by real-time PCR and normalized to cyclophilin levels. The data were expressed as relative expression of each group normalized to that of the female WT group. Only 2 livers from each group were collected and used for analysis.

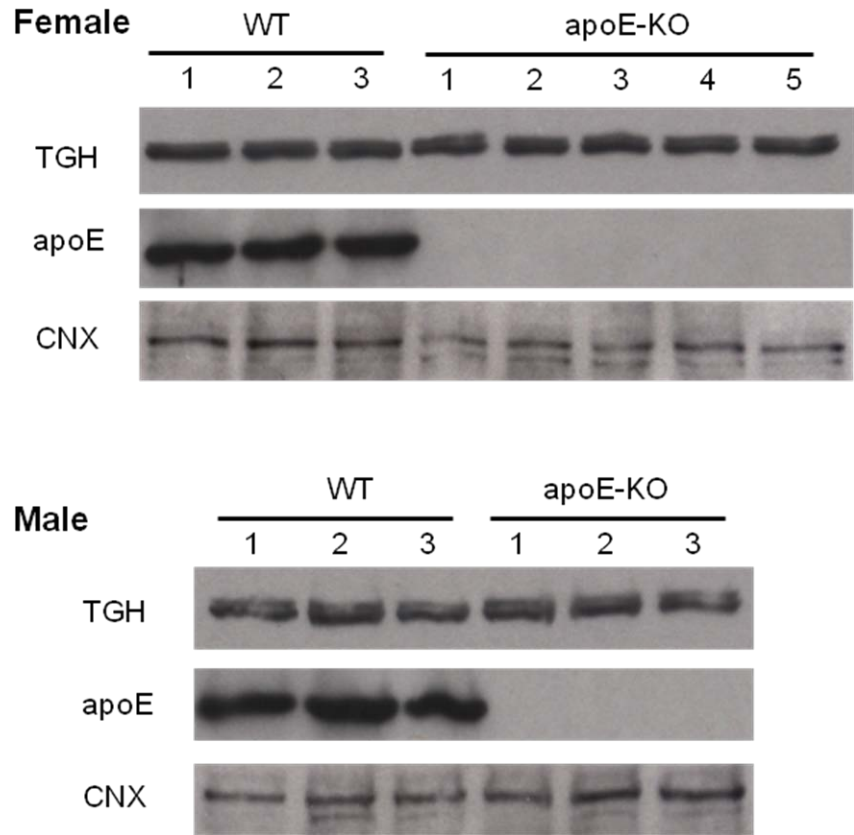


Figure 5-5. TGH protein level in apoE deficient livers. ApoE deficiency does not alter TGH protein level. Livers from 3-5 animals in each group were collected and liver homogenates were analyzed for TGH, apoE, and calnexin levels by Western blotting.

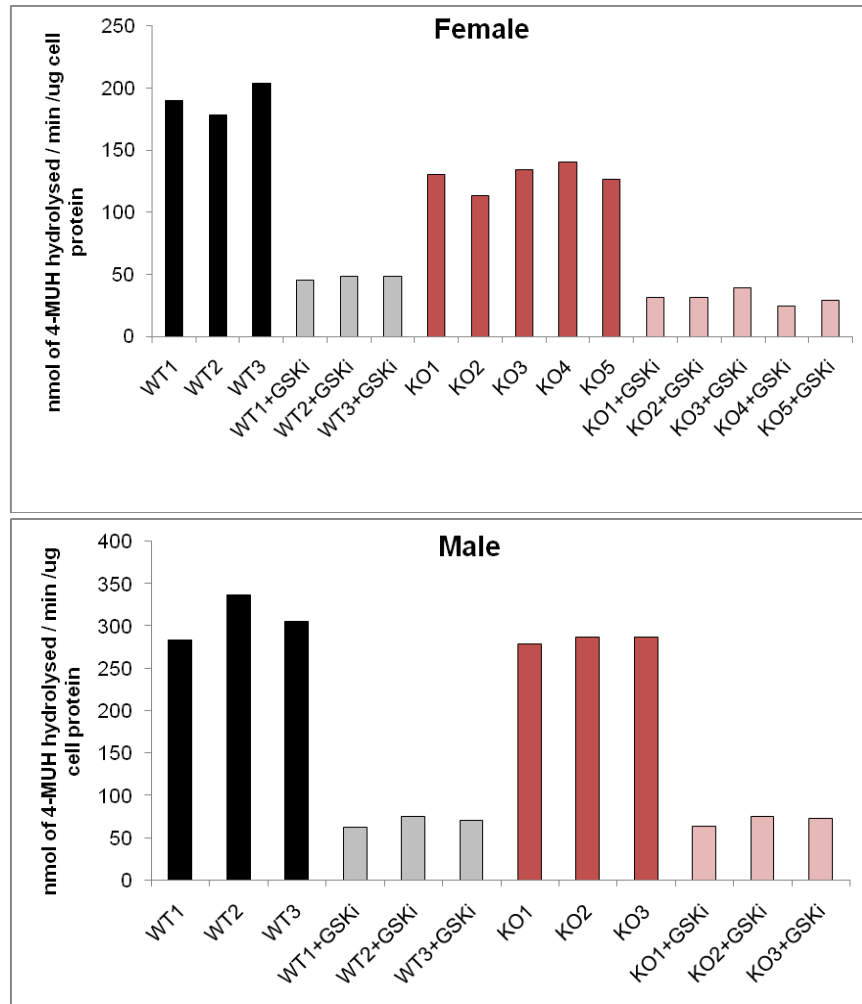


Figure 5-6. ApoE deficiency leads to compromised TGH activity in female but not male mice. The same liver homogenates used in Figure 5-5 were analyzed for *in vitro* lipase activity against 4-MUH in the presence or absence of GSKi, a TGH-specific inhibitor. **(A) General lipase activity and TGH-specific activity.** Data collected from each individual sample were shown.

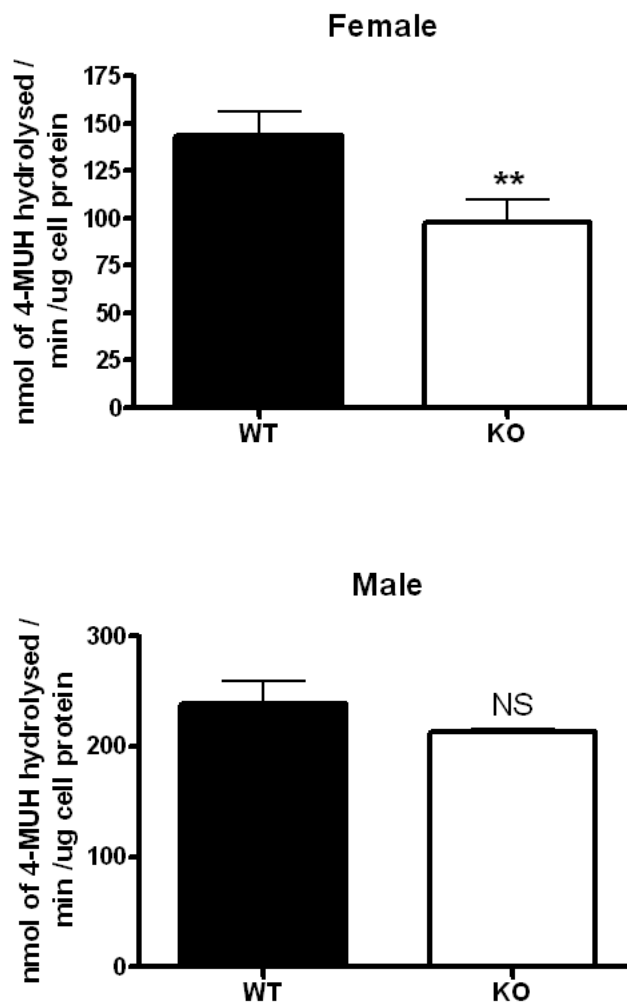


Figure 5-6. ApoE deficiency leads to compromised TGH activity in female but not male mice. (B) TGH specific activity. Activity in the presence of GSKi was subtracted from total activity to reveal TGH-specific activity. Data from all mice in each group were pooled and calculated. **, $p < 0.005$; NS, not significant.

(Figure 5-7). Hepatocytes isolated from female mice were used for these experiments. Lipase inhibitors E600 (a general lipase inhibitor) or GSKi (a TGH specific inhibitor) were introduced to evaluate the contribution of lipolysis to these processes. Consistent with previously reported results (Mensenkamp et al., 2004), ablation of apoE expression led to cellular TG accumulation, but did not affect the percentage of TG turnover during the chase period (Figure 5-7A). [³H]OA labeling revealed that about 6% of total cellular TG was secreted into the media in WT cells during the chase period (Figure 5-7B, upper panel). This percentage was markedly decreased in apoE KO cells, in which only about 2% TG was secreted. Interestingly, the inclusion of lipase inhibitors decreased TG secretion from WT cells, while in apoE deficient cells (in which TG secretion was already compromised), inhibition of lipase activity failed to further reduce TG secretion, indicating that the low amount of TG secreted from apoE deficient cells is not dependent on the lipolysis/re-esterification process. Therefore, the decreased TG secretion in apoE KO cells may be due to compromised lipase activity. A similar trend was also seen in [¹⁴C]glycerol labeling (Figure 5-7B, lower panel).

5.2.4 ApoE is not required for TGH association with lipid droplets

A cofactor could also facilitate lipolysis by targeting the lipase to LDs. To investigate this possibility, I examined the partition of TGH to LDs in the livers of WT and apoE KO mice by subcellular fractionation and western blotting (Figure 5-8). A small amount of TGH was found in the fat cake (LD fraction) in both WT

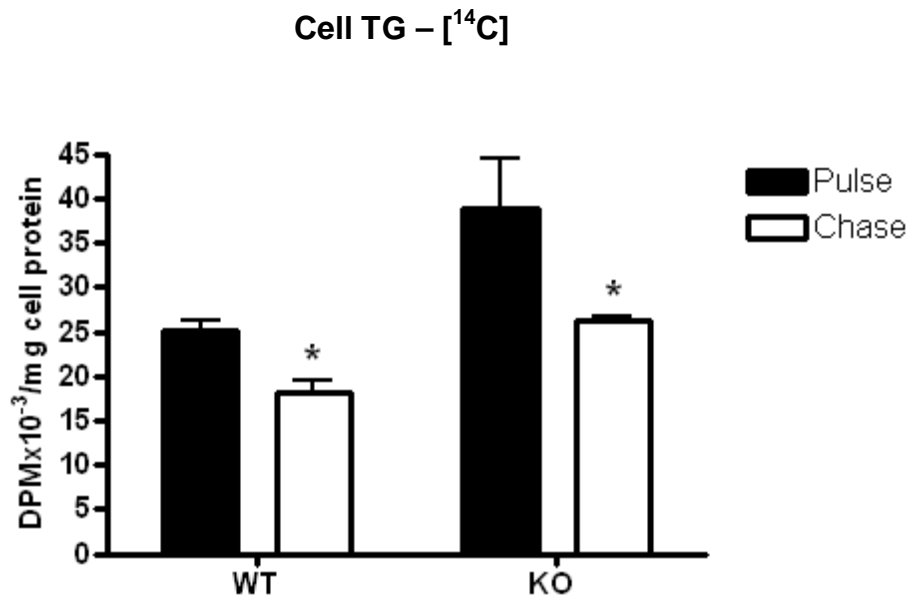


Figure 5-7. TG turnover and secretion in WT and apoE KO hepatocytes. Cells were pulse labeled with [³H]-oleic acid and [¹⁴C]-glycerol for 4 h, followed by a chase period of 12 h. (A) **Cell labeling.** Cells after either the pulse or chase period were collected and analyzed for radioactivity incorporated into TG.

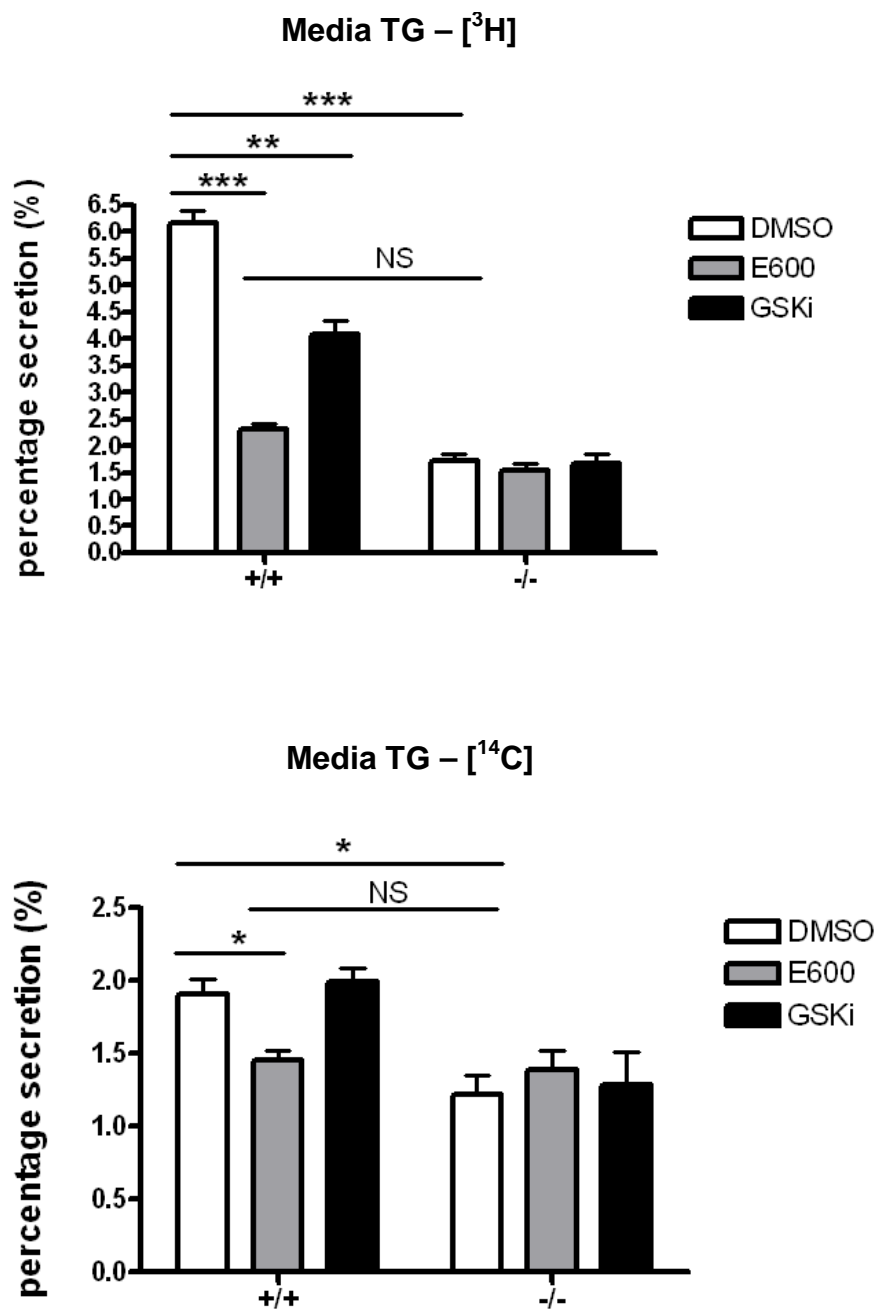


Figure 5-7. TG turnover and secretion in WT and apoE KO hepatocytes. (B) Media labeling. The chase period was performed in the presence of DMSO, E600, or GSKi. Media were then collected and analyzed for radioactivity incorporated into TG.

and apoE KO samples; the ablation of apoE expression did not alter the proportion of TGH associated with LDs. Interestingly, a relatively high proportion of apoE was found to associate with LDs (mainly cytosolic LDs). This phenomenon has never been reported previously. To further address LD apoE association, immunostaining of apoE was performed in WT mouse hepatocytes, and its colocalization with LDs and the LD-coat protein, ADRP, was evaluated (Figure 5-9). In some (~10%), but not all cells, apoE appeared as a ring-like staining pattern surrounding Nile Red-stained LDs. This distribution was confirmed by the co-localization of apoE with ADRP in some of the cells. The reason why the observed LD-association only appeared on some LDs is unknown. The resolution of confocal microscopy cannot unequivocally distinguish whether apoE resides in the ER structure surrounding LDs or actually associates with LDs.

TGH has also been found to associate with LLDs of HDL range (Figure 3-7B). To assess whether apoE affected the association of TGH with LLDs, microsomal luminal contents from WT or apoE KO livers were isolated and the contained particles were separated by gel filtration (the same method as used for results presented in Figure 3-6). Partitioning of TGH in collected fractions was analyzed by western blotting (Figure 5-10). It was predicted that, if the association of TGH with LLDs required apoE, the absence of apoE would have abolished TGH-LLD interaction and therefore TGH would have been detected in fractions corresponding to smaller particles. However, the result suggested that the ablation of apoE expression was not sufficient to cause dissociation of TGH from this fraction. In contrast, TGH seemed to shift to a fraction corresponding to

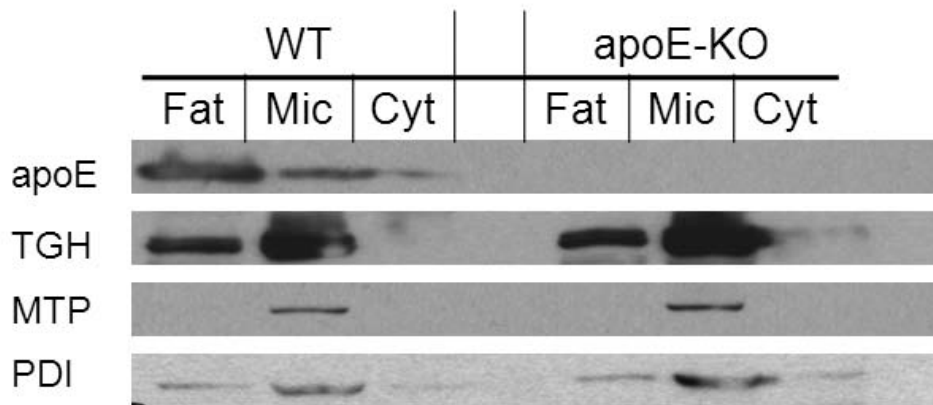


Figure 5-8. Absence of apoE does not affect TGH targeting to CLDs. Fat cake (Fat), microsomes (Mic) and cytosol (Cyt) were isolated from livers of WT or apoE KO mice by centrifugation as described in Chapter 2. Twenty μg of protein were loaded in each lane. Partition of TGH, MTP and PDI were analyzed by Western blotting.

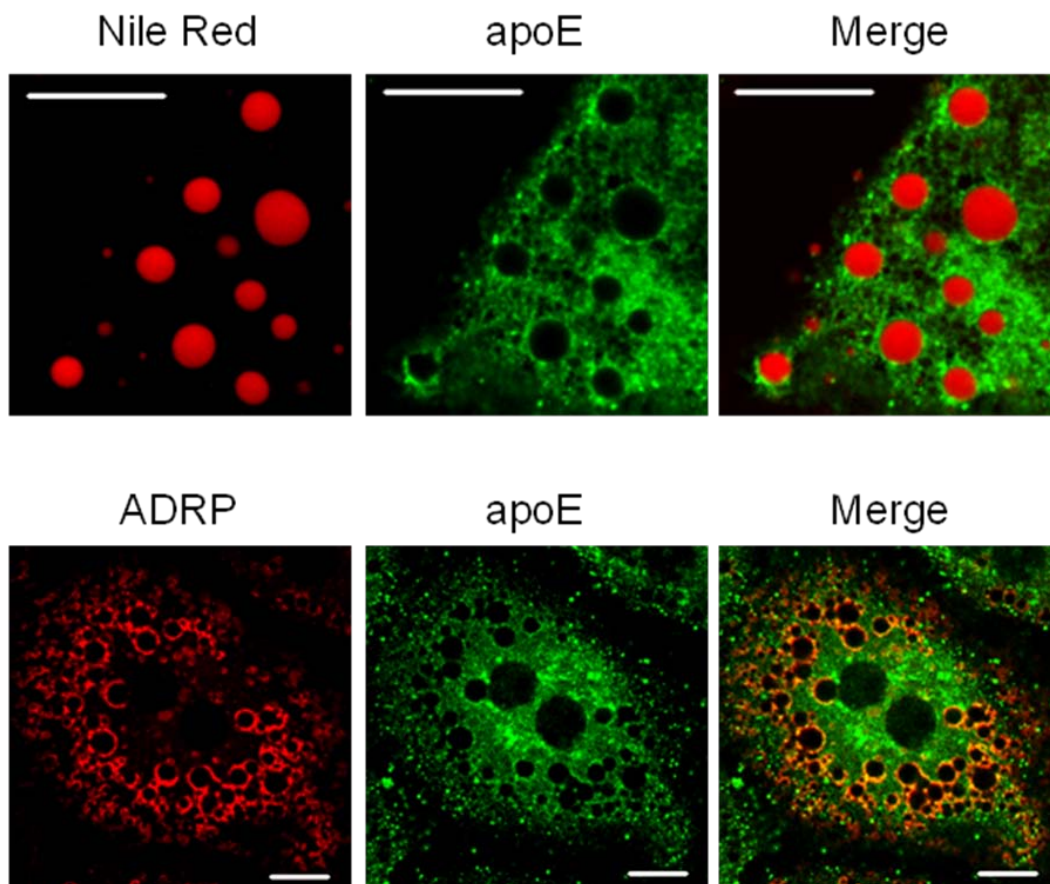


Figure 5-9. ApoE is associated with LDs. Hepatocytes were incubated with DMEM containing OA/BSA and immunostained for apoE. Association of apoE with LDs was determined by colocalization with Nile Red-stained neutral lipids (**A**), or with ADRP, determined by immunostaining with anti-ADRP antibodies (**B**). Bar, 10 μ m.

bigger particles (shifted from fractions 7-9 to fractions 6-8).

5.3 Discussion

In this research, the potential role of apoE as a cofactor for TGH was evaluated. It was observed that *in vitro* lipase activity of TGH against 4-MUH was compromised in livers where apoE expression was ablated, while TGH expression was not affected by the absence of apoE. This compromised lipase activity was only observed in female, but not male, mice. The reason for the observed gender difference is unknown. Interestingly, although TGH levels are lower in male livers at both mRNA (Figure 5-4) and protein (Figure 5-5) levels, homogenates from male livers manifested much higher TGH-specific lipase activity against 4-MUH (250 vs. 150 nmol of 4-MUH hydrolyzed / min / μ g cell protein; Figure 5-6B). The differences in TGH-specific activity between genders suggest that TGH activity might be differently regulated in male and female mice; it is likely that an inhibitor is present in the females, or alternatively, an activator might function in the male mice.

However, whether or not the observed differences are physiologically relevant awaits further investigation. 4-MUH is a synthetic compound established to measure lipase activity *in vitro* in an emulsified solution; a cofactor may not be necessary under these conditions. It has been shown that purified TGH (without association with potential cofactor) was able to hydrolyze 4-MUH with high efficiency. It may be necessary to analyze TGH activity in the presence or absence of apoE using natural substrates such as triolein (or similar).

More physiologically relevant data on TGH activity in the presence or absence of apoE were obtained from metabolic labeling studies in combination with lipase inhibitors. It was shown that apoE deficiency did not affect TG turnover but led to decreased TG secretion. The decreased TG secretion was likely due to the lack of lipolysis in the absence of apoE. It has been well documented that the presence or absence of apoE affects VLDL secretion. Ablation of apoE expression leads to hepatic TG accumulation and reduced VLDL-TG production rate in mice (Mensenkamp et al., 1999; Mensenkamp et al., 2004), while over-expression of apoE stimulates hepatic VLDL-TG secretion (Maugeais et al., 2000). However, despite the prominent correlation of apoE and VLDL production, the mechanism by which apoE regulates VLDL secretion is not clear. The majority of VLDL-TG is derived from the lipolysis of storage TG by lipases (such as TGH), followed by reesterification by DGAT. MTP is indispensable for the integration of TG into nascent VLDL particles. Kuipers' group has shown that MTP and DGAT activities were unchanged in apoE KO mice (Mensenkamp et al., 2004), and they concluded that TG transport through the secretory pathway of hepatocytes was impaired in apoE deficient mice. However, they did not investigate potential changes in lipase activity. In my research, metabolic labeling results revealed that compromised lipase activity, including TGH activity, may have caused decreased VLDL secretion from apoE KO hepatocytes by decreasing TG mobilization. This observation supported the role of apoE as a cofactor to facilitate TGH lipase activity and provided new insight into a plausible mechanism by which apoE regulates VLDL secretion.

The possibility that apoE may facilitate the targeting of TGH to LDs was also investigated. Results suggested that apoE was not required for the targeting of TGH to LDs. However, in the absence of apoE, TGH seemed to have shifted to LLDs of bigger sizes (Figure 5-10). The significance of size differences in LLDs is not clear. Smaller particles may represent a relatively metabolically active pool. They may represent a sub-population of LLDs which provide a preferred substrate for TGH. In this regard, apoE may play a role in stabilizing TGH on its preferred substrate pool. As a consequence, the ablation of apoE expression might have lead to the dissociation of TGH from this preferred pool and its redistribution to a relatively inert pool. However, a firm conclusion cannot be reached from these experiments as to whether the stability of TGH-LD association was altered in the absence of apoE.

Chapter VI: Perspectives and Future Directions

6.1 Synopsis

Studies presented in this thesis investigated the mechanisms by which LLDs and CLDs are regulated by TGH, as well as the contribution of each TG storage pool to VLDL production. LLDs were isolated and characterized, and the presence of proteins involved in VLDL assembly on these droplets was demonstrated. TGH was demonstrated to associate with LLDs, providing new supporting evidence for the lipolysis-reesterification model of VLDL assembly. It was suggested that LLDs comprise a small pool of hepatic TG and may serve as an intermediate reservoir to provide VLDL-TG, while the majority of VLDL-TG was probably mobilized from CLDs. A novel role for TGH in regulating biogenesis of CLDs was demonstrated. It was proposed that more than one mechanism, the TGH dependent mechanism and kiss-and-run fusion, seem to contribute to the regulation of CLD maturation. Further investigation then attempted to evaluate the potential role of apoE as a cofactor for TGH in facilitating its optimal activity.

6.2 Perspectives

6.2.1 Differential pools of intracellular LDs

LDs are metabolically active organelles, and the lipid content in LDs actively goes through synthesis and lipolysis. As a consequence of gaining more knowledge in this field, more compelling questions arise: Are all the LDs metabolized in the same manner? Are there different pools of LDs directed for different metabolic fates? Further, what determines which pool is to be stored and which pool is to be utilized?

Accumulating evidence has suggested the existence of metabolically different pools of TG. There is a certain degree of heterogeneity associated with LDs. Wolins et al. demonstrated that different PAT family proteins coat LDs of different sizes and locations under stimulated conditions (Wolins et al., 2005). Even LDs of identical size have been shown to take up fluorescent polyene lipids at very different rates in COS7 cells (Kuerschner et al., 2008). In the liver and small intestine, heterogeneity of LDs becomes a more outstanding issue since more than one type of LD exists in hepatocytes and enterocytes. Results presented in this thesis (Chapter 3) demonstrated that CLDs and LLDs are clearly distinct entities. Not only do they assume different subcellular localizations, but they also contain different protein and lipid compositions. Even within the population of LLDs, particles were found to be heterogeneous in sizes and protein compositions (Figure 3-7, 3-8), suggesting that heterogeneity is likely to be a general attribute of LDs regardless of the subcellular localization. A recent study using a novel quantitative electron microscopy technique to trace FA incorporation into LDs suggested that heterogeneity exists in adipose-derived 3T3-L1 cells but not in 3Y1 fibroblasts (Cheng et al., 2009). The difference between cell lines may reflect different lipid metabolism in these cells. Results presented in this thesis using Bodipy-labeled fatty acid analogues have demonstrated that FAs are incorporated into different CLDs at different rates (Figure 4-8, 9, 10), suggesting that CLDs are heterogeneous in primary hepatocytes.

Heterogeneity of LDs may be associated with divergent metabolic fates. Although controversial, it was proposed that in 3T3-L1 cells, small LDs may

undergo active lipolysis (Marcinkiewicz et al., 2006; Yamaguchi et al., 2007) and do not incorporate newly synthesized lipid esters significantly (Cheng et al., 2009), while the medium-sized LDs are specialized for incorporating new lipid esters (Cheng et al., 2009). It has been observed that different protocols to increase hepatic TG have led to different results in VLDL secretion. For example, as discussed in **Sections 1.4.3.1**, overexpression of both DGAT isoforms leads to increased TG accumulation, but the increased TG content does not always associate with elevated VLDL secretion. An interesting observation relevant to this phenomenon is that overexpression of the two DGAT isoforms in McA cells resulted in the formation of morphologically different LDs at different subcellular locations (Stone et al., 2004), suggesting that location and morphology of LDs may contribute to regulating their metabolic fate. It was also shown that chemical inhibition of FA oxidation did not affect VLDL production rate despite severe hepatic steatosis (Grefhorst et al., 2005), suggesting that the pool of TG that should have been channeled to β -oxidation cannot be redirected for VLDL secretion when the oxidation pathway is blocked. Results presented in **Chapter 4** of this thesis also support the notion that different pools of LDs are targeted for different metabolic fates. It was demonstrated that preformed LDs seem to represent a metabolically inert pool while nascent LDs are much more dynamic particles that actively transfer their content into the preformed pool (Figure 4-10).

The mechanisms generating heterogeneity in LDs are unknown. The metabolic fate of a specific LD may be affected by its degree of association with lipid metabolism machinery localized in adjacent organelles. The association of

LDs with different organelles such as ER and mitochondria has been extensively reported (**section 1.3.3**). It is not clear how content of CLDs is targeted to the ER for VLDL secretion, but it may require association of CLDs with a specific area of the ER where the lipolysis-reesterification mechanism resides. It was recently reported that when COS-7 cells were treated with OA to drive TG synthesis, DGAT2 translocated to mitochondria associated membranes (MAM) which colocalized with LD surfaces under this condition, suggesting that the association of LDs with MAM is critical for lipid metabolism (Stone et al., 2008). It would be interesting to investigate whether the association between LDs, DGAT2 and MAM exists in hepatocytes and to evaluate whether the degree of association is correlated with the level of TG secretion. TGH was found to channel TG content in CLDs for VLDL secretion. Although TGH does not specifically associate with CLDs, TGH-EGFP appears to preferentially localize to patches of ER area close to CLDs (Figure 4-1A), different from the typical ER localization. It would be interesting to evaluate the significance of this localization and investigate whether it coincides with the area where DGAT enzymes reside. An enticing hypothesis would be that the CLDs which have the ability to access this specified ER area might be the population which is metabolized for VLDL secretion. Similarly, peroxisomes in yeast have been reported to form intimate connections with LDs, and the contact sites are enriched in enzymes of fatty acid oxidation (Binns et al., 2006), suggesting that the lipid content in this population of LDs is possibly targeted for oxidation. Close proximity of LDs and peroxisomes has also been observed in OA-treated hepatocytes by confocal microscopy in one of my pilot

experiments (Figure 6-1). However, it is unknown what determines which LD becomes associated with which organelle and whether the association is a regulated event or simply occurs randomly.

6.2.2 Lipases and the destiny of FAs – is it the location that matters?

Different lipases play different roles in TG metabolism. Other than differences in substrate specificity, subcellular localization of lipases also seems to determine where the hydrolytic products are targeted. It was discussed in **section 1.4.3.4** that lipases responsible for mobilization of TG for VLDL assembly might localize to the ER, and that cytosolic lipases direct FAs to oxidation instead of secretion, indicating ER localization might be necessary for channeling FAs for VLDL assembly. A question raised from this perspective is: is the ER localization sufficient for such a distinct function? This hypothesis is plausible since ER localization would provide convenience for accessing the secretion-coupled pool of TG and for sequestering lipolytic products in the secretory pathway.

A few ER-localized lipases in addition to TGH have been identified in the liver and proposed to play a role in VLDL production. AADA is an ER lipase homologous to HSL and was found to reside in the ER membrane with its active site facing the luminal side of the ER (Lo et al., 2009). It was originally reported by Gibbons et al. that ectopic expression of AADA in HepG2 cells increased TG secretion in those cells by 3-fold (Gibbons et al., 2000). However, results obtained from our laboratory contrast with this observation. Lo et al. have found that McA cells expressing human AADA exhibit decreased intracellular TG, but

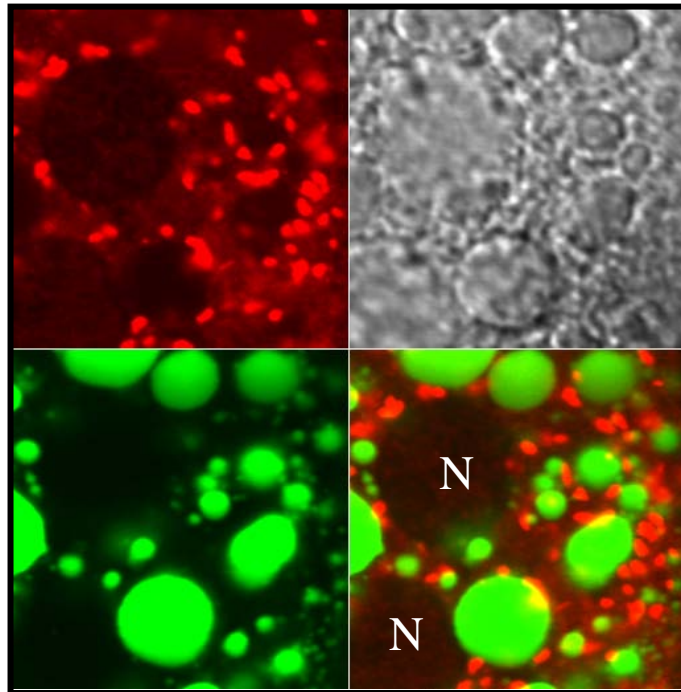


Figure 6-1. Hepatic LDs are at close proximity with peroxisomes. Wild type mouse hepatocytes were cultured in the presence of OA. Cells were fixed, permeabilized and peroxisomes were immunodetected with rabbit anti-SKL (the generic peroxisomal targeting sequence). Following immunostaining, LDs were stained with Bodipy 493/503. N, nuclei; green, LDs; red, peroxisomes.

surprisingly, the mobilized TG seems to be directed to β -oxidation rather than secretion (Lo et al., 2009). It is hard to envision how lipolytic products produced by an ER localized lipase would be directed to the mitochondria for oxidation. One possible explanation would be that the membrane localization of AADA created a microenvironment that allows the lipolytic products to be sequestered in the ER bilayer and further directed to the mitochondria via a mechanism that might involve membrane contact site or MAM. Nonetheless, the case of AADA does not seem to support the hypothesis that ER localization is sufficient to channel FA for VLDL secretion.

AADA is a membrane localized lipase. What about other lumenally localized lipases? Two other candidate lipases, Es-x/Ces1 and Es-22, were shown to reside in the lumen of the ER. Unfortunately, neither the substrate preference, nor their contribution to VLDL secretion has been defined. It is worth mentioning however, that Es-x/Ces1 has been found to associate with LLDs, together with TGH (Table 3-1), suggesting a potential role in mobilizing this pool of lumenally localized TG. Evaluating the role of Es-x/Ces1 and Es-22 in VLDL secretion may provide more insight into the relationship between the localization of a lipase and the metabolic fate of its lipolytic products. Es-x/Ces1 knockout mice have been generated in our laboratory. Characterization of plasma and hepatic lipid profiles, together with metabolic labeling studies in these animals will provide detailed information as to whether this enzyme contributes to directing FA to the secretory pathway.

An alternative approach to investigate the location-metabolic fate enigma is to target an otherwise localized lipase to the lumen of the ER and to assess the destiny of released FA. Such an endeavor has been pursued by our laboratory (unpublished data); hepatic lipase (HL) was retained in the ER by adding HVEL (ER retention signal for mouse TGH) to the C-terminus of the HL sequence. Surprisingly, instead of stimulating VLDL secretion, the ER-retained HL expressed in McA cells suppressed TG and apoB secretion. Under physiological conditions, HL is a secretory lipase that is attached to cell surface heparin sulphate proteoglycans and hydrolyzes TG and PL on VLDL remnants and in HDL. An intracellular lipolytic activity has also been demonstrated [(Verhoeven et al., 1999) and unpublished data]. Because HL hydrolyzes apoB-containing VLDL remnants, it is likely that retention of this lipase in the ER leads to depletion of lipids from VLDL precursor particles and therefore the degradation of apoB, in contrast to TGH, which has been demonstrated not to utilize apoB-containing particles as substrates.

Although inconclusive, the current evidence seems to indicate that localization is not a determining factor, or at least not the only factor that governs whether FA is directed to oxidation or secretion. This question will be better addressed by evaluating the role of another ER luminal lipase, Es-x/Ces1, in VLDL secretion using Es-x/Ces 1 knockout mice. In addition, ATGL and HSL have been reported to direct lipolytic products for oxidation instead of secretion when expressed in hepatoma cell lines or in the liver where their endogenous expression is largely absent (Pease et al., 1999; Reid et al., 2008). It would be

interesting to direct these lipases to a region of the ER similar to where TGH resides by attaching a signal peptide sequence and the HIEL ER retention signal (the ER retention signal for human TGH) to their amino acid sequences. If targeted properly, the ER-localized ATGL or HSL would be predicted to channel TG for VLDL production. However, if the opposite outcome is observed, it would suggest that it is an intrinsic property of a lipase, but less so its localization, that determines the metabolic fate of lipolytic products.

6.2.3 Proposed role of TGH in regulating different pools of LDs

The results presented in this thesis address the mechanism by which TGH regulates LD metabolism. Based on these results, a model is proposed to interpret the potential role of TGH in regulating metabolism of different pools of LDs and channeling different pools of LDs to secretion or oxidation (Figure 6-2). I propose that TGH associates with LLDs in the lumen of the secretory pathway (most likely the ER, see section 3.3) where the bulk lipidation of VLDL primordial particles takes place. Association of TGH and its cofactor (possibly apoE) with LLDs leads to the mobilization of TG content in the LLDs and the liberation of lipolytic products such as FA, DG and MG. At the same time, TGH was also found in the ER area at close proximity with CLDs. If CLDs come into contact with the ER, TGH would also be able to mobilize TG content stored in this pool. The liberated lipolytic intermediates have much more solubility within the ER bilayer than TG and may accumulate in the membrane, where they would be

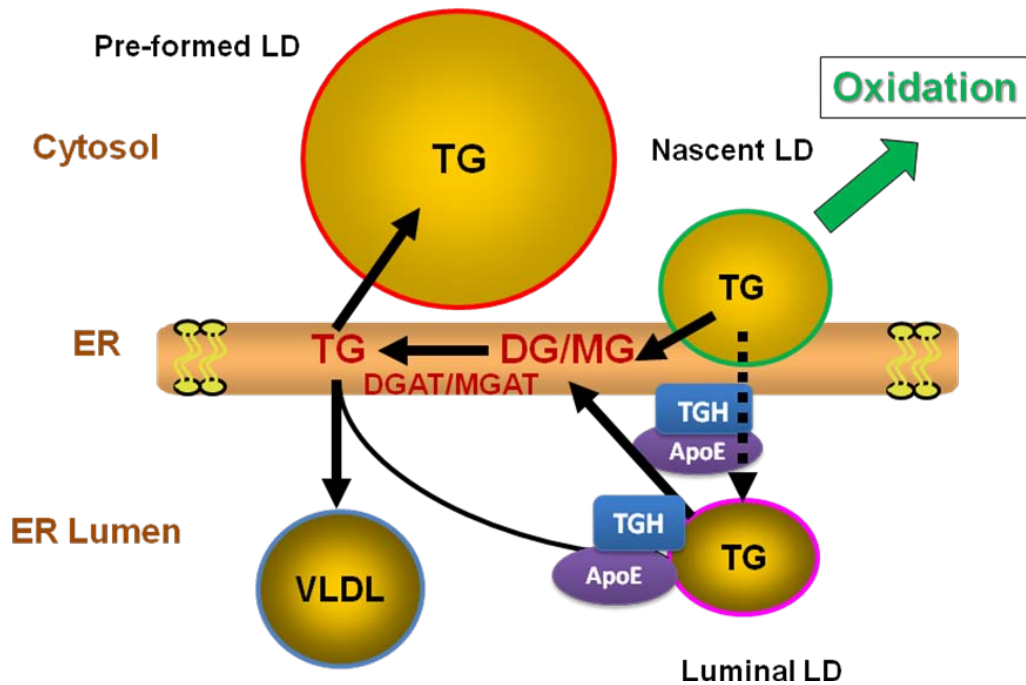


Figure 6-2. Proposed role of TGH in LD metabolism. TGH may mobilize TG content in both small, nascent CLDs and LLDs. The lipolytic products are resynthesized into TG by acyltransferases which may contribute to both the maturation of preformed LDs and VLDL assembly. Optimal catalytic activity of TGH may require association with a cofactor such as apoE. The ablation of TGH leads to accumulation of small CLDs, which may be targeted for oxidation. For simplicity, apoB, MTP and the primordial particle are omitted from this illustration.

resynthesized into TG by acyltransferases such as DGAT and MGAT, accomplishing the previously described lipolysis-reesterification cycle. The resynthesized TG can then be incorporated into VLDL particles. Thus, TG content from both CLDs and LLDs can be directed to VLDL secretion by TGH. Because the pool size of TG in the LLDs is very small compared to that in CLDs, the cytosolic pool may contribute more quantitatively to VLDL-TG. However, the luminal pool might be more readily available for TGH-mediated lipolysis and therefore might function as an intermediate reservoir for VLDL-TG. It is likely that flux through the LLD pool is rapid, and the mass of TG in LLDs is highly regulated to keep the amount constant. A mechanism may exist to replenish the luminal pool from the CLDs by a lipid transfer protein such as MTP (Higashi et al., 2003). This aspect should be further investigated in the future. For example, one could pulse label cells with [³H]-OA in the presence or absence of an MTP inhibitor, then isolate LLDs at different time points during the chase period to evaluate the effect of MTP inhibition on the transfer of radioactivity into these LDs. Alternatively, the replenishment of LLDs could also be accomplished by direct transfer of resynthesized TG into LLDs, possibly when LLDs and ER membranes are in contact. The resynthesized TG can also be incorporated back into CLDs which forms the previously described “futile cycle”. The purpose of the futile cycle has never been clarified. Results presented in this thesis (Chapter 4) suggested that it could be a mechanism utilized for LD remodeling, involving the transfer of lipid content from newly formed LDs to preformed LDs and thus contribute to LD maturation. It was shown that when TGH activity was ablated in

TGH deficient cells, not only was VLDL secretion diminished, but also the maturation rate of preformed CLDs was compromised, supporting the proposed role of a TGH-mediated lipolysis-reesterification cycle in both VLDL and CLD formation. The newly formed CLDs may also serve as a common pool of FAs for both β -oxidation and VLDL formation, as evidenced by the accumulation of smaller LDs in TGH deficient hepatocytes (Figure 4-3) and elevated hepatic FA oxidation rate observed in TGH deficient mice (unpublished data).

6.2.4 Some remaining questions pertinent to TGH function

Enzymology, cell biology and potential physiological roles of TGH have been extensively investigated in our laboratory in the past decade. However, many more compelling questions await further investigation.

6.2.4.1 Which pool of luminal TG does TGH really hydrolyze?

TGH was found to associate with LLDs, however, whether or not TGH directly hydrolyzes TG content from this pool has never been demonstrated. This question can be addressed by incubating purified TGH with radiolabeled, isolated LLDs and examine the release of radioactivity from TG to FA over time. TGH can be easily purified from a McA cell line stably expressing FLAG-tagged TGH without its ER retention sequence to produce active TGH that is continuously secreted into the media (Gilham et al., 2005a). A similar experiment has been performed by a previous member of our laboratory, who demonstrated that TGH does not hydrolyze the intracellular apoB containing LDs immunoprecipitated

with anti-apoB antibodies, or apoB-containing particles secreted into the media (VLDL), thus suggesting that TGH does not utilize apoB containing LDs as substrates (Gilham et al., 2005a). The secreted TGH has been shown to have retained its lipase activity against 4-MUH in vitro. However, a potential problem with this experiment is that the secreted TGH may be missing its cofactor to hydrolyze substrates at a lipid-water interface (LD surface). Therefore, the possibility that TGH could hydrolyze apoB-containing particles cannot be excluded. To reconcile this issue, further investigation would require the use of non-radiolabeled microsomal luminal content as a source of TGH.

If the results of these proposed experiments confirm the previous observations and the hypothesis that TGH uses LLDs but not apoB-containing LDs as substrates, a concurrent question should address the mechanism by which TGH distinguishes these two types of LDs. My hypothesis is that the presence of apoB provides a barrier to prevent TGH from associating with apoB-containing particles and thus accessing its substrate. Conflicting results have been obtained regarding this issue. Gilham et al. have demonstrated that TGH can be crosslinked to apoB (D. Gilham, thesis 2005). In my hands, apoB was found to co-IP with TGH under conditions that preserve the integrity of LDs using anti-mTGH, while reciprocal IP using anti-apoB antibodies under the same conditions did not precipitate TGH (Figure 6-3). Further crosslinking studies using a variety of crosslinkers with different spacer arm lengths are required to investigate TGH-apoB interaction.

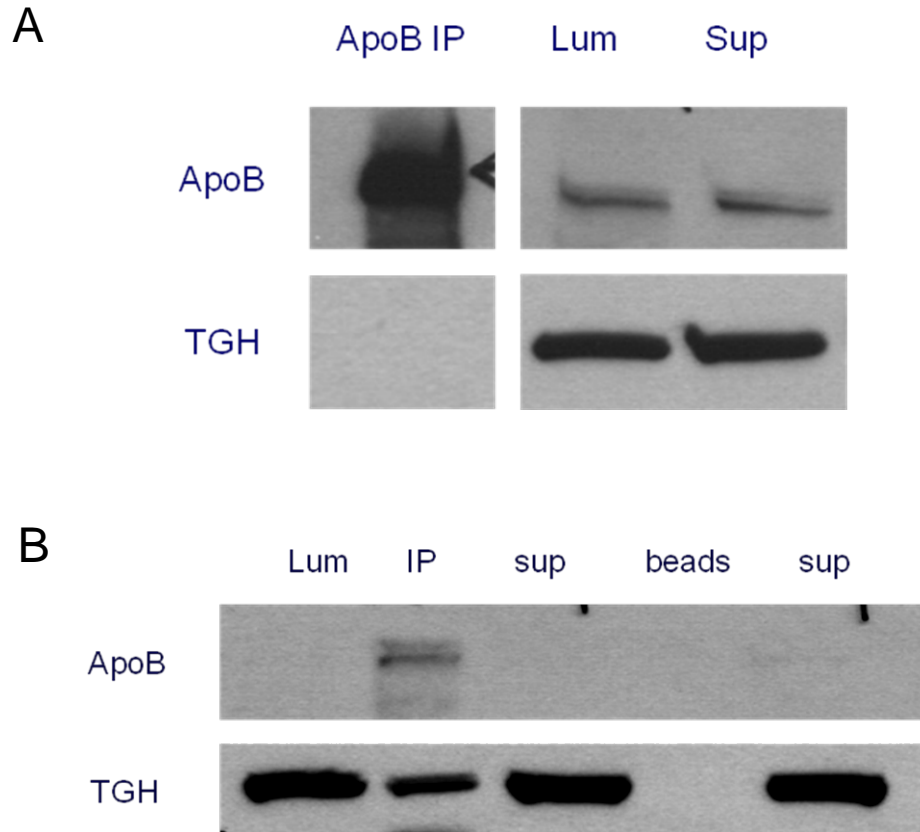


Figure 6-3. Immunoprecipitation of TGH and apoB. Microsomal luminal content was prepared from mouse liver homogenates and IP was performed using anti-apoB (**A**) and anti-mTGH (**B**) antibodies, respectively. Total luminal content, immunoprecipitates (IP) and post IP supernatants (sup) were probed for TGH and apoB. Sepharose protein A beads (beads) with no bound antibodies were used a control for specificity.

6.2.4.2 Cofactor for TGH

Chapter 5 of this thesis investigated the role of apoE as a potential cofactor to facilitate TGH activity. It was concluded that apoE may affect lipase activity of TGH in female mice and potentially affect the affinity of TGH for different subpopulations of LLDs. Figure 6-4 describes a plausible mechanism for apoE to facilitate TGH-mediated lipase activity at the lipid-water interface. TGH may be able to associate with LLD surfaces independently of apoE, as evidenced by the presence of TGH in eluted FPLC fractions lacking apoE (Figure 5-10). Upon interaction with apoE, TGH may undergo a conformational change to stabilize the open-lid conformation, as described in **section 1.5.2**, which may facilitate access of substrates to the catalytic triad at the bottom of the hydrophobic pocket. The specific motif mediating TGH-apoE interaction has yet to be identified. A putative apolipoprotein binding domain found in the TGH primary sequence might play such a role and was under investigation prior to the preparation of this thesis (see next section).

Although spatial proximity of TGH and apoE was demonstrated by IP in the absence of detergent, it is likely that the observed co-IP was due to mutual binding of both proteins to the same pool of LLDs. Direct apoE-TGH interaction has never been clarified and should be determined in the future by performing IP in the presence of detergent or crosslinkers of decreasing spacer arm lengths.

MTP was also found to associate with LLDs (Figure 3-5 and Table 3-1). Several lines of evidence have suggested that it may be a binding partner for TGH, including results observed in FPLC (Figure 3-7), native PAGE (Figure 3-8), and

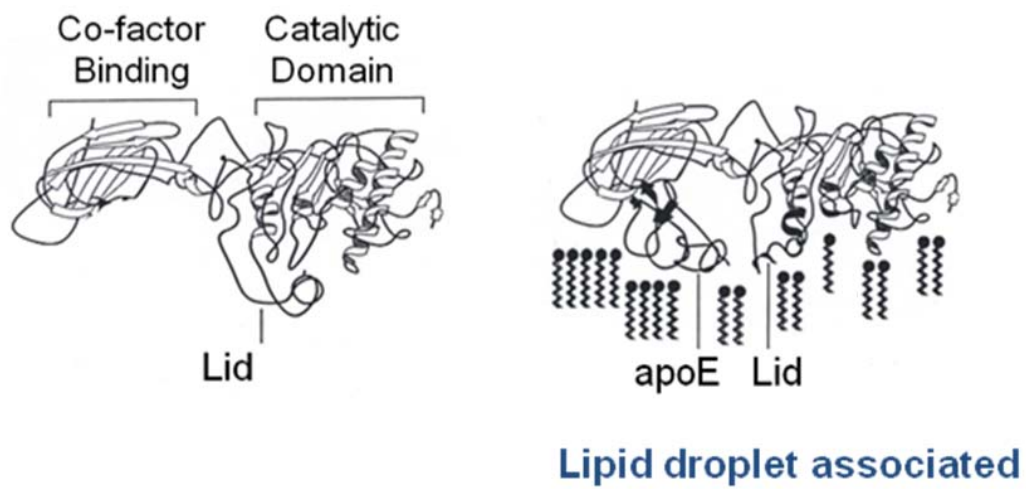


Figure 6-4. Model for apoE stabilizing TGH on lipid-water interface. In the absence of a lipid-water interface (left), TGH maintains a conformation with entrance to the catalytic triad covered by the lid domain. When bound to a lipid-water interface (right), apoE facilitates and stabilizes the open-lid conformation of TGH, allowing the substrates to gain access to the catalytic triad.

IF (Figure 5-1). It was also reported previously that TGH activity is present in two gel filtration fractions, one corresponds to TGH monomer, and the other corresponds to Mw greater than 160kDa. MTP and PDI (an obligatory binding partner for MTP) were both detected in this fraction, suggesting MTP, PDI and TGH may form a protein complex containing TGH activity (D. Gilham, thesis, 2005). The potential role of MTP as a cofactor for TGH should be investigated in future studies. Alternatively, although speculative, MTP could also function as a bridging molecule directing lipolytic products released by TGH to a region of ER close to the site of apoB lipidation. This would require the localization of the TG synthesis mechanism at the vicinity of apoB lipidation.

6.2.4.3 Apolipoprotein binding domain

It was speculated in Chapter 5 that the partition of TGH into the LD fraction remained unchanged in the absence of apoE. Although this speculation may lead to the conclusion that apoE does not play a role in targeting TGH to LDs, it would be premature to exclude the possibility that apoE may regulate the affinity of TGH to its substrate, or facilitate a proper conformation of TGH that is ideal for hydrolysis of its substrates when associated with LDs. In addition to the catalytic domain and lid-domain found in essentially all lipases, a putative apolipoprotein binding domain was identified in the TGH amino acid sequence (Figure 6-5); this led to the hypothesis that this domain may mediate a TGH-apoE interaction. Preliminary experiments have been performed to explore this possibility. We generated McA cell lines stably expressing an EGFP-tagged, mutant TGH in

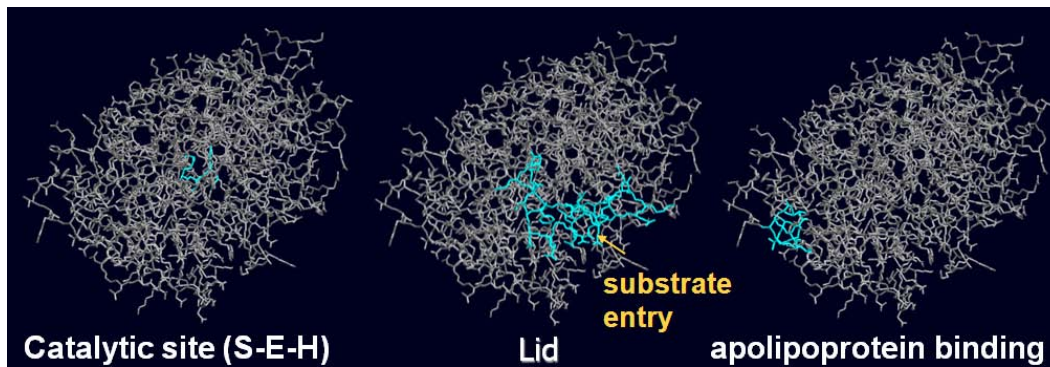
which two conservative Alanines in the lipoprotein binding domain were replaced with two Lysines (AA/KK-EGFP). The expression of mutant and wild type proteins were verified (Figure 6-6) and *in vitro* lipase activity was assessed (Figure 6-7). Although wild type TGH remained active, the mutations from A to K abolished TGH activity almost completely. However, it was observed that although medium- to high- levels of expression were obtained in cells expressing EGFP and wild type TGH, transfection with the mutant TGH failed to yield cells expressing high levels of the protein (Figure 6-5A, B), suggesting that the majority of the expressed mutant proteins might be degraded intracellularly. Potential misfolding or aggregation may have contributed to the lack of activity of the mutant protein. Thus, future studies on this project should assess this possibility. Potential aggregation can be determined by evaluating solubility of this protein in a detergent such as 1% Triton X-100, while misfolding can be assessed by comparing the peptide fingerprint following trypsinization of the protein. If no misfolding or aggregation is found, further investigation should be carried out to evaluate whether the lipoprotein binding domain mediates TGH-apoE interaction by co-immunoprecipitation.

6.3 Concluding remarks

From the initial cloning of TGH in 1997 to the present, when characterization of the TGH global knockout mouse is ready to be published, TGH is emerging as a key enzyme regulating hepatic VLDL assembly and secretion. Interesting

Figure 6-5. Putative lipoprotein binding domain of TGH. (A) The three-dimensional model of human TGH is based on coordinates obtained from crystal structures of acetylcholine esterase and pancreatic lipase. The catalytic triad is located at the bottom of a hydrophobic pocket, which is covered by the lid domain in the absence of a lipid-water interface. The presence of hydrophobic substances allows the open-conformation of the lid and therefore accessibility of the catalytic site to the substrate. The apolipoprotein binding domain may play a regulatory role in stabilizing the open-lid conformation at the lipid-water interface. (B) The location of the apolipoprotein binding domain (blue) in the amino acid sequence of TGH. The two conservative As are highlighted in red. HIEL (brown) is the ER retrieval signal for TGH.

A



B

MWLR AFILATLSASA AWGHPSSPPVVDTVHGKVLGKFVSLEGFAQPVAIFL
GIPFAKPPLGPLRFTPPQPAEPWSFVKNATSYPPMCTQDPKAGQLLSELF
NRKENIPLKLS EDCLYLNIYTPADLTKKNR LPVMVWIHGGGLMVGAASTYD
GLALAAHENVVVVTIQYRLGIWGGFFSTGDEHSRGNWGHLDQVAALRWVQ
DNIA SFGGNPGSVTIFGESAGGESVSVLVLSPLAKNLFHRAISESGVALTSV
LVKKGDV KP **LAEQIAITAGC** KTTTSAVMVHCLRQKTEEELETTLKMK
FLSLDLQGDPRESQPLLGTVIDGM LLLKTPEELQAERNFHTVPYMGINKQ
EFGWLIPMQLMSYPLSEGQLDQKTAMSL LWKSYPLVCI AKELIPEATEKYL
GGTDDTVKKKDLFLDLIADVMFGVPSVIVARNHRDAGAPTYMYEFQYRPS
FSSDMKPKTVIGDHGDELFSVFGAPFLKEGASEEEIRLSKMVMKFWANFA
RNGNPNGEGLPHWPEYNQKEGYLQIGANTQAAQKLKDKEVAFWTNLFAK
KAVEKPPQTE **HIEL**

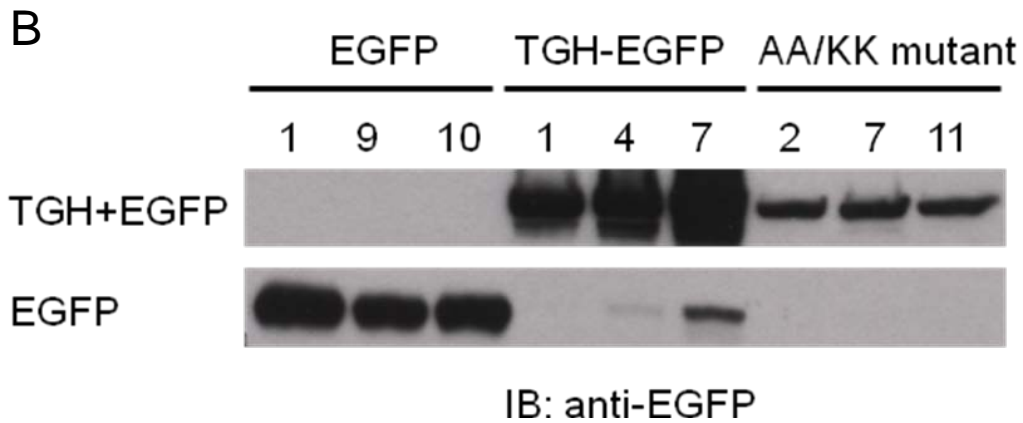
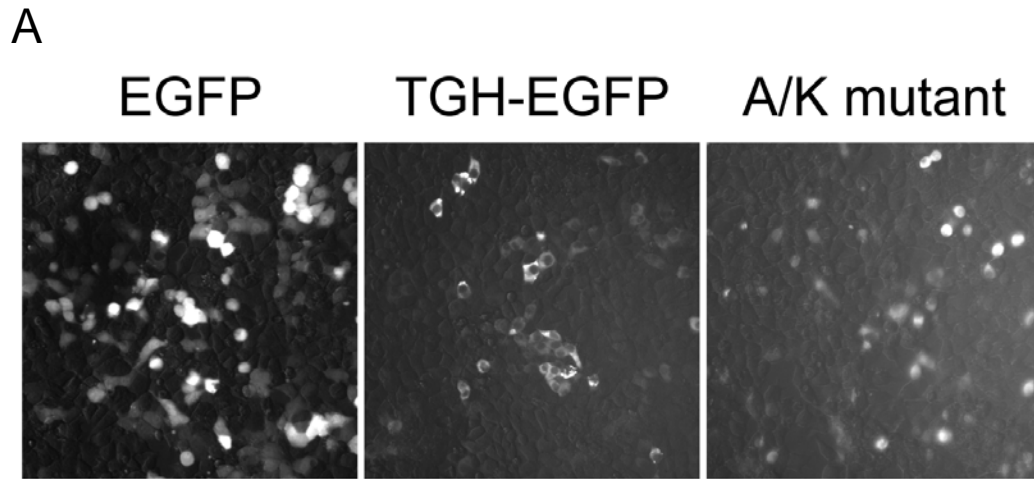


Figure 6-6. McA cells stably expressing wild type or mutant human TGH. Plasmids encoding wild type or mutant hTGH were transfected into McA cells. **(A)** Expression of EGFP tagged proteins were observed by fluorescent microscopy. **(B)** Stable clones were screened. Three colonies from each cell line were selected and cell lysates were analyzed for protein expression using anti-GFP antibodies. Numbers indicate different colonies named during screening.

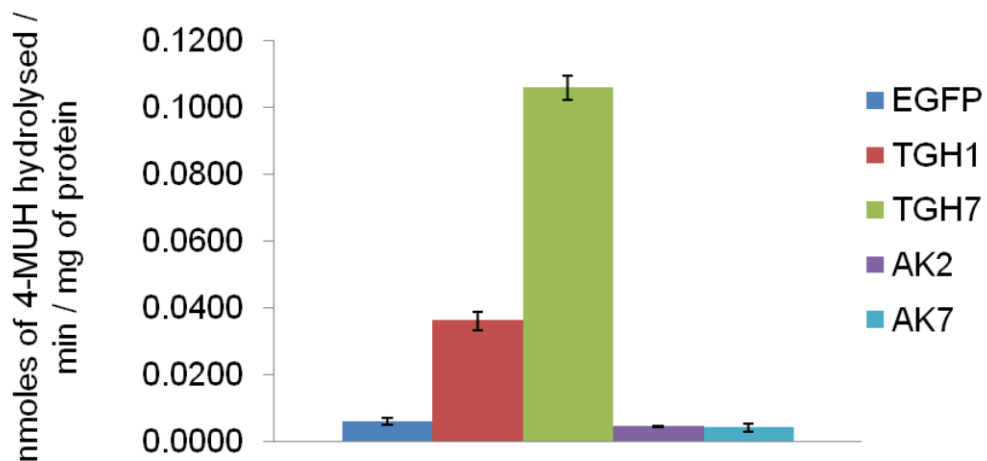


Figure 6-7. In vitro lipase activity of wild type or mutant human TGH. McA cells stably expressing wild type or mutant hTGH were homogenized and analyzed for lipase activity against 4-MUH. TGH 1 and TGH 7 are two cell lines expressing wild type hTGH, AK2 and AK7 are two cell lines expressing mutant hTGH.

phenotypes have been observed in TGH global knockout mice. Despite the compromised TG and apoB secretion due to TGH-deficiency, no TG accumulation was observed in the liver. This effect may be due to increased hepatic FA oxidation, as well as decreased TG mobilization from the adipose tissue. Thus, systemic effects should be taken into account when evaluating physiological roles of TGH. Currently liver-specific TGH knockout mice and liver-specific TGH transgenic mice are under development in our laboratory. Investigating TG metabolism in these animals would eliminate contributions from other tissues to study hepatic phenotypes. In addition, TGH is expressed considerably in adipose tissue and, to some extent, in small intestine. Contribution of TGH to lipid metabolism in these tissues, such as adipose TG mobilization, and TG absorption and CM assembly in the intestine, should be further investigated.

Future studies should also examine detailed mechanisms causing these phenotypes. Results presented in this thesis provide new insight. The isolation and characterization of LLDs provided the first biochemical evidence for the presence of LLDs. These results not only constitute important supporting evidence for the current theory on VLDL assembly, but also added to knowledge of how TGH fits into this picture. This thesis also explored a new aspect of TGH in regulating LDL metabolism. Recently, numerous proteins and genes affecting LDL metabolism have been identified by proteomics and functional genomics studies. Results presented in this thesis add TGH to this rapid-growing list and provide insight into the mechanism by which different pools of LDLs contribute to VLDL

secretion. This is especially valuable, since relatively little is known about the regulation of hepatic LD metabolism compared to that in adipose tissue.

Looking beyond TGH, the liver is a central organ with rapid TG synthesis and lipolysis; however, no intracellular lipase other than TGH has been well characterized in the liver. It has been demonstrated that total liver lipase activity decreased only ~30% in TGH deficient mice, suggesting the presence of other lipases. However, the full repertoire of liver lipases is far from complete. A few known ER-localized lipases were previously discussed in section 6.2.2; their contribution to hepatic neutral lipid metabolism should be further studied. The identities of cytosolic lipases in the liver remain enigmatic. Small amounts of ATGL are expressed in the liver, but ATGL's quantitative contribution to hepatic TG metabolism is unknown. An ongoing project in our laboratory endeavors to identify additional liver lipases using a proteomics approach. Results obtained from this research may shed new light on our understanding of hepatic lipid metabolism.

Chapter VII: References

- Abo-Hashema, K.A., M.H. Cake, G.W. Power, and D. Clarke. 1999. Evidence for triacylglycerol synthesis in the lumen of microsomes via a lipolysis-esterification pathway involving carnitine acyltransferases. *J Biol Chem.* 274:35577-82.
- Adiels, M., C. Packard, M.J. Caslake, P. Stewart, A. Soro, J. Westerbacka, B. Wennberg, S.O. Olofsson, M.R. Taskinen, and J. Boren. 2005. A new combined multicompartamental model for apolipoprotein B-100 and triglyceride metabolism in VLDL subfractions. *J Lipid Res.* 46:58-67.
- Agren, J.J., J.P. Kurvinen, and A. Kuksis. 2005. Isolation of very low density lipoprotein phospholipids enriched in ethanolamine phospholipids from rats injected with Triton WR 1339. *Biochim Biophys Acta.* 1734:34-43.
- Alam, M., D. Gilham, D.E. Vance, and R. Lehner. 2006. Mutation of F417 but not of L418 or L420 in the lipid binding domain decreases the activity of triacylglycerol hydrolase. *J Lipid Res.* 47:375-83.
- Alam, M., S. Ho, D.E. Vance, and R. Lehner. 2002a. Heterologous expression, purification, and characterization of human triacylglycerol hydrolase. *Protein Expr Purif.* 24:33-42.
- Alam, M., D.E. Vance, and R. Lehner. 2002b. Structure-function analysis of human triacylglycerol hydrolase by site-directed mutagenesis: identification of the catalytic triad and a glycosylation site. *Biochemistry.* 41:6679-87.
- Alexander, C.A., R.L. Hamilton, and R.J. Havel. 1976. Subcellular localization of B apoprotein of plasma lipoproteins in rat liver. *J Cell Biol.* 69:241-63.
- Andersson, L., P. Bostrom, J. Ericson, M. Rutberg, B. Magnusson, D. Marchesan, M. Ruiz, L. Asp, P. Huang, M.A. Frohman, J. Boren, and S.O. Olofsson. 2006. PLD1 and ERK2 regulate cytosolic lipid droplet formation. *J Cell Sci.* 119:2246-57.
- Asp, L., C. Claesson, J. Boren, and S.O. Olofsson. 2000. ADP-ribosylation factor 1 and its activation of phospholipase D are important for the assembly of very low density lipoproteins. *J Biol Chem.* 275:26285-92.
- Avramoglu, R.K., and K. Adeli. 2004. Hepatic regulation of apolipoprotein B. *Rev Endocr Metab Disord.* 5:293-301.

- Bamberger, M.J., and M.D. Lane. 1990. Possible role of the Golgi apparatus in the assembly of very low density lipoprotein. *Proc Natl Acad Sci U S A*. 87:2390-4.
- Barrows, B.R., and E.J. Parks. 2006. Contributions of different fatty acid sources to very low-density lipoprotein-triacylglycerol in the fasted and fed states. *J Clin Endocrinol Metab*. 91:1446-52.
- Bartz, R., J.K. Zehmer, M. Zhu, Y. Chen, G. Serrero, Y. Zhao, and P. Liu. 2007. Dynamic activity of lipid droplets: protein phosphorylation and GTP-mediated protein translocation. *J Proteome Res*. 6:3256-65.
- Beckman, M. 2006. Cell biology. Great balls of fat. *Science*. 311:1232-4.
- Bell, M., H. Wang, H. Chen, J.C. McLenithan, D.W. Gong, R.Z. Yang, D. Yu, S.K. Fried, M.J. Quon, C. Londos, and C. Sztalryd. 2008. Consequences of lipid droplet coat protein downregulation in liver cells: abnormal lipid droplet metabolism and induction of insulin resistance. *Diabetes*. 57:2037-45.
- Beller, M., C. Sztalryd, N. Southall, M. Bell, H. Jackle, D.S. Auld, and B. Oliver. 2008. COPI complex is a regulator of lipid homeostasis. *PLoS Biol*. 6:e292.
- Bencharit, S., C.L. Morton, J.L. Hyatt, P. Kuhn, M.K. Danks, P.M. Potter, and M.R. Redinbo. 2003. Crystal structure of human carboxylesterase 1 complexed with the Alzheimer's drug tacrine: from binding promiscuity to selective inhibition. *Chem Biol*. 10:341-9.
- Bickel, P.E., J.T. Tansey, and M.A. Welte. 2009. PAT proteins, an ancient family of lipid droplet proteins that regulate cellular lipid stores. *Biochim Biophys Acta*. 1791:419-440.
- Binns, D., T. Januszewski, Y. Chen, J. Hill, V.S. Markin, Y. Zhao, C. Gilpin, K.D. Chapman, R.G. Anderson, and J.M. Goodman. 2006. An intimate collaboration between peroxisomes and lipid bodies. *J Cell Biol*. 173:719-31.
- Blanchette-Mackie, E.J., N.K. Dwyer, T. Barber, R.A. Coxey, T. Takeda, C.M. Rondinone, J.L. Theodorakis, A.S. Greenberg, and C. Londos. 1995. Perilipin is located on the surface layer of intracellular lipid droplets in adipocytes. *J Lipid Res*. 36:1211-26.

- Borchardt, R.A., and R.A. Davis. 1987. Intrahepatic assembly of very low density lipoproteins. Rate of transport out of the endoplasmic reticulum determines rate of secretion. *J Biol Chem.* 262:16394-402.
- Bostrom, K., M. Wettsten, J. Boren, G. Bondjers, O. Wiklund, and S.O. Olofsson. 1986. Pulse-chase studies of the synthesis and intracellular transport of apolipoprotein B-100 in Hep G2 cells. *J Biol Chem.* 261:13800-6.
- Bostrom, P., L. Andersson, M. Rutberg, J. Perman, U. Lidberg, B.R. Johansson, J. Fernandez-Rodriguez, J. Ericson, T. Nilsson, J. Boren, and S.O. Olofsson. 2007. SNARE proteins mediate fusion between cytosolic lipid droplets and are implicated in insulin sensitivity. *Nat Cell Biol.* 9:1286-93.
- Bostrom, P., M. Rutberg, J. Ericsson, P. Holmdahl, L. Andersson, M.A. Frohman, J. Boren, and S.O. Olofsson. 2005. Cytosolic lipid droplets increase in size by microtubule-dependent complex formation. *Arterioscler Thromb Vasc Biol.* 25:1945-51.
- Bradbury, P., C.J. Mann, S. Kochl, T.A. Anderson, S.A. Chester, J.M. Hancock, P.J. Ritchie, J. Amey, G.B. Harrison, D.G. Levitt, L.J. Banaszak, J. Scott, and C.C. Shoulders. 1999. A common binding site on the microsomal triglyceride transfer protein for apolipoprotein B and protein disulfide isomerase. *J Biol Chem.* 274:3159-64.
- Brasaemle, D.L. 2007. Thematic review series: adipocyte biology. The perilipin family of structural lipid droplet proteins: stabilization of lipid droplets and control of lipolysis. *J Lipid Res.* 48:2547-59.
- Brasaemle, D.L., T. Barber, A.R. Kimmel, and C. Londos. 1997. Post-translational regulation of perilipin expression. Stabilization by stored intracellular neutral lipids. *J Biol Chem.* 272:9378-87.
- Brasaemle, D.L., G. Dolios, L. Shapiro, and R. Wang. 2004. Proteomic analysis of proteins associated with lipid droplets of basal and lipolytically stimulated 3T3-L1 adipocytes. *J Biol Chem.* 279:46835-42.
- Brasaemle, D.L., D.M. Levin, D.C. Adler-Wailes, and C. Londos. 2000a. The lipolytic stimulation of 3T3-L1 adipocytes promotes the translocation of hormone-sensitive lipase to the surfaces of lipid storage droplets. *Biochim Biophys Acta.* 1483:251-62.

- Brasaemle, D.L., B. Rubin, I.A. Harten, J. Gruia-Gray, A.R. Kimmel, and C. Londos. 2000b. Perilipin A increases triacylglycerol storage by decreasing the rate of triacylglycerol hydrolysis. *J Biol Chem.* 275:38486-93.
- Brown, J.M., S. Chung, A. Das, G.S. Shelness, L.L. Rudel, and L. Yu. 2007. CGI-58 facilitates the mobilization of cytoplasmic triglyceride for lipoprotein secretion in hepatoma cells. *J Lipid Res.* 48:2295-305.
- Buhman, K.K., M. Accad, S. Novak, R.S. Choi, J.S. Wong, R.L. Hamilton, S. Turley, and R.V. Farese, Jr. 2000. Resistance to diet-induced hypercholesterolemia and gallstone formation in ACAT2-deficient mice. *Nat Med.* 6:1341-7.
- Cao, J., L. Cheng, and Y. Shi. 2007. Catalytic properties of MGAT3, a putative triacylglycerol synthase. *J Lipid Res.* 48:583-91.
- Carman, G.M., and G.S. Han. 2006. Roles of phosphatidate phosphatase enzymes in lipid metabolism. *Trends Biochem Sci.* 31:694-9.
- Cases, S., S.J. Smith, Y.W. Zheng, H.M. Myers, S.R. Lear, E. Sande, S. Novak, C. Collins, C.B. Welch, A.J. Lusis, S.K. Erickson, and R.V. Farese, Jr. 1998. Identification of a gene encoding an acyl CoA:diacylglycerol acyltransferase, a key enzyme in triacylglycerol synthesis. *Proc Natl Acad Sci U S A.* 95:13018-23.
- Cases, S., S.J. Stone, P. Zhou, E. Yen, B. Tow, K.D. Lardizabal, T. Voelker, and R.V. Farese, Jr. 2001. Cloning of DGAT2, a second mammalian diacylglycerol acyltransferase, and related family members. *J Biol Chem.* 276:38870-6.
- Caviglia, J.M., J.D. Sparks, N. Toraskar, A.M. Brinker, T.C. Yin, J.L. Dixon, and D.L. Brasaemle. 2009. ABHD5/CGI-58 facilitates the assembly and secretion of apolipoprotein B lipoproteins by McA RH7777 rat hepatoma cells. *Biochim Biophys Acta.* 1791:198-205.
- Chang, B.H., L. Li, A. Paul, S. Taniguchi, V. Nannegari, W.C. Heird, and L. Chan. 2006. Protection against fatty liver but normal adipogenesis in mice lacking adipose differentiation-related protein. *Mol Cell Biol.* 26:1063-76.
- Chang, C.C., N. Sakashita, K. Ornvold, O. Lee, E.T. Chang, R. Dong, S. Lin, C.Y. Lee, S.C. Strom, R. Kashyap, J.J. Fung, R.V. Farese, Jr., J.F. Patoiseau, A. Delhon, and T.Y. Chang. 2000. Immunological quantitation and

- localization of ACAT-1 and ACAT-2 in human liver and small intestine. *J Biol Chem.* 275:28083-92.
- Chen, S.H., G. Habib, C.Y. Yang, Z.W. Gu, B.R. Lee, S.A. Weng, S.R. Silberman, S.J. Cai, J.P. Deslypere, M. Rosseneu, and et al. 1987. Apolipoprotein B-48 is the product of a messenger RNA with an organ-specific in-frame stop codon. *Science.* 238:363-6.
- Cheng, J., A. Fujita, Y. Ohsaki, M. Suzuki, Y. Shinohara, and T. Fujimoto. 2009. Quantitative electron microscopy shows uniform incorporation of triglycerides into existing lipid droplets. *Histochem Cell Biol.*
- Cohen, A.W., B. Razani, W. Schubert, T.M. Williams, X.B. Wang, P. Iyengar, D.L. Brasaemle, P.E. Scherer, and M.P. Lisanti. 2004. Role of caveolin-1 in the modulation of lipolysis and lipid droplet formation. *Diabetes.* 53:1261-70.
- Cohen, P., M. Miyazaki, N.D. Socci, A. Hagge-Greenberg, W. Liedtke, A.A. Soukas, R. Sharma, L.C. Hudgins, J.M. Ntambi, and J.M. Friedman. 2002. Role for stearoyl-CoA desaturase-1 in leptin-mediated weight loss. *Science.* 297:240-3.
- Coleman, R.A., and D.P. Lee. 2004. Enzymes of triacylglycerol synthesis and their regulation. *Prog Lipid Res.* 43:134-76.
- Coleman, R.A., T.M. Lewin, and D.M. Muoio. 2000. Physiological and nutritional regulation of enzymes of triacylglycerol synthesis. *Annu Rev Nutr.* 20:77-103.
- Coleman, R.A., T.M. Lewin, C.G. Van Horn, and M.R. Gonzalez-Baro. 2002. Do long-chain acyl-CoA synthetases regulate fatty acid entry into synthetic versus degradative pathways? *J Nutr.* 132:2123-6.
- Cook, H., and C. McMaster. 2002. Fatty acid desaturation and chain elongation in eukaryotes. *In Biochemistry of lipids, lipoproteins, and membranes.* Vol. 36. D.E. Vance and J.E. Vance, editors. Elsevier, Amsterdam. 607 p.
- Cushman, S.W. 1970. Structure-function relationships in the adipose cell. I. Ultrastructure of the isolated adipose cell. *J Cell Biol.* 46:326-41.

- Davidson, N.O., and G.S. Shelness. 2000. APOLIPOPROTEIN B: mRNA editing, lipoprotein assembly, and presecretory degradation. *Annu Rev Nutr.* 20:169-93.
- Davis, R.A. 1999. Cell and molecular biology of the assembly and secretion of apolipoprotein B-containing lipoproteins by the liver. *Biochim Biophys Acta.* 1440:1-31.
- Declercq, P.E., H.P. Haagsman, P. Van Veldhoven, L.J. Debeer, L.M. Van Golde, and G.P. Mannaerts. 1984. Rat liver dihydroxyacetone-phosphate acyltransferases and their contribution to glycerolipid synthesis. *J Biol Chem.* 259:9064-75.
- Dixon, J.L., and H.N. Ginsberg. 1993. Regulation of hepatic secretion of apolipoprotein B-containing lipoproteins: information obtained from cultured liver cells. *J Lipid Res.* 34:167-79.
- Dolinsky, V.W., D. Gilham, M. Alam, D.E. Vance, and R. Lehner. 2004. Triacylglycerol hydrolase: role in intracellular lipid metabolism. *Cell Mol Life Sci.* 61:1633-51.
- Dolinsky, V.W., S. Sipione, R. Lehner, and D.E. Vance. 2001. The cloning and expression of a murine triacylglycerol hydrolase cDNA and the structure of its corresponding gene. *Biochim Biophys Acta.* 1532:162-72.
- Egan, J.J., A.S. Greenberg, M.K. Chang, S.A. Wek, M.C. Moos, Jr., and C. Londos. 1992. Mechanism of hormone-stimulated lipolysis in adipocytes: translocation of hormone-sensitive lipase to the lipid storage droplet. *Proc Natl Acad Sci U S A.* 89:8537-41.
- Ellinghaus, P., U. Seedorf, and G. Assmann. 1998. Cloning and sequencing of a novel murine liver carboxylesterase cDNA. *Biochim Biophys Acta.* 1397:175-9.
- Elovson, J., J.E. Chatterton, G.T. Bell, V.N. Schumaker, M.A. Reuben, D.L. Puppione, J.R. Reeve, Jr., and N.L. Young. 1988. Plasma very low density lipoproteins contain a single molecule of apolipoprotein B. *J Lipid Res.* 29:1461-73.
- Enoch, H.G., and P. Strittmatter. 1978. Role of tyrosyl and arginyl residues in rat liver microsomal stearylcoenzyme A desaturase. *Biochemistry.* 17:4927-32.

- Escary, J.L., H.A. Choy, K. Reue, and M.C. Schotz. 1998. Hormone-sensitive lipase overexpression increases cholesteryl ester hydrolysis in macrophage foam cells. *Arterioscler Thromb Vasc Biol.* 18:991-8.
- Fernandez, M.A., C. Albor, M. Ingelmo-Torres, S.J. Nixon, C. Ferguson, T. Kurzchalia, F. Tebar, C. Enrich, R.G. Parton, and A. Pol. 2006. Caveolin-1 is essential for liver regeneration. *Science.* 313:1628-32.
- Fisher, E.A., and H.N. Ginsberg. 2002. Complexity in the secretory pathway: the assembly and secretion of apolipoprotein B-containing lipoproteins. *J Biol Chem.* 277:17377-80.
- Folch, J., M. Lees, and G.H. Sloane Stanley. 1957. A simple method for the isolation and purification of total lipides from animal tissues. *J Biol Chem.* 226:497-509.
- Fredrikson, G., and P. Belfrage. 1983. Positional specificity of hormone-sensitive lipase from rat adipose tissue. *J Biol Chem.* 258:14253-6.
- Fujimoto, T., H. Kogo, K. Ishiguro, K. Tauchi, and R. Nomura. 2001. Caveolin-2 is targeted to lipid droplets, a new "membrane domain" in the cell. *J Cell Biol.* 152:1079-85.
- Fujimoto, T., Y. Ohsaki, J. Cheng, M. Suzuki, and Y. Shinohara. 2008. Lipid droplets: a classic organelle with new outfits. *Histochem Cell Biol.* 130:263-79.
- Fujimoto, Y., H. Itabe, J. Sakai, M. Makita, J. Noda, M. Mori, Y. Higashi, S. Kojima, and T. Takano. 2004. Identification of major proteins in the lipid droplet-enriched fraction isolated from the human hepatocyte cell line HuH7. *Biochim Biophys Acta.* 1644:47-59.
- Fukao, T., G.D. Lopaschuk, and G.A. Mitchell. 2004. Pathways and control of ketone body metabolism: on the fringe of lipid biochemistry. *Prostaglandins Leukot Essent Fatty Acids.* 70:243-51.
- Fukushima, M., M. Enjoji, M. Kohjima, R. Sugimoto, S. Ohta, K. Kotoh, M. Kuniyoshi, K. Kobayashi, M. Imamura, T. Inoguchi, M. Nakamuta, and H. Nawata. 2005. Adipose differentiation related protein induces lipid accumulation and lipid droplet formation in hepatic stellate cells. *In Vitro Cell Dev Biol Anim.* 41:321-4.

- Gao, J., and G. Serrero. 1999. Adipose differentiation related protein (ADRP) expressed in transfected COS-7 cells selectively stimulates long chain fatty acid uptake. *J Biol Chem.* 274:16825-30.
- Garton, A.J., and S.J. Yeaman. 1990. Identification and role of the basal phosphorylation site on hormone-sensitive lipase. *Eur J Biochem.* 191:245-50.
- Ghosh, A.K., G. Ramakrishnan, C. Chandramohan, and R. Rajasekharan. 2008. CGI-58, the causative gene for Chanarin-Dorfman syndrome, mediates acylation of lysophosphatidic acid. *J Biol Chem.* 283:24525-33.
- Ghosh, S. 2000. Cholesteryl ester hydrolase in human monocyte/macrophage: cloning, sequencing, and expression of full-length cDNA. *Physiol Genomics.* 2:1-8.
- Ghosh, S., R.W. St Clair, and L.L. Rudel. 2003. Mobilization of cytoplasmic CE droplets by overexpression of human macrophage cholesteryl ester hydrolase. *J Lipid Res.* 44:1833-40.
- Gibbons, G.F., S.M. Bartlett, C.E. Sparks, and J.D. Sparks. 1992. Extracellular fatty acids are not utilized directly for the synthesis of very-low-density lipoprotein in primary cultures of rat hepatocytes. *Biochem J.* 287 (Pt 3):749-53.
- Gibbons, G.F., K. Islam, and R.J. Pease. 2000. Mobilisation of triacylglycerol stores. *Biochim Biophys Acta.* 1483:37-57.
- Gilham, D., M. Alam, W. Gao, D.E. Vance, and R. Lehner. 2005a. Triacylglycerol hydrolase is localized to the endoplasmic reticulum by an unusual retrieval sequence where it participates in VLDL assembly without utilizing VLDL lipids as substrates. *Mol Biol Cell.* 16:984-96.
- Gilham, D., S. Ho, M. Rasouli, P. Martres, D.E. Vance, and R. Lehner. 2003. Inhibitors of hepatic microsomal triacylglycerol hydrolase decrease very low density lipoprotein secretion. *Faseb J.* 17:1685-7.
- Gilham, D., and R. Lehner. 2004. The physiological role of triacylglycerol hydrolase in lipid metabolism. *Rev Endocr Metab Disord.* 5:303-9.
- Gilham, D., K.R. Perreault, C.F. Holmes, D.N. Brindley, D.E. Vance, and R. Lehner. 2005b. Insulin, glucagon and fatty acid treatment of hepatocytes

does not result in phosphorylation or changes in activity of triacylglycerol hydrolase. *Biochim Biophys Acta*. 1736:189-99.

Ginsberg, H.N., and E.A. Fisher. 2009. The ever-expanding role of degradation in the regulation of apolipoprotein B metabolism. *J Lipid Res*. 50 Suppl:S162-6.

Goodman, J.M. 2008. The gregarious lipid droplet. *J Biol Chem*. 283:28005-9.

Gordon, D.A., and H. Jamil. 2000. Progress towards understanding the role of microsomal triglyceride transfer protein in apolipoprotein-B lipoprotein assembly. *Biochim Biophys Acta*. 1486:72-83.

Gordon, D.A., H. Jamil, R.E. Gregg, S.O. Olofsson, and J. Boren. 1996. Inhibition of the microsomal triglyceride transfer protein blocks the first step of apolipoprotein B lipoprotein assembly but not the addition of bulk core lipids in the second step. *J Biol Chem*. 271:33047-53.

Granneman, J.G., H.P. Moore, R.L. Granneman, A.S. Greenberg, M.S. Obin, and Z. Zhu. 2007. Analysis of lipolytic protein trafficking and interactions in adipocytes. *J Biol Chem*. 282:5726-35.

Greenberg, A.S., J.J. Egan, S.A. Wek, N.B. Garty, E.J. Blanchette-Mackie, and C. Londos. 1991. Perilipin, a major hormonally regulated adipocyte-specific phosphoprotein associated with the periphery of lipid storage droplets. *J Biol Chem*. 266:11341-6.

Grefhorst, A., J. Hoekstra, T.G. Derks, D.M. Ouwens, J.F. Baller, R. Havinga, L.M. Havekes, J.A. Romijn, and F. Kuipers. 2005. Acute hepatic steatosis in mice by blocking beta-oxidation does not reduce insulin sensitivity of very-low-density lipoprotein production. *Am J Physiol Gastrointest Liver Physiol*. 289:G592-8.

Grundey, S.M. 1990. Cholesterol and atherosclerosis : diagnosis and treatment. Lippincott ; Gower Medical Pub., Philadelphia New York. 1 v. (various pagings) pp.

Guo, Y., T.C. Walther, M. Rao, N. Stuurman, G. Goshima, K. Terayama, J.S. Wong, R.D. Vale, P. Walter, and R.V. Farese. 2008. Functional genomic screen reveals genes involved in lipid-droplet formation and utilization. *Nature*. 453:657-61.

- Gusarova, V., J.L. Brodsky, and E.A. Fisher. 2003. Apolipoprotein B100 exit from the endoplasmic reticulum (ER) is COPII-dependent, and its lipidation to very low density lipoprotein occurs post-ER. *J Biol Chem.* 278:48051-8.
- Gusarova, V., J. Seo, M.L. Sullivan, S.C. Watkins, J.L. Brodsky, and E.A. Fisher. 2007. Golgi-associated maturation of very low density lipoproteins involves conformational changes in apolipoprotein B, but is not dependent on apolipoprotein E. *J Biol Chem.* 282:19453-62.
- Haemmerle, G., A. Lass, R. Zimmermann, G. Gorkiewicz, C. Meyer, J. Rozman, G. Heldmaier, R. Maier, C. Theussl, S. Eder, D. Kratky, E.F. Wagner, M. Klingenspor, G. Hoefler, and R. Zechner. 2006. Defective lipolysis and altered energy metabolism in mice lacking adipose triglyceride lipase. *Science.* 312:734-7.
- Haemmerle, G., R. Zimmermann, J.G. Strauss, D. Kratky, M. Riederer, G. Knipping, and R. Zechner. 2002. Hormone-sensitive lipase deficiency in mice changes the plasma lipid profile by affecting the tissue-specific expression pattern of lipoprotein lipase in adipose tissue and muscle. *J Biol Chem.* 277:12946-52.
- Hamilton, J.A. 1989. Interactions of triglycerides with phospholipids: incorporation into the bilayer structure and formation of emulsions. *Biochemistry.* 28:2514-20.
- Hamilton, J.A., and D.M. Small. 1981. Solubilization and localization of triolein in phosphatidylcholine bilayers: a ¹³C NMR study. *Proc Natl Acad Sci U S A.* 78:6878-82.
- Hamilton, R.L., J.S. Wong, C.M. Cham, L.B. Nielsen, and S.G. Young. 1998. Chylomicron-sized lipid particles are formed in the setting of apolipoprotein B deficiency. *J Lipid Res.* 39:1543-57.
- Hammond, L.E., P.A. Gallagher, S. Wang, S. Hiller, K.D. Kluckman, E.L. Posey-Marcos, N. Maeda, and R.A. Coleman. 2002. Mitochondrial glycerol-3-phosphate acyltransferase-deficient mice have reduced weight and liver triacylglycerol content and altered glycerolipid fatty acid composition. *Mol Cell Biol.* 22:8204-14.
- Havel, R.J., V.G. Shore, B. Shore, and D.M. Bier. 1970. Role of specific glycopeptides of human serum lipoproteins in the activation of lipoprotein lipase. *Circ Res.* 27:595-600.

- Heid, H.W., R. Moll, I. Schwetlick, H.R. Rackwitz, and T.W. Keenan. 1998. Adipophilin is a specific marker of lipid accumulation in diverse cell types and diseases. *Cell Tissue Res.* 294:309-21.
- Higashi, Y., H. Itabe, H. Fukase, M. Mori, Y. Fujimoto, and T. Takano. 2003. Transmembrane lipid transfer is crucial for providing neutral lipids during very low density lipoprotein assembly in endoplasmic reticulum. *J Biol Chem.* 278:21450-8.
- Hilaire, N., A. Negre-Salvayre, and R. Salvayre. 1993. Cytoplasmic triacylglycerols and cholesteryl esters are degraded in two separate catabolic pools in cultured human fibroblasts. *FEBS Lett.* 328:230-4.
- Hilaire, N., A. Negre-Salvayre, and R. Salvayre. 1994. Cellular uptake and catabolism of high-density-lipoprotein triacylglycerols in human cultured fibroblasts: degradation block in neutral lipid storage disease. *Biochem J.* 297 (Pt 3):467-73.
- Holm, C. 2003. Molecular mechanisms regulating hormone-sensitive lipase and lipolysis. *Biochem Soc Trans.* 31:1120-4.
- Hussain, M.M., A. Bakillah, and H. Jamil. 1997. Apolipoprotein B binding to microsomal triglyceride transfer protein decreases with increases in length and lipidation: implications in lipoprotein biosynthesis. *Biochemistry.* 36:13060-7.
- Imamura, M., T. Inoguchi, S. Ikuyama, S. Taniguchi, K. Kobayashi, N. Nakashima, and H. Nawata. 2002. ADRP stimulates lipid accumulation and lipid droplet formation in murine fibroblasts. *Am J Physiol Endocrinol Metab.* 283:E775-83.
- Jacobs, R.L., C. Devlin, I. Tabas, and D.E. Vance. 2004. Targeted deletion of hepatic CTP:phosphocholine cytidyltransferase alpha in mice decreases plasma high density and very low density lipoproteins. *J Biol Chem.* 279:47402-10.
- Jacobs, R.L., S. Lingrell, Y. Zhao, G.A. Francis, and D.E. Vance. 2008. Hepatic CTP:phosphocholine cytidyltransferase-alpha is a critical predictor of plasma high density lipoprotein and very low density lipoprotein. *J Biol Chem.* 283:2147-55.
- Jahn, R., and R.H. Scheller. 2006. SNAREs--engines for membrane fusion. *Nat Rev Mol Cell Biol.* 7:631-43.

- Jamil, H., J.K. Dickson, Jr., C.H. Chu, M.W. Lago, J.K. Rinehart, S.A. Biller, R.E. Gregg, and J.R. Wetterau. 1995. Microsomal triglyceride transfer protein. Specificity of lipid binding and transport. *J Biol Chem.* 270:6549-54.
- Jenkins, C.M., D.J. Mancuso, W. Yan, H.F. Sims, B. Gibson, and R.W. Gross. 2004. Identification, cloning, expression, and purification of three novel human calcium-independent phospholipase A2 family members possessing triacylglycerol lipase and acylglycerol transacylase activities. *J Biol Chem.* 279:48968-75.
- Jonas, A. 2002. Lipoprotein structure. *In Biochemistry of lipids, lipoproteins, and membranes.* Vol. 36. D.E. Vance and J.E. Vance, editors. Elsevier, Amsterdam. 607 p.
- Kayden, H.J., J.R. Senior, and F.H. Mattson. 1967. The monoglyceride pathway of fat absorption in man. *J Clin Invest.* 46:1695-703.
- Kershaw, E.E., J.K. Hamm, L.A. Verhagen, O. Peroni, M. Katic, and J.S. Flier. 2006. Adipose triglyceride lipase: function, regulation by insulin, and comparison with adiponutrin. *Diabetes.* 55:148-57.
- Ko, K.W., B. Erickson, and R. Lehner. 2009. Es-x/Ces1 prevents triacylglycerol accumulation in McArdle-RH7777 hepatocytes. *Biochim Biophys Acta.*
- Kornberg, A., and W.E. Pricer, Jr. 1953. Enzymatic synthesis of the coenzyme A derivatives of long chain fatty acids. *J Biol Chem.* 204:329-43.
- Kuerschner, L., C. Moessinger, and C. Thiele. 2008. Imaging of lipid biosynthesis: how a neutral lipid enters lipid droplets. *Traffic.* 9:338-52.
- Kuipers, F., M.C. Jong, Y. Lin, M. Eck, R. Havinga, V. Bloks, H.J. Verkade, M.H. Hofker, H. Moshage, T.J. Berkel, R.J. Vonk, and L.M. Havekes. 1997. Impaired secretion of very low density lipoprotein-triglycerides by apolipoprotein E- deficient mouse hepatocytes. *J Clin Invest.* 100:2915-22.
- Kuipers, F., J.M. van Ree, M.H. Hofker, H. Wolters, G. In't Veld, R. Havinga, R.J. Vonk, H.M. Princen, and L.M. Havekes. 1996. Altered lipid metabolism in apolipoprotein E-deficient mice does not affect cholesterol balance across the liver. *Hepatology.* 24:241-7.
- Kulinski, A., S. Rustaeus, and J.E. Vance. 2002. Microsomal triacylglycerol transfer protein is required for luminal accretion of triacylglycerol not

associated with ApoB, as well as for ApoB lipidation. *J Biol Chem.* 277:31516-25.

- Lankester, D.L., A.M. Brown, and V.A. Zammit. 1998. Use of cytosolic triacylglycerol hydrolysis products and of exogenous fatty acid for the synthesis of triacylglycerol secreted by cultured rat hepatocytes. *J Lipid Res.* 39:1889-95.
- Lardizabal, K.D., J.T. Mai, N.W. Wagner, A. Wyrick, T. Voelker, and D.J. Hawkins. 2001. DGAT2 is a new diacylglycerol acyltransferase gene family: purification, cloning, and expression in insect cells of two polypeptides from *Mortierella ramanniana* with diacylglycerol acyltransferase activity. *J Biol Chem.* 276:38862-9.
- LaRosa, J.C., R.I. Levy, P. Herbert, S.E. Lux, and D.S. Fredrickson. 1970. A specific apoprotein activator for lipoprotein lipase. *Biochem Biophys Res Commun.* 41:57-62.
- Lass, A., R. Zimmermann, G. Haemmerle, M. Riederer, G. Schoiswohl, M. Schweiger, P. Kienesberger, J.G. Strauss, G. Gorkiewicz, and R. Zechner. 2006. Adipose triglyceride lipase-mediated lipolysis of cellular fat stores is activated by CGI-58 and defective in Chanarin-Dorfman Syndrome. *Cell Metab.* 3:309-19.
- Le Lay, S., E. Hajdich, M.R. Lindsay, X. Le Liepvre, C. Thiele, P. Ferre, R.G. Parton, T. Kurzchalia, K. Simons, and I. Dugail. 2006. Cholesterol-induced caveolin targeting to lipid droplets in adipocytes: a role for caveolar endocytosis. *Traffic.* 7:549-61.
- Lefevre, C., F. Jobard, F. Caux, B. Bouadjar, A. Karaduman, R. Heilig, H. Lakhdar, A. Wollenberg, J.L. Verret, J. Weissenbach, M. Ozguc, M. Lathrop, J.F. Prud'homme, and J. Fischer. 2001. Mutations in CGI-58, the gene encoding a new protein of the esterase/lipase/thioesterase subfamily, in Chanarin-Dorfman syndrome. *Am J Hum Genet.* 69:1002-12.
- Lehner, R., Z. Cui, and D.E. Vance. 1999. Subcellular localization, developmental expression and characterization of a liver triacylglycerol hydrolase. *Biochem J.* 338 (Pt 3):761-8.
- Lehner, R., and A. Kuksis. 1993. Triacylglycerol synthesis by an sn-1,2(2,3)-diacylglycerol transacylase from rat intestinal microsomes. *J Biol Chem.* 268:8781-6.

- Lehner, R., and A. Kuksis. 1996. Biosynthesis of triacylglycerols. *Prog Lipid Res.* 35:169-201.
- Lehner, R., and D.E. Vance. 1999a. Cloning and expression of a cDNA encoding a hepatic microsomal lipase that mobilizes stored triacylglycerol. *Biochem J.* 343:1-10.
- Lehner, R., and D.E. Vance. 1999b. Cloning and expression of a cDNA encoding a hepatic microsomal lipase that mobilizes stored triacylglycerol. *Biochem J.* 343 Pt 1:1-10.
- Lehner, R., and R. Verger. 1997. Purification and characterization of a porcine liver microsomal triacylglycerol hydrolase. *Biochemistry.* 36:1861-8.
- Lessire, R., J.J. Bessoule, L. Cook, D.L. Cinti, and C. Cassagne. 1993. Occurrence and characterization of a dehydratase enzyme in the leek icosanoyl-CoA synthase complex. *Biochim Biophys Acta.* 1169:243-9.
- Levine, T. 2004. Short-range intracellular trafficking of small molecules across endoplasmic reticulum junctions. *Trends Cell Biol.* 14:483-90.
- Levine, T., and C. Loewen. 2006. Inter-organelle membrane contact sites: through a glass, darkly. *Curr Opin Cell Biol.* 18:371-8.
- Levy, E., S. Stan, E. Delvin, D. Menard, C. Shoulders, C. Garofalo, I. Slight, E. Seidman, G. Mayer, and M. Bendayan. 2002. Localization of microsomal triglyceride transfer protein in the Golgi: possible role in the assembly of chylomicrons. *J Biol Chem.* 277:16470-7.
- Li, L., P. Stillemark-Billton, C. Beck, P. Bostrom, L. Andersson, M. Rutberg, J. Ericsson, B. Magnusson, D. Marchesan, A. Ljungberg, J. Boren, and S.O. Olofsson. 2006. Epigallocatechin gallate increases the formation of cytosolic lipid droplets and decreases the secretion of apoB-100 VLDL. *J Lipid Res.* 47:67-77.
- Liang, J.J., P. Oelkers, C. Guo, P.C. Chu, J.L. Dixon, H.N. Ginsberg, and S.L. Sturley. 2004. Overexpression of human diacylglycerol acyltransferase 1, acyl-coa:cholesterol acyltransferase 1, or acyl-CoA:cholesterol acyltransferase 2 stimulates secretion of apolipoprotein B-containing lipoproteins in McA-RH7777 cells. *J Biol Chem.* 279:44938-44.

- Listenberger, L.L., A.G. Ostermeyer-Fay, E.B. Goldberg, W.J. Brown, and D.A. Brown. 2007. Adipocyte differentiation-related protein reduces the lipid droplet association of adipose triglyceride lipase and slows triacylglycerol turnover. *J Lipid Res.* 48:2751-61.
- Liu, P., R. Bartz, J.K. Zehmer, Y.S. Ying, M. Zhu, G. Serrero, and R.G. Anderson. 2007. Rab-regulated interaction of early endosomes with lipid droplets. *Biochim Biophys Acta.* 1773:784-93.
- Liu, P., Y. Ying, Y. Zhao, D.I. Mundy, M. Zhu, and R.G. Anderson. 2004. Chinese hamster ovary K2 cell lipid droplets appear to be metabolic organelles involved in membrane traffic. *J Biol Chem.* 279:3787-92.
- Liu, Y., J.S. Millar, D.A. Cromley, M. Graham, R. Crooke, J.T. Billheimer, and D.J. Rader. 2008. Knockdown of acyl-CoA:diacylglycerol acyltransferase 2 with antisense oligonucleotide reduces VLDL TG and ApoB secretion in mice. *Biochim Biophys Acta.* 1781:97-104.
- Lo, V., B. Erickson, M. Thomason-Hughes, K.W. Ko, V.W. Dolinsky, R. Nelson, and R. Lehner. 2009. Arylacetamide deacetylase attenuates fatty acid-induced triacylglycerol accumulation in rat hepatoma cells. *J Lipid Res.*
- Lowe, M.E. 2002. The triglyceride lipases of the pancreas. *J Lipid Res.* 43:2007-16.
- Lu, X., J. Gruia-Gray, N.G. Copeland, D.J. Gilbert, N.A. Jenkins, C. Londos, and A.R. Kimmel. 2001. The murine perilipin gene: the lipid droplet-associated perilipins derive from tissue-specific, mRNA splice variants and define a gene family of ancient origin. *Mamm Genome.* 12:741-9.
- Magnusson, B., L. Asp, P. Bostrom, M. Ruiz, P. Stillemark-Billton, D. Linden, J. Boren, and S.O. Olofsson. 2006. Adipocyte differentiation-related protein promotes fatty acid storage in cytosolic triglycerides and inhibits secretion of very low-density lipoproteins. *Arterioscler Thromb Vasc Biol.* 26:1566-71.
- Man, W.C., M. Miyazaki, K. Chu, and J. Ntambi. 2006. Colocalization of SCD1 and DGAT2: implying preference for endogenous monounsaturated fatty acids in triglyceride synthesis. *J Lipid Res.* 47:1928-39.
- Marchesan, D., M. Rutberg, L. Andersson, L. Asp, T. Larsson, J. Boren, B.R. Johansson, and S.O. Olofsson. 2003. A phospholipase D-dependent process forms lipid droplets containing caveolin, adipocyte differentiation-

related protein, and vimentin in a cell-free system. *J Biol Chem.* 278:27293-300.

- Marcinkiewicz, A., D. Gauthier, A. Garcia, and D.L. Brasaemle. 2006. The phosphorylation of serine 492 of perilipin directs lipid droplet fragmentation and dispersion. *J Biol Chem.* 281:11901-9.
- Martin, S., K. Driessen, S.J. Nixon, M. Zerial, and R.G. Parton. 2005. Regulated localization of Rab18 to lipid droplets: effects of lipolytic stimulation and inhibition of lipid droplet catabolism. *J Biol Chem.* 280:42325-35.
- Martin, S., and R.G. Parton. 2005. Caveolin, cholesterol, and lipid bodies. *Semin Cell Dev Biol.* 16:163-74.
- Martin, S., and R.G. Parton. 2006. Lipid droplets: a unified view of a dynamic organelle. *Nat Rev Mol Cell Biol.* 7:373-8.
- Martinez-Botas, J., J.B. Anderson, D. Tessier, A. Lapillonne, B.H. Chang, M.J. Quast, D. Gorenstein, K.H. Chen, and L. Chan. 2000. Absence of perilipin results in leanness and reverses obesity in Lepr(db/db) mice. *Nat Genet.* 26:474-9.
- Mattson, F.H., and R.A. Volpenhein. 1964. The Digestion and Absorption of Triglycerides. *J Biol Chem.* 239:2772-7.
- Maugeais, C., U.J. Tietge, K. Tsukamoto, J.M. Glick, and D.J. Rader. 2000. Hepatic apolipoprotein E expression promotes very low density lipoprotein-apolipoprotein B production in vivo in mice. *J Lipid Res.* 41:1673-9.
- Mensenkamp, A.R., L.M. Havekes, J.A. Romijn, and F. Kuipers. 2001. Hepatic steatosis and very low density lipoprotein secretion: the involvement of apolipoprotein E. *J Hepatol.* 35:816-22.
- Mensenkamp, A.R., M.C. Jong, H. van Goor, M.J. van Luyn, V. Bloks, R. Havinga, P.J. Voshol, M.H. Hofker, K.W. van Dijk, L.M. Havekes, and F. Kuipers. 1999. Apolipoprotein E participates in the regulation of very low density lipoprotein-triglyceride secretion by the liver. *J Biol Chem.* 274:35711-8.
- Mensenkamp, A.R., M.J. Van Luyn, R. Havinga, B. Teusink, I.J. Waterman, C.J. Mann, B.M. Elzinga, H.J. Verkade, V.A. Zammit, L.M. Havekes, C.C.

- Shoulders, and F. Kuipers. 2004. The transport of triglycerides through the secretory pathway of hepatocytes is impaired in apolipoprotein E deficient mice. *J Hepatol.* 40:599-606.
- Millar, J.S., S.J. Stone, U.J. Tietge, B. Tow, J.T. Billheimer, J.S. Wong, R.L. Hamilton, R.V. Farese, Jr., and D.J. Rader. 2006. Short-term overexpression of DGAT1 or DGAT2 increases hepatic triglyceride but not VLDL triglyceride or apoB production. *J Lipid Res.* 47:2297-305.
- Mitchell, D.M., M. Zhou, R. Pariyarath, H. Wang, J.D. Aitchison, H.N. Ginsberg, and E.A. Fisher. 1998. Apoprotein B100 has a prolonged interaction with the translocon during which its lipidation and translocation change from dependence on the microsomal triglyceride transfer protein to independence. *Proc Natl Acad Sci U S A.* 95:14733-8.
- Miyazaki, M., M.T. Flowers, H. Sampath, K. Chu, C. Otzelberger, X. Liu, and J.M. Ntambi. 2007. Hepatic stearoyl-CoA desaturase-1 deficiency protects mice from carbohydrate-induced adiposity and hepatic steatosis. *Cell Metab.* 6:484-96.
- Miyoshi, H., S.C. Souza, H.H. Zhang, K.J. Strissel, M.A. Christoffolete, J. Kovsan, A. Rudich, F.B. Kraemer, A.C. Bianco, M.S. Obin, and A.S. Greenberg. 2006. Perilipin promotes hormone-sensitive lipase-mediated adipocyte lipolysis via phosphorylation-dependent and -independent mechanisms. *J Biol Chem.* 281:15837-44.
- Monetti, M., M.C. Levin, M.J. Watt, M.P. Sajan, S. Marmor, B.K. Hubbard, R.D. Stevens, J.R. Bain, C.B. Newgard, R.V. Farese, Sr., A.L. Hevener, and R.V. Farese, Jr. 2007. Dissociation of hepatic steatosis and insulin resistance in mice overexpressing DGAT in the liver. *Cell Metab.* 6:69-78.
- Mu, H., and C.E. Hoy. 2004. The digestion of dietary triacylglycerols. *Prog Lipid Res.* 43:105-33.
- Mulder, H., M. Sorhede-Winzell, J.A. Contreras, M. Fex, K. Strom, T. Ploug, H. Galbo, P. Arner, C. Lundberg, F. Sundler, B. Ahren, and C. Holm. 2003. Hormone-sensitive lipase null mice exhibit signs of impaired insulin sensitivity whereas insulin secretion is intact. *J Biol Chem.* 278:36380-8.
- Murphy, D.J. 2001. The biogenesis and functions of lipid bodies in animals, plants and microorganisms. *Prog Lipid Res.* 40:325-438.

- Murphy, D.J., and J. Vance. 1999. Mechanisms of lipid-body formation. *Trends Biochem Sci.* 24:109-15.
- Murphy, S., S. Martin, and R.G. Parton. 2008. Lipid droplet-organelle interactions; sharing the fats. *Biochim Biophys Acta.*
- Murphy, S., S. Martin, and R.G. Parton. 2009. Lipid droplet-organelle interactions; sharing the fats. *Biochim Biophys Acta.* 1791:441-7.
- Myher, J.J., A. Kuksis, and S. Pind. 1989. Molecular species of glycerophospholipids and sphingomyelins of human plasma: comparison to red blood cells. *Lipids.* 24:408-18.
- Neel, J.V. 1962. Diabetes mellitus: a "thrifty" genotype rendered detrimental by "progress"? *Am J Hum Genet.* 14:353-62.
- Noga, A.A., L.M. Stead, Y. Zhao, M.E. Brosnan, J.T. Brosnan, and D.E. Vance. 2003. Plasma homocysteine is regulated by phospholipid methylation. *J Biol Chem.* 278:5952-5.
- Noga, A.A., Y. Zhao, and D.E. Vance. 2002. An unexpected requirement for phosphatidylethanolamine N-methyltransferase in the secretion of very low density lipoproteins. *J Biol Chem.* 277:42358-65.
- Ntambi, J.M., M. Miyazaki, J.P. Stoehr, H. Lan, C.M. Kendziorski, B.S. Yandell, Y. Song, P. Cohen, J.M. Friedman, and A.D. Attie. 2002. Loss of stearoyl-CoA desaturase-1 function protects mice against adiposity. *Proc Natl Acad Sci U S A.* 99:11482-6.
- Ohsaki, Y., J. Cheng, A. Fujita, T. Tokumoto, and T. Fujimoto. 2006. Cytoplasmic lipid droplets are sites of convergence of proteasomal and autophagic degradation of apolipoprotein B. *Mol Biol Cell.* 17:2674-83.
- Ohsaki, Y., J. Cheng, M. Suzuki, Y. Shinohara, A. Fujita, and T. Fujimoto. 2009. Biogenesis of cytoplasmic lipid droplets: From the lipid ester globule in the membrane to the visible structure. *Biochim Biophys Acta.* 1791:399-407.
- Okazaki, H., J. Osuga, K. Tsukamoto, N. Isoo, T. Kitamine, Y. Tamura, S. Tomita, M. Sekiya, N. Yahagi, Y. Iizuka, K. Ohashi, K. Harada, T. Gotoda, H. Shimano, S. Kimura, R. Nagai, N. Yamada, and S. Ishibashi. 2002. Elimination of cholesterol ester from macrophage foam cells by

- adenovirus-mediated gene transfer of hormone-sensitive lipase. *J Biol Chem.* 277:31893-9.
- Olofsson, S.O., and J. Boren. 2005. Apolipoprotein B: a clinically important apolipoprotein which assembles atherogenic lipoproteins and promotes the development of atherosclerosis. *J Intern Med.* 258:395-410.
- Olofsson, S.O., P. Bostrom, L. Andersson, M. Rutberg, J. Perman, and J. Boren. 2008. Lipid droplets as dynamic organelles connecting storage and efflux of lipids. *Biochim Biophys Acta.*
- Olofsson, S.O., P. Bostrom, L. Andersson, M. Rutberg, J. Perman, and J. Boren. 2009. Lipid droplets as dynamic organelles connecting storage and efflux of lipids. *Biochim Biophys Acta.* 1791:448-58.
- Olofsson, S.O., P. Stillemark-Billton, and L. Asp. 2000. Intracellular assembly of VLDL: two major steps in separate cell compartments. *Trends Cardiovasc Med.* 10:338-45.
- Osuga, J., S. Ishibashi, T. Oka, H. Yagyu, R. Tozawa, A. Fujimoto, F. Shionoiri, N. Yahagi, F.B. Kraemer, O. Tsutsumi, and N. Yamada. 2000. Targeted disruption of hormone-sensitive lipase results in male sterility and adipocyte hypertrophy, but not in obesity. *Proc Natl Acad Sci U S A.* 97:787-92.
- Owen, M.R., C.C. Corstorphine, and V.A. Zammit. 1997. Overt and latent activities of diacylglycerol acyltransferase in rat liver microsomes: possible roles in very-low-density lipoprotein triacylglycerol secretion. *Biochem J.* 323 (Pt 1):17-21.
- Ozeki, S., J. Cheng, K. Tauchi-Sato, N. Hatano, H. Taniguchi, and T. Fujimoto. 2005. Rab18 localizes to lipid droplets and induces their close apposition to the endoplasmic reticulum-derived membrane. *J Cell Sci.* 118:2601-11.
- Parton, R.G., and K. Simons. 2007. The multiple faces of caveolae. *Nat Rev Mol Cell Biol.* 8:185-94.
- Patel, S.B., and S.M. Grundy. 1996. Interactions between microsomal triglyceride transfer protein and apolipoprotein B within the endoplasmic reticulum in a heterologous expression system. *J Biol Chem.* 271:18686-94.

- Pease, R.J., D. Wiggins, E.D. Saggerson, J. Tree, and G.F. Gibbons. 1999. Metabolic characteristics of a human hepatoma cell line stably transfected with hormone-sensitive lipase. *Biochem J.* 341:453-60.
- Pol, A., S. Martin, M.A. Fernandez, C. Ferguson, A. Carozzi, R. Luetterforst, C. Enrich, and R.G. Parton. 2004. Dynamic and regulated association of caveolin with lipid bodies: modulation of lipid body motility and function by a dominant negative mutant. *Mol Biol Cell.* 15:99-110.
- Pol, A., S. Martin, M.A. Fernandez, M. Ingelmo-Torres, C. Ferguson, C. Enrich, and R.G. Parton. 2005. Cholesterol and fatty acids regulate dynamic caveolin trafficking through the Golgi complex and between the cell surface and lipid bodies. *Mol Biol Cell.* 16:2091-105.
- Powell, L.M., S.C. Wallis, R.J. Pease, Y.H. Edwards, T.J. Knott, and J. Scott. 1987. A novel form of tissue-specific RNA processing produces apolipoprotein-B48 in intestine. *Cell.* 50:831-40.
- Raabe, M., M.M. Veniant, M.A. Sullivan, C.H. Zlot, J. Bjorkegren, L.B. Nielsen, J.S. Wong, R.L. Hamilton, and S.G. Young. 1999. Analysis of the role of microsomal triglyceride transfer protein in the liver of tissue-specific knockout mice. *J Clin Invest.* 103:1287-98.
- Razani, B., and M.P. Lisanti. 2001. Two distinct caveolin-1 domains mediate the functional interaction of caveolin-1 with protein kinase A. *Am J Physiol Cell Physiol.* 281:C1241-50.
- Razani, B., C.S. Rubin, and M.P. Lisanti. 1999. Regulation of cAMP-mediated signal transduction via interaction of caveolins with the catalytic subunit of protein kinase A. *J Biol Chem.* 274:26353-60.
- Redgrave, T.G., and L.A. Carlson. 1979. Changes in plasma very low density and low density lipoprotein content, composition, and size after a fatty meal in normo- and hypertriglyceridemic man. *J Lipid Res.* 20:217-29.
- Redgrave, T.G., and D.M. Small. 1979. Quantitation of the transfer of surface phospholipid of chylomicrons to the high density lipoprotein fraction during the catabolism of chylomicrons in the rat. *J Clin Invest.* 64:162-71.
- Reid, B.N., G.P. Ables, O.A. Otlivanchik, G. Schoiswohl, R. Zechner, W.S. Blaner, I.J. Goldberg, R.F. Schwabe, S.C. Chua, Jr., and L.S. Huang. 2008. Hepatic overexpression of hormone-sensitive lipase and adipose

- triglyceride lipase promotes fatty acid oxidation, stimulates direct release of free fatty acids, and ameliorates steatosis. *J Biol Chem.* 283:13087-99.
- Rusinol, A., H. Verkade, and J.E. Vance. 1993. Assembly of rat hepatic very low density lipoproteins in the endoplasmic reticulum. *J Biol Chem.* 268:3555-62.
- Rustaeus, S., K. Lindberg, J. Boren, and S.O. Olofsson. 1995. Brefeldin A reversibly inhibits the assembly of apoB containing lipoproteins in McA-RH7777 cells. *J Biol Chem.* 270:28879-86.
- Rustaeus, S., P. Stillemark, K. Lindberg, D. Gordon, and S.O. Olofsson. 1998. The microsomal triglyceride transfer protein catalyzes the post-translational assembly of apolipoprotein B-100 very low density lipoprotein in McA-RH7777 cells. *J Biol Chem.* 273:5196-203.
- Sahoo, D., T.C. Trischuk, T. Chan, V.A. Drover, S. Ho, G. Chimini, L.B. Agellon, R. Agnihotri, G.A. Francis, and R. Lehner. 2004. ABCA1-dependent lipid efflux to apolipoprotein A-I mediates HDL particle formation and decreases VLDL secretion from murine hepatocytes. *J Lipid Res.* 45:1122-31.
- Sampath, H., M.T. Flowers, X. Liu, C.M. Paton, R. Sullivan, K. Chu, M. Zhao, and J.M. Ntambi. 2009. Skin-specific Deletion of Stearoyl-CoA Desaturase-1 Alters Skin Lipid Composition and Protects Mice from High Fat Diet-induced Obesity. *J Biol Chem.* 284:19961-73.
- Sato, S., M. Fukasawa, Y. Yamakawa, T. Natsume, T. Suzuki, I. Shoji, H. Aizaki, T. Miyamura, and M. Nishijima. 2006. Proteomic profiling of lipid droplet proteins in hepatoma cell lines expressing hepatitis C virus core protein. *J Biochem.* 139:921-30.
- Satoh, T., and M. Hosokawa. 1998. The mammalian carboxylesterases: from molecules to functions. *Annu Rev Pharmacol Toxicol.* 38:257-88.
- Schneider, G., G. Neuberger, M. Wildpaner, S. Tian, I. Berezovsky, and F. Eisenhaber. 2006. Application of a sensitive collection heuristic for very large protein families: evolutionary relationship between adipose triglyceride lipase (ATGL) and classic mammalian lipases. *BMC Bioinformatics.* 7:164.

- Schrader, M. 2001. Tubulo-reticular clusters of peroxisomes in living COS-7 cells: dynamic behavior and association with lipid droplets. *J Histochem Cytochem.* 49:1421-29.
- Shelness, G.S., and J.A. Sellers. 2001. Very-low-density lipoprotein assembly and secretion. *Curr Opin Lipidol.* 12:151-7.
- Shi, Y., and D. Cheng. 2009. Beyond triglyceride synthesis: the dynamic functional roles of MGAT and DGAT enzymes in energy metabolism. *Am J Physiol Endocrinol Metab.* 297:E10-8.
- Singh, R., S. Kaushik, Y. Wang, Y. Xiang, I. Novak, M. Komatsu, K. Tanaka, A.M. Cuervo, and M.J. Czaja. 2009. Autophagy regulates lipid metabolism. *Nature.* 458:1131-5.
- Small, C.A., M.P. Rogers, J.A. Goodacre, and S.J. Yeaman. 1991. Phosphorylation and activation of hormone-sensitive lipase in isolated macrophages. *FEBS Lett.* 279:323-6.
- Smith, S.J., S. Cases, D.R. Jensen, H.C. Chen, E. Sande, B. Tow, D.A. Sanan, J. Raber, R.H. Eckel, and R.V. Farese, Jr. 2000. Obesity resistance and multiple mechanisms of triglyceride synthesis in mice lacking Dgat. *Nat Genet.* 25:87-90.
- Soni, K.G., R. Lehner, P. Metalnikov, P. O'Donnell, M. Semache, W. Gao, K. Ashman, A.V. Pshezhetsky, and G.A. Mitchell. 2004. Carboxylesterase 3 (EC 3.1.1.1) is a major adipocyte lipase. *J Biol Chem.* 279:40683-9.
- Soni, K.G., G.A. Mardones, R. Sougrat, E. Smirnova, C.L. Jackson, and J.S. Bonifacino. 2009. Coatamer-dependent protein delivery to lipid droplets. *J Cell Sci.* 122:1834-41.
- Souza, S.C., K.V. Muliro, L. Liscum, P. Lien, M.T. Yamamoto, J.E. Schaffer, G.E. Dallal, X. Wang, F.B. Kraemer, M. Obin, and A.S. Greenberg. 2002. Modulation of hormone-sensitive lipase and protein kinase A-mediated lipolysis by perilipin A in an adenoviral reconstituted system. *J Biol Chem.* 277:8267-72.
- Spooner, P.J., and D.M. Small. 1987. Effect of free cholesterol on incorporation of triolein in phospholipid bilayers. *Biochemistry.* 26:5820-5.

- Stone, S.J., M.C. Levin, and R.V. Farese, Jr. 2006. Membrane topology and identification of key functional amino acid residues of murine acyl-CoA:diacylglycerol acyltransferase-2. *J Biol Chem.* 281:40273-82.
- Stone, S.J., H.M. Myers, S.M. Watkins, B.E. Brown, K.R. Feingold, P.M. Elias, and R.V. Farese, Jr. 2004. Lipopenia and skin barrier abnormalities in DGAT2-deficient mice. *J Biol Chem.* 279:11767-76.
- Stone, S.S., M.C. Levin, P. Zhou, J. Han, T.C. Walther, and R.V. Farese, Jr. 2008. The endoplasmic reticulum enzyme, DGAT2, is found in mitochondria-associated membranes and has a mitochondrial targeting signal that promotes its association with mitochondria. *J Biol Chem.*
- Stralfors, P., and P. Befrage. 1985. Phosphorylation of hormone-sensitive lipase by cyclic GMP-dependent protein kinase. *FEBS Lett.* 180:280-4.
- Stralfors, P., P. Bjorgell, and P. Befrage. 1984. Hormonal regulation of hormone-sensitive lipase in intact adipocytes: identification of phosphorylated sites and effects on the phosphorylation by lipolytic hormones and insulin. *Proc Natl Acad Sci U S A.* 81:3317-21.
- Sturmey, R.G., P.J. O'Toole, and H.J. Leese. 2006. Fluorescence resonance energy transfer analysis of mitochondrial:lipid association in the porcine oocyte. *Reproduction.* 132:829-37.
- Subramanian, V., A. Rothenberg, C. Gomez, A.W. Cohen, A. Garcia, S. Bhattacharyya, L. Shapiro, G. Dolios, R. Wang, M.P. Lisanti, and D.L. Brasaemle. 2004. Perilipin A mediates the reversible binding of CGI-58 to lipid droplets in 3T3-L1 adipocytes. *J Biol Chem.* 279:42062-71.
- Swift, L.L., M.Y. Zhu, B. Kakkad, A. Jovanovska, M.D. Neely, K. Valyi-Nagy, R.L. Roberts, D.E. Ong, and W.G. Jerome. 2003. Subcellular localization of microsomal triglyceride transfer protein. *J Lipid Res.* 44:1841-9.
- Sztalryd, C., G. Xu, H. Dorward, J.T. Tansey, J.A. Contreras, A.R. Kimmel, and C. Londos. 2003. Perilipin A is essential for the translocation of hormone-sensitive lipase during lipolytic activation. *J Cell Biol.* 161:1093-103.
- Szymanski, K.M., D. Binns, R. Bartz, N.V. Grishin, W.P. Li, A.K. Agarwal, A. Garg, R.G. Anderson, and J.M. Goodman. 2007. The lipodystrophy protein seipin is found at endoplasmic reticulum lipid droplet junctions and is important for droplet morphology. *Proc Natl Acad Sci U S A.* 104:20890-5.

- Takeuchi, K., and K. Reue. 2009. Biochemistry, physiology, and genetics of GPAT, AGPAT, and lipin enzymes in triglyceride synthesis. *Am J Physiol Endocrinol Metab.* 296:E1195-209.
- Tansey, J.T., A.M. Huml, R. Vogt, K.E. Davis, J.M. Jones, K.A. Fraser, D.L. Brasaemle, A.R. Kimmel, and C. Londos. 2003. Functional studies on native and mutated forms of perilipins. A role in protein kinase A-mediated lipolysis of triacylglycerols. *J Biol Chem.* 278:8401-6.
- Tansey, J.T., C. Sztalryd, J. Gruia-Gray, D.L. Roush, J.V. Zee, O. Gavrilova, M.L. Reitman, C.X. Deng, C. Li, A.R. Kimmel, and C. Londos. 2001. Perilipin ablation results in a lean mouse with aberrant adipocyte lipolysis, enhanced leptin production, and resistance to diet-induced obesity. *Proc Natl Acad Sci U S A.* 98:6494-9.
- Tansey, J.T., C. Sztalryd, E.M. Hlavin, A.R. Kimmel, and C. Londos. 2004. The central role of perilipin a in lipid metabolism and adipocyte lipolysis. *IUBMB Life.* 56:379-85.
- Tietge, U.J., A. Bakillah, C. Maugeais, K. Tsukamoto, M. Hussain, and D.J. Rader. 1999. Hepatic overexpression of microsomal triglyceride transfer protein (MTP) results in increased in vivo secretion of VLDL triglycerides and apolipoprotein B. *J Lipid Res.* 40:2134-9.
- Touret, N., P. Paroutis, M. Terebiznik, R.E. Harrison, S. Trombetta, M. Pypaert, A. Chow, A. Jiang, J. Shaw, C. Yip, H.P. Moore, N. van der Wel, D. Houben, P.J. Peters, C. de Chastellier, I. Mellman, and S. Grinstein. 2005. Quantitative and dynamic assessment of the contribution of the ER to phagosome formation. *Cell.* 123:157-70.
- Turro, S., M. Ingelmo-Torres, J.M. Estanyol, F. Tebar, M.A. Fernandez, C.V. Albor, K. Gaus, T. Grewal, C. Enrich, and A. Pol. 2006. Identification and characterization of associated with lipid droplet protein 1: A novel membrane-associated protein that resides on hepatic lipid droplets. *Traffic.* 7:1254-69.
- Valyi-Nagy, K., C. Harris, and L.L. Swift. 2002. The assembly of hepatic very low density lipoproteins: evidence of a role for the Golgi apparatus. *Lipids.* 37:879-84.
- van Tilbeurgh, H., S. Bezzine, C. Cambillau, R. Verger, and F. Carriere. 1999. Colipase: structure and interaction with pancreatic lipase. *Biochim Biophys Acta.* 1441:173-84.

- Vance, D.E. 2008. Role of phosphatidylcholine biosynthesis in the regulation of lipoprotein homeostasis. *Curr Opin Lipidol.* 19:229-34.
- Vance, J.E. 2002. Assembly and secretion of lipoproteins. *In* Biochemistry of lipids, lipoproteins, and membranes. Vol. 36. D.E. Vance and J.E. Vance, editors. Elsevier, Amsterdam. 607 p.
- Verhoeven, A.J., B.P. Neve, and H. Jansen. 1999. Secretion and apparent activation of human hepatic lipase requires proper oligosaccharide processing in the endoplasmic reticulum. *Biochem J.* 337 (Pt 1):133-40.
- Villena, J.A., S. Roy, E. Sarkadi-Nagy, K.H. Kim, and H.S. Sul. 2004. Desnutrin, an adipocyte gene encoding a novel patatin domain-containing protein, is induced by fasting and glucocorticoids: ectopic expression of desnutrin increases triglyceride hydrolysis. *J Biol Chem.* 279:47066-75.
- Voet, D., J.G. Voet, and C.W. Pratt. 2002. Fundamentals of biochemistry. Wiley, New York. 1 v. (various pagings) pp.
- Wakil, S.J., J.K. Stoops, and V.C. Joshi. 1983. Fatty acid synthesis and its regulation. *Annu Rev Biochem.* 52:537-79.
- Walkey, C.J., L.R. Donohue, R. Bronson, L.B. Agellon, and D.E. Vance. 1997. Disruption of the murine gene encoding phosphatidylethanolamine N-methyltransferase. *Proc Natl Acad Sci U S A.* 94:12880-5.
- Walther, T.C., and R.V. Farese, Jr. 2009. The life of lipid droplets. *Biochim Biophys Acta.* 1791:459-66.
- Wang, H., D. Gilham, and R. Lehner. 2007. Proteomic and lipid characterization of apolipoprotein B-free luminal lipid droplets from mouse liver microsomes: implications for very low density lipoprotein assembly. *J Biol Chem.* 282:33218-26.
- Wang, S.P., N. Laurin, J. Himms-Hagen, M.A. Rudnicki, E. Levy, M.F. Robert, L. Pan, L. Oligny, and G.A. Mitchell. 2001. The adipose tissue phenotype of hormone-sensitive lipase deficiency in mice. *Obes Res.* 9:119-28.
- Wang, Y., K. Tran, and Z. Yao. 1999. The activity of microsomal triglyceride transfer protein is essential for accumulation of triglyceride within microsomes in McA-RH7777 cells. A unified model for the assembly of very low density lipoproteins. *J Biol Chem.* 274:27793-800.

- Watt, M.J., and G.R. Steinberg. 2008. Regulation and function of triacylglycerol lipases in cellular metabolism. *Biochem J.* 414:313-25.
- Wei, E., M. Alam, F. Sun, L.B. Agellon, D.E. Vance, and R. Lehner. 2007a. Apolipoprotein B and triacylglycerol secretion in human triacylglycerol hydrolase transgenic mice. *J Lipid Res.* 48:2597-606.
- Wei, E., W. Gao, and R. Lehner. 2007b. Attenuation of adipocyte triacylglycerol hydrolase activity decreases basal fatty acid efflux. *J Biol Chem.* 282:8027-35.
- Welte, M.A., S.P. Gross, M. Postner, S.M. Block, and E.F. Wieschaus. 1998. Developmental regulation of vesicle transport in *Drosophila* embryos: forces and kinetics. *Cell.* 92:547-57.
- Wendel, A.A., T.M. Lewin, and R.A. Coleman. 2009. Glycerol-3-phosphate acyltransferases: Rate limiting enzymes of triacylglycerol biosynthesis. *Biochim Biophys Acta.* 1791:501-6.
- Wetterau, J.R., L.P. Aggerbeck, P.M. Laplaud, and L.R. McLean. 1991a. Structural properties of the microsomal triglyceride-transfer protein complex. *Biochemistry.* 30:4406-12.
- Wetterau, J.R., K.A. Combs, L.R. McLean, S.N. Spinner, and L.P. Aggerbeck. 1991b. Protein disulfide isomerase appears necessary to maintain the catalytically active structure of the microsomal triglyceride transfer protein. *Biochemistry.* 30:9728-35.
- Wetterau, J.R., K.A. Combs, S.N. Spinner, and B.J. Joiner. 1990. Protein disulfide isomerase is a component of the microsomal triglyceride transfer protein complex. *J Biol Chem.* 265:9800-7.
- Wetterau, J.R., and D.B. Zilversmit. 1984. A triglyceride and cholesteryl ester transfer protein associated with liver microsomes. *J Biol Chem.* 259:10863-6.
- Wetterau, J.R., and D.B. Zilversmit. 1986. Localization of intracellular triacylglycerol and cholesteryl ester transfer activity in rat tissues. *Biochim Biophys Acta.* 875:610-7.

- Wiggins, D., and G.F. Gibbons. 1992. The lipolysis/esterification cycle of hepatic triacylglycerol. Its role in the secretion of very-low-density lipoprotein and its response to hormones and sulphonylureas. *Biochem J.* 284:457-62.
- Wolins, N.E., D.L. Brasaemle, and P.E. Bickel. 2006a. A proposed model of fat packaging by exchangeable lipid droplet proteins. *FEBS Lett.* 580:5484-91.
- Wolins, N.E., B.K. Quaynor, J.R. Skinner, M.J. Schoenfish, A. Tzekov, and P.E. Bickel. 2005. S3-12, Adipophilin, and TIP47 package lipid in adipocytes. *J Biol Chem.* 280:19146-55.
- Wolins, N.E., B.K. Quaynor, J.R. Skinner, A. Tzekov, M.A. Croce, M.C. Gropler, V. Varma, A. Yao-Borengasser, N. Rasouli, P.A. Kern, B.N. Finck, and P.E. Bickel. 2006b. OXPAT/PAT-1 is a PPAR-induced lipid droplet protein that promotes fatty acid utilization. *Diabetes.* 55:3418-28.
- Wolins, N.E., B. Rubin, and D.L. Brasaemle. 2001. TIP47 associates with lipid droplets. *J Biol Chem.* 276:5101-8.
- Wolins, N.E., J.R. Skinner, M.J. Schoenfish, A. Tzekov, K.G. Bensch, and P.E. Bickel. 2003. Adipocyte protein S3-12 coats nascent lipid droplets. *J Biol Chem.* 278:37713-21.
- Wu, A.L., and H.G. Windmueller. 1978. Identification of circulating apolipoproteins synthesized by rat small intestine in vivo. *J Biol Chem.* 253:2525-8.
- Wu, X., M. Zhou, L.S. Huang, J. Wetterau, and H.N. Ginsberg. 1996. Demonstration of a physical interaction between microsomal triglyceride transfer protein and apolipoprotein B during the assembly of ApoB-containing lipoproteins. *J Biol Chem.* 271:10277-81.
- Xia, T., N. Mostafa, B.G. Bhat, G.L. Florant, and R.A. Coleman. 1993. Selective retention of essential fatty acids: the role of hepatic monoacylglycerol acyltransferase. *Am J Physiol.* 265:R414-9.
- Xu, G., C. Sztalryd, X. Lu, J.T. Tansey, J. Gan, H. Dorward, A.R. Kimmel, and C. Londos. 2005. Post-translational regulation of adipose differentiation-related protein by the ubiquitin/proteasome pathway. *J Biol Chem.* 280:42841-7.

- Yamaguchi, J., M.V. Gamble, D. Conlon, J.S. Liang, and H.N. Ginsberg. 2003. The conversion of apoB100 low density lipoprotein/high density lipoprotein particles to apoB100 very low density lipoproteins in response to oleic acid occurs in the endoplasmic reticulum and not in the Golgi in McA RH7777 cells. *J Biol Chem.* 278:42643-51.
- Yamaguchi, T., N. Omatsu, E. Morimoto, H. Nakashima, K. Ueno, T. Tanaka, K. Satouchi, F. Hirose, and T. Osumi. 2007. CGI-58 facilitates lipolysis on lipid droplets but is not involved in the vesiculation of lipid droplets caused by hormonal stimulation. *J Lipid Res.* 48:1078-89.
- Yamazaki, T., E. Sasaki, C. Kakinuma, T. Yano, S. Miura, and O. Ezaki. 2005. Increased very low density lipoprotein secretion and gonadal fat mass in mice overexpressing liver DGAT1. *J Biol Chem.* 280:21506-14.
- Yang, L.Y., A. Kuksis, J.J. Myher, and G. Steiner. 1996. Contribution of de novo fatty acid synthesis to very low density lipoprotein triacylglycerols: evidence from mass isotopomer distribution analysis of fatty acids synthesized from [2H6]ethanol. *J Lipid Res.* 37:262-74.
- Yao, Z.M., and D.E. Vance. 1988. The active synthesis of phosphatidylcholine is required for very low density lipoprotein secretion from rat hepatocytes. *J Biol Chem.* 263:2998-3004.
- Ye, J., J.Z. Li, Y. Liu, X. Li, T. Yang, X. Ma, Q. Li, Z. Yao, and P. Li. 2009. Cideb, an ER- and lipid droplet-associated protein, mediates VLDL lipidation and maturation by interacting with apolipoprotein B. *Cell Metab.* 9:177-90.
- Yen, C.L., M.L. Cheong, C. Grueter, P. Zhou, J. Moriwaki, J.S. Wong, B. Hubbard, S. Marmor, and R.V. Farese, Jr. 2009. Deficiency of the intestinal enzyme acyl CoA:monoacylglycerol acyltransferase-2 protects mice from metabolic disorders induced by high-fat feeding. *Nat Med.* 15:442-6.
- Yen, C.L., S.J. Stone, S. Cases, P. Zhou, and R.V. Farese, Jr. 2002. Identification of a gene encoding MGAT1, a monoacylglycerol acyltransferase. *Proc Natl Acad Sci U S A.* 99:8512-7.
- Yen, C.L., S.J. Stone, S. Koliwad, C. Harris, and R.V. Farese, Jr. 2008. Thematic review series: glycerolipids. DGAT enzymes and triacylglycerol biosynthesis. *J Lipid Res.* 49:2283-301.

- Zhao, B., J. Song, W.N. Chow, R.W. St Clair, L.L. Rudel, and S. Ghosh. 2007. Macrophage-specific transgenic expression of cholesteryl ester hydrolase significantly reduces atherosclerosis and lesion necrosis in Ldlr mice. *J Clin Invest.* 117:2983-92.
- Zimmermann, R., A. Lass, G. Haemmerle, and R. Zechner. 2009. Fate of fat: The role of adipose triglyceride lipase in lipolysis. *Biochim Biophys Acta.* 1791:494-500.
- Zimmermann, R., J.G. Strauss, G. Haemmerle, G. Schoiswohl, R. Birner-Gruenberger, M. Riederer, A. Lass, G. Neuberger, F. Eisenhaber, A. Hermetter, and R. Zechner. 2004. Fat mobilization in adipose tissue is promoted by adipose triglyceride lipase. *Science.* 306:1383-6.

Appendices

8.1 Digital data available on CD

Video S1 and Video S2 are continuations to Figure 4-9A and Figure 4-10, respectively. All movies represent 30 min duration in real time and are displayed at 5 frames per second.

Video S1. Lipid transfer from nascent LDs to preformed LDs in WT (A) and TGH KO (B) hepatocytes. Cells were labeled with Bodipy 558/568 C₁₂ containing media overnight and fatty acid uptake reagent (containing Bodipy FL C₁₂) was added immediately before the start of image acquisition (0 min) with time-lapse confocal microscopy. Red, preformed LDs; green, nascent LDs.

Video S2. Dynamic interactions between nascent and preformed LDs in WT (A) and TGH KO (B) hepatocytes. Image stacks were taken at the same conditions as in Video S1 and were magnified and presented at 3-D opacity mode. Red, preformed LDs; green, nascent LDs.